Pathways to Net-Zero Energy Buildings: An Optimization Methodology

Scott Bucking

A Thesis

In the Department

of

Building, Civil, and Environmental Engineering

Presented in Partial Fulfillment of the Requirements

For the Degree of

Doctor of Philosophy (Building Engineering) at

Concordia University

Montréal, Québec, Canada

December 2013

Concordia University

School of Graduate Studies

This is to certify that the thesis prepared

By: **Scott Bucking**

Entitled: **Pathways to Net-Zero Energy Buildings: An Optimization Methodology**

and submitted in partial fulfillment of the requirements for the degree of

DOCTOR OF PHILOSOPHY (Building Engineering)

complies with the regulations of the University and meets the accepted standards with respect to originality and quality.

Signed by the final examining committee:

Dr. W.P. Zhu	Chair
Dr. L. Lamarche	External Examiner
Dr. N. Kharma	External to Program
Dr. H. Ge	Examiner
Dr. F. Haghighat	Examiner
Dr. A. Athienitis	Thesis Co-Supervisor
Dr. R. Zmeureanu	Thesis Co-Supervisor

Approved by Dr. M. Elektorowicz
Graduate Program Director

November 28, 2010 Dr. C. Trueman
Interim Dean, Faculty of Engineering and Computer Science

ABSTRACT

Pathways to Net-Zero Energy Buildings: An Optimization Methodology

Scott Bucking, Ph.D.

Concordia University, 2013

Building Performance Simulation (BPS) is frequently used by decision-makers to estimate building energy consumption at the design stage. However, the true potential of BPS remains unrealized if trial and error methods of building simulation are used to identify combinations of parameters to reduce energy use. Optimization techniques combined with BPS offer many benefits such as: (i) identification of potential optimal designs which best achieve desired performance objectives; (ii) system level component integration by simultaneously considering conflicting trade-offs; and (iii) a process-oriented simulation tool that is complementary to BPS, eliminating the need for repetitive user-initiated model evaluations. However, the capability of optimization algorithms to effectively map out the entire solution space and discover information is farther reaching than building design. As shown in this thesis, optimization datasets are also a valuable resource for conducting uncertainty and sensitivity analyses and evaluating policies to incentivize low-energy building design.

Two performance criteria are considered in this thesis: net-energy consumption and life-cycle cost. The term 'performance-optimized' refers to the extreme of these two criteria that is Net-Zero Energy (NZE) and cost-optimized buildings. A Net-Zero Energy Building (NZEB) generates at least as much renewable energy on-site as it consumes in a given year. A cost-optimized building has the lowest life-cycle cost over a considered period. A focus of this thesis is identifying optimal pathways to NZE and cost-optimized building designs.

This thesis proposes the following approaches to identify pathways to net-zero energy: (i) a redesign case-study of an existing near-Net-Zero Energy Home (NZEH) archetype using a proposed optimization methodology; (ii) the development of an information-driven hybrid evolutionary algorithm for optimal building design; (iii) a methodology for identifying the influence of design variations on building energy performance; (iv) a methodology to evaluate the effect of incentives on life-cycle energy-cost curves; and (v) effect of a time-of-use feed-in tariff on optimal net-zero energy home design.

The optimization methodology consists of: (i) an energy model; (ii) a cost model; (iii) a custom optimization algorithm; (iv) a database; and (v) a statistics module. Several new simulation techniques are proposed to identify pathways to performance-optimized net-zero energy buildings: (i) probability distribution functions extracted from previous simulations; (ii) back-tracking searches; and (iii) importance factors to summarize back-tracking search results.

This thesis provides valuable information related to: (i) the development of performance-based energy codes for buildings; (ii) systematic design of cost-optimized NZEHs; (iii) systematic analysis of the impact of different design parameters on energy consumption and cost; (iv) the study of incentive measures for NZEHs.

Acknowledgments

I thank my supervisors, Drs. Radu Zmeureanu and Andreas Athienitis for their patience and supervision in guiding me through a PhD. My academic training was greatly influenced by my exposure to world class research through my participation in conferences and IEA task meetings in Graz, Kassel, Bassel, Colorado, Barcelona and Chambéry. I have my supervisors to thank for exposing me to such international research events.

I thank my colleagues at the solar building research lab for their support and companionship. It has been a pleasure getting to know you all thus far. I will miss our conversations and have greatly appreciated your feedback over these past years. Special thanks to Matthew Doiron for helping me get involved in commercial energy audits.

I would like to acknowledge several mentors and friends that have helped me through this process: Dr. Eric Ducharme, Dr. Liam O'Brien and Dr. Lukas Swan. I acknowledge Dr. Jose Candandedo, Constantinos Kapsis and Diane Bastien for reviewing and commenting on parts of this thesis. Your comments have greatly improved this document.

All of the content and concepts in this thesis were created using freely available open-source tools. I acknowledge the creators, developers and package maintainers of: Clojure, Python, Matplotlib, GenOpt, R-lang, ggplot, vim, texlive and SQLite.

I thank my family for keeping me grounded over the past years. Family is and will continue to be a priority in my life. To my wife, Shannon: without your love, encouragement, moral support and understanding a PhD would not have been possible. Only you know how easy and yet how hard this experience has been on me. I can't wait for future adventures yet to come.

Table of Contents

List of Figures

List of Tables

Nomenclature

Acronyms and Abbreviations

ASHRAE	American Society of Heating, Refrigerating and Air-Conditioning
BPIE	Building Performance Institute Europe
CMHC	Canada Mortgage and Housing Corporation
DOE	U.S. Department of Energy
ECBCS	Energy Conservation in Building and Community Systems
IBPSA	International Building Performance Simulation Association
IEA	International Energy Agency
IPCC	Intergovernmental Panel on Climate Change
ISES	International Solar Energy Society
LBNL	Lawrence Berkeley National Laboratory
NRC	National Research Council Canada
NRCan	Natural Resources Canada
NREL	National Renewable Energy Laboratory
OEE	Office of Energy Efficiency
OPA	Ontario Power Authority
USGBC	US Green Building Council

Engineering Nomenclature

ACH	Air Changes per Hour
BIPV/T	Building Integrated Photovoltaic-Thermal
BEOpt	Building Energy Optimizer
BPS	Building Performance Simulation
COP	Coefficient of Performance
CTF	Conduction Transfer Function
DAE	Differentiable Algebraic Equation

DE	Differential Evolution
DHW	Domestic Hot Water
EA	Evolutionary Algorithm
ECM	Energy Conservation Measure
EEM	Energy Efficiency Measure
ESP-r	Energy Simulation Program - Research
EUI	Energy Use Intensity
FA	Floor Area
FIT	Feed-in Tariff
GA	Genetic Algorithm
GenOpt	Generic Optimizer Tool
GHG	Green House Gas emissions
HJGPS	Hooke-Jeeves General Pattern Search
HVAC	Heating, Ventilating, and Air Conditioning
IDP	Integrative Design Process
PDF	Probability Distribution Function
MI	Mutual Information
MCA	Monte Carlo Analysis
NPV	Net-Present Value
NSGA-II	Non-dominated Sorting Genetic Algorithm-II
NZE	Net-Zero Energy
NZEB	Net-Zero Energy Building
NZEH	Net-Zero Energy Home
PSO	Particle Swarm Optimization
PV	Photovoltaic
ROI	Return on Investment
SA	Simulated Annealing

SQL	Structured Query Language
TMY	Typical Meteorological Year
TOU	Time of Use Billing
TS	Tabu Search
TRNSYS	TRaNsient SYstems Simulation program
WA	Wall Area
WWR	Window-to-Wall Ratio

Definitions

Building Integrated: A component that is integrated into building façade or roof surface. Typically refers to renewable energy technologies integrated into a exterior surface.

Coefficient of Performance: Used to describe the efficiency of mechanical equipment, particularly heat-pumps. Defined as the ratio of heating or cooling provided divided by the electricity consumed.

Computational Evolution: A probabilistic computer algorithm utilizing selection, genetic operations, and survival of the fittest on simplified design representations to improve objective function(s).

Crossover: An operator in an evolutionary algorithm where information is shared between two individuals create two new individuals. Similar to the biological analogy of mating. Called "recombination" in some textbooks.

Diversity: Used in performance monitoring of evolutionary algorithms, diversity is a measurement of how similar, or different, representations in a population are. This information allows algorithm designers to identify if an optimization algorithm is prematurely converging, or overly randomizing the population.

Energy Conservation: Refers to reduction in total energy consumption by reducing the total load directly. Energy conservation measures reduce the primary energy required to satisfy and given load by reducing the total load to be met. Examples are heating/cooling load reductions due to improvements in envelope air-tightness, insulation and lighting.

Energy Efficiency: Refers to the efficiency of mechanical equipment required to perform work. Energy efficiency measures reduce the primary energy required to satisfy a given load without reducing the total load to be met. Examples of more efficient fans, cooling and heating equipment.

Energy Generation: Refers to reduction in net-energy consumption through the creation of energy preferably using renewable energy technologies. Examples include electricity generated from PV panels and wind turbines.

Generation Gap: The percentage population replaced within an evolutionary cycle. A generation gap of 25% indicates that 75% of the present population was created from previous generations or algorithm iterations.

Interactions: In modelling theory, interactions arise when considering the relationship among three or more variables, and describes a situation in which the simultaneous influence of two variables on a third is not additive.

Monotonic Variable: A variable is monotonic if changing its inputs always makes the model output increase or decrease. Optimal settings of monotonic variables are the extreme values in the set. This relationship may apply to multiple objective functions.

Mutation: An operator in an evolutionary algorithm typically operating on a single individual to emulate random variations similar to DNA mutations in its biological counterpart.

Mutual Information: A measure of dependency between two random variables or the amount of information that can be obtained about one random variable by observing another.

N-arity: Refers to the number of individuals required for a genetic operation within a evolutionary algorithm. Typically operators require two individuals implicating 2-arity.

Nearly Net-zero Energy: A European standard where a building is designed such that heating and cooling energy consumption is cost-optimal over an evaluated life-cycle.

Net-zero Energy: An energy balance, typically over a typical meteorological year, where equal or greater renewable energy is generated than building energy consumption.

Objective Function: An evaluation of fitness of a particular design representation.

Optimization: In this thesis, optimization refers to a systematic algorithmic search of all feasible designs to achieve or exceed a desired energy consumption level or life-cycle cost performance indicator.

Parameter: The set possible values in a discrete variable. Example, the set $x_1, x_2, \cdots, x_N$ which describes the variable $\mathbf{a_1} = (x_1, x_2, \cdots, x_N)^T$.

Probability Distribution Function: Expressing parameters using probabilities for a given variable or variables.

Representation: A particular vector or binary string which encodes the solution space. A simplified representation of all designs.

Selection: An operator in an evolutionary algorithm which determines: (i) which individuals are allowed to sharing information with others, i.e. "mate", or (ii) which population of individuals survive in future algorithm iterations or generations.

Selection Pressure: In an evolutionary algorithm, this term refers to how deterministic a selection operator or genetic operator is. Decreasing selection pressure refers to increasing the randomness of the selection or genetic operator.

Solar Building: A building utilizing solar energy for a significant portion of energy consumption or generation while maintaining occupant comfort.

Solution Space: A higher dimensional space defined by all possible design combinations available to the optimization search. In a discrete optimization problem, the number of possible solutions is described by $M = m^N$ where m is the number of variables, and N is the number of settings in each variable or parameters in the variable set.

Stochastic: Depending on random processes.

Variable: An input to a model, such as $\mathbf{a_1} = (x_1, x_2, \cdots, x_N)^T$ in the model $f(\mathbf{a_1}, \cdots, \mathbf{a_n})$. Can refer to design or non-design aspects.

Chapter 1

Introduction

> Wonder is not knowledge, neither is it ignorance. It's something which is suspended between what we believe we can be, and a tradition we may have forgotten.
>
> –*Emily Dickinson*

> Problems cannot be solved by the same level of thinking that created them.
>
> –*Albert Einstein*

1.1 Motivations

ENERGY is thought to be a keystone of prosperity, security and peace. As of 2013, the primary fuel driving industry, transportation, food production and building operations originates from non-renewable energy reserves. Before the industrial revolution and cheap, abundant coal, society was sustainable by necessity. Master builders embraced functional building design through passive solar strategies, natural ventilation and daylighting with equal or greater importance than architectural æsthetic. The identification of abundant fossil fuel resources initiated a paradigm shift in building design—the same building approaches and materials could be used anywhere in the world for a small energy penalty. Due to dwindling fossil fuel reserves, growing worldwide energy needs and our changing climate another paradigm shift is needed towards new energy sources.

Given the inextricable link between the growing population and energy needs, we must better manage our energy resources while transitioning to new renewable energy

supplies. The International Energy Agency suggested that in 2010, we reached our peak capacity to produce conventional oil (IEA, 2010). Furthermore, the world population is projected to grow annually at 1.9%, resulting in a doubling rate every 37 years (UN, 2013). The United Nations estimates that population will stabilize somewhere around 11 billion. To meet future energy needs, we require energy consumption reductions and new energy resources (IEA, 2010). The impetus toward a renewable energy supply is further strengthened by climate change due to an increase in anthropogenic Green House Gas emissions (GHG) emissions (Arndt et al., 2010; Parry et al., 2007).

Renewable sources of energy can play a key role in the transition away from fossil-based fuels. In fact, every hour our planet receives enough solar energy for the annual needs of humanity (Lewis and Nocera, 2006; World Energy Council, 2007). Furthermore, the peak electrical demand in some provinces such as Ontario is due to air-conditioning needs (OCA, 2007). Air-conditioning is directly correlated with peak solar irradiance and can be offset using Photovoltaic (PV) generated electricity. The cost of manufacturing PV panels is decreasing by 8% per year (Breyer and Gerlach, 2010) with conversion efficiencies now above 22% (SunPower, 2013). Already PV panel cost has reached grid-parity in some countries where electricity costs are high, such as Spain and Germany. PV grid-parity is the point where solar electricity becomes cheaper than grid power on $/kWh basis. In 2012, PV was manufactured at $1.15/W in key-regions and is predicted to decrease to $0.85/W (IEA PVPS, 2013) due to thin-film technology. It is predicted that third generation PV cells will approach the thermodynamic limit for multi-junction cells of 86% or the theoretical limit of 93% (Green, 2001)—a four fold increase in efficiency over present technology. No other renewable energy technology has experienced decreases in price while achieving such increases in efficiencies. Given the vast surface area of buildings, a significant portion which is equatorial-facing, envelope integrated PV is a viable option to offset building energy consumption.

Buildings are often called the 'low-hanging fruit' of GHG and primary energy reductions. In North America, energy used to construct and operate buildings accounts for some 40% of total energy use (DOE, 2009). In Canada, buildings consume about 31% of energy use and about 50% of total electricity produced (NRCan-OEE, 2009). In a consensus report of more than 400 scientists from 120 countries, the IPCC identified

that buildings have the largest economical GHG abatement potential estimated to be in the range of 5.3 to 6.7 $GtCO_2-eq/yr$, representing 18 to 35% of the total abatement potential by 2030 (Parry et al., 2007). Pacala and Socolow (2004) suggested that a set of strategic human actions could result in the stabilization of atmospheric carbon to a 'safe level' using incremental reductions of GHG through stabilization wedges; in this study, the conservation of energy in buildings was recognized as a large potential stabilization wedge. McKinsey (2009) suggested that the USA could benefit from $1.2 trillion in savings through 2020 by investing $520 billion in building improvements. Performance indicators aid in establishing achievable limits of economic and energy savings associated with buildings.

Two performance criteria are considered in this thesis: (i) net-energy consumption, i.e. net meaning consumption minus generation, and (ii) life-cycle cost. The term 'performance-optimized' refers to the extreme of these two criteria, Net-Zero Energy (NZE) and cost-optimized buildings. A Net-Zero Energy Building (NZEB) generates at least as much renewable energy on-site as it consumes in a given year (Torcellini et al., 2006). A cost-optimized building has the lowest life-cycle cost over a designated period. For most individuals, the purchase of a house is the largest expenditure of their lifetime. These buildings last for at least fifty and potentially hundreds of years. The operations and maintenance costs associated with buildings are typically more significant than the initial cost and eventual resale value. Since many performance improvement opportunities cannot be revisited post-construction, optimizing building operations before construction is imperative to reduce life-cycle energy and cost.

There is a growing initiative to transition the construction market towards NZEBs. NZEBs offer many technical benefits: (i) they require an energy balance which offsets primary energy use for construction and operations while eliminating their embodied energy and greenhouse gas emissions over the life-cycle (Berggren et al., 2013); (ii) low operation costs and the potential for a positive investment opportunity if generated electricity is purchased; (iii) lower peak electrical demands relative to other buildings which reduces the need for future grid expansion (Sadineni et al., 2012); and (iv) with additional smart-grid technologies, distributed generation makes the electrical grid more resilient to blackouts (IEEE, 2012) such as unprecedented peak demand or natural events

such as ice-storms (Abley, 1998) and solar coronas (NASA, 2009). Due to these benefits, the European Union has mandated that all member states build to NZEB standards after December 31, 2019 (EU Parliament, 2010). Note that there are many definitions of NZE (Torcellini et al., 2006), however this standard specifies for *nearly NZE* where heating and cooling loads are cost-optimal. Primarily based on EU initiatives, Pike Research (2012) estimated that the NZEB market will be worth $1.3 trillion by 2035. Designing a NZEB requires a delicate balance of energy conservation through more air-tight and better insulated envelopes, more energy efficient lighting and mechanical equipment and renewable energy generation to offset net-energy requirements of the building. Achieving NZE performance in a cost-optimal manner presently requires additional software tools and methodologies to predict how much a building will consume before construction.

1.2 Main Objectives

Creating a NZEB is a challenging task. Pivotal decisions which affect energy consumption must be made using uncertain information. For example, many building properties are not yet known at the design state such as air-tightness, thermal bridging, usage characteristics and site shading. Whole building design is thus an ill-defined problem, meaning that designers are working with limited criteria to identify opportunities for a performance-optimized building. However, insulation levels, building layout and thermal mass sizing, orientation, glazing properties and sizing, natural ventilation, daylighting, renewable energy integration and Heating, Ventilating, and Air Conditioning (HVAC) system selection and sizing must be considered before the detailed design stage. This is because NZEBs require a systems level design approach where all aspects are considered as an interacting whole. Decisions are made within a narrow time frame before the solidification of the final design. Consideration later in the decision process represents a missed opportunity to optimize building performance. An integrated design process involving architects, engineers and trades is recommended (Yudelson, 2008). Collaborative design is a departure from the traditional staged design process, where early designs are passed from architects to engineers for HVAC sizing, back to architects to finalize the design and then to trades for construction. Collaboration between disciplines en-

sures that energy-saving opportunities from the early design stage are incorporated and realized in the final commissioned design. Simulation tools aid decision-makers in identifying cost-optimal opportunities to balance energy efficiency and conservation measures against renewable energy generation.

Building Performance Simulation (BPS) is a powerful means to inexpensively evaluate the potential energy, cost and environmental performance of new and existing buildings. The power to predict the performance of a design before construction can be highly influential since design-stage decisions typically commit 80-90% of a building's life-cycle operational energy demand (Ramesh et al., 2010; UNEP-SBCI, 2007). A software model can simulate future energy consumption under various design strategies and variations. Models can follow bottom-up approaches, such as physics based models, or top-down approaches, such those built from existing building monitored data. Balcomb (1992) categorizes BPS tools as either guidance or evaluation tools. As of 2013, BPS tools are primarily used to evaluate a specific performance indicator. Repeated simulation is required by the user to identify designs which meet or exceed the desired performance outcome. This trade-off analysis becomes particularly cumbersome when conflicting performance objectives are considered such as cost and energy savings. Of particular interest in this thesis are techniques and methodologies which guide users, by summarizing all potentially desirable performance outcomes using repeated model evaluations automated by software. Optimization techniques coupled with BPS is one potential approach to a more process-oriented performance simulation tool.

Optimization techniques in concert with BPS offer the following benefits: (i) identification of potential optimal designs which best achieve desired performance objectives; (ii) system level building integration by simultaneously considering performance trade-offs; and (iii) a process-oriented simulation tool that is complementary to BPS, which eliminates repetitive user-initiated model evaluations. In this thesis, optimization refers to a systematic algorithmic search of all feasible designs to achieve or exceed a desired performance indicator such as an energy consumption or a life-cycle cost target. The use of optimization techniques are a marked departure from typical building design techniques. Present building and energy codes, such as MNECB (NRC, 1997a) or ASHRAE standard 90.1 (ASHRAE, 2011b), recommend minimum building parameters. Energy

codes enforce lower limits for parameters such as ventilation requirements, wall and ceiling insulation levels. Other 'rule-of-thumb' approaches exist for influential design variables. For example, Chiras (2002) suggested typical building options for the design of a low-energy solar home. These design approaches have several disadvantages: (i) limited evidence substantiating the expected performance of each building parameter; (ii) suggested parameters are usually not specific to a site or climate in question; (iii) builders typically select parameters to minimize the initial cost of the building and focus capital on the marketing and curb appeal to maximize profit rather than minimizing life-cycle energy and cost; and (iv) lack of circumstantial guidance related to balancing conflicting performance outcomes such as energy and cost. Optimization algorithms improve information flow by identifying pathways to desired performance targets.

There is a growing need to calculate confidence levels of building performance simulation predictions. For example, a 2013 survey involving fifty optimization researchers indicated a lack of uncertainty techniques applicable to building performance simulation (Attia et al., 2013). Hopfe and Hensen (2011a) suggested several benefits of performing an uncertainty and sensitivity analysis: (i) parameter screening to reduce model complexity; (ii) analysis of model robustness and validation; (iii) quality assurance measures to identify sensitivity of specifications; and (iv) decision support analysis. In the context of this thesis, uncertainty and variational analyses are a key component to understanding interactions in a building model and quantifying confidence in performance-based results.

There are two main views on applying optimization algorithms, BPS, and uncertainty studies to building design. These views originated from the author's participation in the IEA Task 40/ECBCS Annex 52[1] sub-task B whose objective was to identify and refine design approaches and tools to support international industry adoption of NZEBs (IEA/ECBCS, 2013). The first view predicts that future performance-optimized buildings will be designed algorithmically. Proponents argue that only optimization algorithms can identify design strategies which minimize life-cycle costs, while achieving a performance criterion such as net-zero energy; other techniques such as parametric

[1]International Energy Agency joint programme Solar Heating and Cooling Task 40 and Energy Conservation in Buildings and Community Systems Annex 52: Towards Net Zero Energy Solar Buildings

simulation would require decades to identify optimal designs due to the complexity of the design problem. The opposing view is that algorithms will never design buildings since they cannot quantify æsthetic aspects or cultural/social/human implications of a building. Perhaps the truth is between these two extreme views. Optimization techniques are a tool—as with any trade, the expertise resides in the user of that tool. As this thesis will show, the capability of optimization algorithms to effectively map out the entire solution space and provide information is more far-reaching than the traditional trial and error approach (aided by experience and rules of thumb) to building design.

1.3 Scope of Thesis

This thesis focuses on the development of methods and tools which identify and synthesize useful knowledge related to pathways to net-zero energy homes. Residential buildings in Canada are sparsely occupied buildings, with relatively low Energy Use Intensity (EUI) compared to other building types (NRCan-OEE, 2009). They offer large surfaces, such as walls and roofs, for solar panel installation. Optimization algorithms are developed to balance trade-offs between energy conservation and energy generation opportunities. Cost and net-energy consumption are the primary performance objectives used in the optimization analysis. This thesis only considers grid-connected homes as they can benefit from incentives such as feed-in tariffs. Preferential treatment is given to solar energy as a renewable resource because it can be building integrated, particularly when the form of the building is optimized for this purpose. Wind energy was not considered since wind access is limited in urban environments due to city by-laws and reduced generation capacity because of lower geostrophic wind speeds relative to rural landscapes.

This thesis uses an archetype solar home which combines passive solar design, a geothermal heat pump and a building-integrated photovoltaic system to achieve NZE. This archetype solar home is based on ÉcoTerra, a monitored, pre-fabricated near NZE house located in Eastman, Québec. Further design improvements are identified using this already market-proven near NZE design.

The development and evaluation of thermal comfort metrics for NZE homes is not

presented in this thesis. This topic was recently published in a PhD thesis with collaboration of IEA Task 40/ECBCS Annex 52 (Carlucci, 2012). The development and evaluation of advanced control strategies such as model predictive controls is not presented in this thesis. For a detailed evaluation of such technology in a NZE home refer to the PhD research of Candanedo (2011). The development and evaluation of shapes beyond rectangular forms is not considered in this thesis. For an exploratory analysis of this topic refer to the PhD research of Hachem (2012). The focus of this thesis is on the systematic optimization of an archetype NZE house while considering trade-offs in energy conservation, efficiency and generation using energy and economic performance indicators.

The phrase 'pathways to net-zero energy buildings' embodies the following meanings. First and foremost it implies optimization techniques to identify performance-optimized designs. Once optimal solutions are identified, search techniques are used to identify a series of design improvements or pathways from energy-code compliant buildings to performance-optimized designs. A goal is to identify pathways from present construction approaches to energy and cost optimal building designs. The net-zero energy criterion is not a fixed destination nor a primary optimization objective. Net-zero energy is a checkpoint on the path towards performance-optimized design. Finally, the term pathways is used to imply policies or incentives to improve the cost-feasibility of net-zero energy designs and how such policies affect optimal building design approaches. Due to the requirement of additional technologies, NZEBs are associated with a cost-premium even through they have significantly lower operational costs. Policies and incentives establish pathways to cost-optimal scenarios while mitigating cost premiums of additional materials and technology costs to achieve NZE.

This thesis provides valuable information related to: (i) the development of performance-based energy codes for buildings; (ii) systematic design of cost-optimized NZE homes; (iii) systematic analysis of the impact of different design parameters on energy consumption and cost; (iv) the study of incentive measures for Net-Zero Energy Home (NZEH)s.

The techniques described could equally be applied to other performance criteria such as rating systems, life-cycle exergy and embodied energy. The proposed methodologies could be equally applied to commercial and industrial building sectors. The methods

and techniques presented are developed for building applications, however they may be applicable to other engineering disciplines where a product or design must satisfy or exceed a performance criterion.

1.4 Thesis Overview

Chapter 2 reviews components of optimization tools and provides an overview of the current state-of-the-art with regards to building simulation and optimization approaches. Based on this literature review, the research objectives of this thesis are presented at the end of chapter 2.

Chapter 3 provides background on the design concepts used in this thesis. An overview of the optimization methodology is presented in section 3.1. Section 3.2 presents a detailed description of the optimization algorithm developed. Section 3.4 and 3.5 describe details related to energy and cost fitness functions for a NZEH.

Chapter 4 shows a multi-objective design of an archetype solar home using the optimization algorithm, cost and energy model presented in the previous chapter. The archetype home is based on a near NZEH demonstration house located in Eastman, Québec and combines passive solar design, energy efficiency measures including a geothermal heat pump and a building-integrated photovoltaic system to achieve NZE consumption. A redesign case-study is performed to systematically optimize the existing near NZE design to fully balance energy generation with energy consumption. In addition, this chapter explores the integration of deterministic searches into an evolutionary algorithm. Later chapters build on the integration of deterministic searches into an evolutionary algorithm and utilize the archetype solar home proposed in this chapter.

Chapter 5 elaborates on how information obtained from previous simulations can be used to improve search convergence properties and optimization results using deterministic searches coupled with an evolutionary algorithm. This chapter builds on the success of Chapter 4 and fully integrates deterministic searches into a proposed mutual information hybrid evolutionary algorithm. This improved optimization tool is used throughout the thesis for repeated optimization runs.

Chapter 6 introduces a methodology to estimate the influence of building design

parameter variations on the performance an energy model. The previously proposed optimization tool in chapters 3 and 5 is used to build an optimization training dataset for a Monte Carlo analysis. Performing a variability analysis demonstrates that integrating optimization techniques with uncertainty and sensitivity analysis improves the robustness of simulation results and provides information on design aspects requiring quality assurance during construction phases.

Chapter 7 describes an optimization methodology to establish and compare potential policies which incentivize cost optimal net-zero energy buildings. The previously proposed multi-objective optimization algorithm builds energy-cost curves used to compare several economic incentives.

Using the incentive structures proposed in Chapter 7, Chapter 8 explores the effect of a time-of-use feed-in tariff and reductions in PV panel costs on optimal NZEH design.

Finally, Chapter 9 concludes the thesis by summarizing all contributions and potential future work. In support of the previous chapters, Appendix A describes an uncertainty and sensitivity analysis performed on the cost model. Appendix B describes the software structure and design approach used for the optimization methodology. As part of this appendix, a scalability analysis is performed to show how the proposed algorithm scales with problem size. Appendix C describes the formation of reference buildings used throughout the thesis.

Chapter 2

Literature Review

> "Begin at the beginning and go on till you come to the end: then stop."
> –*Lewis Carroll, Alice's Adventures in Wonderland*

2.1 Overview

This chapter provides background on optimization techniques applied to building research. Section 2.3 discusses common components found in previous optimization methodologies. Section 2.4 highlights the state-of-the-art in optimization research. Section 2.5 reviews influential uncertainty and sensitivity analysis relevant to the thesis. Section 2.6 presents a chronological review of relevant research. Section 2.7 summarizes and establishes linkages between the previously presented material. Finally, section 2.8 provides a detailed research plan based on the literature review.

The literature review is restricted to simulation-based optimization studies applied to building research, as specified by the research scope presented in section 1.3.

2.2 Background

There is a growing interest in application of optimization algorithms to building research. Even though the mathematical foundations of optimization were developed centuries ago and algorithmic techniques were developed over fifty years ago, optimization research applied to building design did not appear until shortly after the advent of building energy simulation software in the late 1960s. These studies were limited at the time by

computational resources. It was instead until the mid 1980s and early 1990s that computational resources became cost effective enough for more detailed research to occur. Building optimization research burgeoned in the 2000s due to portable computation. Still, recent surveys suggest optimization research applied to performance driven building design remains largely an academic research topic and is not yet widely used in industry (Attia et al., 2013).

Optimization research related to building design is evolving into more complex applications, which simultaneously consider trade-offs in energy, emissions and cost performance of building geometry, envelope heat transfer and thermal storage, daylighting, HVAC systems and control, and solar energy utilization. Focusing on design trade-offs at the early design stage, prior to solidification of certain design details, allows for energy and cost performance levels otherwise not possible using previous approaches.

2.3 Optimization Methodology Components

This section deconstructs optimization methodologies into several common components. Understanding the function of each component aids in the future development and improvement of optimization methodologies applied to building research.

The following structure was found to be common in most optimization methodologies in the literature: (i) optimization criteria using objective functions; (ii) methods for objective function evaluations; (iii) constraint handling; (iv) representation of design variables; (v) method of simulation file generation; and (vi) optimization algorithm.

Figure 2.1 describes how these components are integrated with each other.

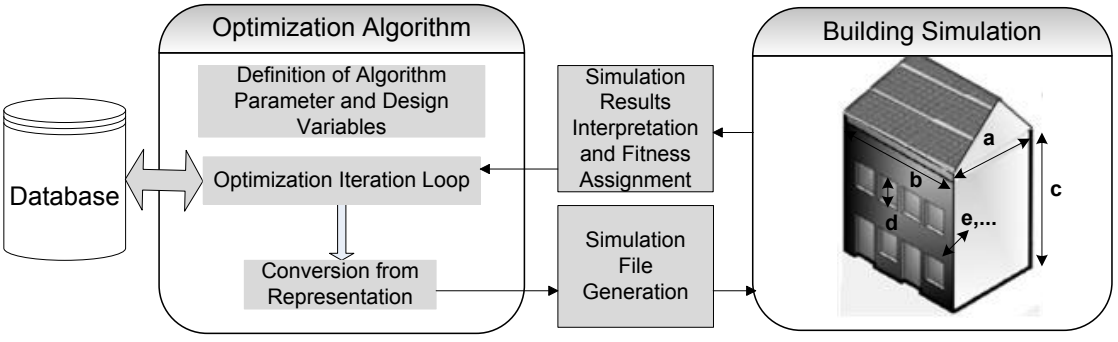

Figure 2.1: Optimization flow chart

First, design variables and their upper and lower limits are defined. Design variable

definitions represent the entire possible set of designs available to the optimization algorithm. Representations of each design are passed to software, which interprets and converts it into a simulation file; a simulation tool evaluates the performance of the representation in question. The optimization algorithm stores previous simulation objective functions and algorithm parameters in a database. The algorithm then selects the best representations, based on their fitness, to enter the next iteration. The process is repeated to find new and improved representations, which are created until a termination criteria is satisfied. Further details regarding each component is provided in the following subsections.

2.3.1 Objective Functions

The selection of objective function(s) defines the criteria of improvement for an optimization study. An objective function refers to the objective of the optimization process, e.g. minimizing cost. When the desired outcome is a minimum, the objective function is often referred to as the cost function. The terms objective function and fitness function are typically used interchangeably. The variation of fitness with respect to design variables forms a fitness landscape or a solution space.

Common objective functions in building research are: (i) energy consumption; (ii) embodied energy; (iii) life-cycle initial and operational costs; (iv) life-cycle carbon; and (v) occupant comfort. Note that comfort may also be treated as an optimization constraint. Prior to discussing each type of objective function, a distinction is made between absolute and relative objective function formulations.

Relative objective functions are calculated relative to a reference point. As such, they are not true optimization studies in the mathematical sense, but rather an improvement over baseline studies. In building design, the typical reference point is an exemplar building formed using an energy code such as ASHRAE 90.1 (ASHRAE, 2011b), MNECB (NRC, 1997a) or a design prototypical of the existing building stock. An advantage of relative objective functions evaluations is that they eliminate the need to model common features in both the reference building and proposed building. For example, in the evaluation of life-cycle cost, the modelling of land-acquisition costs can be ignored since it is the same in both the reference and proposed case. Also, in some cases, relative

objective functions can be compared across locations.

Absolute objective functions require a bottom-up formulation of the design problem. Absolute formulations allow for the identification of theoretical performance limits, i.e. 'the best of the best' within the constrained problem domain. An advantage of using absolute objective functions is that they allow for a better understanding of the design problem couplings encountered throughout the design process. A disadvantage is that they can require significantly more model detail than relative objective functions. Absolute objective functions are backwards compatible with relative objective functions. Relative objective functions can be formed by comparing the absolute objective evaluation of the reference and proposed designs.

Most previous studies have used energy as the basis to formulate an objective function. Life cycle cost and carbon measurements are also common but require additional information regarding embodied carbon of materials used and regional costs implications, for example tools see Athena Impact Estimator (2011), Ecoinvent2000 (Frischknecht, 2003) and Eco-Indicator-99 (2009). Intuitively, comfort could be used as an objective function since the comfort of each individual occupants could be improved by using additional energy and personalized controls. However, perhaps comfort is better handled as a constraint using thermal comfort standards since designs yielding uncomfortable environments are unacceptable no matter how much energy they save. In previous research, Nassif et al. (2004) addressed trade-offs between cost or energy performance indicators and occupant comfort. Examples of previous studies which include life-cycle carbon include Diakaki et al. (2010); Wang (2005); Wang et al. (2005). Examples of previous studies utilizing life-cycle costs include Hasan et al. (2008a); Peippo et al. (1999); Verbeeck (2007).

Engineering problems contain many conflicting objectives, the most evident being cost versus performance where higher costs typically allow for better performance. Although multiple objectives are simulated at the objective function stage, the handling of multiple objectives is done within the optimization algorithm. As such, the topic is discussed in greater detail in the optimization algorithm section.

Once optimization criteria have been selected, techniques and tools for objective function evaluation can be explored.

2.3.2 Methods for Objective Function Evaluations

The tools used for energy simulations must be sophisticated enough to capture dependencies between integrated systems and provide the necessary model resolution to extract essential information from the design process. Many simulation tools exist to model building energy performance, each with specialized capabilities. Literature reviews on the capabilities of building simulation tools have been presented by Crawley et al. (2008); Haltrecht et al. (1999). Validation tests for building energy simulation tools and components, a deliverable of IEA Task 34, are now maintained by National Renewable Energy Laboratory (NREL) (Judkoff and Neymark, 1995).

The majority of building simulation tools were never intended for optimization studies because they have inherent discontinuities that optimization algorithms must address in their search strategies. Discontinuities can be understood as perturbations, $\epsilon(\mathbf{x})$, which cause deviations from the real objective function, $f(\mathbf{x})$, resulting in a modified objective function, $f^*(\mathbf{x}) = f(\mathbf{x}) + \epsilon(\mathbf{x}), \text{for all } \mathbf{x} \in \mathbf{X}$, where, $\mathbf{x}$ are optimization variables. Discontinuities form in building simulation tools due to: (i) distributed numerical solvers with static convergence criteria; (ii) procedural programming styles, such as if-then-else type logic, where changes to model inputs causes different code blocks to be executed resulting in step-changes to simulation outcomes; and (iii) numerical rounding and truncation within simulation engines. There is some indication in literature that using differential equations and Differential Algebraic Equation (DAE) solvers are one possible solution to smooth out the fitness landscape (Wetter, 2004). However, the problem is still susceptible to discontinuities, unless concerted efforts are made to eliminate them. The causes and remedies of discontinuities is a theme in the early work of Wetter (Wetter, 2004, 2005; Wetter and Polak, 2004; Wetter and Wright, 2004).

The scope of optimization studies is limited to the capabilities of the simulation and design tools used. As optimization problems increase in size and complexity, there is a growing need for coupled simulation strategies or, alternatively, simplified simulation strategies. Co-simulation is discussed more in section 2.4.1.

There is a growing trend to approach building energy modelling using simplified methods as an alternative to coupled simulation strategies. For instance, Kämpf and Robinson (2007) used a simplified two-node RC thermal network based on calibration

with a detailed ESP-r model for simulation energy flow in a community of buildings. Similarly, simplified models were used by O'Brien et al. (2010) to calculate the impact of urban density on solar buildings. O'Brien et al. (2011) used parametric studies for identifying an appropriate level of modelling resolution for the design of NZEHs using two-way design parameter interactions. Diminishing returns exist in modelling efforts for thermal, electrical, plant and air-flow models for NZEHs. For example, diminishing returns in modelling effort were found in studies by Christensen et al. (2004), where plug-loads, appliances and lighting in NZE, or near-NZE residential buildings can account for as much as 60% of energy consumption. Yet, the majority of modelling effort is placed on plant, building and air flow models. Simplified models allow for equal modelling effort on all factors of importance, which better estimates the life-cycle energy and costs associated with building operations but have the disadvantage of requiring calibration and validation using measured data or models built from fundamentals. Methods to calibrate and validate building models are further discussed by Kleijnen and Sargent (2000); Reddy (2005).

The following section discusses techniques to ensure design problem constraints are satisfied.

2.3.2.1 Handling Design Constraints

Constraints enforce forbidden regions onto the objective function and consequently onto the fitness landscape. Constraints are important as they enforce design restrictions and direct the optimization away from designs that may not be of interest. In building optimization methodologies, design constraints are typically categorized into three types: (i) inequality constraints; (ii) equality constraints; or (iii) boundary or parameter constraints. Theoretically, boundary constraints are a subset of inequality constraints, but because of their ubiquity, they are typically discussed separately (Feoktistov, 2006, chap. 2.6).

Inequality constraints take the form, $\gamma_j(\mathbf{x}) \leq A, j = 1, 2, \cdots, J$, where J is the number of inequality constraints, γ is the function to be constrained and A is a constant. Methods to ensure inequality constraints include: (i) weighted penalty functions on objective functions; (ii) Lampinen's direct constraining methods; (iii) region of ac-

ceptability methods; and (iv) modifying selection operator methods (Feoktistov, 2006). Some of these methods involve trade-offs such as additional algorithm parameters or loss of information by modifying the objective function to make individuals which do not satisfy constraints less fit. In building optimization methodologies, this type of constraint can impose thermal or visual comfort constraints (Charron, 2007; Wright and Farmani, 2001), or constrain building area, volume or geometry (Kämpf, 2009). It is possible, in some instances, to enforce active constraints within the building simulation and eliminate inequality constraints. For example, thermal comfort can be ensured by sizing HVAC systems to peak loads using design days prior to simulation. Geometry constraints such as area/volume constraints can be used to eliminate geometric variables within the objective function.

Equality constraints are of the type, $\phi_k(\mathbf{x}) = B, k = 1, 2, \cdots, K$, where ϕ is referred to as the *constraining function*, K is the number of equality constraints and B is a constant. Whenever possible, equality constraints should be used to eliminate design variables from the objective function (Price et al., 2005). This method is the only way to ensure equality constraints are met and has the added advantage of shrinking the size of the solution space. An example of enforcing a constraining function would be to use a specified building area or volume to eliminate specific dimensions, such as widths, lengths or heights from design variables.

Boundary constraints are necessary for continuous design variables, such as $x_{j,L} \leq x_j \leq x_{j,U}, j = 0, 1, \cdots, D-1$, where D is the number of design variables involved in the optimization problem. Two techniques ensure values fall within specified boundaries: (i) resetting schemes, and (ii) penalty functions (Price et al., 2005). Resetting schemes push parameter values back within specified ranges if a limit is exceeded. Random processes are preferred, over resetting to the nearest limit, as they preserve diversity within the population by ensuring exceeded limits are not always reset to the same value (Price et al., 2005). Penalty functions are handled using the same methods as described for inequality constraints. An alternative method would be to modify selection operators depending on how far a value exceeds variable limits (Coello Coello, 2002). To ensure the proper functioning of constraint operations, various testing functions and methods have been developed (Michalewicz and Schoenauer, 1996).

2.3.3 Representation of Design Variables

Design variables within building simulation can be discrete, continuous or mixed representations. The selection of design variable type and step-sizes determines the size of the search space and partially determines the set of applicable optimization algorithms. *Representations*, or the design variable set as operated on by the optimization algorithm, can simply be a vector list of a specific design variable set, forming a *phenotype*, or be codified into a *genotype*. Gray-coded binary representations are typically used to represent genotypes (Eiben and Smith, 2003). A good analogy for identifying the difference between phenotypes and genotypes is that phenotypes represent the physical design one is trying to optimize; genotypes are abstractions which are translated into phenotypic space.

Both representations have advantages and disadvantages. An advantage of binary genotypic representations is that they allow for simplified and reusable algorithm operations across different problem domains. Also, operations on binary representations allow for information sharing across variable couplings (Eiben and Smith, 2003). A disadvantage of binary genotypes is that each design variable must be take on step-sizes of 2^N, where N is the number of bits assigned to each design variable, unless redundancies in step-sizes are allowed. For example, a variable is restricted to step-sizes of 2, 4, 8, 16, 32, and so on. This results in a statistical bias and complicates deterministic searches. Thus, where simplicity is gained in algorithm operations, flexibility of parameter ranges is lost. Phenotypic representations allow for flexible design variable step-sizes, but cause added complications when continuous variables exceed specified boundaries, as discussed in section 2.3.2.1. Once design variables and representations have been selected, conversion is required to a format which can be interpreted by the building simulation engine or custom software used for fitness evaluations.

The choice of representation limits one's choice of optimization algorithm. Although modifications can be made to almost any optimization algorithm to allow for continuous and discrete type design variables, other more suitable algorithms likely exist.

2.3.4 Simulation File Generation

The generation of building simulation input files for the purpose of optimization studies is a formidable task. The specification of design variable sets defines a design space. The simulation file generator must ensure that all combinations of design variations are translated into simulation files properly. Evaluations of objective functions aid in the process as they can identify errors that terminate the simulation process. Methods to identify bugs that affect results, but do not terminate the simulation process, are limited due to the sheer amount of design variations and complex configuration of systems in simulation models. Further research is needed, such as comparing objective function evaluations for the same representation using different simulation tools to detect discrepancies in the simulation process.

There is a lack of monolithic building simulation tools to simulate all building processes in an integrated manner and allow timestep energy flows between thermal, electrical, lighting and mechanical domains. Since redeveloping a tool would require a Herculean effort, tool designers prefer to couple existing tools with complimentary capabilities at run-time. Depending on the methods used, this may require additional effort in the creation of simulation configuration files for each engine. Automated methods in creating building simulation files can greatly simplify this process.

Typically, building simulation engines are used for objective function evaluations. Most of these are engines driven by structured text files. Any of the following methods can be used to generate the dynamic content required for optimization studies:

1. Templating systems using: direct variable substitutions, and programming constructs within the simulation file

2. Markup languages

3. Programming languages

Templating of simulation files is the most user-friendly way of generating text files to be used by building simulation engines. The simplest example of templating methods are direct substitutions of design variables into the simulation file. This is the primary method of substitution used by LBNL's Generic Optimizer Tool (GenOpt) (Wetter,

2011a). Additional functionality is made possible in GenOpt through the use of simple math functions in direct substitutions (Wetter, 2011b).

Added complexity can be achieved through templating by using if-then-else statements, loops and other programming logic directly in the simulation file. A good example of this technique can be found in the Building Energy Optimizer (BEOpt) (Anderson et al., 2006; Christensen et al., 2004). Figure 2.2 demonstrates the ability of the BEOpt macro language to make non-trivial substitutions of window materials and constructions in four facade orientations directly in an EnergyPlus Input Description File (IDF). Some programming constructs include: (i) direct variable substitutions (using the '@' variable construct), used to create EnergyPlus construction objects; (ii) looping over each defined facade (where @Facade∈[1,2,3,4]); and (iii) unit conversions (from Btu/(h $\cdot$ ft^2F) to W/m^2K).

```
$- START BEOpt macro language inside an EnergyPlus IDF file (Snippet)
Loop @Facade from 1 to 4                                    $- Point (i,ii)
   WindowMaterial:SimpleGlazingSystem,
      @FacadeDir[@Facade]_Win,                              $- Name (i)
      @WindowUvalue[@Facade]*@Btu_hft2F2W_m2K,              $- U-Factor {W/m2-K}, Point (i,iii)
      @WindowSHGC[@Facade]*@HeatingShadeMultiplier;         $- Solar Heat Gain Coefficient (iii)
   Construction,
      @FacadeDir[@Facade]_Glass,                            $- Name (i)
      @FacadeDir[@Facade]_Win;                              $- Outside Layer (i)
EndLoop
$- END BEOpt macro language inside an EnergyPlus IDF file
```

Figure 2.2: Example of templating substitutions using the BEOpt macro language in an EnergyPlus IDF file (Anderson et al., 2006; Christensen et al., 2004)

Advantages of templating methods are that they preserve readability of the simulation file and can handle the majority of dynamic content required by simulation engines. Disadvantages include: (i) customization is required for each simulation engine encountered; (ii) a separate substitution engine/language is required that may not be open to development; and (iii) conditional statements are required for every case-based substitution. This can cause scaling issues for larger, more detailed optimization problems.

Mark-up languages, such as Extensible Markup Language (XML), solve some scaling issues by allowing for one-to-many substitutions (W3C Consortium, 2011). For example, specifying a window-to-wall ratio can be translated directly into sets of window vertices using XML Stylesheet Language Transformations (XSLT) (W3C Consortium, 2011). Opt-E-Plus is an early-stage commercial building optimization tool which uses XML to translate design variables into EnergyPlus IDF files (NREL, 2011). An advantage of mark-up languages is that they allow developers to specify only the necessary information

to generate a simulation file. A disadvantage is the need for a specification of stylesheet transformations into each simulation engine format. Programming languages may also be used to complete XML transformations that are intractable using XSLT, but an additional XML parser is required.

For added flexibility, programming languages can be used directly for simulation file generation. Although many languages exist, developers typically favour higher-level languages such as Matlab (MathWorks, 2011), Python (van Rossum, 2011), Ruby (Matsumoto, 2013) or Perl (Page, 2012). Abstractions available in most languages allow for code reuse between any simulation file format which facilitates future application using other simulation tools. A trade-off is that techniques may be difficult to interpret for users unfamiliar with the particular programming language. Combinations of these methods can also be used with templating methods to simplify the substitution process.

2.3.5 Optimization Algorithms

An important concept when selecting an optimization algorithm is the "No Free Lunch" theory of Wolpert and Macready (1997). This theory states that all optimization algorithms perform the same, on average, over a large sample of test functions, even random walks, unless expert information regarding the fitness landscape is utilized. Restated, this theory implies that if an approach consistently outperforms other algorithms, it must be due to the algorithm adaptively selecting search strategies based on information gained regarding landscape features of the solution space. The process of selecting an optimization algorithm will have inherent search advantages and disadvantages. If expert information about the design problem is being used to improve convergence speed and resolution of the algorithm, such improvements may not apply to other optimization problems where specialized information no longer applies. Thus, rather than citing performance comparisons found in previous studies, this section focuses on evaluating inherent challenges found in building optimization problems and how each algorithm handles such challenges.

In order for an optimization algorithm to be considered robust in solving building optimization problems, the following problems must be addressed: (i) navigation of large solution spaces; (ii) multi-modal fitness landscapes; (iii) flexible step-sizes in design

variables; and (iv) non-differentiability of the fitness landscape (Price et al., 2005).

Building optimization problems tend to have large solution spaces as they typically require simultaneous design of thermal, electrical, mechanical and visual domains to reach performance targets. Some optimization algorithms are better adapted to smaller solution spaces, whereas others can handle the extreme limit of solvable engineering problems (Luke, 2009). Building design typically falls somewhere in between these two extremes.

Multi-modal problems have fitness landscapes with many peaks and valleys. If an algorithm is not designed or configured properly, optimizations can prematurely converge to non-optimal solutions. Typically, this problem is solved by using individual search strategies with multiple starts, or by using population-based search methods where enough members exist to properly search the design space.

In whole-building optimization studies, often a mix of discrete and continuous parameters are required to properly account for building facade design, HVAC system selection, operation and control. For example, discrete variables such as boolean-based control strategies (ON/OFF) are considered simultaneously with continuous variables such as envelope insulations thickness. These problems are particularly challenging because they involve the design of several highly coupled sub-systems over a very large possible solution space. Deciding on incremental step sizes of design variables can be challenging. Some algorithms have the added advantage of being able to intensify searches around continuous design variables which may yield large improvements in algorithm convergence.

Discontinuities found in most publicly available building simulation tools preclude the use of gradient-based search methods. Although gradient or derivative based optimization techniques are typically faster than non-gradient based algorithms, they require smooth, differentiable fitness landscapes, see Wetter (2004, 2005).

The following algorithm types have been selected for review because they solve, or nearly solve, issues related to navigation of large solution spaces, multi-modal fitness landscapes, flexible step-sizes in design variables and non-differentiability of the fitness landscapes. Two groups of non-gradient search algorithms are identified: (i) local direct searches algorithms which make incremental improvements to a single representation,

and (ii) population-based search algorithms which improve several designs simultaneously. A review of other optimization algorithms can be found in Kicinger et al. (2005); Zang et al. (2010).

The first group of searches relies on incremental improvements to a single representation in order to deterministically arrive at optimal landscapes. They are typically more appropriate for smaller optimization problems with less than 10^{10} possible solutions. An advantage of this group of search algorithms is that in addition to the optimal solution, all intermediate solutions are identified. Since these are local searches, they are not appropriate for multi-modal fitness landscapes. However, initiating searches from several random locations greatly improves the odds of convergence. The meshing of design variable solves the aforementioned non-differentiability and step-size issues.

The *Hooke-Jeeves* (HJ) search (Hooke and Jeeves, 1961), a member of the general pattern search family (Audet and Dennis, 2002), explores defined step-sizes in each design variable coordinate. The algorithm selects the design variable whose step-size best improves fitness and in the next iteration, attempts the same improvement to better the design's fitness. If fitness is not improved, then the process is repeated to find the best step-size improvement in other variable coordinates. When no further improvements are made, the step-size is decreased, as previous step-sizes are assumed to be too large. Decreasing step-sizes requires the algorithm to be constantly converging which is undesirable for multi-modal problem. This disadvantage can be overcome by combining the HJ algorithm with other global searches; this has become a popular algorithm strategy for building design (Holst, 2003; Peippo et al., 1999; Wetter and Polak, 2004; Wetter and Wright, 2003). A similar, yet less robust searching technique is the Nelder and Mead direct search (Nelder and Mead, 1965). Al-Homoud (2005) used this algorithm for a building optimization problem.

Sequential Searches are similar to the HJ algorithm. Rather than using patterns and flexible step-sizes, this approach uses discrete variable representations and identifies the largest incremental improvement to a single design variable at each iteration (Christensen et al., 2004; Vieira et al., 1998). Several modifications can make this type of search suitable for some smaller building optimization problems (Horowitz et al., 2008). In a previous case study, Tuhus-Dubrow and Krarti (2009) found the sequential searches

outperformed a genetic algorithm and particle swarm for smaller problem sizes.

The first algorithm selected for discussion from the group of population-based algorithms is the *Genetic Algorithm*, from the evolutionary algorithm (EA) family. GAs have become popular due to their ease of implementation, ability to navigate discontinuous and large fitness landscapes, and their population-based design to solve highly multi-modal problems. Members of the EA family have been described as being "adaptive systems having a 'basic instinct' to increase the average and maximum fitness of a population", see Eiben and Rudolph (1999). In typical implementations, design variables are defined in binary or discrete format, so additional user knowledge is required for the algorithm to converge on global optima as exact locations, as the requisite mesh sizes to land on optimal solutions are unknown. Although this algorithm does not solve the 'step-size problem', the existence of step-sizes greatly reduces the design space to be searched, which yields faster convergence to regions of global optima. Genetic algorithms are perhaps one of the best studied metaheuristic algorithms in the field of artificial intelligence. Many modifications exist combining the best elements of other search strategies from the evolutionary algorithm family (Luke, 2009; Poli et al., 2008; Weise, 2009). Literature commonly refers to a modified GA by their more general family name to avoid confusion. Studies of genetic algorithms applied to building design are numerous. For example, see Caldas (2001, 2008); Charron (2007); Coley and Schukat (2002); Magnier and Haghighat (2010); Ooka and Komamura (2009); Ouarghi and Krarti (2006); Tuhus-Dubrow and Krarti (2010); Wang et al. (2006); Wright and Alajmi (2005); Wright and Loosemore (2001).

Differential Evolution (DE), another member of the EA family, solves the step-size problem by allowing for mixed-value representations. Feoktistov (2006) suggests that the secret to differential evolution is: "the intelligent use of differences between individuals realized in a simple and fast linear operator, so-called differentiation." Vector differences in DE act as pseudo-gradients, allowing for the exploration of discontinuous and large fitness landscapes. An added feature of DE is that the entire algorithm can be controlled in a very flexible manner using only three algorithm parameters (Price et al., 2005; Storn and Price, 1995). Kämpf et al. (2010) compared a hybrid HJ particle swarm algorithm (HJ/PSO) to a hybrid DE algorithm (CMA-ES/HDE) and found that CMA-ES/HDE

outperformed the HJ/PSO for problems with more complex objective functions, but the HJ/PSO was the better choice for simple objective functions. DE algorithms have been shown to be capable in building simulation problems at the community scale, see Kämpf (2009); Kämpf and Robinson (2010).

Particle Swarm Optimization (PSO) (Kennedy et al., 2001), is fundamentally different from evolutionary cycles found in EAs. Instead of forming a new population of individuals each iteration, the existing population is allowed to gravitate towards other, more fit individuals, or *particles*, in the population. This attraction effect is a form of directed mutation also found in DE. Particles are updated using a balance of best known local and global positions of particles in the swarm. Representations are vectors of continuous design variables, although binary and discrete representations can also be used (Kennedy and Eberhart, 1997). PSO algorithms compare favourably with other optimization algorithms; for example, Elbeltagi et al. (2005) compared five evolutionary based algorithms, albeit for structural optimization problems, and found that a PSO outperformed the other algorithms for a discrete design problem with regards to reproducibility of optimal solutions and scalability with increasing problem sizes. Applications to building design can be found in Hasan et al. (2008b); Reddy and Kumar (2007); Wetter and Wright (2004).

More recently, algorithm developers are adopting global searches to find near optimal landscapes and utilizing more specialized local searches to improve overall convergence. There is no guarantee that global optimization algorithms result in absolute optima due to their probabilistic behaviour. Combinations of optimization algorithms are referred to as *memetic algorithms* (Luke, 2009; Weise, 2009). Although hybridization can occur at many different levels (Feoktistov, 2006, chap. 9), memetic algorithms most commonly refer to a global search combined with a localized hill-climbing search.

Previous research has found that global optimum landscapes in building design are relatively flat and include a large possible set of near optimal solutions. For example, passive solar building design landscapes are typically quite flat near global optima, meaning that many variations of near optimal buildings exist; Balcomb (1992) stated to this effect twenty years ago [emphasis added]:

"The economic trade-off between more insulation and more solar gains leads

to an easily derived optimum design solution that depends on climate. *However, the curve is fairly flat, near-optimum performance can be realized over a reasonably wide range of design choices.* But in all cases, good insulation practices and low infiltration are essential. If this is not done, the required solar area will be too large, thermal mass requirements for adequate heat storage will be too great, and control will be difficult."

More recently, this has been echoed by more modern optimization methodologies. Because the optimal solution space is flat, near-optimal solutions are equally interesting as globally optimal solutions (Christensen et al., 2004). This characteristic of building simulation problems could partially explain the growing trend of using hybrid optimization algorithms to first find global areas of interest, and intensify search resolution locally (Bucking et al., 2010; Kämpf, 2009; Kämpf et al., 2010; Wetter, 2011b).

Some optimization algorithms cater well to multiple conflicting objectives. The most applicable method for handling multiple objectives depends on the optimization algorithm. Summaries can be found in Deb (2001) and Coello Coello (1999) for GA, in Chakraborty (2008) for DE, Kazuhiro et al. (2008); Parsopoulos and Vrahatis (2002) for PSO, and Zitzler et al. (2000) for a comparison of approaches using EAs.

2.3.6 Database

Building performance simulations are computationally expensive and objective function evaluations are typically deterministic. This means that an objective function evaluation on a specific variable set will result in the same outcome, unless probabilistic models are used. Storing previous simulations in a centralized database eliminates re-evaluating previously simulated individuals, which occurs repeatedly in some population based algorithms. From the perspective of information theory (Cover and Tomas, 2006), each model evaluation is a hypothesis test of a design with constantly improving performance. The data-mining of previously stored simulation data can improve the convergence properties of optimization algorithms. However, data-mining requires a database.

Storage of information should not just be reserved for objective functions. For example, peak heating/cooling loads, monthly energy consumption, energy consumption breakdowns are also valuable to store in a database. Furthermore, much can be learned

by storing dynamic algorithm parameters and the historical population of designs that an optimization algorithm has navigated through. Landscapes that provide particular difficulties are of interest, as navigational strategies can be reused in future search applications and investigated to gain a better understanding of the design problem.

In literature, databases are provided using text files (Wetter, 2011a), or using SQL databases (Bucking et al., 2011). Largely, the process of data storage is often not included in previous research. As optimization algorithms increasingly make use of multi-core and distributed computing for simulation purposes, the need for databases that allow for concurrent data access over distributed computers will become necessary.

2.4 State-of-the-Art in Building Optimization Research

This section reviews the present state-of-the-art in building optimization tools, advances in optimization algorithm development and research targeted to the optimization of building models.

Optimization techniques applied to building research are rapidly evolving in several areas. These include: (i) building simulation tools for performance evaluations; (ii) the development of optimization algorithms used for searching optimal designs; and (iii) user interfaces and visualization techniques.

2.4.1 Advances in Building Performance Simulation

This section reviews active research to improve building simulation approaches. Because most optimization tools use building simulation to evaluate building performance, improvements to a building simulation tool directly improve optimization results.

This section describes: (i) differences between compliance, benchmark and performance models in building simulation; (ii) limitations of present BPS tools; (iii) active research to resolve these limitations; and (iv) methods to validate BPS results.

Models in building simulation can be categorized as: (i) compliance models, (ii) benchmark models, and (iii) performance models. Compliance modelling ensures that a proposed design meets specifications or standards. For example, compliance modelling can show that a building, as designed, meets ventilation requirements set forth in ASHRAE

standard 62 (ASHRAE, 2011a). Compliance models often involve comparisons to standardized reference building models. Benchmark models compare the proposed design to the existing building stock using standardized occupant usage and occupancy. An example is the U.S. Environmental Protection Agency's EnergyStar benchmarking program (EPA, 2012) which is based on EUI. BPS assists modellers in making decisions to improve building performance. The remainder of this section refers to BPS.

There is a growing consensus that building simulation tools will further the interaction of physical domains (Hensen and Lamberts, 2011), such as: (i) HVAC systems; (ii) daylighting availability calculations; (iii) electrical systems; (iv) thermodynamics of radiant, conductive and convective heat exchanges; (v) occupant behaviour and comfort; (vi) integration of renewable energy generation; (vii) properties of passive and active building materials (ex. concrete, phase change materials); and (viii) integrative and predicative control strategies and building automation to further link the above domains. At this time, it is believed that no single tool is capable of modelling all of the above domains with an appropriate level of model complexity (Hensen and Lamberts, 2011). For example, there is an absence of monolithic tools which share the best attributes of daylighting tools, such as dynamic daylighting metrics used in Radiance (LBNL, 2011), robust finite-difference methods found in thermal analysis tools such as ESP-r (Clarke, 2001; ESP-r, 2011), and modular-based HVAC/solar system modelling such as TRNSYS (Klein et al., 1976). Two attempts to resolve this problem are presently being researched: (i) time-step coupling of existing monolithic tools, and (ii) development of modular approaches with appropriate levels of model resolution.

Development of coupling between simulation suites with complimentary capabilities is an important on-going research topic. Examples of previous research include: (i) timestep daylight coupling in Radiance-ESP-r (Janak, 1997); (ii) timestep daylight coupling in Radiance-EnergyPlus via OpenStudio (NREL, 2013); (iii) plant and building coupling in TRNSYS-ESP-r (Beausoleil-Morrison et al., 2013, 2011; Wang and Beausoleil-Morrison, 2009); and (iv) multi-tool coupling found in the building controls virtual test bed (Wetter, 2010; Wetter and Haves, 2008). The most prevalent coupling strategies opt for one-way communication between simulation engines, such as the ping-pong method (Clarke, 2001) to simplify possible convergence issues. However, if results

are codependent between linked simulation engines (i.e., inputs of one engine depend on outputs of another and vice-versa) unidirectional solvers may have inaccuracies (Wetter, 2010). For more information, refer to Trčka et al. (2010) for a detailed literature review on building co-simulation strategies.

Modular approaches allow for more intuitive methods of linking building subsystems. It has been argued that the future of building simulation models will involve modular approaches that allow for higher levels of abstraction in the formulation of all building subsystems which more closely match their physical counterparts (Hensen and Lamberts, 2011, chap. 17). To some extent, this can be achieved using equation-centric approaches such as those found in SPARK (Buhl et al., 1993), IDA (Sahlin and Bring, 1991) and Modelica (Fritzson and Engelson, 1998). Modelling of modular components need not be limited to equation-based models and centralized solvers. Mixed-models using distributed solvers can be used to a similar effect but additional care is required to ensure convergence, by using flexible convergence criteria (Wetter, 2004, 2005).

Validating a building model used within an optimization methodology can increase the confidence of optimization results. Two methods to validate models used in optimization tools are: (i) model calibration to monitored data, and (ii) simulation engine validation. Calibration of a model to a monitored building with similar performance and technologies ensures that the ratios of energy used for heating, cooling, plug-loads and lighting are comparable. This approach assumes that variations of model inputs are also validated. The other method is to use a validated simulation engine. Beausoleil-Morrison et al. (2009) suggested that validation is best performed on a component-by-component basis in the simulation engine as opposed to a whole model due to the complexity involved in a typical building simulation tool. Judkoff and Neymark (1995) proposed is the BESTEST method to validate BPS tools. The BESTEST approach validates the simulation engine, rather than the model, by comparing simulation results for several simplified building types. For better validations, both techniques can be used. Perhaps a more sophisticated validation method can look to other dynamic methods of validation, such as validating interactions and coupling strengths within the dynamic model using a different simulation engine as a reference point. Regardless, the validation of building models used within an optimization methodology requires further research.

The number of methods to simulate building dynamics are continuously growing. It is hypothesized that the discussion of which building modelling approach is best will become increasingly irrelevant. Each modelling approach will have scenarios that best fit its formulations. Furthermore, once it has been identified why some approaches are superior to others, improvements can be made to inferior approaches. More important is the non-biased and objective dissemination of knowledge regarding the complexity of integrative building modelling and methods to encapsulate such complexities.

2.4.2 Improvements to Optimization Algorithms

The optimization algorithm is the engine of any optimization tool. Working from the problem definition and user defined boundary conditions, the role of the optimization algorithm is to identify one, or many, designs that meet specified performance criteria. It is important that designers of optimization tools understand not only how to select appropriate search strategies, but also to understand how the algorithm works, how search strategies compare to other approaches and how they can be improved to better meet the goals of the optimization tool.

The following aspects have been identified to greatly improve search performance: (i) improving optimization algorithm performance; and (ii) expediting the optimization process.

2.4.2.1 Improving Optimization Algorithm Performance

Tuning of algorithm parameters can dramatically improve an algorithm's convergence speed and ability to repeatedly identify optimal landscapes (Eiben and Smith, 2003). In previous building optimization research, Wright and Alajmi (2005) realized that genetic algorithms could be calibrated to use much smaller population sizes than typically found in literature at the time. In fact, selection of the best set of control parameter combinations is, in itself, a multi-objective optimization problem, where convergence speed and convergence reliability are conflicting objectives. In population-based algorithms, population diversity acts as a strong indicator of instantaneous algorithm performance over any generation or feed-back iteration. Despite its importance, monitoring and control of algorithm performance is rarely discussed in literature related to building optimization.

To understand how an algorithm can be controlled, some background information on complex systems is required.

Search algorithms based on pseudo-evolution or swarms are, in effect, complex systems; depending on their calibration they can show deterministic or chaotic tendencies. Complex systems are often referred to as being 'on the edge of chaos', meaning that evolution found in evolutionary algorithms occurs when parameters are tuned in such a way that the system's behaviour falls in between deterministic and chaotic regimes (Langton, 1990). Modifications to algorithm parameters can lead to more deterministic or chaotic behaviour. But it is now commonly believed that evolutionary behaviour is maximized 'at the edge' of chaotic behaviour, that is just prior to the algorithm behaviour becoming fully chaotic (Langton, 1990). Algorithms that lean more towards chaotic tendencies improve the exploratory, or global search, nature of the algorithm. Deterministic algorithms tend to act more similar to local searches, or exploitative searches, where the search process is intensified over a local landscape. To better understand transitions between deterministic, complex and chaotic modes found in optimization algorithms, it is useful to approach the topic from cellular automata.

Wolfram (1984) suggested that complex systems can be reduced to simple, deterministic structures, called cellular automata, where the future state depends on modification of a previous state, using a simple set of modification rules. Four classes of cellular automata exist: (i) type 1, static systems, where patterns reach a steady state; (ii) type 2, periodic systems, where periodic patterns emerge; (iii) type 3, chaotic systems, where only random patterns are observed; and (iv) type 4, complex systems, where structured behaviour appears to evolve (Wolfram, 1984, 1994). Types 3 and 4 are connected and are essential to the understanding of optimization algorithms. In type 4, or chaotic systems, information in the system is overpowered by noise, called random attractors, whereas in type 3, or complex systems, induced noise is overpowered by information. The extent of inherent randomness deeply modifies the system's behaviour. In a similar way, optimization practitioners are able to control algorithm parameters such that the algorithm can exhibit behaviour from the above four Wolfram classes of cellular automata.

Transitioning between complex and chaotic modes can be useful in an optimization search. If the search is mired in a local minimum, transitioning to a chaotic regime can

randomize the representation enough to escape from the depression, similar to how a simulated annealing algorithm 'heats up' a representation and allows it to settle into more optimal regions (Davis, 1987). To monitor and establish strategies to control transitioning, a method is needed to calculate the population diversity.

Diversity is a measurement of how similar, or different, representations in a population are. This information allows algorithm designers to identify if an optimization algorithm is prematurely converging, or overly randomizing the population. Diversity measurements can be done using ad-hoc methods or calculated directly using information entropy (Cover and Tomas, 2006). Diversity calculations may include parameter by parameter comparisons for each design variable or, preferably, correlations between design variable settings. For example, in a binary evolutionary algorithm, the diversity of a population of designs at any generation can simply be calculated by comparing each bit in the representation with respect to a reference design, typically the elite design in the population, using an AND operator and normalizing the sum of the correlations by the length of the original representation length. The goal of adaptive control measures are to maintain an acceptable diversity level in the population. The definition of acceptability will vary from problem to problem. It should be noted that measuring and maintaining diversity becomes less important with larger population sizes, but this comes with the major trade-off of an increased number of fitness evaluations.

Diversity can be used as a diagnostic tool to predict and prevent the premature collapse of a population to non-optimal landscapes. If a population is observed to collapse, a common control strategy is to increase the type 4 characteristics of the algorithm by modifying appropriate algorithm parameters. This allows for much smaller population sizes and fewer fitness evaluations per generation, which greatly reduces overall simulation time. Diversity monitoring and control allows for self-configuring optimization algorithms while improving the probability of converging to optimal, or near-optimal, fitness landscapes. Diversity measurements used for algorithm parameter control is an essential ingredient in developing good user interfaces to optimization tools that are both responsive and eliminate the need for users to reconfigure algorithm parameters.

2.4.2.2 Expediting the Optimization Process

There is a preconception in building research that an optimization study requires significant computational resources. This is becoming increasingly false, not only because of increasingly more powerful computers, but also due to better algorithm design strategies and techniques to expedite fitness evaluations. Several strategies have emerged to expedite computational aspects of the optimization process. They include: (i) faster objective function calculations; (ii) parallel computations; (iii) data-mining of previously evaluated designs; and (iv) approximation of fitness evaluations.

Often hundreds or thousands of objective function evaluations are required to find global optima. Reducing time required for fitness evaluations can yield moderate improvements in overall convergence time. In building simulation, researchers have primarily focused on reducing convergence tolerances of solvers and choosing appropriate time steps (Christensen et al., 2004; NREL, 2011). In addition to being CPU intensive, building simulation tools are memory intensive as well. As such, only the essential simulation information is written to disk at the largest possible time step. In addition, solid state drives can represent significant speed gains and mitigate disk-writing bottlenecks. Speed, unfortunately, has not been a primary development objective of present building simulation tools. Likely, opportunities exist for those with software development backgrounds to modify and streamline available source code. For example, the EnergyPlus team reduced simulation time by 40% from version 6 to version 7 (DOE, 2011a). Although it may be tempting to reduce the number of days in the simulation, this is not recommended since most buildings are primarily driven by temperature differentials which depend on typical meteorological conditions (ASHRAE, 2002). Some building energy simulation tools such as Trane Trace utilize shortened simulation periods for energy consumption estimates but do not recommend such approximations for detailed engineering calculations (Trane, 2013).

Population-based optimization algorithms are "embarrassingly parallel" problems. Objective evaluations can be executed in parallel since each individual evaluation is independent of other evaluations (Andre and Koza, 1998). Since most building simulation problems are computationally intense, this strategy alone can yield an improvement proportional to the number of parallel simulations. Strategies might involve local threading

on multi-core processors and graphic processing units and/or distributed computing on dedicated desktops, servers, and clusters, see studies from Kämpf (2009); Kämpf et al. (2010); NREL (2011). Population-based methods allow for individuals to survive from generation to generation. Unnecessary objective evaluations can be avoided by storing previously known outcomes.

Computational strategies to improve convergence efficacy are synergistic, meaning that the impact of combinations of strategies are greater than the sum of improvements of each particular strategy. For best results, a mix of approaches is preferred.

Previous research has indicated the possibility of training simplified methods such as neural networks or regression analyses to calculate approximate objective function evaluations, see Magnier and Haghighat (2010); Ouarghi and Krarti (2006). An advantage of this method is that once models are trained from a reduced set of building simulation, all future objective evaluations can be reduced to milliseconds with only a 5% loss of simulation accuracy (Magnier and Haghighat, 2010). This removes constraints to population sizes found in previous methods. Moreover, if the building simulation is prohibitively long, optimization might not be an option using traditional methods, but possible through trained network methods. Disadvantages are that: (i) training of simplified methods can be prohibitively long; (ii) some important aspects of the fitness landscape may not be sampled during simplified model training which might mask important interactions or linkages between design variables; (iii) training is required for every optimization study, whereas other speed improvements can be applied directly to other applications; (iv) trained data may not model near optimal landscapes; (v) training of simplified methods risks statistical over-fitting; and (vi) some building simulation software already suffers from a loss of modelling accuracy due to numerical discontinuities, thus training of simplified models might lead to further discrepancies. Further research on using trained simplified models, such as neural networks or ensemble tree methods, to approximate building simulations is required.

2.4.3 Advances in the Design of Interfaces for Optimization Tools

The last critical aspect is improving how users interact with optimization tools. This section describes: (i) how optimization tools are deployed, (ii) tool integration using

common file formats, and (iii) applicable visualization techniques.

The first aspect of any interface is how it is deployed. Presently, user interface designers can select from the present deployment options: (i) operating system (OS) dependent; (ii) OS independent; and (iii) web-based, or cloud-based deployment.

OS dependent deployments are the most common type of present building optimization tool deployment. OS dependent optimization tools are developed for a specified OS. An advantage of this approach is a relatively quick deployment time to industry due to well established packaging systems. However, repeated downloads to update existing software to include new features are required and reproducing software defects can be difficult as they depend on combinations of local software. OS independent deployments enhance the user base by catering to all popular operating systems. Open source tools, that is tools where source code is made available for further development, can broaden the application of the tool since distributed developers can expand the tools application areas. Examples of OS dependent tools include the BEOpt tool (Christensen et al., 2004) and EnergyGaugePro (Vieira et al., 1998). The GenOpt optimization tool is an example of an open-source tool which can be further developed (Wetter, 2011b).

Web-based interfaces rely on browsers to access software. Cloud-based approaches do not require browser and can interface using a variety of technologies such as smartphones and tablets in addition to desktops and laptops. Sometimes this approach is referred to as software as a service. Centralized systems allow for reduced initial prices due to economies of scale, portability, transfer of computationally expensive components to dedicated servers, quick implementation of new features and reuse of previous simulation data. Disadvantages of centralized service is that the tool cannot be open-sourced to allow for distributed development and possible privacy issues regarding specific building details. An example of a web-based design and optimization tool is the Massachusetts Institute of Technology Design Advisor (MIT-DA) (Glicksman et al., 2011). The MIT-DA was originally created for the design of building facades, but has since been expanded to include daylighting design, ventilation design, comfort analysis and scenario optimization using simulated annealing algorithms (Lehar, 2005).

An ongoing objective in applied building modelling is to integrate all aspects of building design into a common file format. Presently, members of industry and research are

forced to work with separate files for architectural computer aided drafting (CAD), life-cycle, environmental impact and energy performance models. Changes to one file, even minor, can require time expensive changes to all other files required during the design process. Augenbroe et al. (2004) and more recently Wetter (Hensen and Lamberts, 2011, chap. 17) commented on the need for more fundamental research in mapping between disparate models. The Berkeley Building Design Advisor (BDA) integrates CAD models and performance simulation models by synchronizing and converting to independent formats at the 'load' and 'save' levels of the program (Papamichael et al., 1999) but the method only supports one type of data exchange. Presently, the only standard to integrate all file formats conveniently into one common format under active development is the National Building Information Model Standard (NIBS, 2011).

Optimization studies require innovative methods to visualize simulation results. In the BEOpt tool, this was partly accomplished by comparing a given building to any number of scenarios or to a reference building using defined energy codes (Christensen et al., 2004). O'Brien et al. (2011) utilized one dimensional interaction diagrams to aid visualization interdependencies between conflicting design variables. Both strategies simplify the design process by providing guidance to further optimization a given performance metric. The *Design Desktop* module within the BDA tool allows for a comparison of illuminance and energy consumption in several zones as well as across several design scenarios (LBNL, 2001, pg.41-48). Integrated performance views found in ESP-r also offer a robust solution to the lack of higher resolution information required to select between competing designs (Hand, 2010, pg.131-136)

2.5 Uncertainty and Sensitivity Approaches in Building Simulation

This section describes the state-of-the-art in uncertainty and sensitivity analysis applied to performance simulation. This section provides background information for Chapter 5 and Appendix A.

Kim and Augenbroe (2013) defined several areas of uncertainty in building simulation research: (i) statistical uncertainty or uncertainty which can be estimated using historical data, for example variations in climate, exterior temperatures, solar radiation

and cloud coverage; (ii) uncertainty caused by discrepancies in the model and the as-built building; (iii) measurement errors such as thermal or optical proprieties of building materials; and (iv) statistical uncertainty where no historical data exists, for example occupant behaviour such as occupancy, utility usage, window operation and conditioning schedules. Variations are defined as discrepancies in the model and the as-built building. Causes of such variations could include: (i) early appraisal of unknown and influential model inputs, such as energy related occupant behaviour; (ii) late-stage design modifications; and (iii) modifications to a design due to unavailable or less expensive building materials.

An uncertainty analysis estimates the effect of variations in inputs collectively with regards to an output. A common technique to perform an uncertainty analysis is a Monte Carlo analysis (MCA). A MCA repeatedly samples input distributions to form representative designs, which once simulated result in an outcome distribution that approximates the effect of uncertainty in the model (Liu, 2001). The decomposition of model inputs into probability distribution functions (PDFs) allows for an examination of cumulative changes in an outcome due to variations in inputs. Sampling refers to the formation of a representative design by selecting the value of each model input using a probabilistically weighted distribution of possible values. A limitation of a MCA is that it cannot attribute the significance of individual parameter variations on model uncertainty. A sensitivity analysis is commonly used for this purpose.

A sensitivity analysis determines the importance of individual variations in model inputs with respect to a model output. A variable is sensitive if a small variation causes a disproportionately large change to an outcome. In building performance simulation, a sensitivity analysis identifies and ranks sensitive variables in a building model using a simulation objective, such as energy consumption. A variety of suitable methods exist to conduct a sensitivity analysis. Regression analyses, such as standardized regression coefficients (SRC) (Saltelli et al., 2000), attribute sensitivity coefficients to model inputs by building a regression model of uncertainty results. The Morris method (1991) determines which variations are: negligible, linear and additive, or non-linear or involve interactions with other factors. The Morris method uses two statistical quantities, the mean and standard deviation, calculated from a Morris design sampling strategy (Saltelli

et al., 2008), as sensitivity measures. These quantities are calculated by using a sampling strategy of many local sensitivities. The mean represents the overall influence of the input on the output. The standard deviation estimates the ensemble effects of input variations on the output. A variable with a small mean but large a variance indicates the influence of non-linear couplings between other variables is significant. The Sobol method (1993) attributes the variance in a model's output to its parameters and their interactions. This method calculates the first order, total order and second order sensitivities and reports confidence intervals for each factor. Other techniques such as Fourier methods, one-at-a-time methods are applicable to building energy research (Tian, 2013).

2.6 Summary of Previous Studies

The remainder of this chapter focuses on the chronological development of previous research to better understand research trends. Two areas of research are presented: (i) optimization studies, and (ii) uncertainty and sensitivity research applied to BPS.

2.6.1 Summary of Previous Optimization Studies

Although the mathematical foundations of stochastic optimization algorithms were developed over fifty years ago, most notably Monte Carlo methods developed by Bledsoe and Browning (1959); Friedberg (1958); Robbins and Monro (1951), they did not become of academic interest until the 1970s, when computers were less cost prohibitive.

Optimization methods applied to building design have been developed for over forty years. Early optimization studies compared layout and space optimization was an earlier application of optimization methods (Balachandran and Gero, 1987; Jo and Gero, 1998; Liggett, 1985; Liggett and Mitchell, 1981; Michalek et al., 2002; Mitchell et al., 1976). The primary objective in these studies was to use various optimization techniques to identify optimal configurations of building layout and planning problems. Later studies focused on multi-objective criteria.

The impact of trade-offs in building design studies has been an on-going theme in building optimization studies. Studies of trade-offs in daylighting and internal temperature swings using multi-objective Pareto approaches were carried out by Radford

and Gero (1980). D'Cruze and Radford (1987); D'Cruze et al. (1983) considered multi-criteria trade-offs in thermal loads, daylighting and cost of open planned office spaces using dynamic programming techniques.

The period roughly from 1987 to 1995 is often referred to as the 'AI winter', a play on the term 'nuclear winter' (Russell and Norvig, 2010). During this time, applications of artificial intelligence (AI) research saw a rapid reduction in funding from public and private sectors due to applied AI research not meeting target levels of market penetration. In applied building studies, it appears that the application of optimization algorithms to building design also saw a reduced interest during this period.

Peippo et al. (1999) applied a Hooke-Jeeves General Pattern Search (HJGPS) algorithm to the design of a residential building in Helsinki, Finland with renewable energy systems. It was found that a 20% energy savings was possible with only a 3% increase in cost. NZE was possible in Trapani, Italy for an increased cost of 16% in contrast to a 40% increase in Helsinki, but required a burdensome investment into PV systems. It was concluded that optimization using simple single-zone thermal models could be used to find solutions comparable to high performance buildings on the market. It was suggested that a more sophisticated algorithm be used to improve convergence to optimal solutions.

Application of multi-objective optimization allowed for a clearer visualization of convergence to optimal solutions using Pareto Fronts, or solution surfaces. Wright and Loosemore (2001) utilized a multi-objective Genetic Algorithm (GA) to identify optimum payoff characteristics between facade construction, HVAC systems, and control strategy elements of the building design problem using criteria for thermal comfort and cost. The initial population converged rapidly after only 50 generations.

Caldas (2001) utilized a multi-objective GA and a shape generation algorithm that modifies geometry directly to explore the optimization of commercial building shape with reference to building loads (heating, cooling, and lighting), operation costs, and daylighting potential using DOE-2.1E as a simulation engine (DOE, 2007). Several other optimization algorithms were explored, such as simulated annealing (SA) and tabu searches (TS), but a multi-objective GA was found to be more agreeable as it allowed architects to observe trade-offs between elite designs. The cost feasibility of complex

geometries was not considered in this study and penalties had to be used wisely to maintain structural sanity while meeting architectural objectives. It was noted that a 3D CAD interface would be essential for this tool to have commercial applications.

Wright and Farmani (2001) were the first to carry out a whole building design optimization by simultaneously varying systems, controls and fabric construction. Constraints were placed on the solution space, allowing only solutions that met thermal comfort. Building fabric parameters were limited only to thermal mass and window glazing. Simulation was performed on a single zone model only. To demonstrate the utility of the optimization methodology, it was shown through further exhaustive simulations that no valid solutions were found that met thermal comfort restrictions, even if one were to run one hundred thousand randomly generated solutions. A modification of this study was published later by Wright et al. (2002).

Wetter and Wright (2003) commented that optimization methodologies can be applied with little effort to reduce baseline commercial energy usage from 7% to 32% depending on the building location.

Holst (2003) conducted a simple study to reduce the energy usage of a small school located outside of Trondheim, Norway. By optimizing wall insulation values, window types, internal thermal mass, as well as nightly set backs, a energy reduction of 22% was possible relative to the actual design. Generic Optimizer Tool (GenOpt) (Wetter, 2011a) was used with a sequential search HJGPS algorithm using EnergyPlus (EnergyPlus, 2011) to simulation energy related objective functions.

Wetter and Wright (2003) compared a GA with a HJ pattern search. It was found that stochastic methods are effective at finding global areas of interest but were unable to find local minima, whereas sequential search techniques were effective at finding local minima but failed to find global areas of interest. It was suggested that a hybrid HJGPS and GA methodology would be highly effective in finding general areas of interest and then converging the population onto local optima. It was concluded that complimentary algorithms can be combined to improve the performance of an optimization methodology.

Couchoulas (2003) presented a tool for conceptual architectural design shape generation. A GA was used to modify a sequence of rules that were applied to generate a design shape. The tool did not modify geometry directly as with Caldas (2001).

Choudhary (2004); Choudhary et al. (2003, 2005) developed a hierarchical optimization framework for architectural applications. The method is based on analytical target cascading, a design approach where top level system design approaches cascaded down to lower levels of the modelling hierarchy (Kim et al., 2003). At the lowest level, a computationally expensive cost function, calculated using EnergyPlus, is approximated by a simplified mathematical function. At a higher system level, sequential quadratic programming is used to solve an optimization problem using smooth cost functions.

BuildOpt is a DAE-driven simulation suite (Wetter, 2004, 2005) based on smooth models developed to ensure that optimization algorithms within GenOpt (Wetter, 2011a) converge to a stationary point. A notable outcome was the utility of adaptive precision for numerical solvers. A desirable feature of the pattern search used in this study was coarse precision approximations to the cost function when far from a region of interest, with the precision progressively increased as the optimal solution landscape is approached.

Wetter and Wright (2004) concluded that a Particle Swarm Optimization (PSO) was the most likely algorithm to reach a global stationary minimum, but required considerably more time to converge than a simple GA.

A more recent application of comparative optimization with respect to NZE buildings is the BEOpt simulation tool (Christensen et al., 2004). Building Energy Optimizer is an optimization tool created by Christensen et al. (2004) which applies a sequential search algorithm to optimize residential homes for the Building America initiative (DOE, 2010). Energy savings of 100% relative to a baseline building was considered to be a NZE building, even though the standard chosen to represent the baseline design will reflect what is considered the optimal design. Construction variables such as window and wall types were modelled using DOE-2.1 for energy modelling and TRNSYS to implement solar modules (DOE, 2007; Klein et al., 1976). Beyond the initial cost savings, diminishing returns causes energy efficiency to become less cost effective than renewable energy. Electricity from PV was used to account for the remaining energy needs. More recent versions of BEOpt use EnergyPlus for building simulation (EnergyPlus, 2011).

Wright and Alajmi (2005) performed a detailed analysis regarding the robustness of a GA for solving optimization problems. They found that GAs are robust in finding

optimal solutions using a variety of population sizes.

In most optimization problems, there is considerable room for improvement by tuning optimization algorithm parameters. Wright and Alajmi (2005) repeated the optimization experiment carried out by Wetter and Wright (2004), paying special attention to GA performance. It was found that small populations (five to fifteen individuals) with high crossover rates converged the quickest. Originally, 585 simulations were needed to converge to optimal solutions. Using a smaller population and higher crossover rates, convergence occurred after 300 simulations. This GA configuration strategy was later applied to a multi-objective problem and again, rapid convergence was found.

Wang (2005) approached the building optimization problem with a more structured software engineering approach by emphasizing object-oriented design to maximize the flexibility of the optimization tool. Structured variables were used to allow variables within variables. Optimization was limited to envelope-related design variables only. A multi-objective GA was utilized to optimize life-cycle cost, and life-cycle energy/exergy, using ASHRAE Toolkit as a simulation engine (Pedersen et al., 2000).

Wang et al. (2005) applied a two-stage optimization methodology to an office building in Montreal. The goal of the first stage was to find a diverse population of Pareto solutions allowing identification of design trade-offs. The purpose of the second stage was to explore an area of interest around Pareto solutions to allow designers more flexibility in choosing a final design. This methodology allowed designers more flexibility for other trade-offs while still using near optimal designs.

Wang et al. (2006) performed a multi-objective shape generation optimization on a two dimensional polygonal floor plan using a whole-part strategy with a length-angle abstraction technique. It was found that solutions with near pentagon shapes had the lowest life-cycle cost. Solutions with lowest life-cycle exergy were a pentagon form, but had elongated edges on south and north facades.

Ouarghi and Krarti (2006) utilized a hybrid GA and artificial neural network to optimize building shape using energy and cost objectives. A Bayesian neural network was used to predict annual energy usage for any building shape by using training data as it was found to be more accurate than a feed-forward ANN model. Optimal building dimensions were found using a GA.

Charron (2007) applied a GA to simultaneously optimize HVAC and renewable energy systems, simple control strategies and building facade and geometries against a building operational and embodied costs. TRNSYS was used as a simulation engine (Klein et al., 1976) and RSMeans data was used for cost information (RSMeans, 2013). A battery of design scenarios were considered such as: (i) changes in government policy, (ii) consequences of simple control, (iii) implications of indoor finishes, and (iv) the effect of feed-in tariffs on cost-effectiveness of renewable energy systems. Charron (2007) used monetary penalties to discourage solutions with low thermal and visual comfort.

Torres and Sakamoto (2007) explored the usage of daylighting to reduce lighting loads and visual discomfort by varying facade geometries and blind action using a GA and Radiance (LBNL, 2011) for lighting simulation. It was found that optimal solutions reduced lighting loads by 75% relative to a baseline design.

Reddy and Kumar (2007) compared a PSO to the popular Non-dominated Sorting Genetic Algorithm-II (NSGA-II) algorithm (Deb et al., 2002), for three multi-objective engineering problems. The results demonstrated that a PSO is efficiently able to yield a wide spread of solutions with good coverage and convergence to Pareto-optimal fronts.

Norton and Christensen (2008) confirmed the performance of a constructed net-positive energy home designed using an optimization algorithm. The home, located in Denver, Colorado, was designed using BEOpt (Christensen et al., 2004). It was noted that 34% of energy usage originated from plug-loads and occupant energy usage behaviour was well below Building America benchmarks (DOE, 2005). Due to the NZE goal, it was found to be extremely difficult to size PV systems without user behaviour models.

Hasan et al. (2008b) utilized GenOpt's PSO algorithm (Wetter, 2011a) to optimize envelope and HVAC systems with respect to life cycle cost of a single detached home in Finland. The investigation showed that the optimized house had a reduction in space heating of 23-49% relative to a reference case based on traditional construction techniques.

Ooka and Komamura (2009) utilized a distributed GA or multi-island GA to carry out an HVAC sizing, scheduling and control optimization. The salient feature of a

multi-island GA is that the population of one generation is divided into several sub-populations, or 'islands', and genetic operations are performed on each sub-population separately. Information regarding individuals is then exchanged periodically between sub-populations, called 'migrations'. The optimization is effectively reduced to two separate optimizations with data exchange. Optimization is broken into four stages: (i) basic energy system definition, (ii) tiered optimization stages (second and third stages cannot be uncoupled due to strong dependencies), and (iii) optimal solution selection. The optimization methodology was applied to HVAC systems design of a Japanese hospital.

Caldas (2008) presented an overview regarding the present capabilities of her optimization tool, GENE_ARCH, for building shape, energy efficiency and visual comfort. Since 2001, the optimization methodology has been expanded to include electrical and mechanical installations. GENE_ARCH was applied to several exemplar building designs located world-wide to explore trade-offs between heating loads and daylighting loads using up to two objective functions.

Castro-Lacouture et al. (2009) utilized an optimization methodology to aid industry in minimizing costs associated with green building material selection for a green building rating system (USGBC, 2011). A case study building located in Columbia was used. A mixed integer approach was used to select wood carpentry and metallic finishes used in the building interior, material temporally used during construction, adhesives, paints, finishes and sealants, carpets, roofing material, glass and window assemblies. Using a multi-objective approach, the author was able to compare trade-offs between awarded points and monetary costs, although results are strongly correlated with location.

Magnier (2009) and Magnier and Haghighat (2010) utilized a custom multi-objective GA to optimize an equivalent neural net model of a commercial building. Custom algorithms outperformed the popular NSGA-II algorithm (Deb et al., 2002) for equivalent neural-network models only. It was found that neural networks are able to approximate building load simulations by $\pm 2\%$, but have difficultly predicting thermal comfort with a loss in resolution of $\pm 10\%$. Case studies were performed on the Twin-House project in Ottawa, Canada and the Grong Media school in Norway.

Kämpf (2009) explored optimization applied to community energy fluxes. The goal of the study was to optimize the layout and form of buildings to maximize solar ra-

diation while considering simple design parameters such as insulation in ceilings and walls, window types and areas, infiltration and thermal mass. ESP-r was used to calibrate a simplified two-node thermal network (Kämpf and Robinson, 2007). A hybrid differential evolution algorithm was used to find optimal combinations of the 41 design parameters (Kämpf, 2009; Kämpf and Robinson, 2010).

2.6.2 Summary of Previous Research using Uncertainty and Sensitivity Techniques in Building Simulation

This section describes previous uncertainty and sensitivity research which influenced the proposed methodology used later in this thesis. Previous research in building simulation primarily focused on uncertainty analysis to improve: (i) information for decision making; (ii) confidence in simulation results; and (iii) sensitivity and uncertainty techniques for building simulation.

Uncertainty analysis techniques can improve decision making during building design. De Wit (2001) demonstrated the potential for thermal comfort uncertainty estimation in a naturally ventilated office building. De Wit and Augenbroe (2004) showed the effect of variations in heat transfer and climate variables on thermal comfort and energy consumption to facilitate rationale design decisions under uncertainty. Hopfe et al. (2007) showed the effect of variations to physical parameters in an energy model on heating and cooling energy use in relation to unmet building loads. Heiselberg et al. (2009) identified a few influential design parameters using sensitivity techniques to optimize a building's sustainability. Breesch and Janssens (2010) estimated the performance of natural ventilation strategies using building energy simulation while considering uncertainties using a MCA with SRC. Domínguez-Muñoz et al. (2010) showed the significance of uncertainty on peak cooling load calculations under various weather and building use scenarios using a Monte Carlo analysis with SRC. They showed that peak load uncertainty was sufficiently addressed using three variables related to charging and discharging of thermal mass. Tian and de Wilde (2011) proposed a methodology to model uncertainties in building energy consumption and greenhouse gas emissions under climate change projections. A case-study showed that heating energy consumption is likely to decrease and cooling energy consumption will increase. Hu and Augenbroe (2012) used a MCA to

estimate the effect of uncertainty in the power systems of an off-grid house on thermal comfort and power reliability. Rysanek and Choudhary (2013) explored the technical and economic uncertainties of building retrofits using optimized greenhouse gas emissions and cost criteria. The study provided decision-makers information for identifying retrofit opportunities in existing buildings under various uncertainties. Wang et al. (2012) explored uncertainties in climate, physical and mechanical system parameters on the energy consumption of an office building. They found that mechanical system operations significantly influenced energy consumption. Booth and Choudhary (2013) identified a limited number of energy saving measures using uncertainty techniques to cost-effectively reduce GHG emissions and energy consumption in the UK housing stock.

Another area of research to improve simulation results was to include confidence factors along using uncertainty and sensitivity analysis. Aude et al. (2000); Borchiellini and Fürbringer (1999) utilized uncertainty and sensitivity techniques to validate energy models. Purdy and Beausoleil-Morrison (2001) calculated the sensitivity of variations to individual building model inputs to improve modelling decisions by varying each input independently using a stationary building model. Struck et al. (2006) utilized the Morris method with linear partial correlation coefficients to estimate the importance of material properties variations on annual cooling and heating loads. Hopfe et al. (2007) compared the results of four building performance simulation tools using uncertainty analysis. Corrado and Mechri (2009) used the Morris method to estimate the sensitivity and uncertainty of building energy rating systems. Spitz et al. (2012) applied a Monte Carlo uncertainty and sensitivity analysis using 139 physical parameters within an energy model. The Sobol method attributed 6 significant variables to uncertainty propagation. Hopfe and Hensen (2011a) applied a MCA and sensitivity analysis using step-wise and rank regressions to three groups of uncertain parameters: physical, design, and scenarios. Burhenne et al. (2010) analyzed uncertainty associated with model parameters of a building using a solar thermal collector for heating and domestic hot water.

Additional research has been explored to improve uncertainty analysis techniques for building simulation problems. Lomas and Eppel (1992) recommended differential sensitivity methods for sensitivity predictions in building thermal simulation programs over stochastic sensitivity approaches. Macdonald (2002) described how to embed uncertain-

ties within a simulation tool's conservation equations using a differential and factorial analysis (Macdonald and Clarke, 2007; Macdonald and Strachan, 2001). De Wit (2001); De Wit and Augenbroe (2002) used the Morris method to identify and rank which variations contributed to uncertainty in building energy model outputs. Macdonald (2009) recommended about one hundred samples for a MCA, independent of the number of model inputs, to estimate the mean and variance of the outcome distribution. O'Brien et al. (2011) extracted one-way and two-way interactions from a net-zero energy house model. Heo et al. (2011, 2012) updated PDFs using a Bayesian approach in the calibration of an energy model for energy performance contracts. Previous studies estimating the effect of uncertainty in building simulation indicated that few input parameters affect energy performance outcomes significantly (Corrado and Mechri, 2009; Déqué et al., 2000; Hopfe and Hensen, 2011b). In one study, about 100 of the 1009 input parameters of a building model had statistical significance (Eisenhower et al., 2011). Brohus et al. (2012) quantified the uncertainty of building energy consumption using stochastic differential equations and applied the method to an arbitrary number of loads and zones in a building. Burhenne et al. (2013) proposed a cost-benefit analysis using a MCA with Monte Carlo filtering to find which variables drive model uncertainty. Infiltration was identified has having the largest effect on the solar fraction of a solar thermal system. Sun et al. (2013) defined uncertainty quantification of micro-climate variables affecting building simulation results.

2.7 Summary

Optimization methodologies applied to building design allow for design-at-once approaches that facilitate understanding of potential performance opportunities. Present day computing power and progress in the design of optimization algorithms allow for complex design scenarios to be considered.

Although building optimization tool development is still in its infancy, an optimization approach has several attractive aspects, including: (i) direct user interaction with design trade-offs, such as cost, energy consumption and environmental impact throughout the building life-cycle; (ii) automation of repetitive tasks such as creation of build-

ing simulation configuration files; and (iii) performance-based comparisons of building design. Building optimization tools represent a shift in design paradigms, where the designer no longer depends on parametric runs of a limited set of local design variations, but specifies boundary conditions on the design problem itself. In this way, the tool can be used to identify combinations of design variables which most significantly determine the performance of the building.

Components of existing optimization approaches in building design were reviewed in detail as follows: (i) methods for objective evaluations; (ii) objective function definitions, (iii) constraint handling; (iv) representation of design variables; (v) methods of simulation file generation; and (vi) optimization algorithm selection.

Three specific areas of rapid development in key optimization research domains were identified that would greatly aid in the progress of industry tools. They included developments in: (i) building simulation tools for fitness evaluations, (ii) optimization algorithms used for search of optimal designs, and (iii) user interfaces and visualization techniques.

Developments in building simulation are allowing for more highly coupled performance evaluations which involve trade-offs in cost, energy consumption and environmental impact. By automating the control of optimization algorithm parameters, details regarding the challenges of algorithm design can be abstracted away from the end-user while improving convergence speed and reproducibility of optimal or near optimal building designs. Visualization techniques within an interface allow the user to better understand complex interactions with the design of a building. Web, or cloud-based interfaces allow users to interact with design tools independent of location using personal computers or hand-held devices.

2.8 Overview of Research Plan

The literature review identified the following research areas: (i) identify performance enhancements to optimization algorithms applied to building research; (ii) apply the optimization approach to the design of a near net-zero energy home using an archetype solar home; (iii) utilize optimization algorithms in variability analysis around perfor-

mance criterion; (iv) evaluate the potential for economic incentives to affect energy-cost optimal curves; and (v) evaluate the effect of incentives on performance-optimized net-zero energy home design.

Previous research applied optimization algorithms to find an optimal solution to various design problems. This thesis focuses on the information finding ability of optimization algorithms rather than only finding particular solutions. Focus will be placed on identifying pathways to performance-optimized net-zero energy buildings. An additional goal is to identify variations which cause significant performance criterion changes. Identifying optimal configurations and theoretical building performance is considered secondary to identifying new and innovative approaches of using stored optimization data.

A redesign of a near NZE demonstration home is formulated within the context of a systematic multi-objective optimization problem using the previous designed optimization tool. The ÉcoTerra home is a proven near NZE design approach for cold-climates by combining passive solar design, energy efficiency measures including a geothermal heat pump and a building-integrated photovoltaic system. The commissioned design indicated that there might be potential for ÉcoTerra to achieve NZE with new, more efficient PV technology (Doiron, 2010). An archetype solar home model will be optimized using economic and energy objective functions to identify pathways to NZE.

Previous research showed that optimization algorithms required 40–50 hours to identify optimal building configurations for 20 to 30 design variables. This time requirement is a major barrier limiting future research that requires repetitive optimization runs to explore the solution space (Attia et al., 2013). Thus, improving optimization results while reducing optimization time requirements is an important contribution of this thesis.

There is an opportunity for optimization algorithms to play a pivotal role in variability analyses. It may be possible for previous building performance simulations to be saved and data-mined around performance criteria such as NZE. Sampling this information might suggest scenarios where the performance criterion is no longer met. Previous research has yet to use such information to enhance a designer's ability to identify changes to building designs that compromise expected performance.

The final research area focuses on the cost feasibility of energy-optimized buildings. Previous research has not yet explored economic incentives that affect the relationship between a cost-optimized building and an energy-optimized building. This research area explores the potential effect of incentives on energy-cost curves.

2.8.1 Objectives of PhD Thesis

To accomplish the research plan, several objectives for this thesis are identified. These objectives are as follows:

1. Build an optimization tool using two objective functions: i) net-energy consumption, ii) life-cycle cost.
    - develop a new evolutionary algorithm which drastically reduces computational and time-requirements while improving algorithm convergence by investigating opportunities for information data-mining and integration of deterministic searches
    - develop a cost model to use energy simulation results to calculate life-cycle costs
    - develop a reference building for comparisons in life-cycle cost objective functions
2. Perform a redesign of the ÉcoTerra home using a systematic multi-objective optimization approach
3. Evaluate the potential for an optimization tool to guide a variability analysis around a performance criterion
4. Evaluate how economic incentives affect optimal building design

This thesis uses a previously developed energy model for NZEH design (O'Brien, 2011). This is model is described in a later concept of design chapter. The model uses EnergyPlus (Crawley et al., 2000) to evaluate energy consumption over a typical meteorological year. A modified version of this model is used as an archetype solar home for chapter case-studies. This model was augmented with a life-cycle cost model

to evaluate the economic performance of each potential design. Details related to the algorithm design, energy and cost model formulation are described in the following concept of design chapter.

Chapter 3

Concept of Design: Optimization Methodology, Energy Model, Cost Model

> "The machine does not isolate man from the great problems of nature but plunges him more deeply into them.
>
> –*Antoine de Saint-Exupéry*"

3.1 Overview

This chapter describes details regarding algorithm design, energy model and cost model formation. The energy and cost models define objective functions used by the optimization algorithm. These components are used in future chapters.

This section provides an overview of the optimization methodology using the component framework described in the literature review, section 2.3. Table 3.1 shows an overview of the methodology. Section 3.2 describes the custom multi-objective EA used for optimizations. The representation types are described in section 3.3.1. Genetic operators, such as cross-overs, mutations and differential mutations are described in section 3.3.3. Section 3.3.6 describes the database used to store simulation results. Two objective functions are defined in this chapter, an energy consumption function defined in section 3.4 and a life-cycle cost function defined in section 3.5. Both of these sections include relevant details regarding the formulation and evaluation of each objective function. Section 3.3.8 describes four core concepts used in later chapters: (i) back-tracking searches; (ii) solution space exploration; (iii) probability distribution functions; and (iv)

extracting variable interactions using mutual information.

Table 3.1: Overview of optimization methodology

Component	Specification
objective function	net-energy consumption, life-cycle cost (multi-objective)
evaluation method	EnergyPlus simulation, Python script for LCC
file generation	Python script (programmed)
database	relational database (SQLite)
optimization algorithm	custom designed evolutionary algorithm
representation	grey-coded binary or discrete (convertible)
constraints	boundary and active equality constraints
genetic operators	crossover, mutation, differential evolution
selection operators	tournament and NSGA-II
termination criteria	number of generations

Before describing each component, requirements were established to ensure the streamlined development of the optimization tool.

3.1.1 Optimization Tool Requirements

This section describes primary requirements or objectives of the optimization methodology. The primary objectives of the optimization tool are: (i) focus on finding populations of good candidate building designs more quickly than the present state-of-the-art techniques; (ii) exemplify methods of visualizing and interacting with data that aids the design of NZEBs; (iii) design the proposed optimization tool to be easily interfaced with; (iv) store previously evaluated building simulation results, including performance measurements in a database; (v) store all optimization algorithm data in a database; (vi) modular design of major optimization components (optimization algorithm, building model, database, statistics tool-kit).

Making the tool simple to interface with, primary objective (iii), requires a readable and easily understandable design. A consequence of this requirement is that the energy and cost simulation tools must also be open-source, cross-platform compatible, well-documented and extensible.

Database storage and specialized search strategies, objective (iv), allow emphasis on pathways to optimal designs, not just a single 'optimal' result. This data was later used to characterize all designs satisfying a performance objective.

Modular design, primary objective (vi), allows for upgrades to any major components

without affecting the functioning of other modules. A software development strategy of highly-cohesive modules (serving a single functional purpose) which is loosely-coupled to other modules (limiting cross-dependencies) was deployed. This strategy allows for modifications in each module without requiring changes to other components. For example, upgrades to the building simulation tool could be made without affecting other modules.

A few non-critical implementation features were also proposed, which included: (a) isolate the tool to a single directory for ease of distribution thus constraining development to a single directory allows for simple drag and drop installation of the complete tool facilitating primary objective (iii) stated above; (b) allow for user interaction at runtime, such as the injection of user specified designs allowing hypothesis testing and visualizing how algorithms arrive at optimal building designs; and (c) include visualization techniques and feedback to aid the understanding of solar building design and improve user experience.

Recall the major components of an optimization tool shown previously in Figure 2.1. Major components include the optimization algorithm, building model, database, and statistics module. The optimization algorithm provides the necessary information to the building simulation module to create the energy and cost simulation files. The building simulation module then simulates the given building design and passes the simulated data back to the optimization algorithm. The optimization algorithm associates a fitness level to the representation using simulated data, and stores all valuable information into the database. The statistics module connects directly to the database to recover and present information for analysis and visualization at any point during or after an optimization run.

Notably, most previous optimization studies do not include a building simulation module and work with energy simulation files directly. The limitation of this approach is that the study cannot handle more complicated substitutions such as the translation of a Window-to-Wall Ratio (WWR) onto window co-ordinates or geometry studies beyond very simple shapes. Separate wrapper scripts, one for each simulation engine used, are required to interpret optimization variables into proper simulation format. Matlab (MathWorks, 2011) and Python (van Rossum, 2011) are presently used to script building

simulation files.

Major algorithm components are discussed in greater detail in the next section.

3.2 Concept of Design: Optimization Algorithm

> "The worst potential competition for any organism comes from its own kind."
> –*Frank Herbert, Dune*

3.3 Evolutionary Algorithm

A simplified Evolutionary Algorithm (EA) is summarized in Figure 3.1. Clojure (Hickey, 2012), a LISP programming language, was used to integrate mixed optimization strategies into an evolutionary algorithm, see Appendix B.

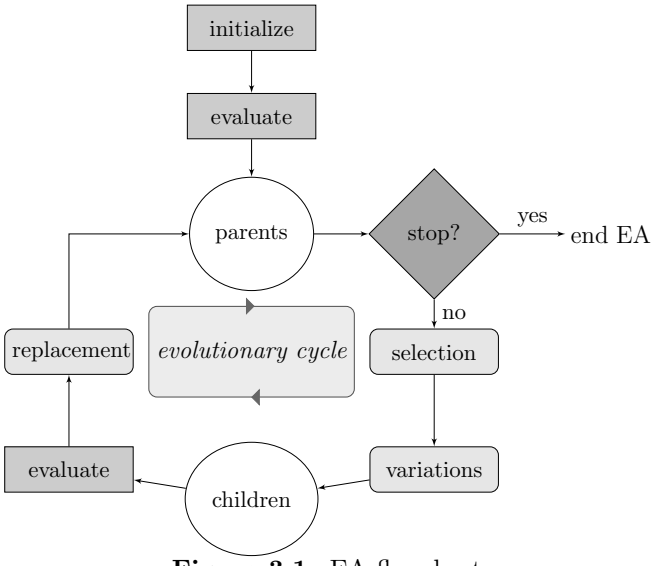

Figure 3.1: EA flowchart

A set of *genomes*, or simplified representations of building designs, form a *population*. The population is *initialized* by randomly creating the specified population size and performing energy/cost simulations to evaluate *fitness*. This population becomes the *parent* population as it enters the *evolutionary cycle*. Prior to further operations, a *terminal criteria* is evaluated to ensure that an optimal solution as yet to be found or a defined number of iterations, or *generation* has not yet been satisfied. *Parent selection* is used to select genomes for *variation* operators such as *crossover* and *mutations*. The

fitness of new individuals is evaluated. *Survivor selection* chooses which genomes from the old and new population will *replace* others in the next generation. The process is repeated until a *termination* criteria is reached, typically a set number of generations. Individuals are said to be *elite* if there exists no other individual in the present population with a higher fitness. *Elitism* refers to a mode where the elite individual always passes to the next generation.

In a sense, individuals compete with each other for mating resources. Once desirable characteristics have been identified, they can quickly be shared with other individuals. The components and requirements of the EA are considered in greater depth in the following subsections.

3.3.1 Representation

The selection of individual representation will also determine the available methods that can be used for genetic operations.

Due to primary objectives, the representation must satisfy the following requirements: (a) remain discrete as per primary objective (i); (b) be competitive with the fastest known representation with regards to convergence speed, primary objective (i); (c) allow for robust diversity measurements, primary objective (i); (d) remain consistent with building representations, primary objective (ii); and (e) be flexible in defining the set of design parameters, primary objective (iii).

The primary representation used in the EA was grey-coded binary (Eiben and Smith, 2003). Grey-coding refers to a binary representation where adjacent parameters differ by at most one bit, see Table 3.2. Binary representation allows for the most effective mutation and crossover operators, excellent diversity estimates and the fastest convergence performance. In binary format, crossover can occur both inside and outside the representation, i.e. data cannot only be shared between similar design variables but also between non-similar design variables. This information sharing strategy is very effective in improving convergence performance, as it allows for information transfer between variable couplings without suffering positional bias (Eiben and Smith, 2003). The limitation of binary representation is that all design variables must be represented using 2^N step-sizes, where N is the number of bits, hence requirement (e) is not satisfied. This is

a minor issue as the user cannot specify any desirable set of design parameters without having some redundancy, or a finer resolution than originally desired. To overcome this limitation for some genetic operations, a discrete representation was used.

Table 3.2: Comparison of numerical encoding of representations

Decimal	Gray	Binary
0	000	000
1	001	001
2	011	010
3	010	011
4	110	100
5	111	101
6	101	110
7	100	111

Alternatively, a discrete representation was allowed for some operations. Discrete representation allowed for flexible step-sizes and enabled the use of uncommon genetic operations, such as differential mutations, so long as individuals were converted back into binary representations before re-entering the binary-based optimization algorithm.

An alternative solution would be to use a mixed continuous and integer representation from an evolutionary strategy or differential evolution. These representation types focus on continuous parameter optimization and apply rounding operators prior to objective evaluations to keep representations discrete. Unfortunately this option fails requirement (b) as the crossover will no longer be able to share data inside and outside representation thus convergence performance is lost. In addition, boundary conditions of continuous variables need to be enforced.

3.3.2 Constraints

Several of the constraints discussed in section 2.3.2.1 were used in the methodology.

Boundary constraints specified the allowable minimum and maximum values for design or decision variables to take. Furthermore, boundary constraints ensured that values in the representation adhered to the discrete values allowed in the binary representation. In the case of variational operations where continuous variables were used, rounding to the nearest discrete values was always performed.

Inequality constraints operated on the objective function to ensure value constraints were not exceeded. Barrier functions as recommended by Wetter were used (Wetter, 2011b). For example, in Chapter 5, an inequality constraint ensured that designs did not exceed an economic budget. Barrier functions were applied to the energy objective functions to deter the algorithm from selecting cost-prohibitive designs. Crossing the constrained barriers results in objective functions of infinity.

3.3.3 Genetic Operations

As mentioned previously, the choice of genetic operators are a consequence of individual representation. The effectiveness of binary operators has been well studied and requires little exploration (Eiben and Smith, 2003). As per the No-Free-Lunch theory (Wolpert and Macready, 1997), each search algorithm and genetic operators have inherent advantages and disadvantages which depend on the fitness landscape (Weise, 2009).

The arity of the operator refers to the number of individuals or genomes that are operated on. Typical operators have an n-arity, where n is in the range of one to four.

Two types of mutation operators were explored: (i) a binary mutation operator, and (ii) a differential mutation. A binary mutation operator accepts a binary genome and with a probability, p_m, typically 1 to 4%, flips each bit and returns the resulting binary representation. Thus this operator has 1-arity. The diversity of the population can be increased by using higher mutation rates, but at the detriment of possibly losing progress made within evolutionary cycles. The second method used was a differential mutation. Differential mutations are the primary evolutionary mechanism found in Differential Evolution (DE) and PSO algorithms. This proposed discrete mutation operated on a single parent using gradient information from three unique, randomly selected individuals from the population. Thus the operator had 3-arity. A modified version of differential mutation, created by Storn and Price (1995), was adapted to work within a binary EA, shown in Algorithm 1. The scaling factor (SF) determined the scaling of the gradient difference used in the operator. The mutation rate (MR) was identical to the probability of mutation used in the bit-flip operator. After the differential mutation, the resulting continuous representation required rounding to conform to the specified variable step-sizes. Thus the representation was rounded back into a discrete vector before conversion

into binary format. If values exceeded specified ranges within the differential mutation, they were randomly reset to an allowed value, as recommended by Feoktistov (2006). An algorithm parameter, the probability of selecting mutation method 1 versus method 2, specified which method was used; the higher the parameter, the more likely method 1 would be used over method 2 and vice versa.

Algorithm 1 Modified differential mutation operator

Precondition: **a** is a grey-coded binary string

```
1  function DIFF_MUTATE(a)
2      a ← binary2discrete(a)                    ▷ Convert binary representation to discrete
3      d, e, f ← getnRandomIndiv(n=3)            ▷ select 3 random individuals from population
4      for i ← 1 to N do                         ▷ Note: a = (a_1, ··· , a_N)^T
5          if MR ≥ rand(0,100) then              ▷ Mutation rate, MR ∈ [0, 100]
6              g_i ← d_i + SF ∗ (e_i − f_i)      ▷ Scaling factor, SF ∈ [0, 2]
7          else
8              g_i ← a_i
9          g ← round2discrete(g)                 ▷ Round resulting representation to discrete
10         return discrete2binary(g)             ▷ Convert discrete representation to binary
```

Two variations of the uniform type crossovers were used. Uniform crossover operates on each parent on a bit-by-bit basis. Across the representation, there is equal probability that the bit setting of each parent will be used to build the first child. The opposite information is used to build the second child, see Figure 3.2 (Eiben and Smith, 2003).

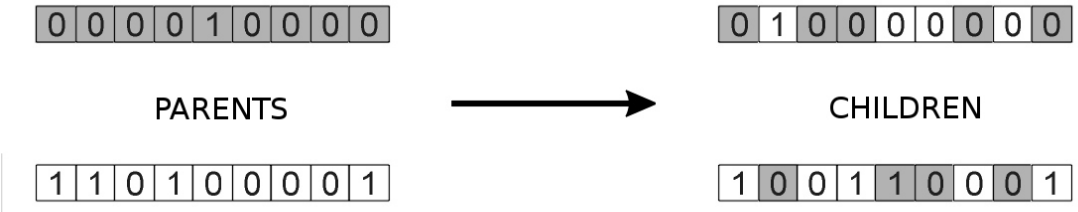

Figure 3.2: Bit-by-bit uniform recombination (modified from Eiben and Smith (2003))

An advantage of uniform crossover is that slight mutations may be introduced as information is shared both inside and outside of the variable representation, which aids in exploring new fitness landscapes. One disadvantage of a uniform crossover is that the operator suffers from distribution bias. Positional information that may be advantageous to share between two individuals is often lost due to random effects while creating new genomes. This issue is compounded for longer genome lengths.

To counteract the disadvantages of bit-by-bit uniform crossover, a variable uniform

crossover operator was also used. This crossover operator operated across variables only, see Figure 3.3.

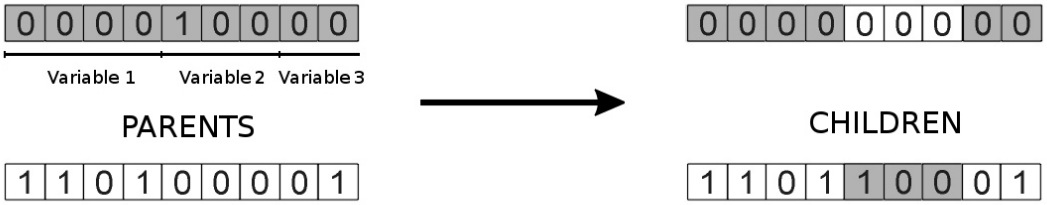

Figure 3.3: Variable uniform recombination

Variable uniform crossover does not suffer greatly from distribution bias, as variable information is strictly shared. However, since bit information is taken in chunks, the operator is susceptible to positional bias. This recombination strategy is important in the stages of evolution, when one, or several variables of elite individuals open up landscapes in the solution space where optimums are located.

3.3.4 Selection

Two selection operators are required in an EA. The parent selection operator selects two genomes from a population of possible mating candidates. Representations exchange information to form new individuals which are then reintroduced back into the population. This process, like its biological counterpart, is referred to as mating. Survivor selection selects a finite number of genomes to move onto the next generation in the EA loops. Survivor selection is often referred to as replacement as it replaces the previous population with a pool of new or existing candidates. Note that the choice of selection operators are made independently of representation and genetic operators.

The term *selection pressure* is often used when considering a selection operator. Selection pressure refers to how deterministic a selection operator or genetic operator is. Decreasing selection pressure refers to increasing the randomness of the selection or genetic operator. A deterministic selection operator will always allow the best representations to produce offspring and survive each generation. At first thought this seems beneficial, however, it allows the population to prematurely converge to local optimums and is said to disrupt the diversity of the population, see section 3.3.5.

Tournaments were used for parent selection. A tournament randomly chooses k individuals from a given population and takes the fittest representation of the local tournament. This process is repeated until the required population is formed. The variable k controls the tournament size and hence the selection pressure. Smaller tournament sizes decrease the likelihood of the best individual in the population being chosen for mating, but ensures at least good individuals are selected.

A (μ, λ) or a $(\mu + \lambda)$ selection operator was used for survivor selection (Eiben and Smith, 2003). This type of operator is highly deterministic. Given a population of representations, it sorts and returns the best individuals, where the size is defined by the specified population size. The operator is said to be (μ, λ) if it uses only the newly created population, called children (μ), for selection. A $(\mu + \lambda)$ selection operator uses the original population, called parents (λ), and their children for selection. Selection operators are also solely responsible for handling multiple objectives in an EA. Multi-objective selection operators are discussed in a later section.

3.3.5 Diversity Definition and Control Strategy

Diversity is a measure of how similar or different individuals in a population are. Diversity calculations may include parameter-by-parameter comparisons for each design variable or more favourably correlations between design variable settings. The comparison operators will depend on the representation method chosen. Note that the larger the EA population size is, the less important measuring and maintaining diversity becomes. However, this comes with the trade-off of an increase in required fitness evaluations.

Diversity can be used as a diagnostic to predict and prevent the premature collapse of a population to non-optimal landscapes. This allows for much smaller population sizes and fewer required fitness evaluations per generation, which greatly reduces overall simulation time. Diversity monitoring also ensures exceptional algorithm performance without requiring user interventions made possible by using self-adaptive algorithm parameter control.

A self-adaptive feedback model was used for algorithm parameter control. EAs have three typical modes of operation (Eiben and Smith, 2003): (i) deterministic mode; (ii) chaotic mode; and (iii) complex, or evolutionary mode. Evolutionary mode is desired

unless problems are encountered. If the population becomes mired in a local minimum, selection pressure can be reduced by decreasing tournament sizes and increasing mutation rates to induce the algorithm into a chaotic mode until the minimum has been escaped similar to simulated annealing (Weise, 2009). Often this 'randomness injection' is sufficient to average local optimums in the landscape enough for evolution to continue. This strategy is useful in any situation where a collapse of diversity is observed. If the population has approached the global optimum, the deterministic behaviour of the algorithm can be utilized to locally search the landscape. This is best done by changing the genetic operators completely to local search operators. Another useful method is to increase population sizes to recuperate from a loss of diversity, but this was avoided due to an increase in required fitness evaluations. Injecting previously evaluated individuals is useful if the fitness is comparable and sufficiently diverse from the present members of the population. The power of adaptive feedback is that no user interaction is required to ensure the algorithm is operating properly.

Recall that grey-coded binary representation was used. The diversity metric employed was the number of bits shared with the elite individual, normalized by the total number of bits in an individual, see Figure 3.4. Two exact genomes would have relative diversity equal to 0, while two individuals sharing no bits would have a relative diversity equal to 1. Since the comparison involves a population compared to an elite individual, the diversity metric is the average of all comparisons. An advantage of a binary representation is that diversity calculations are numerically simple.

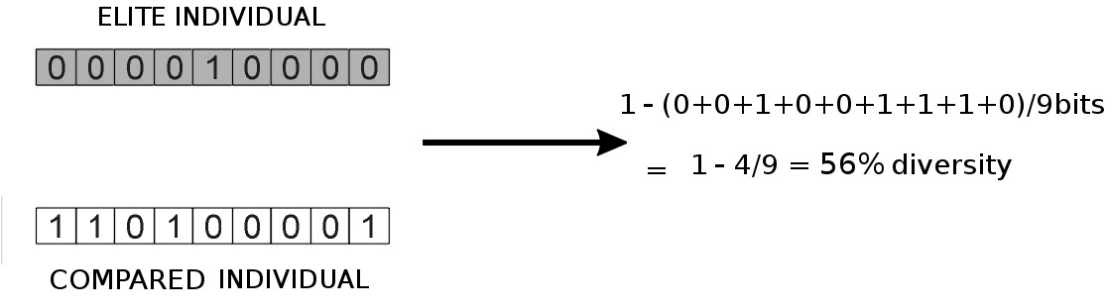

Figure 3.4: Demonstration of diversity calculation for a single individual

3.3.6 Database

To satisfy primary objective (vi), see page 53, a modular approach is used to separate the storage of building simulation results from the optimization algorithm and separate statistical analysis from both the optimization algorithm and building models. Furthermore, a database is needed to store important simulation data for previously evaluated representations and recall of previous convergence information of the optimization algorithm as per primary objectives (iv, v).

SQLite (2012) was selected as a database, as it could be isolated to a working directory, as per non-critical objective (a), and was simple to interface with any programming language, primary objective (iii). By using a database with excellent support in most programming languages, the author was not limited to one single programming toolkit. For example, statistical analysis could be done using other sophisticated statistical packages such as R (R Foundation, 2012).

A consequence of a parallel programming approach to energy simulation is that a concurrent queue had to be developed to handle simultaneous insertions and queries of energy simulation data from the optimization algorithm. The write-ahead logging (WAL) feature in SQLite was used in a new versions to allow for concurrent database reading and writing.

Table 3.3 describes the database table 'indiv' used to store simulation results for new evaluations. If the identical individual was later requested for simulation results, this table was utilized to save computational time. Descriptions and selection variables for optimization is discussed in later chapters.

Table 3.4 describes the database table 'vmap'. It stored the representation method used to evaluate in individual described in Table 3.3. This table was referenced to convert binary representation to and from discrete representations. Individuals with continuous representations, i.e. those with differential mutations, were rounded to discrete representations and later to binary representations (if necessary) using information from this table. Note that each individual has a relational key which refers every individual to a variable representation in this table. This allowed for genetic operations to be performed on individuals with different variable step-sizes.

Table 3.3: Database table 'indiv' for representation simulation results

Name	SQL Type	Description
pkey	INTEGER PRIMARY KEY	Primary key of 'indiv' SQL table
vmapkey	INTEGER	Primary key of 'vmap' SQL table, see Table 3.4
indiv	VARCHAR(200)	Representation of individual (binary or discrete)
keyvar	TEXT	Variable hash map of individual
gen	INTEGER	Generation number where individual was evaluated
heat	REAL	Heating consumption using heat-pump, kWh
pk_heat	REAL	Peak heating load, kW
cool	REAL	Cooling consumption using heat-pump, kWh
pk_cool	REAL	Peak cooling load, kW
light	REAL	Lighting energy consumption, kWh
dhw	REAL	DHW energy consumption, kWh
fan	REAL	Fan energy consumption, kWh
app	REAL	Appliances energy consumption, kWh
pv	REAL	PV generation, kWh
fit	REAL	fitness function (net-energy consumption), see equation 3.13
datetime	DATETIME	Date and time stamp of when simulation was initiated
simtime	REAL	Duration of simulation (in minutes)
conscst	REAL	Initial construction costs
pvcst	REAL	Initial PV cost
pvrev	REAL	Revenue from feed-in tariff (PV generated electricity)
npv	REAL	Net Present Value, see equation 3.17
lcc_cf	TEXT	Vector of cash-flows for each year in life-cycle
t_lc	REAL	Life cycle period (years)
elec_rate	REAL	Rates used for electricity billing
pv_rebate	REAL	PV array initial cost rebate
mort_rate	REAL	Amortization rate for mortgage loan
pv_feedin	REAL	PV Feed-in tariff

Table 3.4: Database table 'vmap' for variable representation

Name	SQL Type	Description
pkey	INTEGER PRIMARY KEY	Primary key of 'vmap' SQL table
vmap	TEXT	Variable mapping used to convert binary$\Longleftrightarrow$discrete representations
datetime	DATETIME	Date and time stamp of when new representation was created

3.3.7 Multi-Objective Selection Operator

This section discusses the implementation of an additional objective function into an EA. The multi-objective selection operator determines the formation of the Pareto front. The inclusion of cost as an objective function, in addition to net-energy consumption, allows for much more complex interactions between variables. The details of calculating cost objective functions is discussed in section 3.5. This section discusses EA design modifications to accommodate additional objective functions. This multi-objective selection operator is later used in Chapter 7.

This section describes the implementation of multiple objectives into a evolutionary algorithm. However it is not intended to be an exhaustive resource on multi-objective optimization techniques. For an in-depth analysis, refer to the textbook by Deb (2001) from which this section is based on.

Multi-objective optimization depends on two concepts: (i) dominance and (ii) Pareto optimal fronts.

The definition of dominance is described in the following. For a minimization problem, a vector of decision variables $\mathbf{x} \in \mathbf{X}$ is said to dominate another vector $\mathbf{y} \in \mathbf{X}$ *iff* $f_i(\mathbf{x}) \geq f_i(\mathbf{y})$ for all $i = 1, \cdots, k$ and $f_j(\mathbf{x}) > f_j(\mathbf{y})$ for at least one j. If there does not exist any other decision vector in $\mathbf{X}$ that dominates vector $\mathbf{x}^*$, then $\mathbf{x}^*$ is said to be Pareto optimal.

Dominance allows for comparison of fitness evaluations on individuals using several objective functions. This concept is necessary as individuals can no longer be compared using one objective function—comparisons of design alternatives must use all objective functions. Non-dominated individuals form the optimal solution set indicating that each individual in the Pareto set has performance characteristics which are unique. This is a departure from the single objective optimization where one individual dominates all others.

A population is said to converge if it approaches the Pareto front, see Figure 3.5. Most multi-objective operators encourage spreading across Pareto fronts using non-dominated individuals. Crowding distance equations are used to quantify the density of individuals. Preference is given to individuals which are Pareto optimal and have the largest spreading relative to other individuals in the population. Spreading of indi-

viduals across Pareto fronts is a form of diversity management that improves algorithm performance (Deb, 2001).

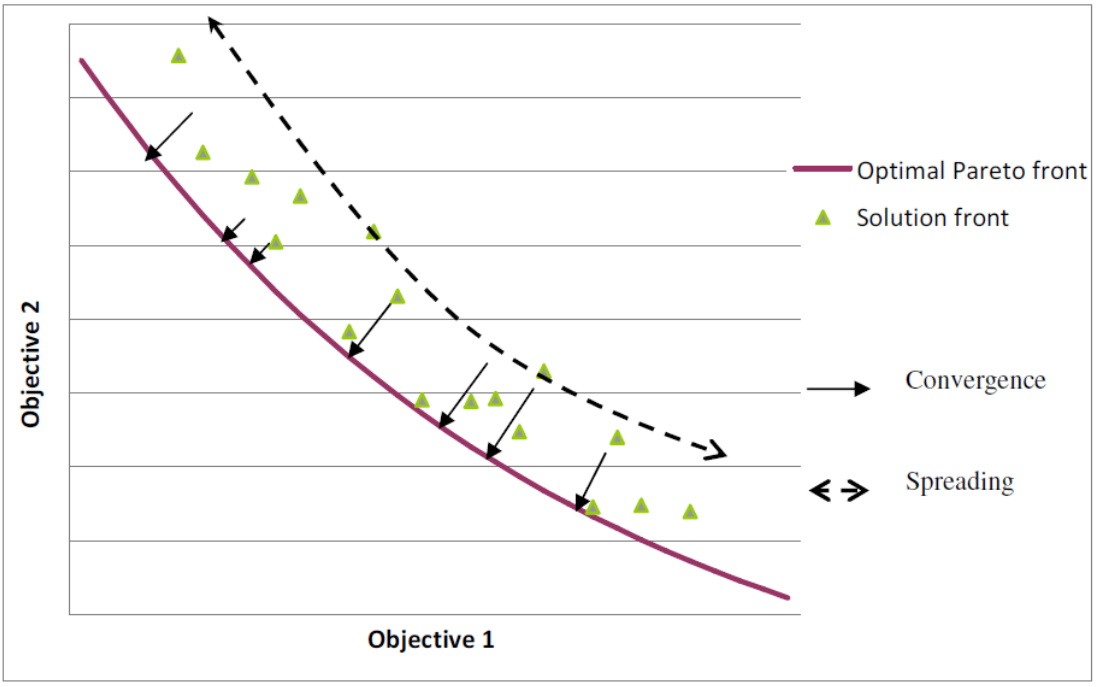

Figure 3.5: Convergence and spreading in the NSGAII selection operator (Magnier, 2009)

The inclusion of multiple objectives is accomplished in an EA by modifying the parent selection operator. The elitist non-dominated sorting genetic algorithm (NSGA-II) was selected as a parent selection operator for multi-objective optimization as described in Deb (2001, chap. 6.2, pg. 233). This selection operator preserves elite individuals through non-dominance and explicitly maintains population diversity using crowding distances. NSGA-II uses a crowding strategy which is more computational efficient ($O(M \cdot N \cdot \log N)$) as compared to other selection operators such as SPEA which is $O(M \cdot N^2)$ (Deb et al., 2002).

In NSGA-II, crowding distance calculations are performed using equation 3.1 (Deb, 2001).

$$d^m = d_i^m + \frac{f_{i-1}^m - f_{i+1}^m}{f_{max}^m - f_{min}^m} \tag{3.1}$$

where: $f_{i-1} - f_{i+1}$ is the difference in objective functions between two sorted individuals, $f_{max} - f_{min}$ is the difference in objective functions between the population max/min of the mth objective function, and d_i^m is an estimate of the perimeter of the cuboid, see

Figure 3.6. The crowding distance of individuals with no neighbours (extrema) is set to infinity.

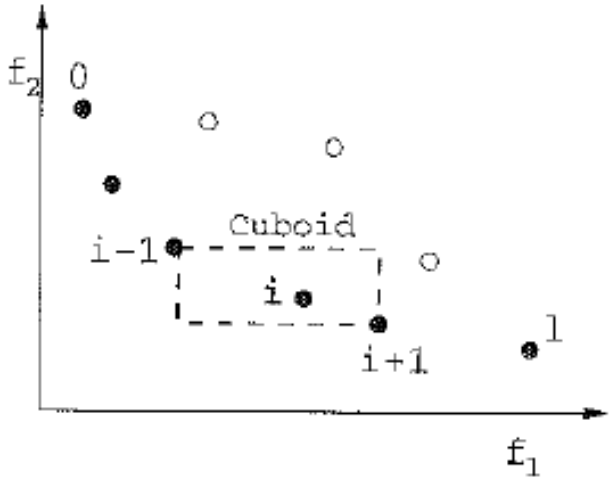

Figure 3.6: NSGA-II distance calculation (Deb, 2001)

After crowding distance calculations, individuals are ranked into fronts, and the selection process is conducted, see Figure 3.7. Individuals common to fronts F1 and F2 survive to the next population based on rank. Individuals from front F3 are selected based on crowding distance to form the remaining population which is used for genetic operators. Deb (2001) recommended that since the NSGA-II parent selection is deterministic, the survivor selection operator must have some probabilistic characteristics.

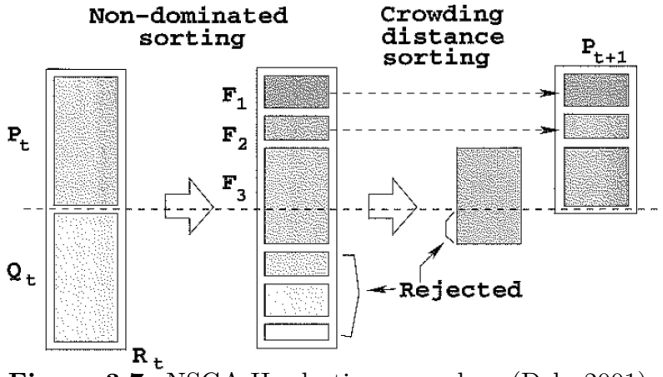

Figure 3.7: NSGA-II selection procedure (Deb, 2001)

Multi-objective optimizations require larger population sizes to spread across Pareto fronts; however early objective function evaluations rarely contribute the identification of non-dominated individuals. Thus, it is desirable to restrict population sizes and use over-selection to grow a population of individuals, see Figure 3.8. This innovation allowed for an identical number of fitness evaluations as the single objective EA by using

a $(\mu+\lambda)$ tournament selection operator. Note that population sizes, shown in Figure 3.8, grow from 10 individuals in generation no. 1, to 20 individuals in generation no. 2, until the desired population size of 40 is met in generation no. 4. At this point, a population of 40 individuals is used to spread across the Pareto front. The percentage population replacement is referred to as the *generation gap*. In this case, a generation gap of 25% indicated that 75% of the population was selected from previous generations.

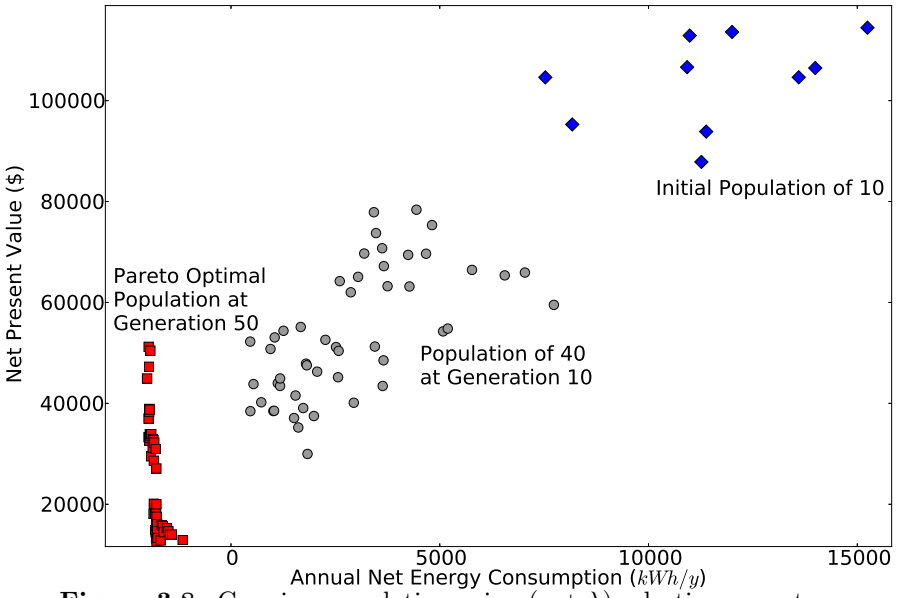

Figure 3.8: Growing population using $(\mu + \lambda)$ selection operators

3.3.8 Core Concepts

This section describes core concepts instrumental to the optimization methodology, but outside the scope of typical EA design. Core concepts arise repeatedly in future chapters and thus this section provides background information necessary to understand later chapters which are more application focused. The following core concepts are described below: back-tracking searches, solution space exploration, probability distribution functions and data-mining using mutual information.

3.3.8.1 Back-tracking Search

A core concept used throughout this thesis is the back-tracking search. Back-tracking searches are a new proposed search technique. Figure 3.9 exemplifies the back-tracking search using a simplified example. A back-tracking search identifies the order in which

each variable should be changed to result in the steepest objective function gradients from a selected individual, A, to a known reference individual, B. In Figure 3.9, starting from A three potential variable changes are tested. The variables, x_1, x_2, x_3, are changed from the value found in the selected individual to the value known in the reference individual. Thus three new intermediate individuals, C, C_1, C_2, are created and evaluated using the objective function. The variable x_3 resulted in the steepest change in the objective evaluation and is identified as the variable with the highest importance as listed in the x-axis. The objective function gradient from A to C is recorded. Now, the variable x_3 can be excluded from the remaining back-tracking searches. Starting from the intermediate individual, C, the variable x_2 with the next steepest gradient is identified for individual D. This process is repeated until all variables of A are back-tracked to B. Importance factors, as described in chapter 6, are used to summarize back-tracking results.

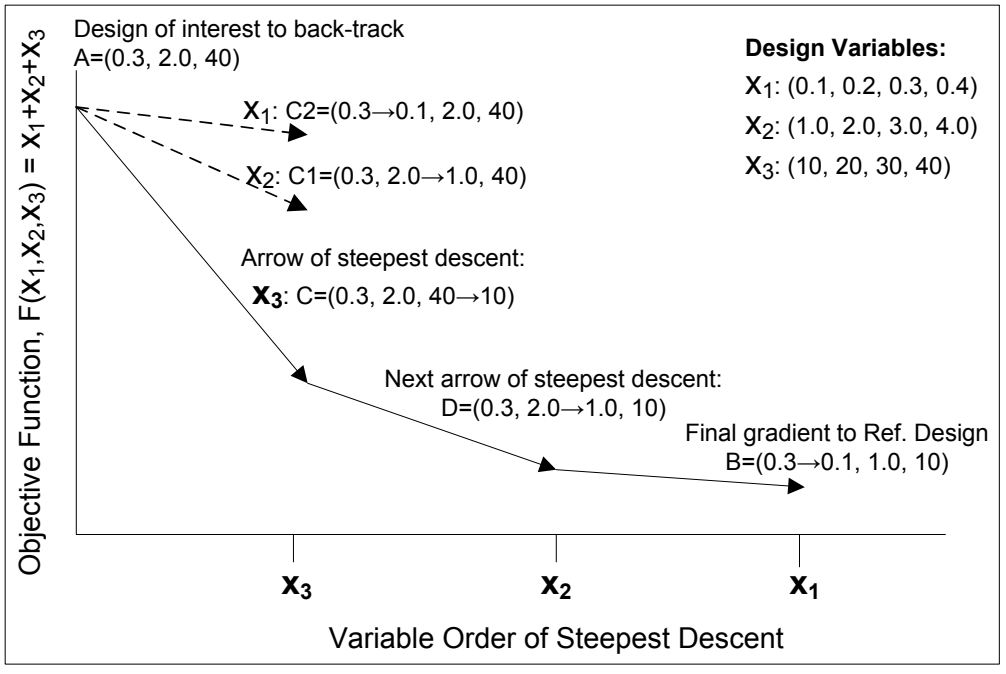

Figure 3.9: Simplified back-tracking search of vector A back-tracked to reference design vector B

3.3.8.2 Exploration of Solution Space using Repeated Optimization Runs

Repeated optimization runs are required to use optimization algorithms to extract information from the solutions space. Consider the solutions space shown in Figure 3.10

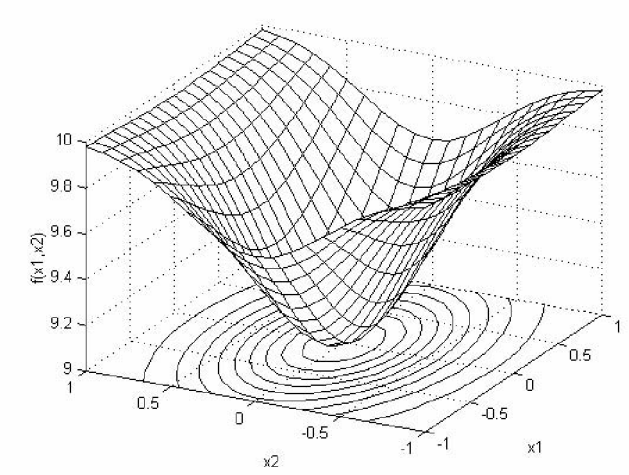

Figure 3.10: Formation of contours from solution space (Feoktistov, 2006)

This simplified solution space includes two design variables and one objective function. A contour map is formed by representing fitness using contours, similar to how maps describe elevations. Figure 3.11 shows several sequential searches on this solution space.

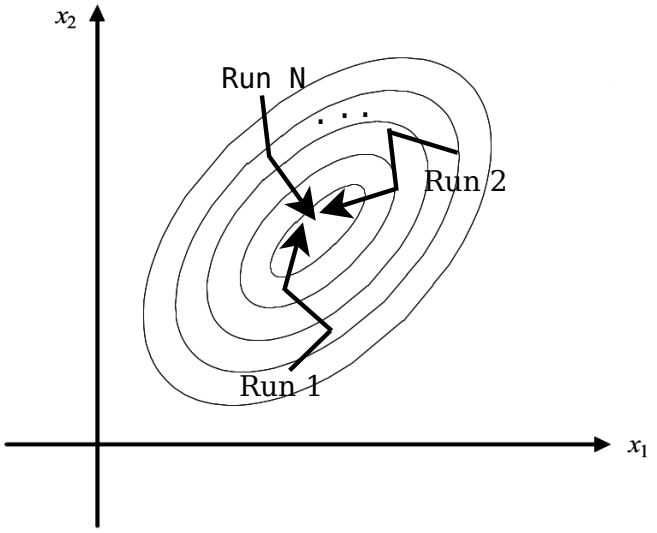

Figure 3.11: Navigation of solution spaces using repeated sequential searches (modified from Feoktistov (2006)

Note in Figure 3.11 that each optimization run only explores a small portion of the total solution space. Each run starts from a different part of the solution space and converges to the same global optimum. Many optimization runs are required to build statistical significance and a representative dataset. The sample size is dependent on the effect size one observes, the significance level and the statistical power required. For

optimization studies of 20 or 30 variables, a sample of 10 to 20 optimization runs is sufficient depending on the number of algorithm iterations.

3.3.8.3 Probability Distribution Functions

> "There are known knowns; there are things we know that we know. There are known unknowns; that is to say there are things that, we now know we don't know. But there are also unknown unknowns—there are things we do not know we don't know."
>
> –*United States Secretary of Defense, Donald Rumsfeld*

In previous sections, the goal of an optimization study was to identify the best performing designs. This section describes a departure from this perspective. Optimization approaches coupled with visualization tools can aid in identifying trade-offs in the solution space. This can be accomplished using Probability Distribution Function (PDF).

Recall that the formation of building models relies on many assumptions. Assumptions arise from known-unknowns such as occupancy patterns and envelope compositions. However, unknown-unknowns can also arise from overlooked or underestimate aspects of the simulation process. For example, consider design changes due to budget restrictions or unavailable materials or equipment. Unknown or uncertain variables can be included by associating variables to PDFs and simulating all possible scenarios.

Building simulation can be performed using deterministic or probabilistic models, see Figure 3.12. Traditional deterministic models require all variables to be unique prior to simulation. Probabilistic models require PDFs to be assigned to input variables. The probabilistic inputs are sampled to select individual values, then evaluated in the model to form output distributions. The sampling and analysis to probabilistic input distribution is referred to as a type of uncertainty analysis called a Monte Carlo simulation.

The following steps are required to form PDFs from optimization data: (i) create dataset using repeated optimization analysis; (ii) query sets of designs with interesting characteristics; and (iii) convert query results to PDFs for each variable.

For example, in the following database query, the window frame types variable (FT) which includes parameters (1, 2) would be associated with a PDF of $(\frac{4}{5}, \frac{1}{5})$. Stating this mathematically $FT \in (1, 2) \rightarrow (\frac{4}{5}, \frac{1}{5})$. Similarly for variable for glazing type GT_s $\in (3, 4, 5) \rightarrow (\frac{1}{5}, \frac{2}{5}, \frac{2}{5})$. These results can then be exported into a statistical tool such as R (R Foundation, 2012) for analyses or be converted directly into PDFs for sampling.

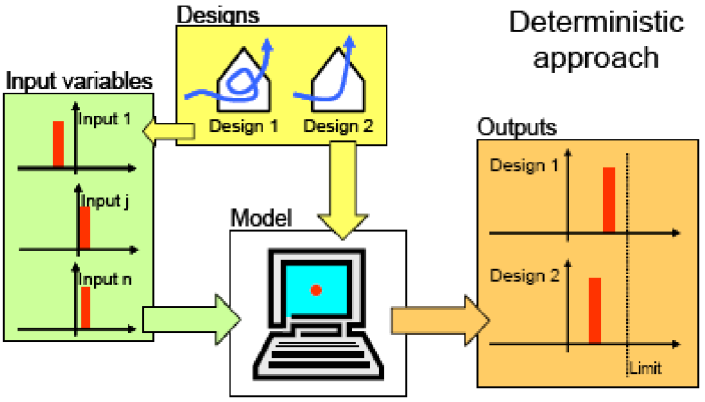

(a) Deterministic Model

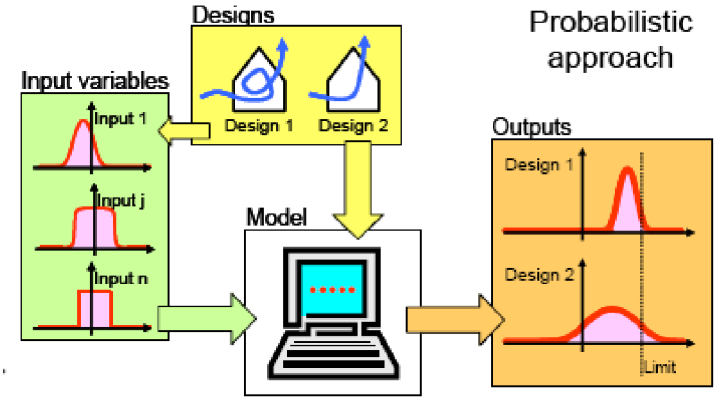

(b) Probabilistic Model

Figure 3.12: Deterministic versus probabilistic models (Heo et al., 2011)

```
-- Select unique variable descriptions and fitness...
-- for all NZE homes from table 'indiv'.
-- Randomly select 5 representative designs.
-- Round fitness to one decimal place.
SELECT DISTINCT keyvar,ROUND(fit,1) FROM indiv
   WHERE fit<0 ORDER BY RANDOM() LIMIT 5;
```

Listing 3.1: SQL query for extracting information for probability densities

```
--                                                  KEYVAR                                                  | FIT
{:FT 1, :GT_n 5, :GT_s 4, :aspect 1.8, :azi -5.6, ...}|-2069.7
{:FT 1, :GT_n 5, :GT_s 3, :aspect 1.1, :azi -5.6, ...}|-1817.7
{:FT 1, :GT_n 4, :GT_s 5, :aspect 1.9, :azi  0.0, ...}|-1593.8
{:FT 1, :GT_n 5, :GT_s 4, :aspect 1.6, :azi 16.9, ...}|-1534.6
{:FT 2, :GT_n 4, :GT_s 5, :aspect 2.1, :azi 16.9, ...}|-1994.6
```

Listing 3.2: Results from above SQL query

PDFs extracted from optimization results exhibit emergent properties and depend on the performance of the designs they are extracted from. Some variables might be monotonic meaning that increasing or decreasing an input variable will always increase or decrease the outcome. These variables are not interesting in the optimization sense since

they behave predictably. However, they are interesting with regards to an uncertainty analysis. For example, at what variable limit is a performance target no longer met? What other variables are codependent on a particular variable? Figure 3.13 shows how PDFs can change with decreasing EUI. In this Figure, note that variable 2 is monotonic and has a parameter cut-off. Variable 1 shows two probable regions for low EUI and all parameter combinations are possible.

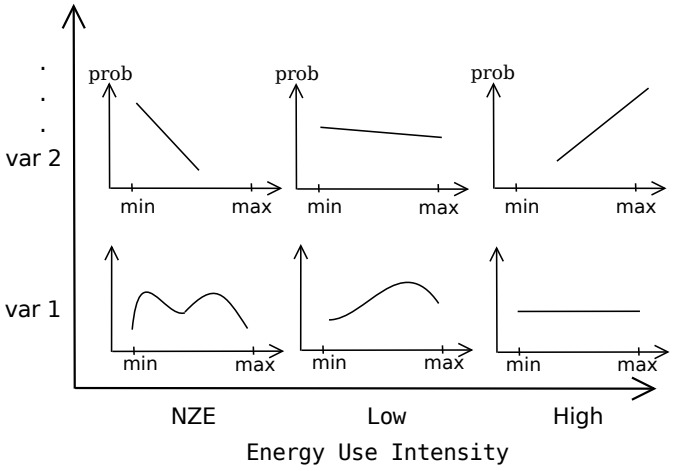

Figure 3.13: Emergent properties of PDFs with EUI reductions

PDFs are used later in chapter 6. Using a completely different approach, in Appendix A PDFs are specified using normal distribution functions. The goal of this appendix is to build confidence in economic estimates by conducting an uncertainty and sensitivity analysis on the cost-model used.

3.3.8.4 Variable Interaction Extraction using Mutual Information

This section describes how mutual information can extract variable interactions. By definition, mutual information is a measure of dependency between two random variables (Cover and Tomas, 2006). Due to its Bayesian roots, the updating of mutual information throughout the optimization search reduces the uncertainty and builds confidence in selected variables interactions.

In communication theory, variable interdependencies are leveraged to shrink the capacity of the communication channel (Shannon and Weaver, 1947). If the value of one interdependent variable is known and sent through the channel, then the other variable can be inferred indirectly. The notion of using predicted variable interactions can be

used in an optimization algorithm.

One effective way to extract variable interdependencies is to use the mutual information shared between two design variables denoted by $I(X_i, X_j)$ in equation 3.2 (Cover and Tomas, 2006), noting that x_i belongs to the set X_i ($x_i \in X_i$) and x_j belongs to the set X_j ($x_j \in X_j$).

$$I(X_i, X_j) = \sum_{x_i, x_j} p(x_i, x_j) \cdot \log_2 \left(\frac{p(x_i, x_j)}{p(x_i) \cdot p(x_j)} \right) \tag{3.2}$$

Probability calculations are made using representations of previously simulated individuals. The functions $p(x_i)$ and $p(x_j)$ are the marginal probability functions of discrete random variables X_i and X_j for a given performance range. Similarly, $p(x_i, x_j)$ is the joint probability for discrete variables X_i and X_j for a specified performance range. From $p(x_i, x_j)$, $p(x_i)$, and $p(x_j)$ the mutual information common to variables X_i and X_j can be calculated.

If variables X_i and X_j are independent, then $p(x_i, x_j) = p(x_i) \cdot p(x_j)$ and $I(X_i, X_j) = 0$, indicating that no information is shared. Larger values of $I(X_i, X_j)$ indicates that more information is shared between variables X_i and X_j. Given these relations, $I(X_i, X_j) \geq 0$.

The following example shows how mutual information is calculated for simplified simulation results. Consider the simulation results for two design variables framing type (FT) and glazing type north (GT_n). Note that mutual information calculations for only two variables are shown for 6 different building designs.

```
-- KEYVAR                                          | FIT
{:FT 1, :GT_n 5, :aspect 1.8, :azi -5.6, ...}|-2069.7
{:FT 1, :GT_n 5, :aspect 1.1, :azi -5.6, ...}|-1817.7
{:FT 1, :GT_n 4, :aspect 1.9, :azi  0.0, ...}|-1593.8
{:FT 1, :GT_n 5, :aspect 1.6, :azi 16.9, ...}|-1534.6
{:FT 2, :GT_n 4, :aspect 2.1, :azi 16.9, ...}|-1994.6
{:FT 2, :GT_n 5, :aspect 2.1, :azi 16.9, ...}|-1600.0
```

Listing 3.3: Results from above SQL query

The marginal probabilities of variables FT and GT_n are $p(FT = 1) = \frac{4}{6}, p(FT = 2) = \frac{2}{6}$ and $p(GT\_n = 4) = \frac{2}{6}, p(GT\_n = 5) = \frac{4}{6}$. Joint probabilities for these two variables are calculated as $p(FT = 1, GT\_n = 4) = \frac{1}{6}, p(FT = 2, GT\_n = 4) = \frac{1}{6}, p(FT = 1, GT\_s = 5) = \frac{3}{6}, p(FT = 2, GT\_n = 5) = \frac{1}{6}$. The mutual information shared between these two variables is:

$$I(FT, GT\_n) = \frac{1}{6}\cdot\log_2\left(\frac{\frac{1}{6}}{\frac{4}{6}\cdot\frac{2}{6}}\right)+\frac{1}{6}\cdot\log_2\left(\frac{\frac{1}{6}}{\frac{2}{6}\cdot\frac{2}{6}}\right)+\frac{3}{6}\cdot\log_2\left(\frac{\frac{3}{6}}{\frac{4}{6}\cdot\frac{4}{6}}\right)+\frac{1}{6}\cdot\log_2\left(\frac{\frac{1}{6}}{\frac{2}{6}\cdot\frac{4}{6}}\right) = 0.0441 \tag{3.3}$$

Finally, equation 3.4 describes the total information that design variable X_i shares with all other design variables for a given performance range.

$$I_i = \sum_{j=1}^{N} I(X_i, X_j) \qquad \text{where, } j \neq i \tag{3.4}$$

Note that deterministic searches work best on variables that are loosely coupled to other variables in the model, that is variables with low shared information. The identification and strategic searching of weakly interacting variables improves upon one shortcoming of population-based optimization searches such as EAs.

Information depends on the fitness of the set of design vectors used for the calculation. For example, in a building simulation problem, information calculated from the objective space for a set of design vectors which are evaluated in a range of annual energy consumption of $[800, 1200)$ MJ/m^2 would be different than information calculated from design vectors evaluated within $[400, 800)$ MJ/m^2. Mutual information tends to increase as EUI decreases since building designs with lower energy consumption tend to have more strongly coupled variables to achieve a given performance levels. As described in chapter 4, clustering methods exist to better visualize variable interactions.

Mutual information is used later in chapter 5.

3.4 Concept of Design: Energy Model

> Simplify, simplify, simplify—without sacrificing the truth
>
> –*Richard Feynman*

> With a good model comes discovery, with discovery comes understanding, with understanding comes control.
>
> –*K. Still, Crowd Dynamics*

This section highlights important aspects in calculating the energy consumption of a home in a cold climate. The descriptions in this section are not intended to be exhaustive and cover all topics involved in a cold climate energy model as this is outside the

scope of this thesis. The intent is to familiarize the reader with important design aspects of modelling heating and cooling loads and renewable energy generation for residential buildings. For detailed engineering calculations, refer to the EnergyPlus engineering documentation (DOE, 2011b). For more detailed information regarding the energy model refer to the research of O'Brien (2011); a modified version of this energy model was used for optimization case-studies. Modifications included: (i) inclusion of additional design variables (see below), (ii) modelling of windows and glazing using WINDOW 6 (LBNL, 2012), (iii) specialized control strategies for mixing of solar gains, (iv) life-cycle cost analysis using post-processing of energy simulation results, and (v) model updates to most recent version of EnergyPlus (v8).

Building energy models involve complex interactions between occupants, mechanical systems and interior and exterior environments, see Figure 3.14 which represents such energy flows in a generalized case. For example, interactions in air-movement and convective heat transfer are coupled to infrared radiation from solar gains and internal loads simultaneously while air-temperatures are modulated via mechnical equipment. Inevitably, some approximations must be made to achieve the necessary model resolution while retaining an appropriate level of model simplicity to estimate energy usage.

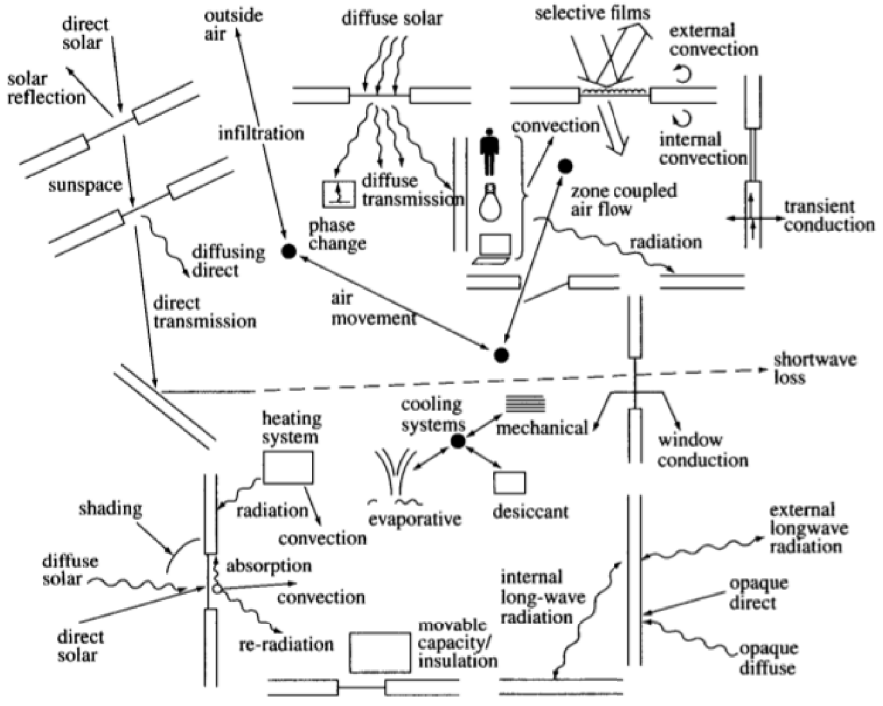

Figure 3.14: Energy flow paths in a typical building (Clarke, 2001)

3.4.1 Energy Balance

EnergyPlus uses a heat balance method to model heat transfer, see equation 3.5 (DOE, 2011b).

$$C_z \frac{dT_z}{dt} = \sum_{i=0}^{N_{CL}} \dot{Q}_i + \sum_{i=0}^{N_{surf}} h_i A_i (T_{si,others} - T_z) + \sum_{i=0}^{N_{zones}} \dot{m}_i C_p (T_{zi} - T_z) + \dot{m}_{inf} C_p (T_\infty - T_z) + \dot{Q}_{sys} \tag{3.5}$$

where:

$$\begin{aligned}
C_z \frac{dT_z}{dt} &= \text{Stored energy in zone air} \\
\sum_{i=0}^{N_{CL}} \dot{Q}_i &= \text{Sum of Convective Internal Loads} \\
\sum_{i=0}^{N_{surf}} h_i A_i (T_{si,others} - T_z) &= \text{Sum of heat transferred by convection from zone surfaces} \\
\sum_{i=0}^{N_{zones}} \dot{m}_i C_p (T_{zi} - T_z) &= \text{Heat transferred due to interzone mixing} \\
\dot{m}_{inf} C_p (T_\infty - T_z) &= \text{Heat transferred due to outdoor air infiltration} \\
\dot{Q}_{sys} &= \text{Supplied system load (heating or cooling)}
\end{aligned}$$

Note: (i) T_z is the zone air temperature; (ii) T_∞ is the outdoor air temperature; (iii) $C_z = \rho_{air} C_p C_T$ is the zone air capacitance; (iv) ρ is the zone air density; (v) C_p is the zone air specific heat; and (vi) C_T is the sensible heat capacity multiplier. The sensible heat capacity multiplier represents additional thermal mass, such as furniture, that is equilibrium with the zone air.

Assuming a centralized heating/cooling system and that the zone supply air flow equals the zone return flow in each zone, the system load is proportional to the difference of supply air enthalpy and zone temperature, or $\dot{Q}_{sys} = \dot{m}_{sys} C_p (T_{supply} - T_z)$.

The building load, $\dot{Q}_{load}$ is described by the sum of all right hand terms, excluding the system load. When the capacitance of the air is assumed to be zero, the heat balance is described by equation 3.5 reduces to $\dot{Q}_{sys} = \dot{Q}_{load}$.

The EnergyPlus solver allows for three potential heat balance algorithms: (i) Euler method; (ii) analytical solution; and (iii) third-order backward finite difference. The

third order backward finite difference method was selected to balance accuracy with computation time without requiring a prohibitively small time-step.

The derivative term in equation 3.5 can be substituted using a backward finite difference approximation. Note this could also be formulated using a central or forward difference in addition to a backward difference (Clarke, 2001).

$$\frac{dT}{dt} \approx (\delta t^{-1}) \left(T_z^t - T_z^{t-\delta t} \right) + O(\delta t) \tag{3.6}$$

where: $O(\delta t)$ is the truncation error; $T_z^{t-\delta t}$ is the node temperature at the previous time-step.

This first order finite difference model, called the Euler formation, suffers from higher-order truncation errors for larger time-steps. Taylor et al. (1990) recommended a third order finite difference method, see equation 3.7.

$$\left.\frac{dT_z}{dt}\right|_t \approx (\delta t^{-1}) \left(\frac{11}{6} T_z^t - 3T_z^{t-\delta t} + \frac{3}{2} T_z^{t-2\delta t} - \frac{1}{3} T_z^{t-3\delta t} \right) + O(\delta t^3) \tag{3.7}$$

where: $O(\delta t^3)$ is the third order truncation error; $T^{t-n\delta t}$ is the node temperature at the nth previous time-step. This implicit finite difference method reduces numerical error by incorporating results from the three previous time-steps.

This equation in combination with equation 3.5 forms the EnergyPlus heat balance engine.

3.4.1.1 Surface Heat Balance

This section describes the surface heat balance between air-nodes, exterior and interior surfaces. In EnergyPlus, a first-law heat balance approach ensures that energy is conserved over each time-step.

The surface heat balance equations require several terms: (i) conduction through a material; (ii) convection with surfaces and air nodes; (iii) longwave radiant interchange between surfaces; and (iv) shortwave radiant interchange between surfaces. Longwave interchanges include radiant exchanges between low-temperature (infrared) objects such as people, equipment, and other surfaces. Shortwave interchanges include exchanges such as solar radiation through transparent wall elements and other visible and ultraviolet

light sources.

EnergyPlus performs a surface heat balance on the following control volumes: (i) outside wall face; (ii) inside wall face; and (iii) inside air heat balance. The heat balances considered by EnergyPlus are shown below:

$$\dot{q}_{\alpha sol} + \dot{q}_{LWR} + \dot{q}_{conv} - \dot{q}_{ko} = 0 \qquad \text{(Outside Surface Heat Balance)}$$

$$\dot{q}_{LWX} + \dot{q}_{SWRL} + \dot{q}_{LWS} + \dot{q}_{ki} + \dot{q}_{sol} + \dot{q}_{conv} = 0 \qquad \text{(Inside Surface Heat Balance)}$$

$$\dot{Q}_{conv} + \dot{Q}_{CE} + \dot{Q}_{IV} + \dot{Q}_{sys} = 0 \qquad \text{(Air Node Heat Balance)}$$

where:

$\dot{q}_{\alpha sol}$**:** absorbed beam and diffused solar radiation flux on the exterior wall, W/m^2

$\dot{q}_{LWR}$**:** net long-wave radiative flux exchange with the air and exterior environment (incoming − outgoing), W/m^2

$\dot{q}_{conv_o}$**:** convective exchange flux with the outside air, W/m^2

$\dot{q}_{ko}$**:** conductive exchange flux into the wall from the exterior, W/m^2. Term is positive for heat flow into the wall

$\dot{q}_{ki}$**:** conductive exchange flux through the wall, W/m^2. Term is positive for heat flow into the wall

$\dot{q}_{LWX}$**:** net long-wave radiative flux exchange between surfaces (incoming − outgoing), W/m^2

$\dot{q}_{SWRL}$**:** net short-wave radiative flux exchange to surfaces from lights, W/m^2

$\dot{q}_{LWS}$**:** net long-wave radiative flux from equipment to surfaces in zone, W/m^2

$\dot{q}_{sol}$**:** transmitted exterior solar radiative flux absorbed at surfaces, W/m^2

$\dot{Q}_{conv_i}$**:** convective heat transfer from interior surfaces to the air node, W

$\dot{Q}_{CE}$**:** convective portions of internal loads (people, lights and equipment), W

$\dot{Q}_{IV}$**:** sensible loads caused by infiltration and ventilation (fresh air into zones), W

$\dot{Q}_{sys}$: heat transfer to and from HVAC system, W

Figure 3.15 shows the heat balance for the inside surface. The heat balance equation is coupled to the air-node heat balance through convective terms and the exterior heat balance equation through the exterior conduction term.

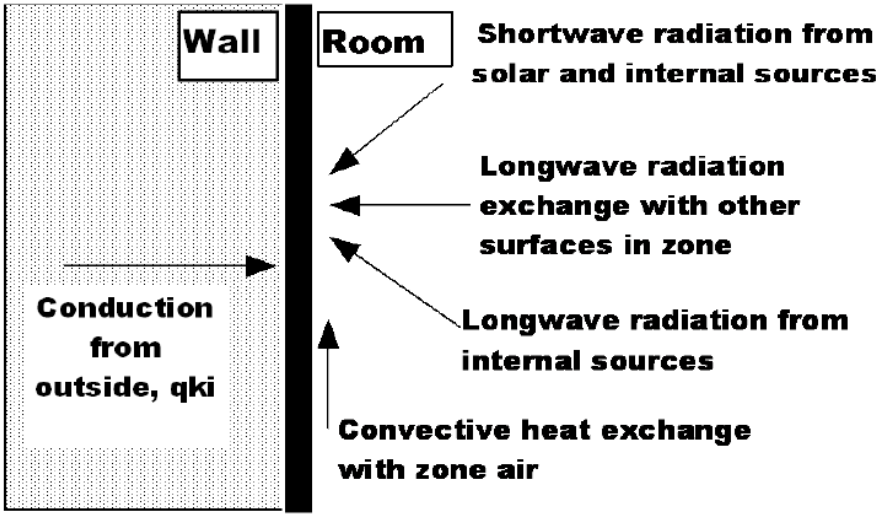

Figure 3.15: Inside surface heat balance diagram (DOE, 2011b)

Long-wave radiation exchanges between zone-surfaces are calculated using simplified view factors (DOE, 2011b). The calculation requires a matrix of view factor exchange coefficients for all exchange paths between surfaces. An assumption is made that all surface radiation properties are grey and all radiation is diffuse. Light introduced into the zone by mechanical equipment is defined using a radiative/convective split. Once the view factor coefficients are determined, the long-wave radiant exchange is calculated for each surface using (DOE, 2011b):

$$q_{LWX(i,j)} = A_i F_{i,j} (T_i^4 - T_j^4) \tag{3.8}$$

where: A_i is the area of surface i; $F_{i,j}$ is the view factor between surface i and j; and T_i, T_j is the temperature of surfaces i, j.

The distribution of short-wave radiation consists of beam solar radiation, diffuse solar radiation, and short-wave radiation from electric lights. EnergyPlus determines the amount of radiation absorbed by opaque surfaces, glass and shading layers, transmitted through windows into zones and transmitted back out to the exterior windows. Light transmitted into the zone is distributed to surfaces within the zone using view factors.

Material absorptance and reflectance properties determine how much energy is absorbed and reflected by a given surface. After a single bounce, light is assumed to be diffused to the zone surfaces.

EnergyPlus allows for the adaptive selection of convection coefficients depending on the flow regime (Beausoleil-Morrison, 2000). In EnergyPlus, convective terms are specified using the *SurfaceProperty:ConvectionCoefficients* object.

The conduction terms are formulated using transfer functions. EnergyPlus calculates Conduction Transfer Function (CTF) using the state-space method (DOE, 2011b). CTFs require special consideration if they are to be used for conductive heat transfer through massive wall elements (Beccali et al., 2005). This thesis uses implicit finite difference to describe conductive heat transfer through massive elements such as concrete walls and slabs; CTFs were used to described heat transfer through light-weight elements. As of EnergyPlus version 7.2, users can specify different heat transfer methods for each surface.

The CTF term for the inside-face is:

$$\dot{q}_{ki}(t) = -Z_o T_{si,\theta} - \sum_{j=1}^{nz} Z_j T_{si,\theta-j\delta} + Y_o T_{so,\theta} + \sum_{j=1}^{nz} Y_j T_{so,\theta-j\delta} + \sum_{j=1}^{nq} \Phi_j \dot{q}_{ki,\theta-j\delta} \qquad (3.9)$$

The outside heat flux relates conductive heat fluxes to current and past exterior surface temperatures and past heat fluxes

$$\dot{q}_{ko}(t) = -Y_o T_{si,\theta} - \sum_{j=1}^{nz} Y_j T_{si,\theta-j\delta} + X_o T_{so,\theta} + \sum_{j=1}^{nz} X_j T_{so,\theta-j\delta} + \sum_{j=1}^{nq} \Phi_j \dot{q}_{ko,\theta-j\delta} \qquad (3.10)$$

where:

X_j**:** Outside CTF, for surfaces $j = 0, \cdots, nz$

Y_j**:** Outside-Inside CTF, for surfaces $j = 0, \cdots, nz$

Z_j**:** Inside CTF, for surfaces $j = 0, \cdots, nz$

Φ_j**:** Inside CTF, for surfaces $j = 0, \cdots, nz$

δ: time step

T_{si}: Inside-face temperature, °C

T_{so}: Outside-face temperature, °C

$\dot{q}_{ki}$: conductive heat transfer on inside face, W/m^2

$\dot{q}_{ko}$: conductive heat transfer on outside face, W/m^2

EnergyPlus uses an integrative, simultaneous solver to calculate heat-balances between plant, building and systems modules, see Figure 3.16. The integrated solution manager relies on successive substitution iteration to reconcile energy supplies and demand between plant, building and systems modules. This solver is an evolved version of previous solvers which only allow unidirectional energy flows between modules such as DOE-2 (DOE, 2011b). For detailed heat transfer formulation using Fourier partial differential equations and finite difference refer to Clarke (2001).

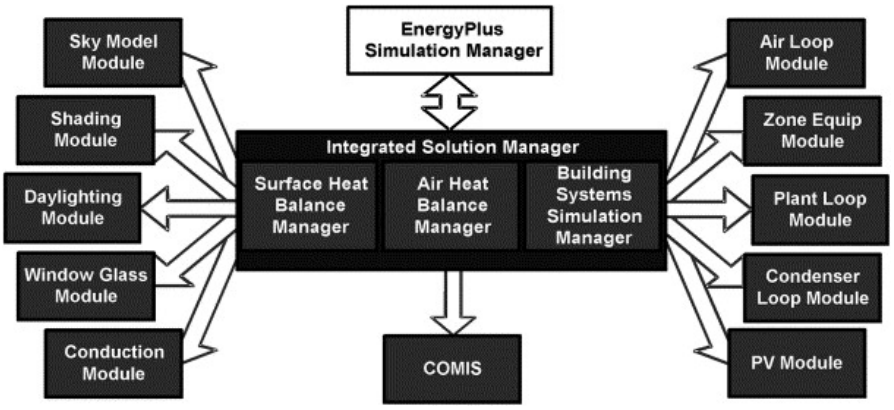

Figure 3.16: EnergyPlus Integrated Solution Manager (DOE, 2011b)

3.4.1.2 Sparse Matrix Solutions using Finite Difference

This section describes an alternative method of expressing energy balances using a finite difference method as used by ESP-r (Clarke, 2001). The purpose of this section is to exemplify an exploitable characteristic of energy balances in building simulation tools that can improve optimization algorithm convergence properties. Although EnergyPlus does not use sparse matrix solvers, the loosely-coupled relationship between heat balance nodes is equally applicable.

The heat balance equations can be solved simultaneously using matrix inversion. For example, equation 3.11 determines future air-temperatures for a single zone by multiplying a characteristic matrix to the present air-temperatures, see Figure 3.17.

$$A\theta_{t+\delta t} = B\theta_t + C = Z \tag{3.11}$$

where: θ_{n+1} is the temperature vectors at all nodes in the future time-step, θ_n is the temperature vectors of all nodes at the present time-step, A is the future time-step temperature coefficients, B is the present time-step temperature coefficients, and C are the boundary conditions for the zone. To solve for future node temperatures requires inversion, i.e. $\theta_{n+1} = A^{-1}Z$.

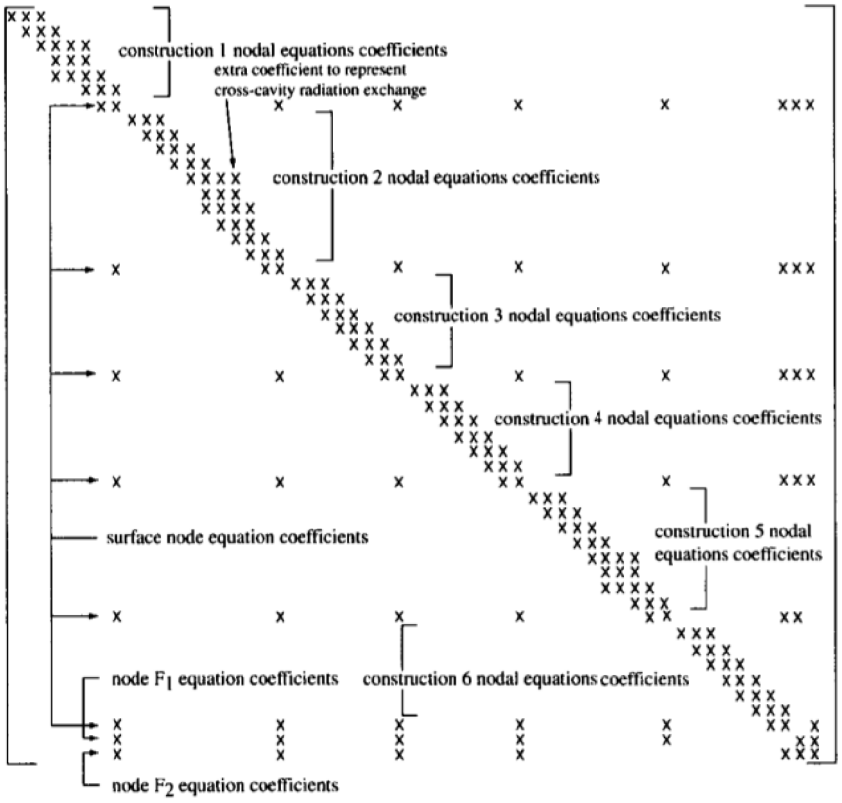

Figure 3.17: Matrix formation of future-time coefficients (A) for a single thermal zone, where $A\theta_{n+1} = B\theta_n + C$ (Clarke, 2001)

The characteristic matrix in equation 3.11 is N by N, where N is the number of temperature nodes. During a typical annual simulation, over five thousand matrix inversions are required for a simple single-zone model using one hour time-step (Clarke, 2001). Often, energy models require tens to hundreds of thermal zones.

The inversion of future temperature coefficient matrix is computationally intensive. However, specialized solvers can simplify the solution scheme since these matrices are sparsely populated. Sparse matrices are primarily populated with zeros meaning that nodes are largely loosely-coupled to other nodes; these matrices are more densely populated on the diagonal than on the upper and lower quadrants. Loosely-coupled systems are sometimes referred to as being approximately linear. In fact, the only reason that step-wise solvers work for energy simulation is because the building energy models are loosely-coupled and approximately linear. Tightly coupled systems typically require simultaneous solutions. ESP-r uses the sparse-matrix property to simplify numerical solutions (Clarke, 2001). Several thermal zones and potentially a mechanical system are partitioned and processed independently, see Figure 3.18.

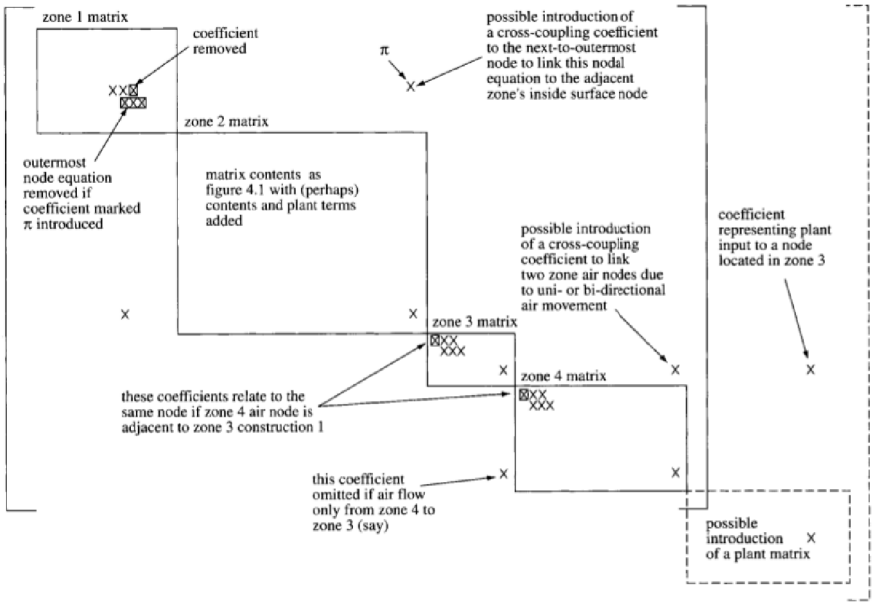

Figure 3.18: Sparse matrix for systems solution to building heat loss in four zone model (Clarke, 2001)

Note, nodes not marked by 'x' are zero. Building energy simulation can be viewed as the solution of interlocking of partitioned matrices. The fact that energy models are loosely-coupled can also expedite the optimization process. System matrices clearly show that some heat balance nodes are more tightly coupled than other nodes. This characteristic is later data-mined and exploited by a new proposed optimization approach. Optimization strategies to solve loosely-couple engineering problems are discussed in Chapter 5.

3.4.2 Energy Objective Function

This section describes the objective function used for energy-consumption optimizations.

The formal goal of an energy-consumption minimization study is to find a design variable vector, $\mathbf{x}$, such that:

$$min\{f(\mathbf{x})\} \tag{3.12}$$

where: $\mathbf{x}$ is the design variable vector $\mathbf{x} = (x_1, x_2, \cdots, x_N)^T$, in design space $\mathbf{X} \subset \mathbb{R}^N$; the objective or fitness function, $f()$, evaluates set of design variables onto an 'objective' vector $\mathbf{y} = (y_1, y_2, \cdots, y_M)^T$ where $f_i \in \mathbb{R}^M$, $y_i = f_i(\mathbf{x})$, $f_i : \mathbb{R}^N \rightarrow \mathbb{R}^1$ for $i = 1, 2, \cdots, M$, describes the objective or solution space $\mathbf{Y} \subset \mathbb{R}^M$; $min\{f(\mathbf{x})\}$ is subject to L constraints $g_i(\mathbf{x}) \leq 0$ where $i = 1, 2, \cdots, L$; feasible design vectors set $\mathbf{x}|g_i(\mathbf{x}) \leq 0$ form the feasible design space $\mathbf{X}^*$, and corresponding objective vectors set $\mathbf{y}|\mathbf{x} \in \mathbf{X}^*$ form feasible objective space $\mathbf{Y}^*$; for a minimization problem, a design vector $\mathbf{a} \in \mathbf{X}^*$ is Pareto optimum if no design vector $\mathbf{b} \in \mathbf{X}^*$ exists such that $y_i(\mathbf{b}) \leq y_i(\mathbf{a}), i = 1, 2, \cdots, M$.

The objective is to minimize the net-annual energy consumption of a near net-zero energy home. The objective function is the annual net-electricity consumption of the building, see equation 3.13. Sub-hourly time-steps of 15 minutes were used to solve energy balances in EnergyPlus.

$$f(\mathbf{x}) = Q_{heat}/COP_H + Q_{cool}/COP_C + E_{elec} - E_{PV} \tag{3.13}$$

where: $\mathbf{x} = (x_1, x_2, \cdots, x_N)^T$ is a design variable vector; $f(\mathbf{x})$ is the annual net-electricity consumption of the building (kWh); COP is the average annual coefficient of performance of the ground-source heat pump in heating and cooling mode, 3.77 and 2.77 respectively; Q is the annual heating and cooling load of the house (kWh); E_{elec} is the gross annual electricity consumption in lighting, appliances and plug-loads (kWh) and; E_{PV} is the electricity generated by the roof-top PV (kWh). When $f(\mathbf{x}) < 0$ this implies the net-generation of electricity, or a positive-energy house. Energy consumption calculations include both sensible and latent loads. Modelling of energy related aspects of a net-zero energy solar house are discussed in this following section.

3.4.3 Energy Model Details

This section provides and overview of influential energy modelling considerations. Influential design elements were identified partly by design of experiment techniques (Goos and Jones, 2011) such as significance tests within generalized linear models and partly from previous studies (Charron, 2007; O'Brien, 2011; Verbeeck, 2007; Wang, 2005).

3.4.3.1 Weather Data

Typical weather data was used for energy simulation purposes since real weather data for a thirty year period would be computationally prohibitive. Typical weather data is intended to use typical monthly weather based on measured weather data. EnergyPlus uses Typical Meteorological Year (TMY) version two weather data (DOE, 2011b). Canadian weather information is provided for 144 locations through the Canadian Weather Energy and Engineering Data Sets (CWEEDS); CWEEDS weather data contains typical weather for the period 1974–1993. Weather data was recorded typically on an hourly basis; EnergyPlus interpolates this information down to sub-hourly time-steps.

In BPS, TMY weather data is intended to calculate building loads during a typical weather period; TMY data is inappropriate to use for peak mechanical system sizing. Previous research indicated that building simulation results using TMY data is comparable to using real weather data over a yearly period (Crawley and Huang, 1997). It was assumed that an oversizing factor of 10% was used to size heat pump equipment to account for additional capacity during peak weather periods.

3.4.3.2 Occupant Behaviour and Internal Heat Gains

Energy related occupant behaviour is an important, but challenging aspect to incorporate into building simulation. Although occupant behaviour is not actually a design variable, it greatly influences on energy consumption. For example, energy-related occupant behaviour accounted for 37% of ÉcoTerra's gross energy consumption (Doiron et al., 2011).

Monitoring of energy consumption and occupant feedback is an important energy conservation measure in a NZEH. In the ÉcoTerra house, monitoring identified that the occupants had installed a 5 kW of electric baseboard heaters in the garage space

which had doubled their instantaneous electricity consumption when in use. This behaviour was simple to correct after the occupants were made aware how much electricity was being consumed.

In this thesis, the term 'energy related occupant behaviour' considers indirect energy consumption related to occupant behaviour. This includes electricity consumption in appliances, Domestic Hot Water (DHW) and lighting. The goal is to model differences in total energy consumption based on average Canadian consumption profiles and not to model consumption differences due to individual occupants. This section describes an approach to examine the affect of energy related occupant behaviour on NZEH design based on research on residential energy consumption in Canada. Energy related occupant behaviour is a significant modelling aspect since electricity consumption will dictate the sizing of roof-based PV in a NZEH.

Ideally, monitored data from a large sample of NZEHs would be preferred to estimate energy related occupant behaviour for a given location. Since such data was not available, usage scenarios were created from published data. Previously published hourly occupancy, domestic hot-water (DHW) loads, appliance and lighting usage profiles were used (Armstrong et al., 2009). These were determined from monitored data specific to Canadian housing stock. The amplitude of energy-use profiles were normalized to match published consumption data for lighting, DHW, and appliance loads (NRCan-OEE, 2009). In 2009 Canadians used, on average, 95 kWh/m^2 of total energy for lighting, DHW and appliances. An assumption was made that an above average user of lighting, was also an above average consumer of DHW and appliance loads and vice versa.

Peak electricity profiles suggested by Armstrong et al. (2009) were used, see Figure 3.19. In the figure, a high energy users uses 150% of the Canadian national average. An average consumer uses 100% of the national consumption average. A low energy user consumes 50% of the national average. For this thesis, a lower bound of 50% for DHW, appliance and lighting energy consumption was selected based on monitored data from the ÉcoTerra house. An upper bound of 100%, indicating an average Canadian, was chosen for an electricity consumption profile.

Total consumption profiles were deconstructed into internal heat gain profiles, see

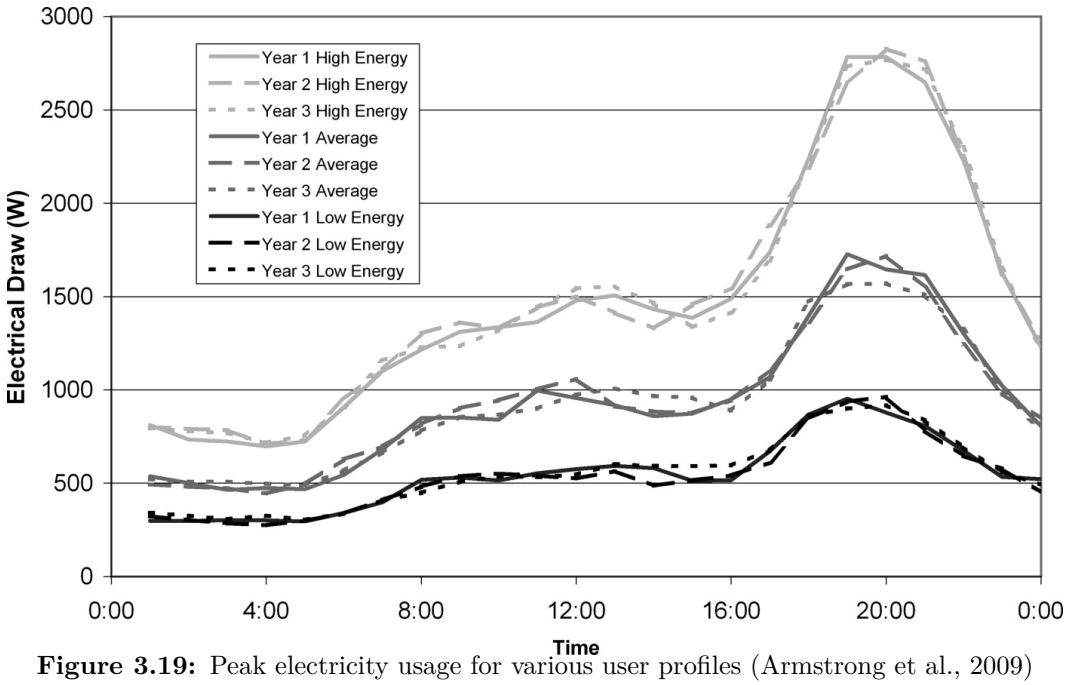

Figure 3.19: Peak electricity usage for various user profiles (Armstrong et al., 2009)

Figure 3.20.

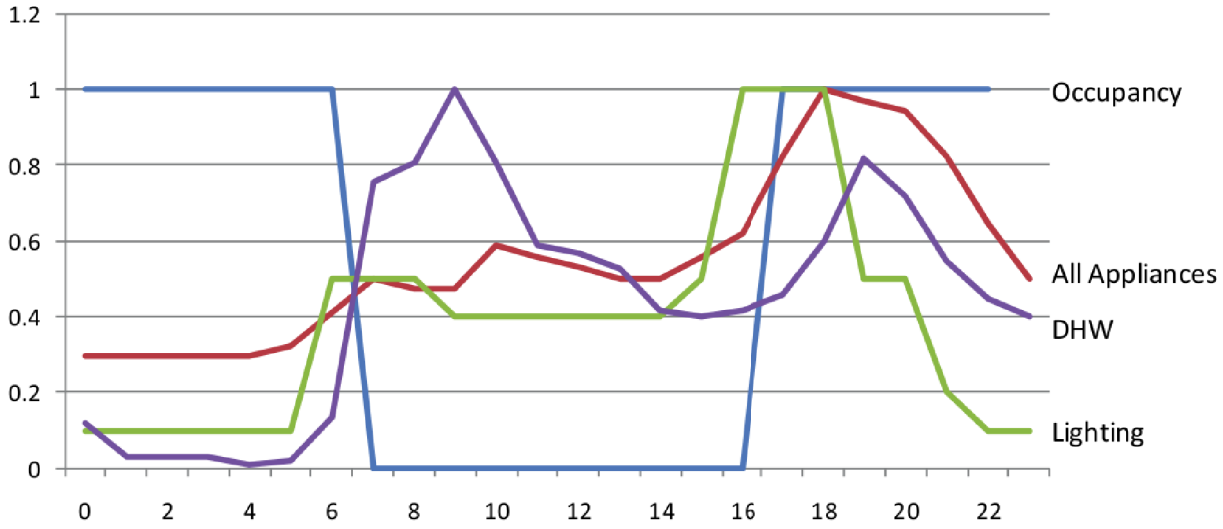

Figure 3.20: Breakdown of occupant loads into daily internal gain profiles (O'Brien, 2011)

Phantom loads refer to baseline electricity used for stand-by power in minor and major appliances, such as electronic devices, wires and appliances. Armstrong et al. (2009) found the average Canadian home had 65 Watts of standby loss. Occupants were assumed to generate 120 Watts of heat per occupant. Simulations assumed a family of four (two parents, two children) occupying the home 50% of the day, see occupancy schedule in Figure 3.20.

3.4.3.3 Building Geometry and Solar Orientation

> In houses that look towards the south [in the northern hemisphere], the sun penetrates the portico in winter.
>
> –*Socrates*

This section describes the interplay between solar orientation and building geometry. Although Greek philosophers have documented proper solar orientation over 2500 years ago, interactions between orientation and geometry and other design aspects are still essential to solar building design today.

In the energy model, rectangular geometries were preferred for optimization studies. All floor plans were specified using the total floor area and an aspect ratio. From these two variables, widths and lengths of the building were calculated. In the energy model, a one or two story floor plan could be specified. Results are relevant to other more complex geometries if both buildings are thermodynamically equivalent, or have identical directional heat-loss surfaces, self-shading characteristics and internal air-volumes. Previous research related to building shape optimization (Wang, 2005) indicated that rectangular floor plans are comparable to optimal shapes such as pentagonal plans; exotic shapes such as L-shaped or U-shaped floor plans performed poorly due to their large heat-loss surface areas compared to other more compact shapes. Furthermore, rectangular shaped buildings can easily be integrated in to existing grid-based urban environment.

Solar orientation is an important factor in modelling a solar home. Since simulation studies occur in Canada, south-facing implicates orientation towards the sun, or equatorial-facing. The orientation of the solar home determines the available solar fraction and the peak solar electricity generation using roof-based PV panels. The solar fraction refers to the percent of heating loads offset using solar gains. Figure 3.21 shows how orientation affects solar gains and the time of peak temperature gains in a solar house (Henderson and Roscoe, 2010).

The following sections discuss several envelope modelling considerations for exterior above-grade walls, below-grade basement walls, basement slabs and the ceiling envelope.

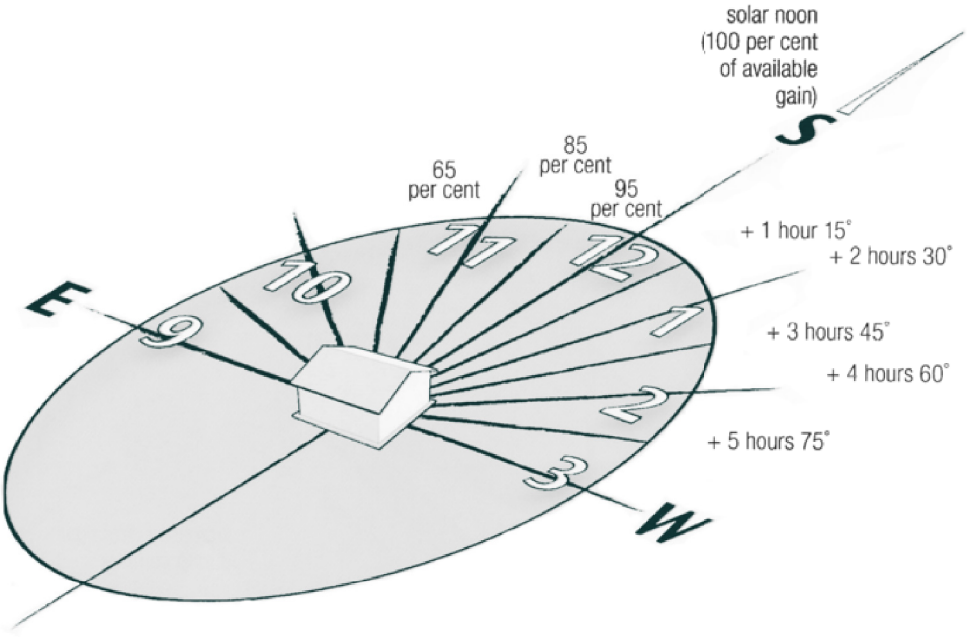

Figure 3.21: Relation of azimuth to peak solar gains (Modified from Henderson and Roscoe (2010))

3.4.3.4 Above-grade Walls

This section describes the wall construction used for this thesis, see Figure 3.22. A cold climate construction consisted of two inches of rigid extruded polystyrene insulation, two 2x4" walls filled with dense-pack cellulose insulation. The advantage of having exterior rigid insulation is that thermal bridging is eliminated by using a continuous layer of insulation continued from below the slab, up the basement walls to the ceiling envelope.

A double 2x4" wall was considered for all designs. This wall construction has several advantages, a double 2x4" wall: (i) can be insulated to any amount by increasing the spacing between the two frames; (ii) is simple to air-seal; (iii) is roughly cost equivalent to a 2x6" wall due to 2x4"s studs being less expensive than 2x6" studs; and (iv) has few thermal bridges due to use of dense-packed cellulose insulation. Figure 3.23 shows the framing method used in a double 2x4" wall (courtesy of Habitat Studio).

The following assumptions were made when modelling wall envelopes: (i) a rain-screen using naturally ventilated exterior brick prevented rain from saturating the wall envelope; (ii) the envelope was sufficiently air-tight such that moisture in air transport through the wall cavity into the zone could be ignored from cooling load calculations; (iii) an interior vapour barrier decoupled the majority of moisture transfer mechanisms;

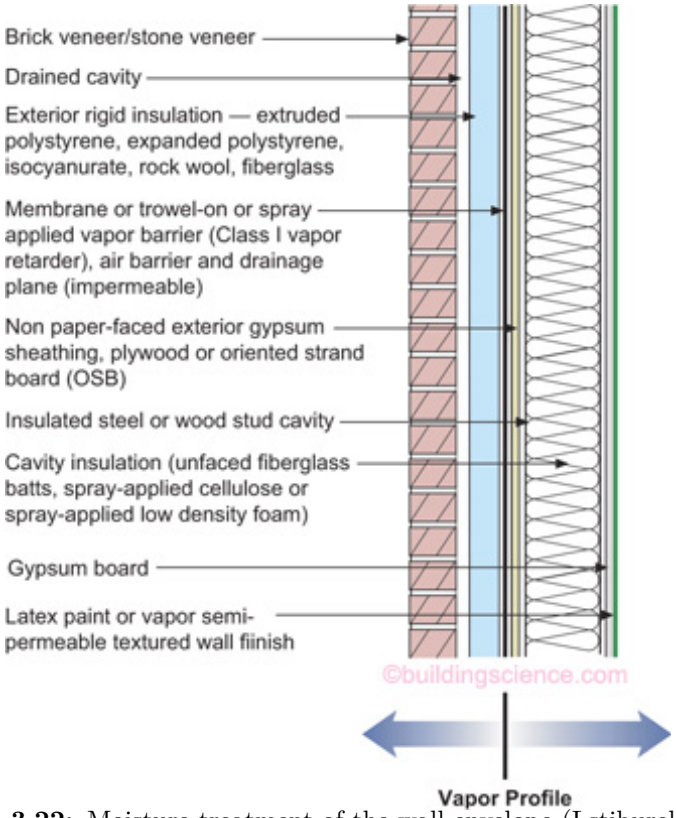

Figure 3.22: Moisture treatment of the wall envelope (Lstiburek, 2009)

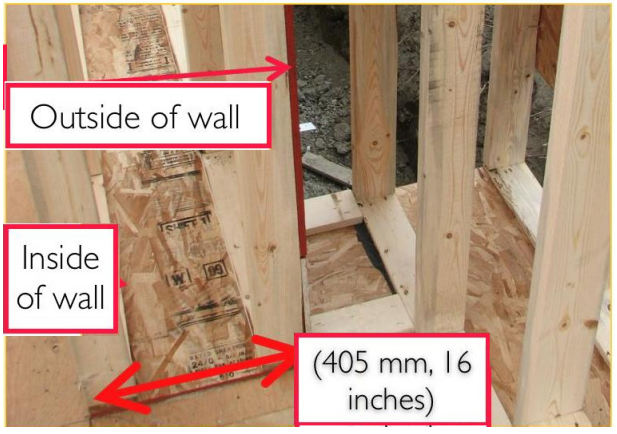

Figure 3.23: Construction of a double 2x4" wall (courtesy of Habitat Studio)

and (iv) two inches of rigid insulation was sufficient to keep the interior surface of the rigid foam above the dew-point temperature.

3.4.3.5 Ceiling Envelope

Ceilings heat loss is typically the most significant envelope due to heat stratification in a multi-story home. Ceiling envelopes require moisture control and attic ventilation to control potential condensation issues. The following assumptions were made when modelling the ceiling envelope: (i) 3.5 inches of closed-cell polyurethane spray foam provided air-sealing and decoupled moisture transfer to the attic to the ceiling; (ii) remaining level achieved using loose-pack blown-in insulation; (iii) eve compression was eliminated using raised heel trusses, see Figure 3.24; and (iv) attic was ventilated at 6 ACH using baffles and ridge vents to prevent moisture build-up in the attic space.

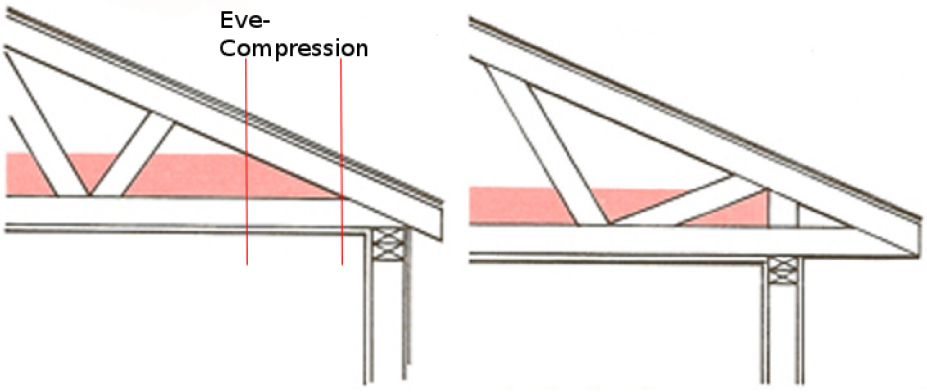

(a) Section of Common Roof Truss (b) Section of Raised Roof Truss

Figure 3.24: Section of common and raised roof trusses

The presence of eve-compression in a ceiling envelope, shown in Figure 3.24, results in greater heat loss near the top of walls than through mid-centre attic sections. Eve-compression can cause a reduction in the effective insulation value of the ceiling envelope and moisture damage through ice-damns. Raised heel trusses allowed for a uniform layer of insulation throughout the attic space.

3.4.3.6 Below-grade Walls

Basement heat-loss is thought to account for 10–40% of total heat-loss in Canadian housing (Beausoleil-Morrison, 1996). Since basement heat-loss depends on insulation levels and the presence of thermal bridging, one-dimensional heat-loss calculations do

not result in accurate energy consumption estimates. Modelling of below-grade surfaces is challenging due to: (i) seasonal time-lag thermal effects; (ii) moisture on wall surfaces; and (iii) thermal bridging which necessitates three-dimensional heat-transfer models.

Basements were insulated using exterior and under-slab rigid-foam insulation, see Figure 3.25.

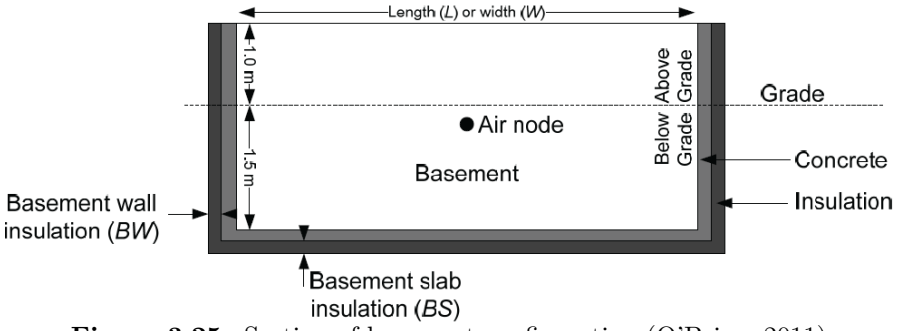

Figure 3.25: Section of basement configuration (O'Brien, 2011)

As described in O'Brien (2011), coupling of basement walls to the ground was accomplishing using a regression model of 2D heat-loss results from the BASECALC tool (Beausoleil-Morrison, 1996).

The following assumptions were made when forming regression models: (i) exterior insulation was covered using a water-proof membrane decoupling moisture exchange from outside to inside; (ii) concrete thickness: walls 0.2 meters, slab 0.1 meters thick; (iii) no windows in basement walls; (iv) constant basement air temperature of 20 °C; (v) basement wall height: one meter above-grade, 1.5 meter below-grade; (vi) solar gains in main-floor were recirculated using a fan throughout the basement;

3.4.3.7 Thermal Zoning

Thermal zoning is an important determinant of energy consumption. A trade-off exists between model simplicity and accuracy. Simplified one-zone models tend to under predict energy consumption due to the assumption that internal and solar gains are well mixed. A model with many zones requires significantly more computational resources due to coupling between zones. In addition, including more thermal zones may not improve the accuracy of energy simulation results. O'Brien (2011) found that a three zone model was sufficient to encapsulate heat transfers in a solar house, see Figure 3.26.

The energy model uses three thermal zones: a south-facing zone; a north-facing

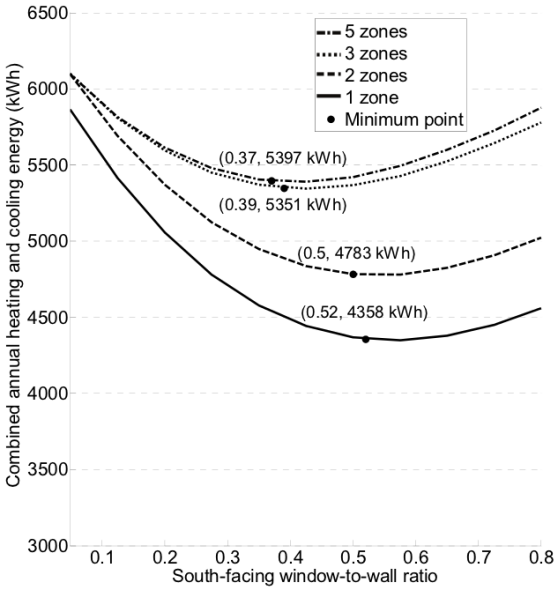

Figure 3.26: Effect of thermal zoning on electrical energy-consumption (O'Brien, 2011)

zone; and a basement zone. An additional unconditioned roof zone couples roof heat-gains to the adjacent ceiling. Thermal gains from plug-loads and solar radiation are re-distributed through conditioned spaces using an air-flow network. A trade-off between air recirculation and electricity cost for fans was modelled; thus, the recirculation rate between thermal zones is considered as an optimization variable.

3.4.3.8 Thermal Mass

Thermal mass can reduce peak heating and cooling loads of a solar heated house. Passive storage of solar gains during periods of peak solar gains acts like a thermal capacitor. An additional advantage is that surplus solar gains can be stored and discharged during later periods. This reduces the reliance on mechanical systems for heating. Stated simply, thermal storage regulates air-temperature fluctuations and can reduce over-heating and over-cooling. From the perspective of frequency domain analysis, thermal mass acts as a low-pass filter to moderate high-frequency variations in solar or plug-load heat gains (Athienitis and Santamouris, 2002).

The primary form of thermal mass is concrete in direct contact with solar gains through glazing. Warmer floors then reradiate to the surrounding cooling walls and furniture. It is well documented that a large surface area of thermal mass is more effective than a concentrate volume (Candanedo, 2011; Charron, 2007; Tzempelikos, 2005). Thus,

the energy model just considers thermal mass on concrete floors and on the vertical wall surface separating the south and north zones. An assumption was made that all floors were not covered with carpets or flooring. It is well known that the effectiveness of thermal mass is compromised if covered (Charron, 2007; Chiras, 2002). Concrete floor and wall thickness was considered as an optimization variable. All concrete was assumed to have the following properties: (i) conductivity of 1.95 W/mK; (ii) density of 2240 kg/m^3; (iii) specific heat of 900 J/kgK; (iv) emissivity of 0.5; (v) reflectance of 0.9; and (vi) absorptance of 0.7.

A secondary form of mass is the thermal capacitance of air and other massive objects in the thermal zone such as furniture. The energy model uses an air capacitance multiplier of 20, see variable C_T in equation 3.5, to add additional thermal inertia to the environment as recommended by the EnergyPlus engineering guide (DOE, 2011b).

Centralized thermal storage in the form of seasonal storage, water cisterns, or ground storage is outside the scope of this thesis. For further information refer to IEA Annexes 21–26 (IEA, 2013).

3.4.3.9 Comfort Models

This section describes the assumptions made to consider acceptable comfort in energy simulations.

Popular comfort models, such as the Fanger model (1971), require several unknown parameters such as metabolic rates, clothing insulation levels as well as known parameters from simulation such as air-speeds, relative humidity levels and mean-radiant temperatures. In the Fanger model, comfort is calculated using a predictive mean vote on a scale from -4 to 4 where 0 is the 'ideal' comfort level. This model is static since occupants cannot interact with their environment to adapt their comfort. Adaptive comfort models (Nicol and Humphreys, 2002) assume that occupants can modify their clothing and adapt to seasonal temperatures. These models are appropriate for residential environments or office environments where individualized environmental control is provided. Adaptive models were not considered since they require additional uncertain information to make comfort calculations and thus were outside the scope of this thesis.

There is on-going debate about whether comfort should be considered an optimiza-

tion criterion or as an optimization constraint. One perspective argues that comfort is quantifiable in early simulations and a given design can be more comfortable than another, so comfort is an added objective function in a optimization study. The other perspective is that comfort models are too uncertain since they depend on hourly values of temperature, air velocity, relative humidity, intra-zone mixing and occupant clothing levels, all variables which are difficult to predict over an annual period.

Perhaps comfort is better handled as an optimization constraint and that mechanical systems should be sized to ensure that heating and cooling setpoints are satisfied throughout the simulation period. The automatic sizing of mechanical systems to meet setpoints under peak seasonal conditions actively constrains air-temperatures to an acceptable level. Thus, comfort in this thesis is not considered directly but indirectly using zone air-temperatures modulated by HVAC systems. This approach has the following advantages: (i) all designs considered have acceptable air temperature throughout the simulation period but may require larger HVAC systems; and (ii) the relationship between energy consumption and air-temperature setpoints can be examined. The detailed simulation of models which do not achieve acceptable set-point schedules is considered a waste of computational resources. Active constraining of comfort enables the data-mining of all previous simulations to identify interesting design features. If comfort was considered as an objective function, only a subset of simulations would be usable for data-mining. This approach assumes that occupants will adapt clothing levels or metabolic activities to air temperature setpoints.

The heating and cooling needs are determined via a setpoint schedule. Models used nightly setback schedules during the evening (10pm–7am). Cooling systems were enabled from May to September. The lower and upper temperature setpoints define the temperature dead-band, i.e. the range of temperature were no heating or cooling interventions are required, see Figure 3.27.

The temperature dead-band is a major determinant of energy consumption and occupant comfort. If the dead-band is narrow, then an over-reliance on short-cycling of mechanical systems is required to satisfy temperature schedules and charge passive thermal storage. As shown in Figure 3.27, a wide dead-band allows for free-floating conditions but at the risk of occupant discomfort. As previously mentioned, the implementation of

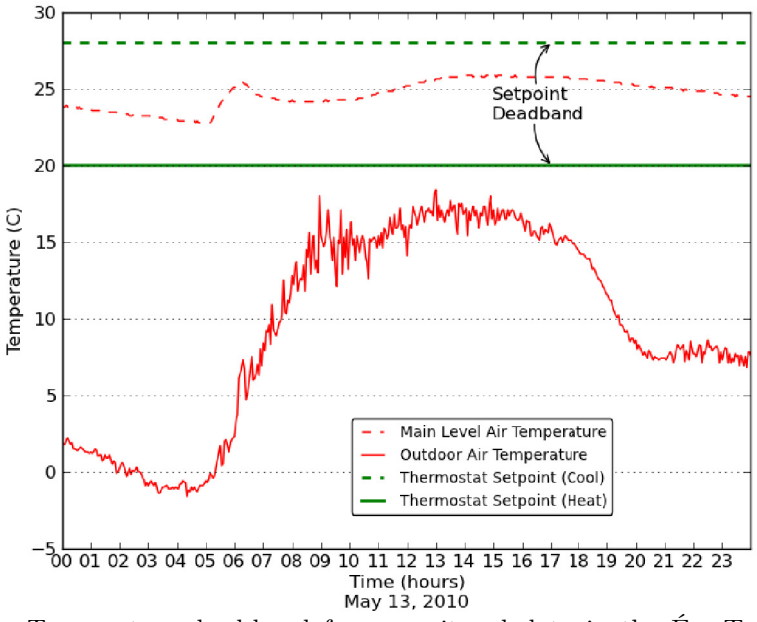

Figure 3.27: Temperature dead-band from monitored data in the ÉCOTERRA solar home (Modified from Doiron (2010))

thermal comfort models in the energy methodology is outside the scope of this thesis. Comfort is considered indirectly by controlling mean radiant air-temperatures.

3.4.3.10 Window, Overhangs and Blind models

This section describes modelling details related to window, blinds and overhangs. The combination of these three technologies determines the utilization of impinging, useful solar radiation on the transparent facade. A solar optimized house uses solar gains during the heating seasons to offset heating loads and protects the interior from overheating during the cooling season. The WWR is defined as the area of glazing and framing relative to the total facade areas for each directional wall surface.

WINDOW 6 was used to specify glazing properties (LBNL, 2012). EnergyPlus can use WINDOW 6 results to specify several important window system properties such as: (i) average window-frame heat transfer properties from 2D calculations; (ii) inside and outside projection distances; (iii) conduction and optical properties due to different gas mixes (up to three gases); (iv) hemispherical emissivity properties for each pane; (v) edge conduction properties; and (vi) glazing optical properties for different incident angles and solar spectrum wavelengths.

Table 3.5 describes window types available in the energy model. In EnergyPlus, windows are defined by construction layers and the optical properties of the glazing unit. Two window framing types, wood and vinyl could be specified as optimization variables (wood denoted by 1, vinyl by 2). Window sizing was calculated from facade area and the WWR fraction. Windows were grouped into a single window object for each wall surface. Note windows were not modelled in the basement zone.

Name (GT_i index)	DGLEAR (1)	TGCLAR (2)	TGLEAR (3)	QGLEAR (4)
Outside Layer	Clear 3mm	Clear 3mm	Clear 3mm	Clear 3mm
.	Argon 12.7 mm	Argon 12.7 mm	Argon 12.7 mm	Argon 12.7 mm
.	Low-e 3.8mm	Clear 3mm	Clear 3mm	Low-e 3.8mm
.		Argon 12.7 mm	Argon 12.7 mm	Argon 12.7 mm
Inside Layer		Clear 3mm	Low-e 3.8mm	Low-e 3.8mm
				Argon 12.7 mm
				Low-e 3.8mm
Air space between inner glass layer and shade (if shade present)	5 cm air space	5 cm air space	5 cm air space	5 cm air space
Shade (if present)	Reflective roller shade	Reflective roller shade	Reflective roller shade	Reflective roller shade
U-value (W/m^2K)	1.499	1.629	1.055	0.525
Edge U-value (W/m^2K)	2.625	2.680	2.473	2.363
SHGC (normal incidence)	0.690	0.685	0.612	0.533
SHGC (hemispherical average)	0.601	0.579	0.516	0.441

Table 3.5: Window properties used in energy model (O'Brien, 2011)

Roller shading with visible spectrum reflectance of 0.8, emissivity of 0.9 and conductivity of 0.3 W/m^2K were used. Roller shades were automatically deployed if exterior solar radiation on the exterior window surface exceeded 150 W/m^2 and if exterior temperature on the window exceeded 20 °C. These values ensured that blinds were closed if there was potential for zone overheating. This was determined via a previous simulation study (O'Brien, 2011).

Depending on the orientation of the main solar collecting surface, glazings could account for a net-heat gain over the heating season. This indicates that more solar radiation is gained over the simulation period than lost due to heat transfer. Figure 3.28 (O'Brien, 2011) shows all double and triple glazed windows described in Table 3.5 have net-solar gains if oriented south.

Exterior shading prevents unwanted solar gains during the cooling season. Deployable canvas window awnings provided shading for south facing windows, see Figure 3.29. The overhang distance was calculated using maximum and minimum solar angles or

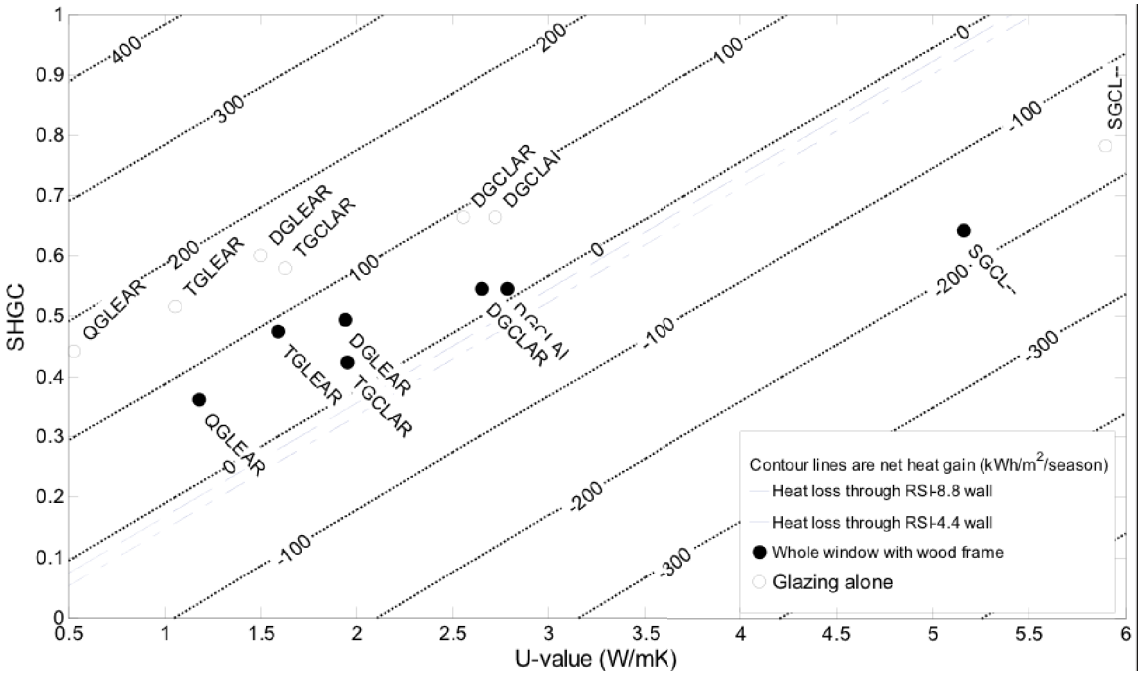

Figure 3.28: Heat-gain for various window types during heating season (O'Brien, 2011)

within the optimization algorithm. Charron (2007); Wang (2005) commented that overhangs on east and west-facing facades provided minimal utility due to low solar angles, and thus were ignored.

Figure 3.29: Window awning

3.4.3.11 Infiltration and Exfiltration

Infiltration is the rate at which air is exchanged between the inside of a building enclosure and the outdoors. In northern climates, air-tightness is a strong indicator of

how much energy a building will consume, especially during peak heating and cooling seasons. One air-change per hour indicates that the air volume in a building is replenish with fresh outdoor air every hour. Uncontrolled air flow during peak heating season can significantly increase heating loads. The adage of home builders is to 'build tight, ventilate right' encouraging builders to build as air-tight as possible and use mechanical equipment to control air into the building.

Infiltration is most commonly measured after post-construction using a blower-door test. To calculate air-tightness, one must calculate the air-volume of the building, then measure the air-flow entering the building at various air-pressures. It is recommended that infiltration be measured by both pressurizing and depressurizing the building (ASHRAE, 2011a), see Figure 3.30 (Krarti, 2011). With this information the equivalent leakage area, infiltration at 50 Pa and natural infiltration can be calculated.

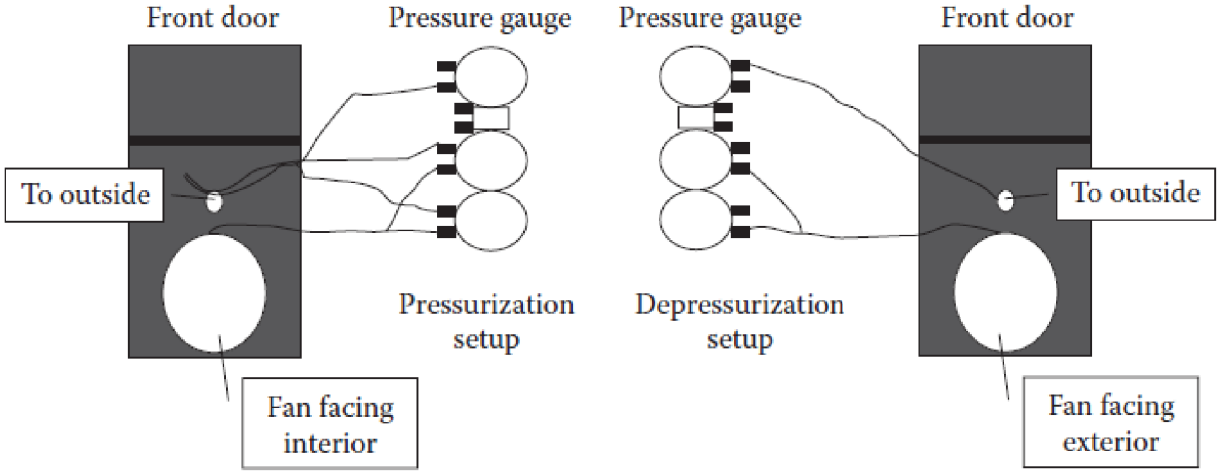

Figure 3.30: Blower door setup (Krarti, 2011)

Figure C.2, Appendix C, shows blower door measurements for 180,000 homes in Canada; this data was provided by Natural Resources Canada (NRCan) and collected through the ecoEnergy programme (NRCan, 2012). The most probable infiltration measurement in this dataset was 3.5 Air Changes per Hour (ACH) at 50 Pa. The tightest home in this dataset had an air-tightness of 0.48 ACH at 50 Pa. These values determined the limits of air-tightness in the energy model.

One accurate infiltration method supported by EnergyPlus is the AIM-2 (Walker and Wilson, 1998) model to calculate infiltration for a given exterior wind speed and weather conditions using an assumed or measured air-flow rate (DOE, 2011b).

Inter-zonal air mixing was considered using a design variable, *zone_mix*. It was possible to recirculate air between thermal zones using a fan. However, the fan consumed electricity proportional to the cube of the fan speed. This lead to an interesting interaction which allowed the energy model to effectively behave like a single thermal zone if a sufficient amount of electricity was consumed for air recirculation.

Exfiltration refers to the intentional introduction of fresh air for ventilation purposes. Fresh air can be provided by depressurizing the building using bathroom and kitchen fans or control exhaust through heat-exchange process in a heat-recovery ventilator.

ASHRAE 62.2 standard (ASHRAE, 2011a) for residential ventilation requires: (i) 8 L/s per person; (ii) additional 0.1 L/s per square foot of floor area; (iii) CO2 concentration in indoor air do not exceed 700ppm; and (iv) satisfies 80% or more people. Federal programs in Canada simplified this requirement to 0.3 ACH including mechanical and natural sources of air during occupied periods (NRCan, 2012). This requirement was imposed during energy simulations. This requirement allows for some buildings not to have ventilation equipment if they are not air-tight; very air-tight buildings require HRVs to satisfy fresh air requirements. An HRV with an efficiency of 60% was used to provide 0.3 ACH of fresh air during occupied periods.

3.4.3.12 Renewable Energy Generation using Photovoltaic Panels

> "If each energy quantum of the exciting light releases its energy independently from all others to the electrons, the distribution of velocities of the electrons, which means the quality of the generated cathode radiation, will be independent of the intensity of the exciting light; the number of electrons that exits the body, on the other hand, will, in otherwise equal circumstances, be proportional to the intensity of the exciting light."
>
> –*Albert Einstein on the Photoelectric Effect (1905)*

Electrical generation via PV panels was the primary source of renewable energy. Advantages of PV panels include: (i) rapidly decreasing costs due to a surplus international supplies and streaming-lined manufacturing; (ii) electricity has more applications than process heat from solar thermal; and (iii) electricity can be stored and grid-distributed.

Photovoltaic panels use the photoelectric effect (Einstein, 1905) to generate electricity. The photoelectric effect is a quantum phenomena where an absorbed photon in a material frees a photo-electron. Photons can only be absorbed if their energy exceeds the

band-gap of the material. Multi-junction PV can absorbed multiple photo-electrons at different wavelengths. In PV cells, electrical conduits conduct photo-electrons through an inverter and to battery storage or the grid.

Day4 Energy PV polycrystalline silicon modules with 15% efficiency (Day4Energy, 2012) were used in the model. In some chapters, variable cell efficiency, roof slope and roof coverage is considered in optimization studies. The number of panels was calculated using the allowable roof area. The panels were wired to stay within the max voltage and current characteristics of the inverter. PV modules were fixed to the roof surface—tracking modules were not considered. The allowed PV area was dictated by the slope of the gable roof and fractional PV area; other roof types such as hip-roofs were not considered. It was assumed that all electricity was exported to the grid. No electrical storage devices were considered. It was assumed that the panels were not self-shaded and that no peripheral shading such as trees existed.

Since the panels are installed on a potentially hot roof surface, a one-diode model was used to couple PV cell efficiency to module temperature, see Figure 3.31. It was assumed that cell efficiency decreases over time.

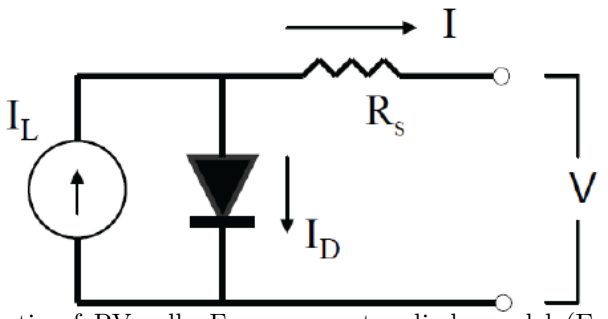

Figure 3.31: Schematic of PV cell: Four parameter diode model (EnergyPlus engineering manual, (DOE, 2011b))

Production losses due to poor electrical connections, snow coverage dust coverage are presently thought to account for an electrical loss of only 5% of total electricity production (Thevenard et al., 2010; Thevenard and Pelland, 2011). For this thesis, these losses were ignored.

3.5 Concept of Design: Cost Model

Cost is a primary factor in the economic viability of any new technology, especially capital intensive project such as building design. Including initial and operating costs as an additional objective function in NZEH performance evaluations results in a more complex and non-intuitive solution space. Navigating this problem space using trial and error simulation strategies is burdensome. In fact, previous researchers attempting to do so have commented that as many as 10,000 building simulations using parametric runs was insufficient to find the optimal design (Wright and Farmani, 2001). However, the exploration of such multi-objective optimization problems could be achieved using an algorithmic approach such as an EA.

This section describes the cost objective function used to determine a proposed designs cost effectiveness. The primary source for material and labour costs is the most recent RSMeans cost catalogue for residential construction (RSMeans, 2013). The cost analysis presented in this section is an *incremental cost analysis*. This means that costs are only considered valid with respect to a reference building, such as the reference building described in chapter 7. Considering incremental costs relative to a reference building greatly simplifies the life-cycle analysis, see Appendix C. Detailed costing is not required for all aspect if they are identical in the actual and reference building. For example, land acquisition, building inspection and excavation costs can be ignored. One disadvantage of this approach is that the life-cycle cost of the actual building is valid only if compared to a particular reference building. An uncertainty and sensitivity analysis of the cost model is conducted in Appendix A.

3.5.1 Cost Calculation Procedures

ASHRAE (2011c) recommends that economic evaluations be performed with in a life-cycle analysis. A detailed LCC analysis involves the following terms (Doty and Turner, 2012):

$$\mathrm{LCC}_{NPV} = C_{NPV} + \mathrm{O\&M}_{NPV} + E_{NPV} - S_{NPV} - I_{NPV} \tag{3.14}$$

where: C_{NPV}: represents capital costs of materials; $\mathrm{O\&M}_{NPV}$: is non-energy related

operations, maintenance and replacement costs; E_{NPV}: represents operational energy costs; S_{NPV}: is the salvage or residual value; I_{NPV}: is the income generated through incentives such as feed-in tariffs.

The Net-Present Value (NPV) of each term is calculated using (Doty and Turner, 2012):

$$\text{NPV} = \sum_{t=0}^{N} \frac{C_t}{(1+a)^t} \tag{3.15}$$

where: C_t: Net-cash flow at time, t (Net meaning $C_t = cash_{out} - cash_{in}$); a: is the minimal acceptable rate of return; and N: number of years considered in the life-cycle (t=0 is the present year).

If $NPV = 0$, the investment is considered to be cost neutral over the considered life-cycle. For this thesis, $NPV < 0$ is considered to be a profitable opportunity, and if $NPV > 0$, the investment is considered to unprofitable over the evaluated life-cycle period. The transition between non-profitable and cost neutral deserves a special cost-metric, called the internal rate of return, which is discussed in greater detail later. The goal of the cost optimization study is to minimize NPV. The goal of a multi-objective analysis is to minimize net-energy consumption and life-cycle cost using Pareto fronts.

NPV transforms future cash flow into present value using an minimal acceptable rate of return (MARR) or an expected Return on Investment (ROI). This term is often referred to as the discount rate. Real and nominal discount rates were used in life-cycle analyses. Real discount rates represent the loss of money value due to inflation. Nominal discount rates represent the investor opportunity costs which could be achievable using other investment vehicles. Nominal discounts rates include inflationary terms. Investors expect a MARR of 8–12% depending on the risks involved.

To compare a potential investments, economists use guaranteed investment options such as bank rates, government bonds or Guaranteed Investment Certificates (GIC) to determine the MARR. The MARR is calculated from equation 3.16 (Doty and Turner, 2012):

$$a = (1+r)(1+i) - 1 \tag{3.16}$$

where: r is assumed bank rate, 2.14% a return from a 10 year GIC from 2002 to

2012 (Bank of Canada, 2009); i is the annual inflation rate, 2.0% in Canada (Bank of Canada, 2009); a is the minimal acceptable rate of return, 4.18%.

A detailed cost analysis is not possible at the conceptual design stage due to missing or uncertain information. Thus, some of the terms as described in equation 3.14 are simplified or ignored based on the criteria outlined below:

- Only material and labour are considered in capital costs. Cost associated with design or consulting fees, land acquisition and development are not considered. It is assumed that the appreciation/depreciation of non-design aspects are similar for all design alternatives.

- Salvage or residual values are considered. Residual values are not used in the sense that all building materials are to be re-sold. They are used as a method to allow for variable life-cycle periods. Including salvage values allow for the comparison of life-cycle periods where some, or all, materials have just been replaced with a life-cycle period where materials are due for replacement in the following year. It is assumed that material salvage values depreciate linearly from the initial purchase until the year of replacement.

- Cost items unaffected by design variables are excluded because they are equal values for all design alternatives.

- Replacement costs are only considered if they fall within the specified life-cycle. Capital cost are assume to grow with inflation. Reductions in costs due to experience curves and improved manufacturing are not considered.

- Non-energy operation and maintenance costs, such as painting, servicing, etc., are not considered.

- Soft costs, or penalty functions, related to comfort (visual and thermal) are excluded due to their difficulty to quantify.

In previous research, soft costs or penalty functions penalized designs with visual or thermal occupant discomfort (Charron, 2007). This approach steers the optimization algorithm away from solution landscapes which lead to undesirable performance criteria.

A disadvantage is that the determination of penalty functions is subjective and may not be all appropriate for all occupants. To avoid this, active constraints were used in the optimization algorithm to ensure potential design which do not satisfy temperature setpoints or work-plane illuminance criteria are not considered.

Based on the aforementioned assumptions, the life-cycle cost equation used for the analysis is reduced to equation 3.17.

$$\mathrm{LCC}_{NPV} = C_{NPV} + E_{NPV} + R_{NPV} - S_{NPV} - I_{NPV} \tag{3.17}$$

where: C_{NPV}: represents capital costs; E_{NPV}: represents operational energy costs; R_{NPV}: is replacement costs; S_{NPV}: is the salvage or residual value using linear depreciation; and I_{NPV}: is the income generated through incentives such as feed-in tariffs.

3.5.2 Life-Cycle Period

Few standards suggest an appropriate evaluation period for a life-cycle cost analysis. For case-studies, a period of 30 years is considered, although longer period may be used to project the payback period for building upgrades. European standards, such as *EN 15459: Energy performance of buildings—economic evaluation procedure for energy systems in buildings* (2010) does not recommend life-cycle periods greater than 30. Beyond a 30 year horizon, estimation of interest rates and energy escalation indexes become near impossible to estimate. Note that the selection of a life-cycle period will affect the replacement costs of some materials. The use of salvage values allows for variable life-cycle periods.

3.5.3 Salvage Values

Including replacement costs creates a potential problem: the possibility that costs are incurred just before the end of the life-cycle results in an artificially high NPV. Thus, some salvage values need to be associated with each material. This is especially important for equipment, such as PV panels and inverters, where costs can vary significantly from design to design depending on the array size.

Salvage values were incorporated using a linear depreciation method, see Figure 3.32.

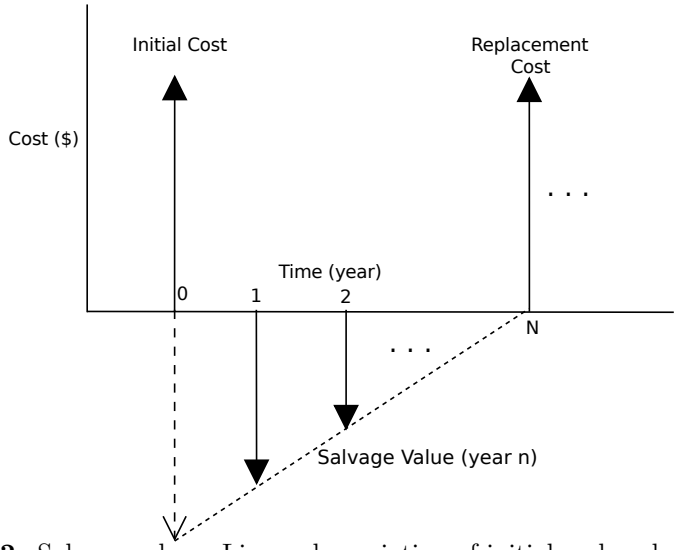

Figure 3.32: Salvage values: Linear depreciation of initial and replacement costs

It was assumed that materials depreciate linearly over-time until replacement is required. Thus, at the end of the specified life-cycle period, it is assumed that the materials purchased have some residual value. In some instances this can be related to a real resale value, such as PV panels, whereas in other instances, such as insulation replacement, salvage values are strictly used to compare different life-cycle periods. Note that other depreciation methods are also available (Doty and Turner, 2012).

Specification of initial and replacement costs are discussed in the following sections.

3.5.4 Material Initial and Replacement Costs

Initial costs were broken down as follows:

$$C = \text{wallinsCost} + \text{ceilinsCost} + \text{baseinsCost} + \text{slabinsCost} + \text{roofCost} + \text{overhangCost} + \text{concrCost} + \text{PVCost} + \text{winCost} + \text{airtightCost} \quad (3.18)$$

Each of these capital costs is described in the following sections.

3.5.4.1 Envelope and Insulation Costs

This section describes pricing of exposed wall, ceiling, slab and basement envelopes.

The wall envelope was constructed using a double 2x4" wall with 2" of exterior rigid closed cell extruded polystyrene, 25 PSI compressive strength insulation board. Exterior

rigid insulation reduces thermal bridging and improves envelope tightness. Blown-in cellulose filled in the cavity in the double 2x4" wall. The incremental framing costs associated with insulating double 2x4" walls was assumed zero since spacing could be modified to allow for any wall insulation value.

The costs associated with the construction of a wall section is given by equation 3.19.

$$\text{wallinsCost} = \text{wallArea} \cdot \text{wallUnitCost} \tag{3.19}$$

Wall areas are calculated based on the specified WWR; thus, trade-offs between collection of solar energy versus reductions in heat loss using better insulated walls is embodied in the analysis. A breakdown of wall constructions cost is shown in Table 3.6. Cellulose insulation in the wall cavities was also scheduled for replacement every 25 years. It was assumed that cellulose required replacement due to material compression and deterioration.

Table 3.6: Incremental costing data for wall construction

Description	thickness (in)	Resistance (R-val/in)	Incremental Cost ($/($in \cdot m^2$) WA)
Extruded polystyrene rigid insulation	2.0	5.0	8.88
Dense pack cellulose in double 2x4 staggered framed wall	$x \geq 3$	3.6	1.20

The ceiling attached to the attic space was insulated using a mix of closed cell polyurethane over 2x4" rafters and loose-pack blown-in cellulose. Truss heels were assumed to be raised to reduce additional heat loss through eve-compression. Table 3.7 summarizes ceiling insulation costs. Cellulose attic insulation was scheduled for replacement every 25 years.

Table 3.7: Incremental costing data for ceiling construction

Description	thickness (in)	Resistance (R-val/in)	Cost ($/($in ft^2$) FA)
Sprayed polyurethane insulation (closed cell) on 2x4 rafters	3.5	5.0	7.10
Loose blown-in cellulose insulation	$x > 7$	3.4	1.20

Foundation walls were a concrete structure—insulation was accomplished using a closed-cell polyurethane foam on a 2x4" wall of various distance from the concrete wall to reach the desired insulation level. A cost of $\$7.10/m^2/in$ for spray foam was sourced from RSMeans 2011 data. It is assumed that basement walls are finished in the reference and upgrade cases, so costing related to drywall and framing can be ignored.

Slab insulation was used to deter heat-loss through the ground and footings of the basement. Rigid extruded polystyrene insulation was assumed to be place under the slab at varying thicknesses. RSMeans 2011 data suggested a cost of $\$8.88/m^2/in$.

3.5.4.2 Passive Thermal Storage using Concrete

As previously mentioned, concrete slabs and a single vertical concrete wall was used to passively store solar gains.

Costs were determined for both the concrete floors and wall using RSMeans 2011 data. Table 3.8 shows the cost per concrete thickness.

Table 3.8: Costing data for concrete floor and wall construction

Description	Total ($\$/cm/m^2$ FA)
Concrete Floor, mesh reinforcing, with labour	2.28
Concrete Wall, light reinforcing, with labour	5.89

The combined cost for all poured concrete is shown in equation 3.20.

$$\begin{aligned} \text{concCost} = A_{floor} \cdot \text{floorUnitCost} \cdot d_{floor} \cdot N_{floor} + \\ A_{wall} \cdot \text{conWallUnitCost} \cdot d_{wall} \end{aligned} \tag{3.20}$$

where: N_{floor} is the number of stories; d_{floor} is the thickness of the floor; d_{wall} is the thickness of the wall.

3.5.4.3 Window Costs

Window costs were calculated based on the WWR ratio and the total wall area, see equation 3.21.

$$\text{winCost} = \text{WWR} \cdot \text{facadeArea} \cdot \text{winUnitCost} \tag{3.21}$$

The window cost data was sourced from RSMean 2011 data, see Table 3.9.

Table 3.9: Window costing data

Description	Total ($/m^2$)
2-pane, 12.7mm air cavity	477.90
2-pane, 12.7mm argon cavity, low-e	520.53
3-pane, 12.7mm air cavity	565.74
3-pane, 12.7mm argon cavity, low-e	585.74

3.5.4.4 Roofing and Overhang Costs

Roofing and overhangs costing is presented in this section. Recall, that PV is mounted directly on the roof-top surface. Since there is potential for partial coverage of roof area using PV, shingles were used to cover the remaining roof area. The unit cost for shingling from RSMeans 2011 is $\$37.36/m^2$ for labour and material. This includes a water-proof ice-guard membrane for an underlay. Gable roofs were specified to maximize the area for PV panels. Other roof styles, such as hip roofs were not considered.

Various roof slopes were consider in the cost analysis, see Table 3.10. This created an interaction between PV-based energy production and material costs. A steeper roof allowed for a larger area of PV panels and the opportunity for revenue through feed-in tariffs programs but at the expense of higher roof framing costs and investment into PV panels.

Table 3.10: Costing data for gable roofs at various pitches

Roof Pitch	Roof Slope (°)	Roof Cost ($/m^2$ FA)
3-12	14	79.64
6-12	27	84.37
9-12	37	91.48
12-12	45	100.42
15-12	51	110.64
18-12	56	121.62

Canvas window awnings provided shading for south facing windows. Costing data, sourced from RSMeans 2011, depended on the width of the window requiring coverage. Each linear foot of window awning was assumed to cost $22 for materials and labour. Since the protruding distance of the awning is adjustable, this cost is independent of the awning depth.

3.5.4.5 Air-Tightness Costing

Air-tightness cost is difficult to quantify since it depends on the experience and talent of the builder. Additional costs should lead to a more air-tight house due to better material selection and a more meticulous installation process. RSMeans has yet to quantify added costs associated with improving a homes air-tightness. Particularly, we are interested in additional costs to achieve R2000 air-tightness ($1.5ACH@50Pa$) down to PassiveHaus air-tightness standards ($0.6ACH@50Pa$).

In a conversation with the director of Habitat Studio a designer and builder of several NZEHs in Canada, and a participant in the Net-Zero Energy Home Coalition (NZEH Coalition, 2012), the following details were shared. Getting to 3ACH should be possible without any special materials or additional labour. Achieving an air-tightness of 1.5ACH requires an additional $3200 of labour and material costs for a 2500 ft^2 home. Achieving PassiveHaus air-tightness standards requires specialized air-sealing products originating from European markets but is possible for an additional cost of $4000 of labour and material costs for a 2500 ft^2 home. These costs are normalized by the square footage to arrive at Table 3.11.

Table 3.11: Envelope air-tightness: combined labour and material costs

Air-tightness (ACH at 50 Pa)	Incremental Cost ($/m^2$ FA)
>3.0	0.000
1.5	13.773
0.6	17.216

3.5.4.6 Photovoltaic Costing

> We need to invest dramatically in green energy, making solar panels so cheap that everybody wants them. Nobody wanted to buy a computer in 1950, but once they got cheap, everyone bought them.
>
> *–Bjorn Lomborg*

As previously mentioned, a PV array was integrated into the building roof-top. It is assumed that some combination of PV panels and wiring configurations exist to fill any roof area. Thus the design of PV strings, inverter sizing, etc. is abstracted away from this cost analysis. A breakdown of costs for a 10kW PV array, see Figure 3.33, is shown in Table 3.12.

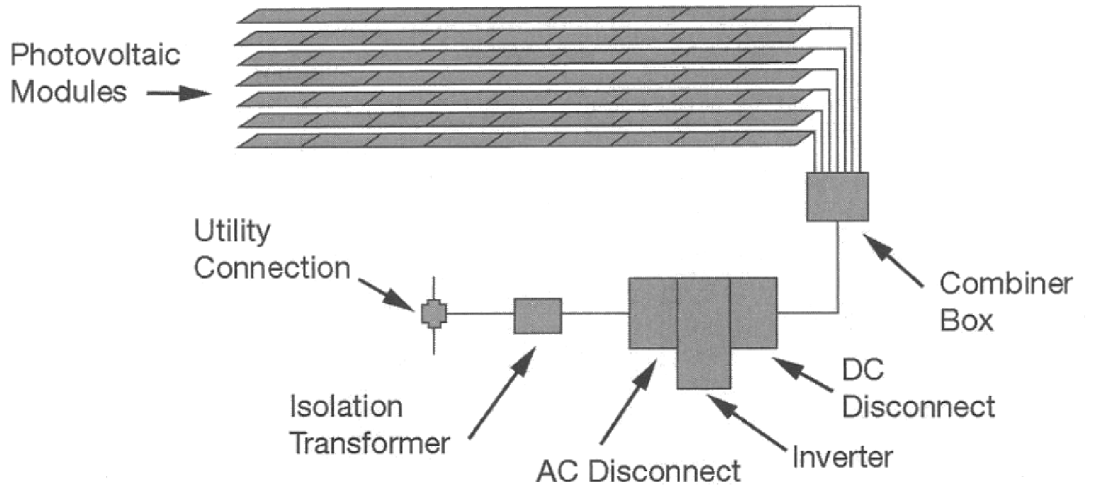

Figure 3.33: Diagram of 10kW grid connected PV system (RSMeans, 2012)

Note that although PV module prices have decreased to almost \$1/W, modules account for less than half of the total installation price of a 10 kW PV system shown in Table 3.12. The material and labour costs associated in safely connecting a grid-tied PV system also need to be considered in a life-cycle cost-analysis. These miscellaneous costs were determined to be 3.43 $\$/W$. The cost per watt for a PV panel base case analysis was \$1.50, however, scenarios were considered with PV panel less than this value. Inverters were intentionally oversized by 20%, a common practice to ensure inverters are never overloaded.

It was assumed that PV panels were replaced after 40 years and that the inverter was replaced every 15 years, see Figure 3.34. Chow et al. (2003) suggested that cell efficiency decreases by 0.1% per year; this was used to model decreasing PV electricity production over the life-cycle.

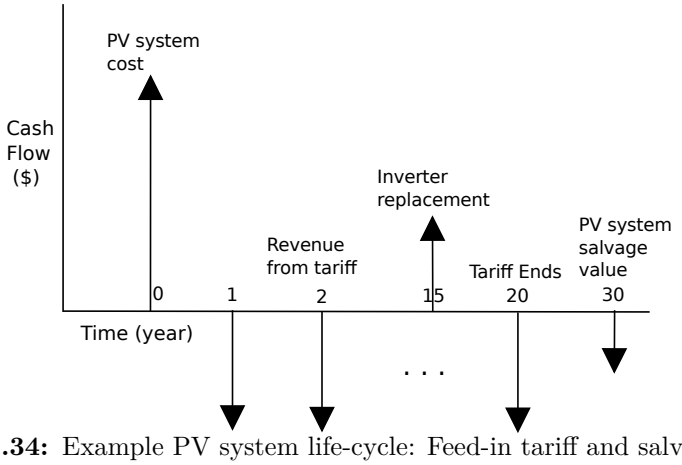

Figure 3.34: Example PV system life-cycle: Feed-in tariff and salvage value

Table 3.12: Material and labour costs for a 10kW grid connected PV system (RSMeans, 2012)

Description	Quanity	Unit	Material ($)	Labour ($)	Total ($)
PV modules, 167 Watt, 23.5 V	60	Ea	42300	4620	46920
Mounting Frames, 6 modules	10	Ea	9650	1250	10900
Steel Angle Support	400.0	LF	184	5696	5880
# 12 wire	4.0	CLF	146	224	370
AC Disconnect switch, 60 A	1	Ea	595	280	875
Fuse, 75 A	3	Ea	75	46.20	121.20
4/0 wire	2.0	CLF	930	432	1362
Module Connector 4/0	4	Ea	40.20	352	392.20
Combiner box 10 lug, NEMA 3R	1	Ea	206	154	360
Utility connection, 3 pl breaker	1	Ea	257	99.50	256.50
15 A fuses	10	Ea	135.50	154	289.50
Enclosure 24x24x10", NEMA 4	1	Ea	5150	1225	6375
Inverter, 12kW	1	Ea	1075	930	11655
Conduit w/fittings	200.0	LF	426	1070	1496
# 6 ground wire	8	CLF	504	760	1264
60 A fuse	3	Ea	33.45	37.05	70.50
DC disconnect switch, 75A	1	Ea	1100	340	1440
10 kVA isolation transformer	1	Ea	1800	770	2570
# 6 ground wire	0.4	CLF	25.2	38	63.20
# 6 ground connection	2.0	Ea	34.80	103	137.80
Total($)			74317.15	18580.75	92897.90
Total($/W)			7.43	1.86	9.29

C.L.F.: Centi-linear feet, L.F: Linear feet, Ea.: Each

3.5.5 Miscellaneous Costs

The following elements were not included in the cost analysis: (i) lighting fixture cost, (ii) mechanical system cost, (iii) ventilation fans including heat recovery ventilators. It was assumed that the same equipment was used in both the reference and actual building.

Presently, LED lighting is not cost effective enough to compete with CFL tubes and bulbs at present occupancy patterns in residential buildings. Thus, it was assumed that identical lighting fixtures were used in all cases. However, this is quickly changing. There are many LED replacements coming to market. For example, a LED replacement for pot-lights (MR-16) are quickly becoming cost-competitive. Likely this saving opportunity will become feasible over the next few years.

Identical heat pumps were assumed in all design cases. This assumption under-estimates the cost benefits of achieving NZEH. There were two reasons for this. First, there are no heat pump products sized properly for NZEHs (less than one ton). Thus, in most design scenarios there is no realized cost savings for using a smaller heat pump, Second, comparisons of building performance do not compare different fuel escalation rate estimates. The specification of system level heating and cooling COPs of the GSHP

depends on soil properties and aquifer flows which are unknown prior to drilling. To simplify, system level heating and cooling COPs were taken from monitored data from existing NZEH projects. Thus, it was assumed that identical systems were used in both reference and proposed cases.

Finally, ventilation fans and specialized heat recovery ventilators were assumed to be identical in all design cases. Building ventilation is a requirement by code. It was assumed that envelopes were air-tight enough to necessitate a heat recovery ventilator to control moisture build-up and reduce energy consumption for ventilation. In the case of inter-mixing solar gains between zones, additional costs were considered to operate fans to provide the required air-flow rate.

3.5.5.1 Summary of Replacement Costs

The replacement costs from the previous section are summarized in Table 3.13. Columns with dashes indicate that replacement costs are not considered.

Table 3.13: Replacement cost and serviceable life-cycle of materials

Material Category	Replaced?	Replacement Period (years)
Cellulose insulation in Walls	✓	25
Cellulose insulation in Attic	✓	25
Spray insulation in Attic/Basement	✓	25
Rigid insulation under Slab, exterior wall	✗	–
Windows	✓	40
Shingles on Roof	✓	25
Inverters	✓	15
PV Panels	✓	40
Miscellaneous PV array costs	✗	–

3.5.6 Income Generation: Feed-in Tariffs

Income generation refers to positive cash-flow in equation 3.17. A Feed-in Tariff (FIT) was explored as an opportunity to obtain payback for the higher initial costs associated with a NZEH. The FIT used in this dissertation was modelled after the microFIT program presently offered in Ontario. Income refers to electricity that is generated on-site and sold back to a utility company.

The Ontario micro Feed-in Tariff (microFIT) program presently offers the most competitive feed-in tariff for photovoltaic (PV) generated electricity in North America. No other Canadian province presently offers tariffs for renewable energy generation. Historically, as much as 80.2 ¢/kWh was offered for ground and roof-installed PV. Presently, 54.9 ¢/kWh is offered for roof-top installations up to 10kW, with a 20 year standard contract. This PV array size can be integrated on the roof of a NZEH (Candanedo, 2011; Chen, 2009). A PV array represents a significant capital cost and incentives such as a FIT could make a NZEH an attractive investment opportunity. The offered tariff is not inflated over time. Thus, this incentive becomes less attractive towards the end of the investment period.

The following assumptions were made: (i) FIT program lasted for 20 years; (ii) tariffs are not adjusted for inflation; and (iii) future revenue is not paid if life-cycle period is shorter than feed-in tariff period.

3.5.7 Utility Rates and Operation Costs

This section details the calculation of energy operational cost from simulated energy consumption. Of importance isthe utility billing structure, escalation of energy prices, and new billing methods involving smart metering.

3.5.7.1 Utility Billing Structure

Operational electricity costs can been calculated using two methods: (i) equivalent annual billing rate, or (ii) breakdown of electricity fees as specified from the utility.

ASHRAE (2011c) recommends a breakdown of energy costs using daily charges, peak load charges and charges based on total use to estimate annual electricity costs from an energy model. This method would be appropriate if the objective was to calculate operating costs at hourly or shorter periods. However, since the objective was to evaluate energy operations costs over an annual period, an equivalent annual billing rate was used.

3.5.7.2 Energy Escalation Rates

The cost of energy is rising in Canada. This is partially due to limited fossil fuel reserves, conflicts in oil producing countries, as well as investments made by utilities to incorporate

renewable energy into their energy stocks. The increased cost due to escalating energy prices can be calculated using equation 3.22 (Doty and Turner, 2012):

$$C_n = C_o \cdot (1 + e)^n \tag{3.22}$$

where: C_n is the annual electricity billing rate at year n (\$/kWh); C_o is the annual electricity billing rate at year 0; e is the energy escalation rate.

Energy cost escalation rate = 1.97%, which is calculated as the average of energy escalation rate between 2004 and 2008 for residential use in Montréal (Hydro-Québec, 2010)

3.5.7.3 Time of Use Rates

Many utility providers have mandated that smart meters be installed in all residential and commercial buildings. Smart meters have been installed in almost every home and business served by utility providers in Ontario and BC. Time of Use Billing (TOU) enables utilities to influence peak grid demands by charging clients more during peak periods. It is likely that TOU will be common place in most Canadian locations.

TOU rates imply that the price of electricity will depend on the time of day it is used, as recorded by a local smart meter. The cost of electricity will increase during peak hours, see Table 3.14. Peak hours are defined by the utility, but typically are the hours in which electricity demand is the highest.

Table 3.14: Time of use billing

Pricing Schedule	Hours	TOU	Price (¢)
Summer Weekdays	21:00–07:00	off-peak	5.3
	07:00–11:00	mid-peak	8.0
	11:00–17:00	on-peak	9.9
	17:00–21:00	mid-peak	8.0
Winter Weekdays	21:00–07:00	off-peak	5.3
	07:00–11:00	on-peak	9.9
	11:00–17:00	mid-peak	8.0
	17:00–21:00	on-peak	9.9
Weekends and Holidays	00:00–24:00	off-peak	5.3

TOU was calculated by post-processing hourly EnergyPlus results and implementing billing schedules based on Table 3.14. Note that since TOU results require detailed simulation data, updating billing rates could not be calculated from the database and

required additional energy simulations.

3.5.8 Location Cost Multipliers

The incorporation of detailed location specific material and labour costs is unrealistic for a research optimization study. Location factors are used from the most recent RSMeans cost database (RSMeans, 2013). RSMeans recommends that linear multipliers be used to convert costs from one location to another, see Table 3.15. RSMeans uses American currency. In 2012, Canadian and American currency were at parity so this data could be used directly.

Table 3.15: RSMeans location multipliers (RSMeans, 2013)

City	Province	Residential Cost Multiplier
Montréal	Québec	1.18
Regina	Saskatchewan	1.07
Toronto	Ontario	1.18
Vancouver	British Columbia	1.10

3.5.9 Other Economic Metrics

Although NPV is the preferred method to establish cost performance, it alone is insufficient to properly characterize important elements of a building's cost. A few additional cost metrics are used in this thesis: (i) internal rate of return; (ii) mortgage loans; (iii) simple payback; and (iv) capital payback. This metrics are discussed the following sections.

3.5.9.1 Internal Rate of Return

Internal rate of return or return on investment (ROI), see equation 3.23, is the rate of return, or discount rate, at which an investment yields a NPV of zero, or in other words, the investment becomes cost-neutral. An advantage of this cost metric is that options can quickly be compared over their life-cycle. However, IRR not able to clearly represent non-simple cash flows, such as positive and negative cash flow. Problems arise when costing of mutually exclusive projects, which is common in an energy efficiency measure (Doty and Turner, 2012):

$$\text{NPV} = \sum_{t=0}^{N} \frac{R_t}{(1+\bar{r})^t} = 0 \tag{3.23}$$

where:

R_t Net-cash flow at time, t. Net meaning $R_t = \text{cash}_{out} - \text{cash}in$

$\bar{r}$: internal rate of return, average percent growth at which an invest becomes cost neutral

N: number of years considered in the life-cycle (t=0 is the present year).

3.5.9.2 Mortgage Loan

A mortgage loan is a loan secured by the ownership of property. Mortgages allow for a large initial loan amount to be paid over an agreed time period for an interest penalty.

Mortgages can be issued at a fixed interest rate or at an adjustable rate. Fixed-rate mortgages typically have higher borrowing rates due to the perceived risk that the rate might be less than inflation over the period of the loan. Adjustable mortgage rates are recalculated annually based on market indexes. The following discusses details related to a fixed-rate mortgage. Note, other fees such as application, origination and title fees are not included.

Equation 3.24 shows the monthly payment, c, due to maintain a mortgage loan of principle, P_o (CMHC, 2012).

$$c = \frac{P_o \cdot r_{APR}}{1-(1+r_{APR})^{-M}} \tag{3.24}$$

where: (a) P_o is the principle loan amount (b) M is the number of monthly payments, ex. 30 year mortgage will have $30 \cdot 12 = 360$ payment cycles (c) r_{APR} is the annual percent rate (APR), split by the number of payment cycles each year, ex. monthly payments with a 6.5% APR, $r_{APR} = 6.5/100/12 = 0.0054$

Most banks require that a down-payment be made to secure a mortgage. The best interest rates for a Canada Mortgage and Housing Corporation (CMHC) insured loan, require a down payment of 20% or more for a 25 year mortgage (CMHC, 2012). For the purpose of this thesis, mortgage loans are assumed to have a 25 year repayment

period with a 20% initial payment on the principle. Note in Canada, mortgages are compounded every 6 months; this effects how annual interest rates are calculated.

The balance owing at after any month, m, is given by equation 3.25 (CMHC, 2012):

$$P_n = P_o \cdot (1+r)^m - c \cdot \frac{(1+r)^m - 1}{r} \tag{3.25}$$

where: (a) P_o is the principle loan amount; (b) m is the number of monthly payments made; (c) r is the annual percent rate (APR); (d) c is the monthly mortgage payment, see equation 3.24

An assumption was made that additional technology and energy conservation and efficiency measures were covered by a mortgage with the initial home purchase. This reduced the initial cost of technology but increased the life-cycle cost.

3.5.9.3 Simple Payback

Simple payback is the initial capital cost divided by the annual operational savings, see equation 3.26 (Doty and Turner, 2012). It can be used roughly estimate the time, in number of years, required to recover an initial investment.

$$t_{sp} = \frac{R_0}{C_{ann}} \tag{3.26}$$

This metric can be used for relatively quick paybacks, say less than three years, but is inappropriate to be used as a primary cost metric for investments beyond a three year horizon; simple paybacks do not consider the time value of money. Life-cycle cost is a more appropriate decision making metric as it considers inflation and cost escalation rates.

3.5.9.4 Capital Payback

Capital payback is the period of time required for an investment to payback the initial capital invested while considering the time value of money (Doty and Turner, 2012). This is a key cost metric of a life-cycle cash-flow. The capital payback is calculated by identifying the year where the cumulative cash-flow diagram passes from a negative cash-flow to a positive cash-flow.

Figure 3.35 shows an example cash-flow diagram for an life-cycle comparison of a

reference building to a hypothetical net-zero energy home; the cash-flow diagram shows a primary capital payback of 9 years and secondary paybacks in year 14 and year 24. As shown in Figure 3.35, a cash-flow diagram may have several capital paybacks due to replacement costs of equipment in future time periods. Typically, the first capital payback period is used so long as the cash-flow has a favourable NPV.

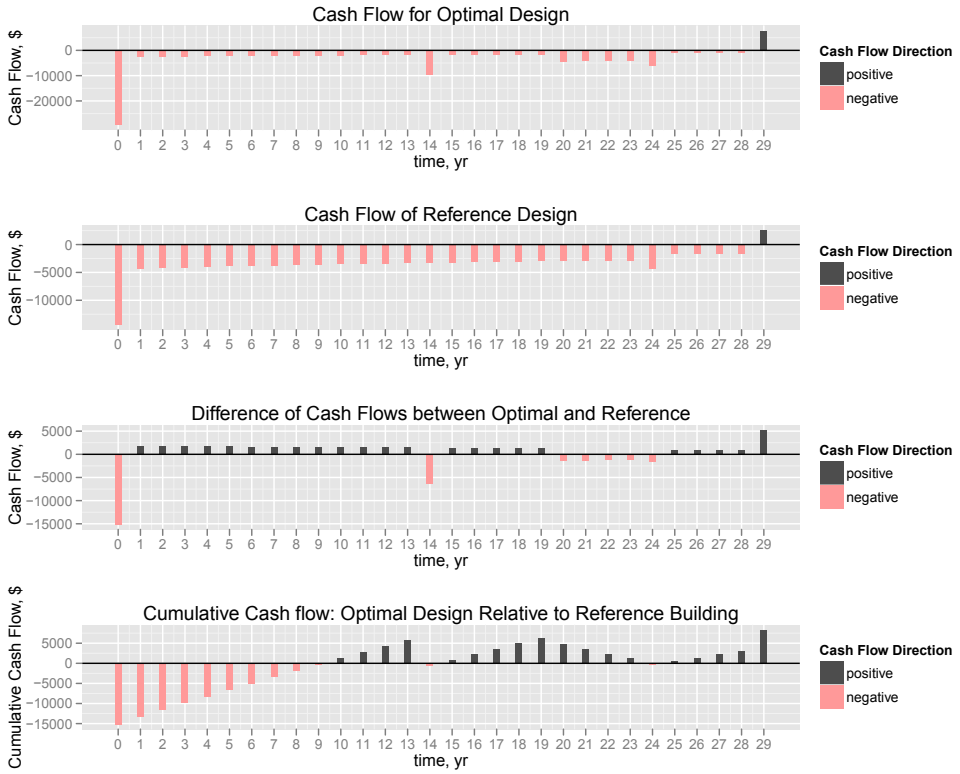

Figure 3.35: Example cash flow diagram of optimal design compared to reference design

3.6 Concept of Design: Summary

This chapter developed the essential components of the optimization methodology. These include the optimization algorithm, energy and cost models. These components are used in the next chapter.

Chapter 4

Multi-Objective Optimal Design of a Near Net-Zero Energy Solar House

> "Few things are harder to put up with than the annoyance of a good example."
> –*Mark Twain*

4.1 Overview

This chapter presents a redesign case study of the ÉcoTerra^{TM} house[1]. This research originated as a conference paper (Bucking et al., 2010). A modified version was accepted for publication in ASHRAE Transactions (Bucking et al., 2013a). This chapter uses the optimization methodology presented in chapter 3 including the optimization algorithm (section 3.2), energy model (section 3.4) and cost model (section 3.5). This chapter builds the concept of the archetype solar home that combines passive solar design, energy efficiency measures including a geothermal heat pump and a building-integrated photovoltaic system. This archetype is used in later chapters as a case-study.

This chapter shows how strategic deterministic searches can be deployed using information extracted from a database to improve performance of an evolutionary algorithm. The information extraction approach was previously described in section 3.3.8. These findings in improving algorithm performance are incorporated into an information driven EA presented in Chapter 5.

[1] ÉcoTerra is a registered trade-mark of Alouette homes.

4.2 Background

ÉcoTerra^{TM} is a detached near NZE home located in Eastman, Québec, see Figure 4.1. This home was one of the winners of the Canadian Mortgage and Housing Corporation Equilibrium Net Zero Energy Home competition and the first demonstration house built under this program (CMHC, 2008). The primary goal of the house design was to be cost competitive with other pre-fabricated homes, while greatly reducing energy intensity compared to the Canadian building stock.

Figure 4.1: ÉcoTerra House.

The ÉcoTerra design has a heated floor area of 211.1 m^2 (2,272 ft^2) and a heated volume of 609.1 m^3 (21,510 ft^3). The house is heated and cooled using a well-tied ground source heat pump (GSHP). Domestic hot-water (DHW) energy consumption is offset using a desuperheater and thermal energy collected from an open-loop solar thermal collector on the roof surface. The design features an innovative dual-energy roof system which uses 6% efficient amorphous silicon photovoltaic (PV) panels and an air-channel to simultaneously collect thermal and electrical energy.

The ÉcoTerra home was the first pre-fabricated home design with a customized building-integrated photovoltaic/thermal (BIPV/T) roof linked to a hybrid thermal energy storage system (Chen et al., 2010a,b). This technology combined with passive solar design strategies resulted in an annual net-energy consumption less than $50kWh/m^2$, or one fifth of the average national energy consumption or one half of the R2000 standard, see Figure 4.2 (Doiron et al., 2011). R2000 is a voluntary standard which promotes cost-effective energy-efficient building practices and technologies in Canada.

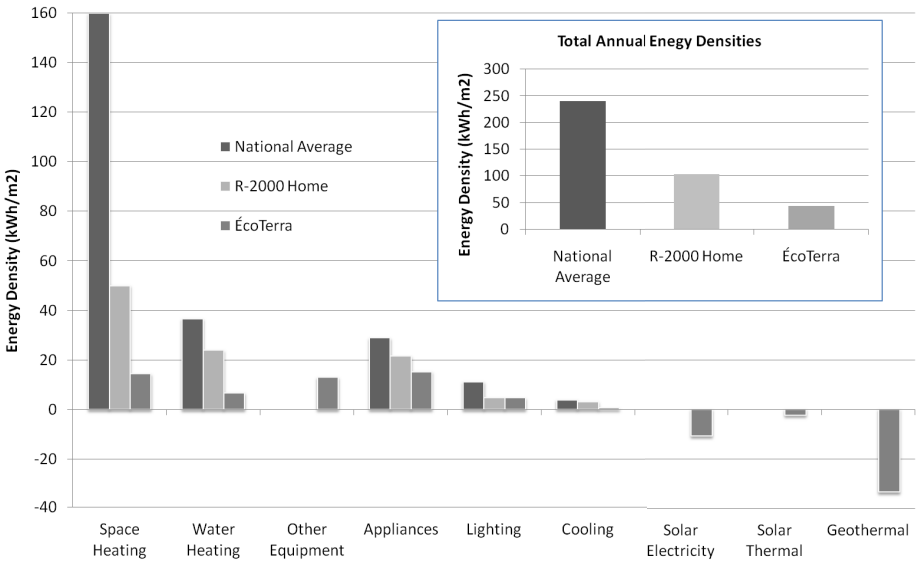

Figure 4.2: ÉcoTerra annual energy consumption (Doiron et al., 2011).

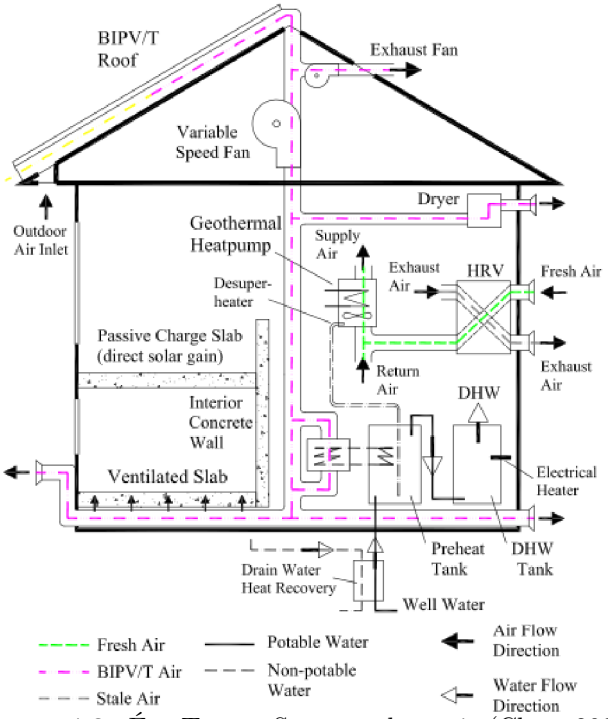

Figure 4.3: ÉcoTerra System schematic (Chen, 2009).

Approximately 40% percent of the gross heating demand is met through passive solar gains. Some thermal energy is offset by the roof integrated 2.84 kWe BIPV/T system, which can produce up to 10 kW_p of useful heat (Candanedo et al., 2010). The remaining auxiliary heating is provided by a GSHP. The thermal energy from the BIPV/T is delivered directly through an open-loop air system to a concrete slab in the basement or to a DHW pre-heat tank through an air-water heat exchanger, see Figure 4.3 (Chen, 2009). The slab serves as an active charge/passive discharge storage device.

Data was recorded from early 2008 until 2012 using over 100 temperature sensors distributed within the roof, slab and thermal zones. The PV generation, DHW and heat pump electrical demand of the home was monitored separately. This information permits the study of each design parameter and offers a unique opportunity to evaluate the present operation as well as to assess the impact of design improvements.

4.3 Method and Problem Formulation

Two redesign approaches were used in this chapter: (1) identify minor upgrades that could help ÉcoTerra reach NZE or reduce life-cycle costs without significant design modification, and (2) perform a full redesign with significant design modifications and a feed-in tariff to reduce operational costs.

For the first redesign approach, upgrades were restricted to simple renovations and control strategies modifications. These included modifying envelope insulation, air-sealing, and fine-tuning control strategies. Geometry, orientation, roof area and slope were fixed. Adding more PV panels was allowed if a similar PV product was used to match the æsthetic and electrical characteristics of the existing PV strings.

In the second redesign approach, the complete design was reconsidered including all aspects of passive solar design, renewable energy generation and control strategies. Changes to the rectangular shape were allowed only if the same floor area and number of floors were used. A feed-in tariff created revenue from on-site PV generated electricity. Including an incentive shows how economics can influence optimal building design approaches.

Additional goals of this study are to: (i) evaluate the potential of hybrid deterministic-

evolutionary algorithms in design optimization, (ii) extract information regarding variable interdependencies, and (iii) expedite the optimization process using extracted information.

The information extraction approach was previously described in section 3.3.8.

The design of net-zero energy solar buildings is dependent on local climate and site constraints. Any significant deviations in heating or cooling degree days or the amount of solar exposure would require the optimization process to be repeated on a new design. This fact precludes the utility of training methods such as decision tree ensembles and neural networks. However, restarting the entire optimization process is unnecessary as previous simulation data can be used to identify the relative importance of each design variable and suggest possible search strategies. There will be similarities between many optimal design parameters in elite design, even across different locations.

To complete the study, an energy model, database and optimization algorithm were necessary. This components were previously discussed in chapter 3. SQLite was used as a database to store variable mappings and fitness evaluations (SQLite, 2012).

The objective of the case-study was to conduct a multi-objective optimization analysis using net annual electricity consumption and the life-cycle cost. Time-of-use electricity billing and feed-in tariffs will change design variable interactions and are considered in chapter 7.

Design variables included in the optimization have been restricted to upgrades that could be done via simple renovation and control strategies to reduce electricity consumed for heating and cooling loads such as blind controls; free cooling and modifications to temperature schedules. Adding more PV was allowed if the type and efficiency remained the same (6% efficient amorphous silicon), but changes to the roof slope were prohibited. An exhaustive list of design variables used for the optimization and parameters for the ÉcoTerra design are presented in Table 4.1. Note that glazing types and WWR were considered separate design variables for all four walls.

The following sections elaborate on the energy model, optimization algorithm, strategies to integrate deterministic searches into an evolutionary algorithm and methods to extract information regarding design variable importance and interdependencies.

Table 4.1: Definition of optimization variables and parameters used for the Ecoterra redesign study

Variable	Units	Min.	Max.	No. Steps	EcoTerra	Description
wall_ins	m^2K/W	3.50	12	8	5.89	Effective resistance of wall insulation
ceil_ins	m^2K/W	5.6	15	8	8.2	Effective resistance of ceiling insulation
base_ins	m^2K/W	0	7	8	5.2	Effective resistance of basement wall insulation
slab_ins	m^2K/W	0	2.32	4	1.32	Effective resistance of slab insulation
ovr_south	m	0	0.45	4	0	Width of southern window overhangs
int_loads	% CAD_{avg}	50	80	8	50	Occupant loads (% Canadian average consumption)
pv_area	%	0	90	8	50	Percent of PV area on roof
wwr_s	%	1	80	8	35	Window to Wall Ratio South (also N,E,W)
GT_s	–	1	4	1	4	Glazing type (also N,E,W)
set_heat	°C	18	25	4	22	Heating setpoint
set_cool	°C	25	28	4	26	Cooling setpoint
FT	–	1	2	2	2	Window framing types (ex. 1:Wood, 2:Vinyl)
blind_irr	W/m^2	0	1000	4	500	Incident solar radiation for blind deployment
slab_th	m	0.1	0.2	8	0.1	Concrete slab thickness
vwall_th	m	0	0.35	8	0.1	Concrete wall thickness
zone_mix	L/s	0	400	4	400	Air circulation rate between thermal zones
infil	ACH	0.025	0.179	8	0.047	Natural infiltration rate

4.4 Energy and Cost Model

Details regarding the energy model were described previously in section 3.4.

The cost model was described previously in section 3.5.

4.5 Optimization Algorithm

A summary of algorithm parameters and setting used for this study is summarized in Table 4.2. A 54 grey-coded binary string was used to represent each candidate building design. Two types of recombination were used. The first shares data between two parents on a bit-by-bit basis using a uniform crossover and the second shares data on a variable-by-variable basis. Uniform recombination on a variable-by-variable basis should be included as it is unlikely that a binary string representing a sensitive design parameter will be transferred from a parent to a candidate child for a representation greater than 50 bits, an important aspect in convergence to optimal solutions. Diversity was measured by averaging the number of bits that any individual shared with the elite member in the

population (lowest annual net-electricity consumption). Diversity control becomes important for small population sizes, where there is a risk that the population prematurely converges to a local minimum, or the average diversity in the population converges to one. The problem was fixed by injecting noise into the population by increasing mutation rates and decreasing tournament sizes in the event of collapsing diversity. The concept of injecting noise to escape local minima is found in many optimization algorithms catered to navigating highly multi-modal solution spaces (Eiben and Smith, 2003). A more elaborate discussion of algorithm configuration and performance is presented in the concept of design, see section 3.2.

Table 4.2: Summary of algorithm configuration

Algorithm Parameter	Setting
Representation	54 bit binary string
Population Size	10
Recombination	50% bit-by-bit Uniform, 50% variable Uniform
Recombination Prob	100%
Mutation	bit-by-bit mutation
Mutation Prob	1.5%
Elitism?	Yes, best individual
Parent Selection	NSGA-II, see section 3.3.7
No. of Children	10
Survivor Selection	Best of parents and children, (μ+λ)
Diversity Control	NSGA-II crowding distances

It is well known that Evolutionary Algorithms work well at finding good combinations of design parameters, but are less adapted to resolve local minima without a 'lucky' random effect (Eiben and Smith, 2003). Resolving local minima, or search intensification, is the expertise of a deterministic search. Deterministic searches were attempted: (i) after initial population fitness evaluation, (ii) as a mutation operator, and (iii) after the termination criteria was reached.

A hill climbing algorithm was used for the deterministic search. The hill climbing search increments or decrements each design parameter such that the fitness function is reduced. The process was repeated across each design variable and variable setting until the fitness function could not be further reduced.

The most effective way to extract variable interdependencies at a defined energy consumption interval was to use the Mutual Information (MI) shared between two design

variables. This was described previously in section 3.3.8.4. Variables having low MI were targeted for hill-climbing searches.

Results and a discussion are presented in the following section.

4.6 Results and Discussion

Recall that two redesign approaches were used in this chapter: (1) identify minor upgrades that could help ÉcoTerra reach NZE for minimal life-cycle cost without significant design modification, and (2) perform a full redesign with significant design modifications and a feed-in tariff to reduce operational costs. The first multi-objective redesign study is show in Figure 4.4.

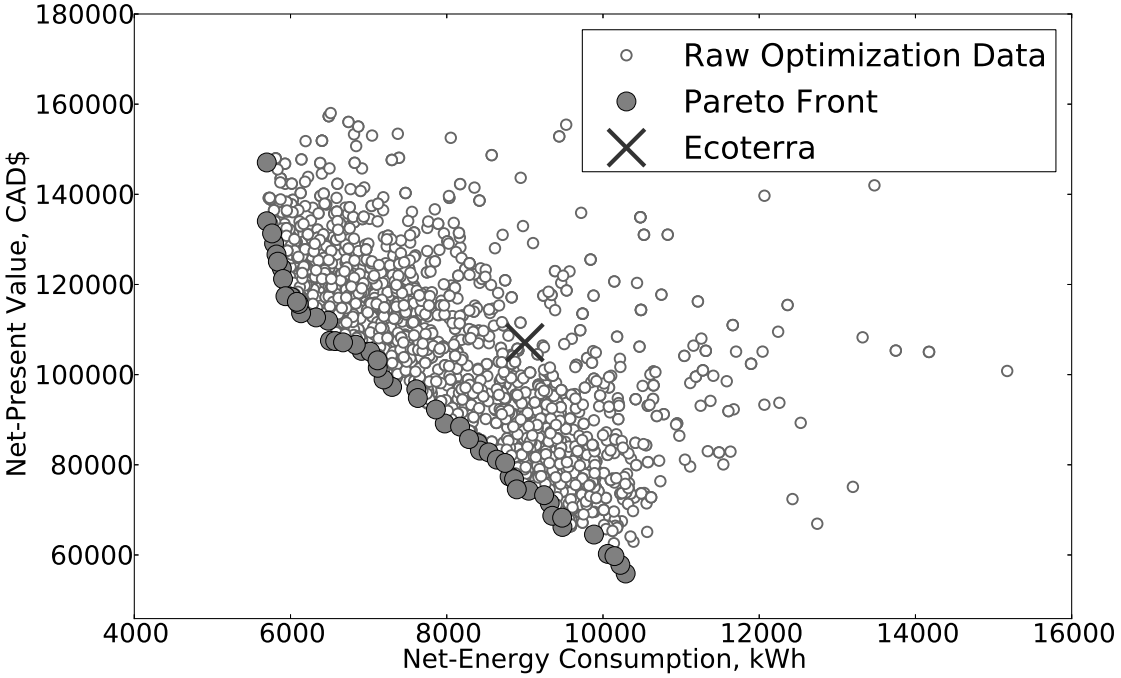

Figure 4.4: Multi-objective constrained redesign of ÉcoTerra home.

From Figure 4.4, the best design found had a net energy consumption of 5300kWh, a decrease in energy intensity from 50 kWh/m^2 to 20 kWh/m^2. Important changes included adding PV to the remaining area of the roof and modifying the heating and cooling dead-band limits, resulting in a combined net-electricity consumption reduction of 3500kWh. Of the redesign opportunities identified, none required significant changes to the passive solar design of the house. For example, fine tuning the thermal storage (slab and basement wall), increasing the slab and wall insulation levels, increasing the

southern window area to 50%, increasing air tightness to 0.5 ACH at 50Pa (approximately 0.025 ACH natural infiltration rate) from 0.8 ACH at 50Pa (approximately 0.047 ACH natural infiltration rate), cumulatively amounted to only 500kWh of annual electricity savings. This indicates that the ÉcoTerra design was near a local optimum with regards to passive solar design.

Figure 4.5 shows results for the second part of the redesign case-study. In this part, all variables were reconsidered including PV panel efficiency, roof-slope, orientation and geometry. Note that all designs were compliant with local building codes. The diversity in results shows that there significant opportunity to better improve energy codes and reduce energy consumption and life-cycle cost of residential homes in Canada.

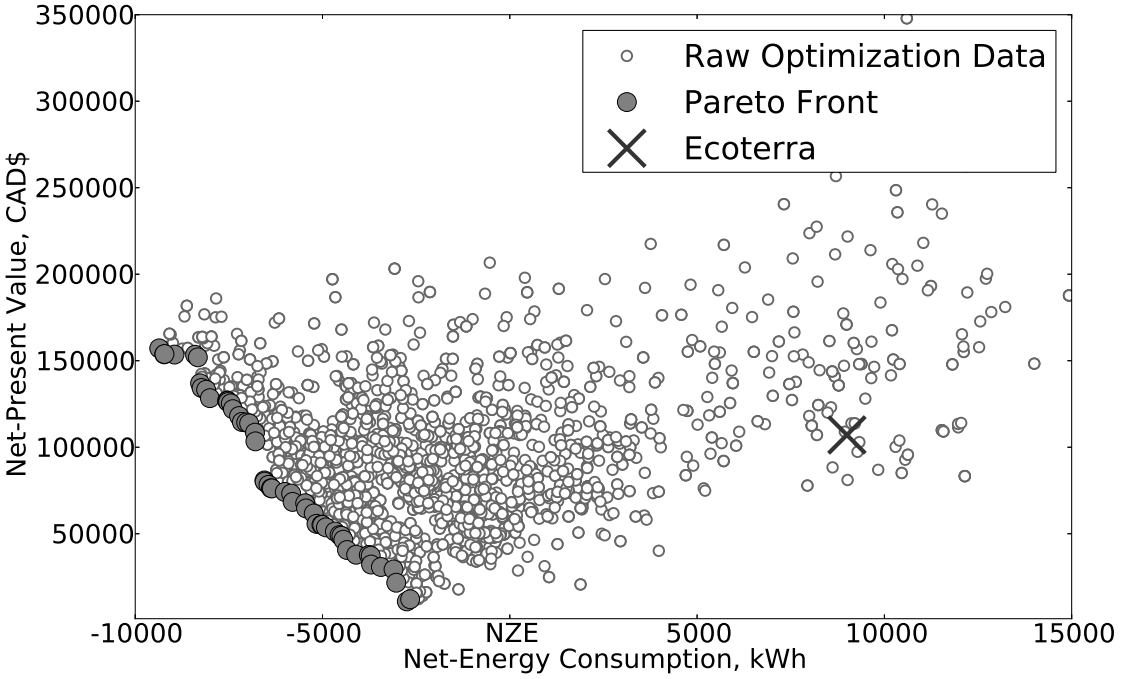

Figure 4.5: Multi-objective complete redesign of ÉcoTerra home.

The primary inhibitor to NZE with the ÉcoTerra design is the lack of renewable energy generation. More than doubling the PV efficiency from 6% to 15% alone would reduce net-electricity consumption from 5300kWh to 400kWh. A secondary inhibitor was high appliance loads which were measured from monitored data to be approximately 4000kWh/yr. Further research on implementing conservation measures on appliance, lighting, and DHW loads and their effect on occupant energy behaviour is recommended.

Although Figure 4.5 shows a spectrum of costs and energy consumption, we shall consider a single optimal design to examine improvements. The optimal design with

the lowest net-energy consumption generated a net of 3150 kWh of electricity and cost $\$32,000$ over the life-cycle. This design was selected since it had the lowest LCC while achieving the NZE target. To achieve this optimal design required integrated approach. A balance of passive solar strategies, such as: air-tight envelopes (0.025 ACH natural infiltration rate), sufficient wall envelope insulation values, RSI 8.56 ($R49$) and ceiling insulation RSI 10.57 ($R60$), sufficient south-facing glazing area (48% WWR), sufficient air circulation between zones to distribute solar gains, 133 L/s (280 cfm) and sizing of concrete floor thermal mass, 0.25 m (10 in.). Thermal mass allowed storage of solar gains and interacted with solar gain control strategies. Blind control strategies and exterior shading allowed for a larger window-to-wall fraction while maintaining acceptable visual comfort. The identification of trade-offs between passive solar design, energy efficiency and active solar electricity generation resulted in a sufficient improvement to achieve NZE. Figure 4.6 shows the optimal design energy balance compared to the national average and the existing ÉcoTerra design.

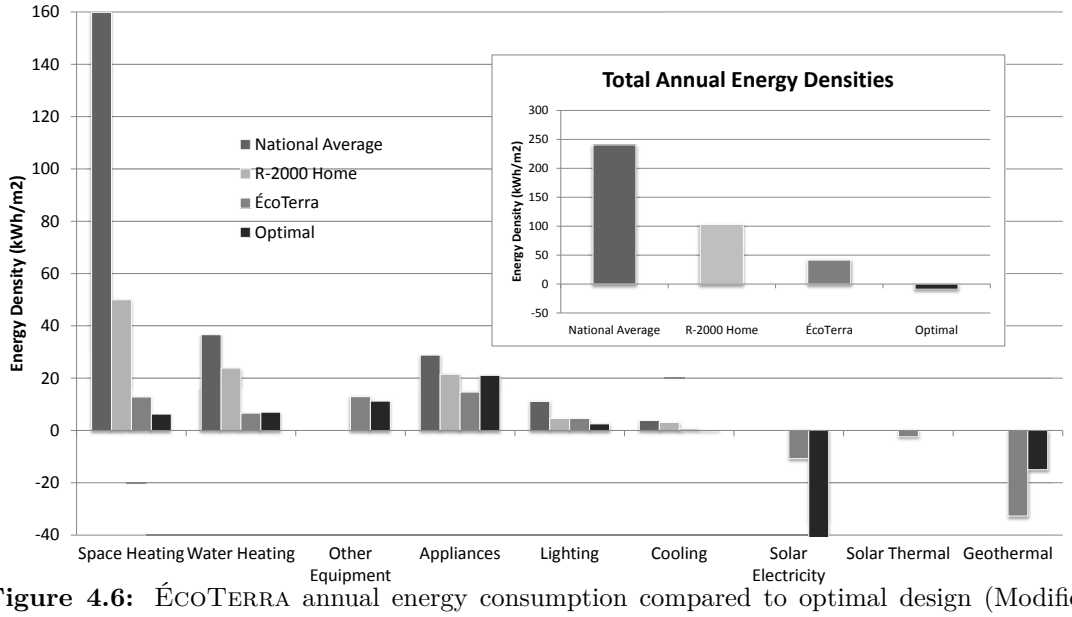

Figure 4.6: ÉcoTerra annual energy consumption compared to optimal design (Modified from Doiron (2010)).

The EA with incremental diversity control, as described in section 4.5, was used as a baseline comparison, see Figure 4.7. The simulation was run 20 times and averaged. The red bars represent the standard deviation of the fittest individual at each generation across all runs. The solid red line represents the average fitness of population. The red shaded area represents the average fitness of the best and worst individual in the popu-

lation across the 20 simulation runs. The solid black line is the average diversity of the population, a measure of the average number of bits shared with the elite individual in that particular generation. It can be concluded that, on average, 160 energy simulations are required to find an optimal building design with a fitness of 5536 kWh.

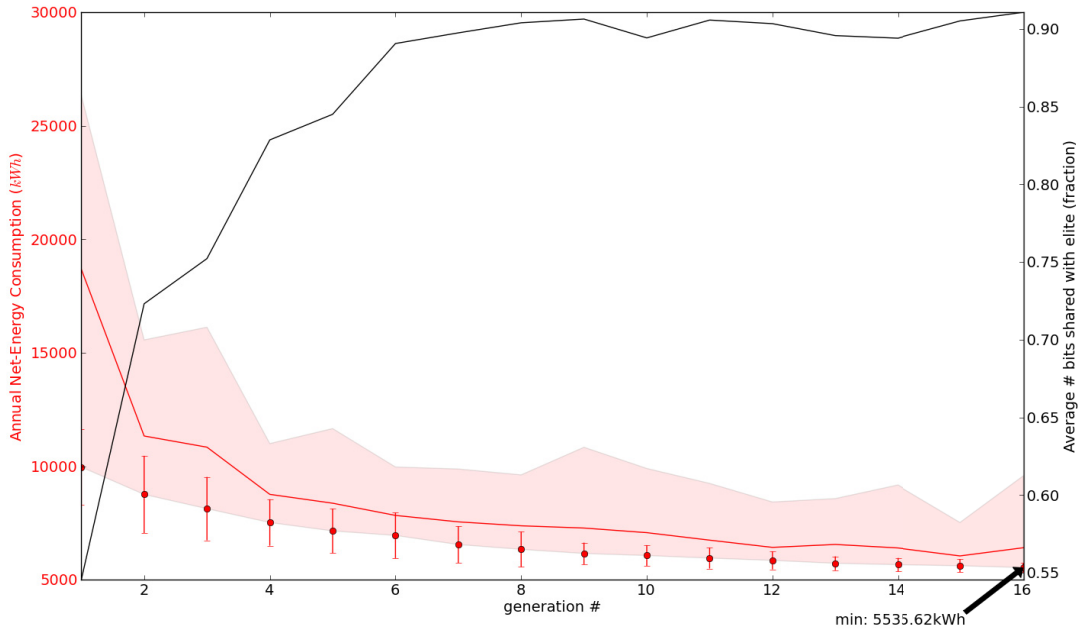

Figure 4.7: Average of 20 runs of the baseline EA

Of the three identified locations for deterministic search integration only one was found to be of significance. Searching sensitive design variables after the initialization of the population was the best way to integrate deterministic searches into a single hybrid deterministic-evolutionary approach. For instance, the fittest individuals always maximized the available roof area to offset unavoidable user loads. The relative importance of each design variable was decided on by randomly selecting a building design and calculating, variable-by-variable, the steepest descent to the best known building design. Variables that interacted weakly with the population were considered to be independent and could be locked after a brief search. Each design variable that was lockable contracted the size of the solution space significantly and expedited the search process. By using a hybrid deterministic-evolutionary algorithm, identification of optimal designs could be reproduced by deterministically searching the PV area and occupant load variables and as few as five evolutionary generations to result in a building design with a fitness of 5306 kWh, see Figure 4.8.

Initiating a deterministic search at the end of the evolutionary algorithm successfully

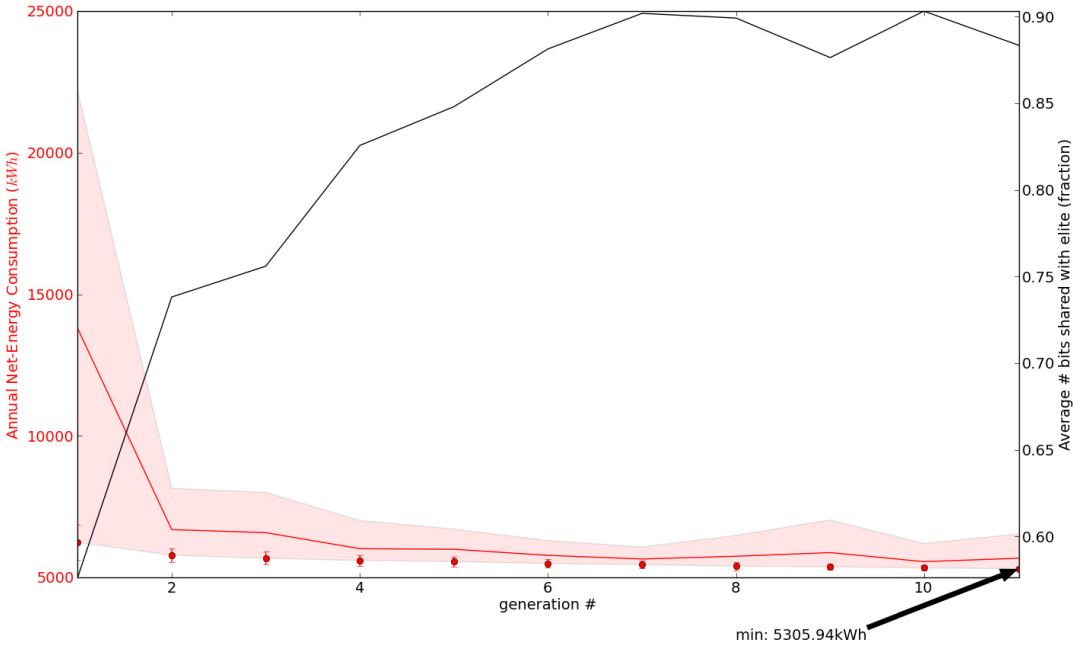

Figure 4.8: Average of 20 runs of hybrid EA

resolves designs to local minima, but required a substantial amount of computations, often as much as the original EA, for a negligible improvement in fitness. This was primarily because the model had already maximized renewable energy generation and was trying to further reduce heating and cooling loads, but any improvements were devalued by the Coefficient of Performance (COP) of the heat pump, that is, reduced by a factor of one third. This result enforces the idea that there is little benefit in finding the truly optimal design since the surrounding design space is nearly as good for this specific case study.

Probabilistically incrementing or decrementing the setting of a design parameter as a mutation operator was inadequate to inject diversity into the population. As previously mentioned, the purpose of the mutation operator is to explore new territory in the solution space and if necessary, to intentionally randomize the population to escape from local minima. Randomly incrementing or decrementing the setting of a design parameter was simply not random enough to escape from local minima.

In conclusion, the importance of an evolutionary algorithm is to find good design variable combinations quickly and locate near optimal solutions. Deterministic searches are best used to initiate a steepest descent search on sensitive variables prior to the evolutionary search.

Variable interactions for all buildings with energy consumption of less than 6500kWh are shown in Figure 4.9. Variable interactions were extracted using techniques discussed in the section 3.3.8.4. Design variables that form their own hierarchy could be highly sensitive to setting variations or could be very weakly interacting with all other design variables. Either situation indicates that the variable is susceptible to a deterministic search. For example, the PV area and occupant behaviour interact weakly with other design variables, but exhibit some mutual interactions as PV is used to offset electrical loads. Sub-clusters identify variables that are better handled by the evolutionary algorithm due to design variable interdependencies.

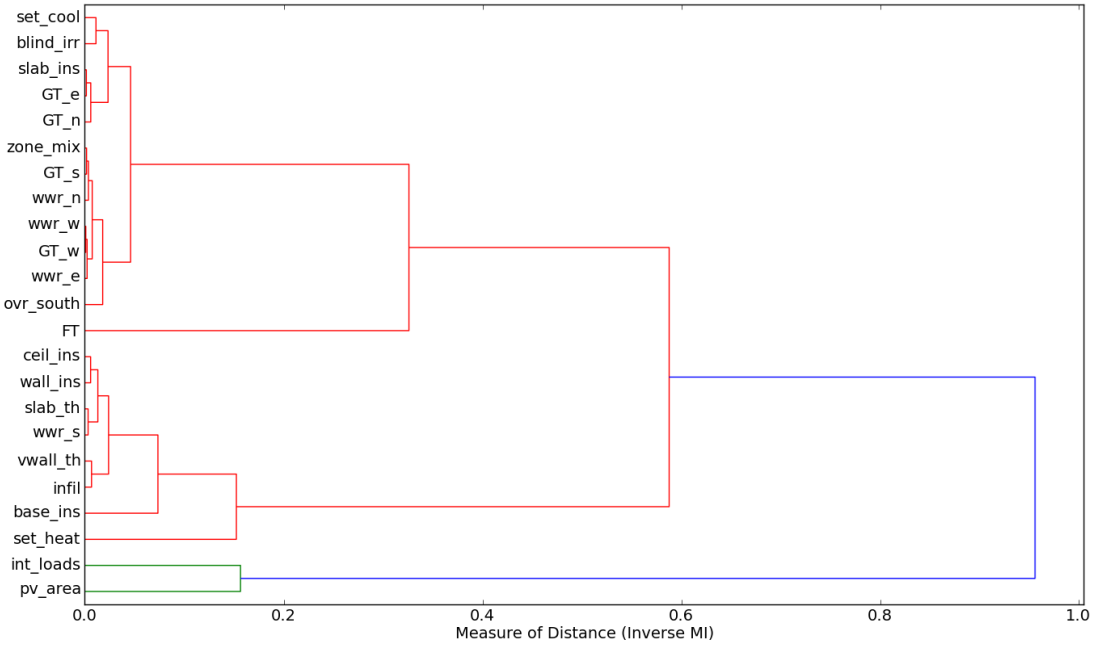

Figure 4.9: Dendrogram of variable interactions where inverse mutual information is used as a distance metric, using agglomerative clustering (complete method with Canberra distance)

Figure 4.10 shows the back-tracking search, core concept in section 3.3.8.1, from the initial ÉcoTerra design, to the optimal solution found in the defined solution space. Note that the first ten parameters have the largest impact on fitness, as they open new solution space landscapes and that the last few parameter changes are largely inconsequential. This is due to the fact that they were either near optimal values, or are insensitive to variations in the vicinity of the solution space landscape (they may be very sensitive at a different region of search space). Important changes included adding PV to the remaining area of the roof and modifying the heating and cooling dead-band to the limits of ASHRAE thermal comfort, resulting in a combined net-electricity consumption

reduction of 3500kWh.

Note the small hump in Figure 4.10. The algorithm had to back track the search process to arrive at the global optimum from a near optimum. This process is very difficult to do manually with a design tool as one has to know when and where to back track to arrive at the optimal landscape. This shows the benefit of using a optimization tool.

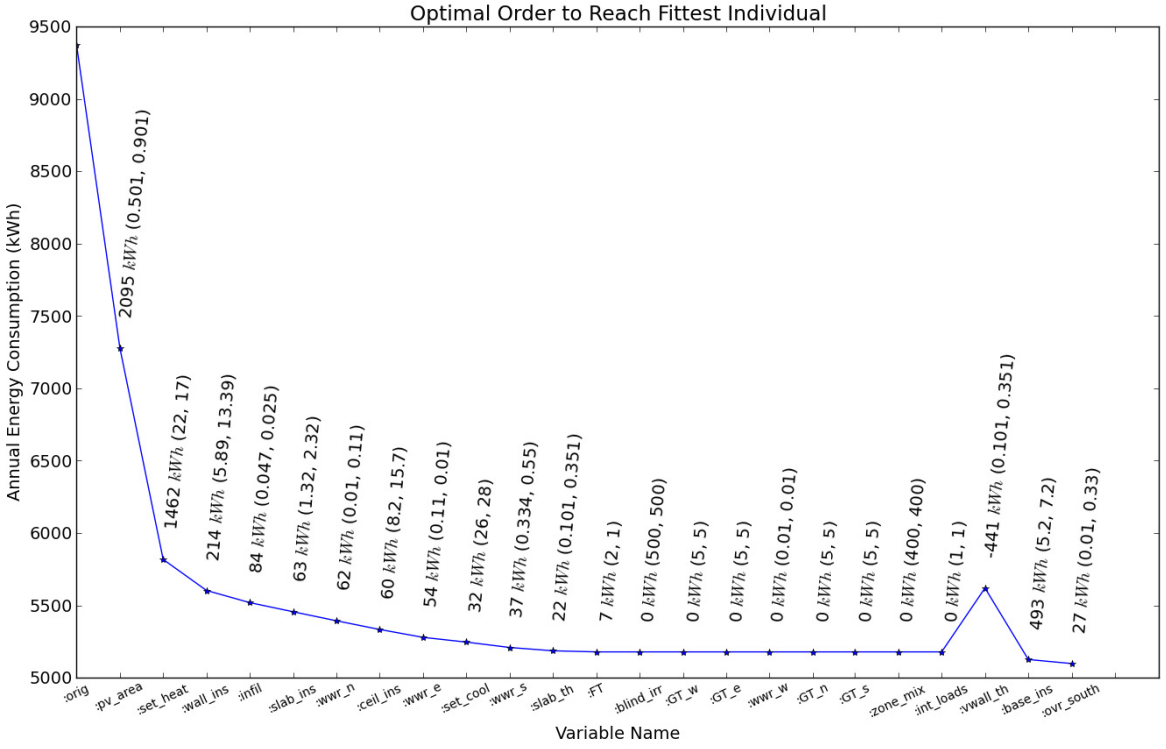

Figure 4.10: Back-tracking search from initial ÉcoTerra design to global optimum

The optimization time required was reduced by a factor of ten relative to previous studies by: (i) parallelizing energy simulations, (ii) deterministically searching weakly coupled design variables and (iii) monitoring diversity at each generation to avoid premature convergence and still enable the use of small population sizes. The coupling between variables is further exploited in chapter 5 to improve algorithm performance.

Chapter 5

An Information Driven Hybrid Evolutionary Algorithm for Optimal Building Design

> "In God we trust, all others bring evidence."
>
> –*W. Edwards Deming*

5.1 Overview

This chapter proposes a hybrid evolutionary algorithm which utilizes information gained during previous simulations to expedite and improve algorithm convergence using targeted deterministic searches. This chapter builds on the success of strategic deterministic searches first explored in chapter 4. Strategic deterministic searches are now integrated into the EA. Similar to the earlier chapters, this chapter uses the archetype solar home that combines passive solar design, energy efficiency measures including a geothermal heat pump and a building-integrated photovoltaic system previously described in chapter 4. This methodology was published and peer reviewed in a Solar Energy paper (Bucking et al., 2013b).

5.2 Background

Most previous research involving building simulation and optimization algorithms emphasized the importance of identifying a single optimal solution or a set of Pareto optimal solutions, see chapter 2. However, optimization algorithms extract other valuable in-

formation about the design problem during the optimization process, which is seldom used. Of equal importance is the collection and use of information gained during the optimization process. For example, other interesting information is the identification of: (i) automated search and discovery of potential optimal designs which best achieve desired performance objectives; and (ii) consideration of conflicting system level design trade-offs. Data-mining within the optimization process allows for a broader knowledge of the design problem and the feasible solution set. The inclusion and application of information obtained during the search process still remains unexplored in BPS.

This chapter proposes a method to extract and strategically apply information gained within an optimization algorithm to improve search resolution and expedite algorithm convergence for building simulation problems.

Since each building simulation problem has a unique set of constraints, climate conditions, shape characteristics and occupant usage characteristics, optimization studies must inevitably be performed on a case-by-case basis. Reducing time requirements for optimization studies while improving search resolution is an important research area of BPS.

The utilization of information obtained during the search process still remains unexplored in building optimization research. This paper proposes a data-mining technique within the optimization process. A new algorithm is presented to extract and strategically apply information gained using sub-searches to improve search resolution and expedite algorithm convergence for building simulation problems.

This chapter contains the following sections. Section 5.3 presents the proposed methodology, and the algorithm is applied to a case study in section 5.4. Discussions of results are presented in section 5.5, followed by conclusions.

5.3 Methodology

This section integrates strategic deterministic search, first explored in chapter 4, into the EA. Two evolutionary algorithms are proposed.

In addition, effective search strategies are borrowed from other optimization algorithms and incorporated into the proposed EA. For example, pseudo-differential gradi-

ents originating from DE were explored as a mutation operator. Hill-climbing searches from the deterministic family are examined to perform searches on isolated design variables. The proposed optimization algorithms are discussed in the next section.

5.3.1 Proposed Optimization Algorithms

Two algorithms are used in this chapter, a modified evolutionary algorithm (previously presented in section 3.3) and an information-driven hybrid evolutionary algorithm (section 5.3.1.2). The performance of both algorithms are benchmarked and discussed in later sections.

5.3.1.1 Proposed Modified Evolutionary Algorithm (EA)

Recall that three innovations, presented previously in section 3.3, were applied typical EA to improve algorithm performance: (i) mixed crossover operations (inside and outside representations), (ii) mixed mutation operators (differential mutation and bit-flip mutation), and (iii) algorithm parameter control using diversity measurements.

5.3.1.2 Incorporation of Mutual Information into a Hybrid Evolutionary Algorithm (MIHEA)

The proposed EA from the previous section was augmented with a module to data-mine previous simulation information. This hybrid EA was developed to extract information regarding variable interdependencies and strategically deploy deterministic searches to improve algorithm performance.

EAs are best suited for finding near-optimal solutions and there is no guarantee that searches will resolve to absolute minima. Deterministic searches are better suited for resolving local minima, or search intensification. In building optimization, interactions between variables are treated as a hindrance when they could improve the search process. For example, weakly dependent design variables might be susceptible to deterministic searches. Similarly, if interactions are identified between sub-clusters of design variables, sub-population search strategies might expedite the search process.

A hill-climbing algorithm was used for the deterministic search. A hill-climbing search increments or decrements each design parameter such that fitness is improved. The difficulty lies in identifying which design variables may be weakly interacting and

thus susceptible to deterministic searches within the present landscape of the solution space. Mutual information calculations, a concept originating from information theory (Cover and Tomas, 2006), identified weakly interacting variables.

By definition, mutual information is a measure of dependency between two random variables (Cover and Tomas, 2006). Due to its Bayesian roots, the updating of mutual information throughout the optimization search reduces the uncertainty in interaction calculations and builds confidence in selected variables for deterministic searches.

One effective way to extract variable interdependencies is to use the mutual information shared between two design variables. This was described previously in section 3.3.8.4.

Recall the previous discussion in section 3.3.8.4 related to mutual information calculations. Again equation 5.1 describes the total information that design variable X_i shares with all other design variables for a given performance range.

$$I_i = \sum_{j=1}^{N} I(X_i, X_j) \qquad \text{where, } j \neq i \tag{5.1}$$

Equation 5.1 calculates the total information that design variable X_i shares with all other design variables for a given performance range. Note that deterministic searches work best on variables that are loosely coupled to other variables in the model, i.e. variables with the lowest I_i. The identification and strategic searching of weakly interacting variables improves upon one shortcoming of population-based optimization searches such as EAs.

Figure 5.1 and Algorithm 2 presents the proposed mutual information hybrid EA (MIHEA). The evolutionary cycle was identical to Figure 3.1 except for the addition of a data-mining module which identified weakly-interacting variables and performed a hill-climbing search on the elite individual in the present population. The data-mining of variable interactions was repeated every two generations as determined by the 'datamine?' decision block. After the formation and evaluation of the child population, the elite member of the previous population entered the data-mining module.

Three variables were selected for a hill-climbing search. Selecting more than one variable for simultaneous deterministic searches allowed for better use of multi-processor

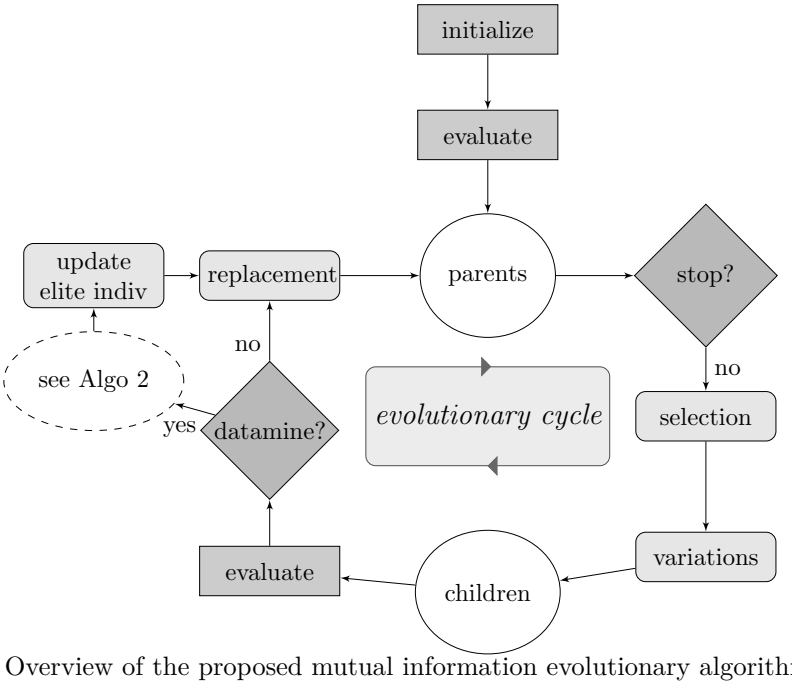

Figure 5.1: Overview of the proposed mutual information evolutionary algorithm (MIHEA)

Algorithm 2 Information-driven deterministic hill-climbing search

Precondition: **a** is a grey-coded binary string and the elite individual in the population

```
1 function MIDETSEARCH(a)
2     a ← binary2discrete(a)                          ▷ Note: a = (a_1, ··· , a_N)^T
3     data ← getnBestIndiv(n=100)                     ▷ Select 100 fittest individuals from database
4     I ← calcMI(data)                                ▷ Calculate and sum mutual information
5     freq_vars ← calcFreq()                          ▷ Calculate frequency of previously searched variables
6     vars ← tournSelect(I, freq_vars)                ▷ Select variables using tournament
7     for var ∈ vars do                               ▷ Hill-climbing increments and decrements variable var
8         b ← hillclimb_inc_dec(a,var)                ▷ Conduct hill-climbing search
9     return discrete2binary(b)                       ▷ Convert discrete representation to binary
```

computational resources. Variables were selected for the hill-climbing search using two criteria: (i) the mutual information shared with other design variables, and, (ii) the frequency that each variable had been deterministically searched in all previous generations. Mutual information calculations used at most 100 unique individuals from the database ordered by improving fitness to calculate interactions. The MIHEA selected variables for hill-climbing searches using a tournament selection operator to identify variables with low total mutual information, see equation 3.4, and a low frequency of being previously hill-climbed. Tournament operators ensured that the same variables were not searched repeatability every generation but still gave preference to variables that were weakly interacting.

The follow section describes how the proposed algorithms were benchmarked.

5.3.2 Optimization Algorithm Performance Comparison

Comparing the performance of the proposed optimization algorithms was challenging because both proposed EA and MIHEA algorithms depend on stochastic processes and simulations in this study were conducted in batches on multi-core processors.

The performance of the proposed EA and MIHEA were compared to GenOpt's particle swarm inertial weight (PSOIW) algorithm (Wetter, 2011b). Initial populations were randomized for each optimization run to ensure that algorithms were compared under different initial fitness landscapes. Identical design variables and variable step-sizes were used to constrain algorithms to the same solution spaces.

The following measures compared algorithm performance: (i) sensitivity of algorithm configurations, (ii) repeatability studies, and (iii) convergence analysis. The sensitivity study compares the sensitivity of each algorithm to its initial configuration. In addition, this study determines which initial configuration resulted in the best algorithm performance. A repeatability study explores how consistently each algorithm will find optimal or near optimal solutions and the expected fitness value for each algorithm given a single optimization run. The repeatability study also compares algorithms to determine reductions in computational and time requirements. Because the optimization algorithm used in the study depends on stochastic processes, a significant sample of optimization runs is required to conduct the repeatability study. Finally, a convergence analysis com-

pares how quickly each algorithm converges to optimal landscapes from a random initial population.

In the following case study, we compare the performance of the proposed EA and MIHEA to the GenOpt PSOIW algorithm. The proposed EA and MIHEA are also compared separately to estimate the performance improvement from augmenting the EA with information-driven deterministic searches.

5.4 Case Study: Net-Zero Energy House

The case study involves the optimization of a net-zero energy home (NZEH) located in Montréal, Québec. The energy model was previously described in chapter 3 section 3.4. The case study was presented previously in chapter 4. Table 5.1 shows the variables used in this case-study.

5.4.1 Objective function

The objective of the study was to minimize the net-annual energy consumption of a near net-zero energy home. Heating, cooling, fan loads, PV generation and lighting loads were simulated using EnergyPlus (Crawley et al., 2000). The objective function used for this case study was the annual net-electricity consumption of the building, see equation 5.2,

$$f(\mathbf{x}) = Q_{heat}/COP_H + Q_{cool}/COP_C + E_{elec} - E_{PV} \tag{5.2}$$

where: $\mathbf{x} = (x_1, x_2, \cdots, x_N)^T$ is a design variable vector; $f(\mathbf{x})$ is the annual net-electricity consumption of the building (kWh); COP is the average annual coefficient of performance of the ground-source heat pump in heating and cooling mode, 3.77 and 2.77 respectively; Q is the annual heating and cooling load (kWh); E_{elec} is the annual electricity consumption in lighting, domestic hot-water (DHW), appliances and plug-loads (kWh) and; E_{PV} is the electricity generated by the roof-top photovoltaic panels (kWh). When $f(\mathbf{x}) < 0$ this implies the net-generation of electricity, or a positive-energy house.

Note that variable descriptions are shown for the south orientation only; also, the PV slope is equal to the roof slope. Table 5.2 shows the binary encoding used in the representation for a sample of variables. Equation 5.3 demonstrates the translation of a

Table 5.1: Sample of influential variables for NZEH case study

Variable	Units	Min.	Max.	No. Steps	Description
azi	degrees	-45	45	32	Building orientation/azimuth
aspect	–	0.7	2.2	8	Aspect ratio (south facing width to depth ratio)
wall_ins	m^2K/W	3.5	13.0	8	Effective resistance of wall insulation
ceil_ins	m^2K/W	5.6	15.0	8	Effective resistance of ceiling insulation
base_ins	m^2K/W	0.0	7.0	8	Effective resistance of basement wall insulation
slab_ins	m^2K/W	0.0	2.3	4	Effective resistance of slab insulation
ovr_south	m	0.00	0.45	4	Width of Southern Window Overhangs
pv_area	%	0	90	8	Percent of PV area on roof
pv_eff	%	12	15	4	PV efficiency
roof_slope	degrees	30	45	8	South facing roof/PV slope
wwr_s	%	5	80	8	Percent of window to wall ratio, south (also N,E,W)
GT_s	–	1	4	4	Glazing type, south (also N,E,W)
heating_sp	°C	18	25	4	Heating setpoint
cooling_sp	°C	25	28	4	Cooling setpoint
FT	–	1	2	2	Window Framing Types (1:Wood, 2:Vinyl)
slab_th	m	0.1	0.2	8	Concrete slab thickness
vwall_th	m	0.00	0.35	8	Concrete wall thickness (basement)
zone_mix	L/s	0	400	4	Air circulation rate between thermal zones
infil	ACH	0.025	0.179	8	Natural infiltration rate

partial representation from binary to vector space using the encodings of Table 5.2.

Table 5.2: Sample of grey-coded binary representation of design variables

Variable: aspect		Variable: wall_ins		Variable: ceil_ins	
encoding	value, –	encoding	value, m^2K/W	encoding	value, m^2K/W
000	0.7	000	3.50	000	5.60
001	0.9	001	4.86	001	6.94
011	1.1	011	6.21	011	8.29
010	1.3	010	7.57	010	9.63
110	1.6	110	8.93	110	10.97
111	1.8	111	10.29	111	12.31
101	2.0	101	11.64	101	13.66
100	2.2	100	13.00	100	15.00

$$\overbrace{\text{“ } \underbrace{010}_{\text{aspect}} \quad \underbrace{110}_{\text{wall\_ins}} \quad \underbrace{000}_{\text{ceil\_ins}} \quad \dots \text{”}}^{\text{Binary Representation}} \rightarrow \overbrace{(1.3,\ 8.93,\ 5.60,\ \dots)}^{\text{Vector Representation}} \tag{5.3}$$

5.4.2 Cost Constraint

This section describes the formulation of a cost constraint used in the case-study. A cost constraint required the algorithm to minimize net-energy consumption cost-effectively. Establishing a cost-constraint ensured that algorithm identified cost-effective design trade-offs between passive-solar design and renewable energy generation. If the cost-constraint was exceeded, a barrier function was applied to the objective function and net-energy consumption was set to infinity.

Incremental cost of materials and operational energy costs over the life-cycle is shown in equation 5.4. A cost constraint of $90,000 was determined based on published cost premiums of NZEHs in Canada (CMHC, 2008). Costs were evaluated over the life-cycle of the building. Hence, initial, operational, and replacement costs are evaluated

using the net-present value (NPV) of each design. Cost calculations were performed by post-processing energy simulation results.

$$\begin{aligned} g(\mathbf{x}) &= C_{NPV} + E_{NPV} + R_{NPV} - S_{NPV} \\ &\leq \$90,000 \end{aligned} \tag{5.4}$$

where: C_{NPV}: is the capital costs of materials and equipment in Canadian dollars; E_{NPV}: is the operational energy costs calculated from energy simulation results; R_{NPV}: is the replacement cost for materials and equipment; and S_{NPV}: is the salvage or residual value using a linear depreciation method.

Materials were scheduled for replacement based on an expected serviceable lifetime (RSMeans, 2013). A marginal electricity rate of 7 cents with an escalation rate of 2.0% was used (Hydro-Québec, 2010). Note that all monetary amounts refer to Canadian dollars. Life-cycle costs were calculated over a 30 year time horizon.

Initial costs were broken down as follows:

$$\begin{aligned} C = {} & \text{wallinsCost} + \text{ceilinsCost} + \text{baseinsCost} + \text{slabinsCost} + \\ & \text{roofCost} + \text{overhangCost} + \text{concrCost} + \text{PVCost} + \\ & \text{winCost} + \text{airtightCost} \end{aligned} \tag{5.5}$$

where: C is the total material cost; insCost is the cost of wall, ceiling, basement and slab insulation; winCost is the cost of windows based on glazing area; roofCost is the incremental cost of additional roof framing beyond 30 degrees slope; overhangCost is the cost of overhangs; concrCost is the cost of concrete walls and slab for passive thermal storage; PVCost is the cost of PV panels and inverters; and airtightCost is the incremental cost associate with tighter envelopes. These costs were specified from RS-Means data (RSMeans, 2012, 2013).

5.5 Results and Discussion

To ensure that the EA and PSOIW algorithms were operating properly, the sensitivity of several algorithm configurations were explored. The algorithm settings which resulted in the lowest fitness values were selected for future optimization runs, see run no. 1 of Tables 5.3 and 5.4.

Table 5.3: Parametric run for various algorithm parameters, EA

EA Parameters	Run 1	Run 2	Run 3	Run 4	Run 5
Representation	62 bit binary string	–	–	–	–
Population Size	10	–	–	–	–
Recombination *	60% Method 1	60% Method 1	60% Method 2	80% Method 2	60% Method 2
Mutation ⊙	60% Method 2	60% Method 2	60% Method 1	60% Method 1	80% Method 2
Mutation Prob	2.0%	3.0%	2.0%	2.0%	1.0%
Scaling Factor	0.7	0.5	0.5	0.5	0.1
No. Generations	35	–	–	–	–
Fitness (kWh)	−1481	−1400	−1367	−1104	−934

* Recombination: Method 1: Bit-by-bit Uniform; Method 2: Variable Uniform
⊙ Mutation: Method 1: Bit-by-bit Mutation; Method 2: Differential Mutation
–: No change as compared to Run 1

Table 5.4: Parametric run for various algorithm parameters, GenOpt PSOIW

GenOpt PSOIW Parameters	Run 1	Run 2	Run 3	Run 4	Run 5
Representation	Discrete	–	–	–	–
Topology	gbest	–	–	–	–
Population Size	10	–	–	–	–
Neighborhood Size	5	–	–	–	–
Cognitive Acceleration	2.8	1.0	3.4	1.8	2.8
Social Acceleration	1.3	1.0	1.5	1.8	2.3
Max Velocity Discrete	4	3	3	4	2
Initial Inertia Weight	1.2	–	1.6	1.4	–
Final Inertia Weight	1.0	–	1.4	1.2	–
No. Iterations	35	–	–	–	–
Fitness (kWh)	−1205	−1003	−1171	−1202	−861

–: No change as compared to Run 1

Parallelization of building simulations to multi-core processors was used extensively for this study. Parallel simulations can greatly reduce optimization time requirements but do so with diminishing returns, as per Amdahl's law of computational parallelization (Amdahl, 1967). To identify the optimal population size or number of particles, a parallelization simulation study was performed. Figure 5.2 shows that five simultaneous building simulations allows for an optimal speed-up of four times compared to a sequential simulation strategy. The improvement factor of Figure 5.2 shows that it is most computationally efficient to conduct energy simulations in batches of five. Since a population of five individuals was insufficient to maintain population diversity within the evolutionary and PSOIW algorithms, a population of ten individuals was selected. Thus, two simulation batches of five individuals were required per algorithm iteration

and they were approximately time equivalent to two separate energy simulations.

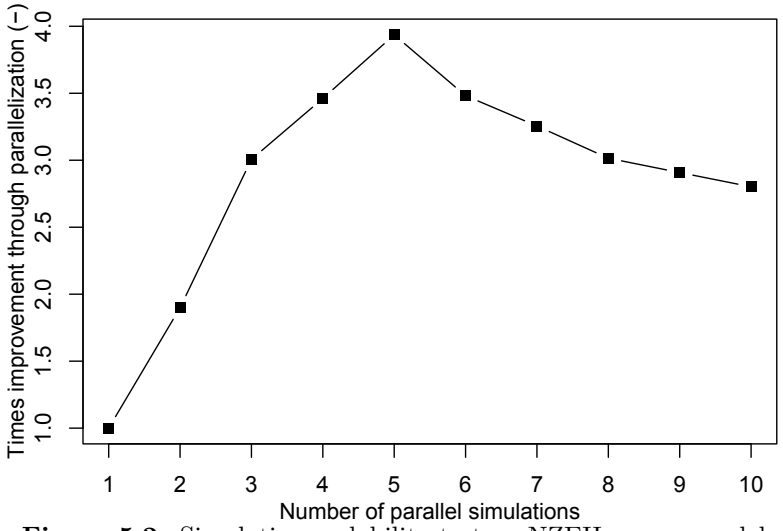

Figure 5.2: Simulation scalability test on NZEH energy model

Table 5.5 shows the results of the repeatability study. The results in Table 5.5 represent the expected fitness value for each algorithm given a single optimization run. This data was built using 20 repeated optimization runs. A sample size of 20 repeated optimization runs yielded 97% statistical power using a p-value of 5%. One standard deviation of data is shown with the average fitness value of optimal solutions.

Table 5.5: Expected optimal fitness for the proposed EA, proposed MIHEA and PSOIW based on 20 repeated optimization runs, NZEH case study

	Proposed EA	Proposed MIHEA	GenOpt PSOIW
No. of energy simulations	350	364	350
No. of deterministic searches	0	14	0
No. of simulations batches	70	70	70
Algorithm generations/iterations	35	28	35
Mean fitness (kWh)	-1250 ± 172	-1411 ± 119	-1112 ± 213

In Table 5.5 the expected optimal value of the proposed EA is slightly improved over the PSOIW. A larger disparity was observed when comparing the MIHEA to the PSOIW algorithm. The MIHEA algorithm found designs which had 20% lower fitness values with less variance. Since simulations were conducted in batches on multi-core processors, each algorithm was allowed an equal number of simulation batches rather than an equal number of building simulations. Recall that each batch consisted of five energy simulations. Thus the proposed EA and PSOIW were allowed 70 simulation batches over 35 algorithm iterations. Since MIHEA required one batch of six deterministic searches every other generation the total number of generations was reduced to 28 for a total of 70 simulation batches. MIHEA required 14 more energy simulations than the other algo-

rithms because simulation batches of six were used for deterministic searches instead of batches of five for each algorithm generation. However, the computational requirements are equivalent across all compared algorithms.

Table 5.6: Optimization results with MIHEA: Optimal design for case study

Variable	Description	Units	Optimal Values
azi	Building orientation/azimuth	degrees	0
aspect	Aspect ratio (south facing width to depth ratio)	–	1.3
wall_ins	Effective resistance of wall insulation	m^2K/W	8.93
ceil_ins	Effective resistance of ceiling insulation	m^2K/W	10.97
base_ins	Effective resistance of basement wall insulation	m^2K/W	5.08
slab_ins	Effective resistance of slab insulation	m^2K/W	1.39
ovr_south	Width of Southern Window Overhangs	m	0.34
pv_area	Percent of PV area on roof	%	90
pv_eff	PV efficiency	%	15
roof_slope	South facing roof/PV slope	degrees	45
wwr_s	Percent of window to wall ratio, south	%	48
wwr_n	Percent of window to wall ratio, north	%	10
wwr_e	Percent of window to wall ratio, east	%	10
wwr_w	Percent of window to wall ratio, west	%	10
GT_s	Glazing type, south (also N,E,W)	–	2
FT	Window Framing Types (1:Wood, 2:Vinyl)	–	2
slab_th	Concrete slab thickness	m	0.2
vwall_th	Concrete wall thickness (basement)	m	0.251
zone_mix	Air circulation rate between thermal zones	L/s	133
infil	Natural infiltration rate	ACH	0.025
Fitness of Individual (kWh)			-1491

Table 7.4 shows the optimal NZEH parameter sets for the case study. The optimal design shown in Table 7.4 generated a net of 1491 kWh of electricity and was found using MIHEA. The cost constraint was sufficiently large to allow for the full roof-surface to be covered in PV panels and achieve the NZE target. To achieve this optimal design required integrated design approach. A balance of passive solar strategies, such as: air-tight envelopes (0.025 ACH natural infiltration rate), sufficient wall envelope insulation values (8.56 m^2K/W), appropriate south-facing window-to-wall percentage (48%), sufficient air circulation between zones to distribute solar gains (133 L/s) and sizing of thermal mass (0.25 m central thermal storage wall in basement). Thermal mass allowed storage of solar gains and interacted with solar gain control strategies. Blind control strategies and exterior shading allowed for a larger window-to-wall fraction while maintaining acceptable visual comfort. The identification of trade-offs between passive solar design, energy efficiency and active solar electricity generation is a significant application of the proposed optimization algorithm.

Table 5.7 shows the deterministic search probability for a sample of design variables

from the case study. The search probability is defined as the probability that a given design variable will be searched deterministically within the MIHEA. The probability of selecting a variable for a deterministic search with no prior information is $1/N$, where N is the number of design variables. The actual search probability was calculated by post-processing previous MIHEA optimization runs. The variables with the highest deterministic search probability were the sizing of renewable energy generation, such as PV efficiency, area of PV coverage, roof/PV slope and heating/cooling setpoints. Variables that were rarely selected for deterministic searches were the solar orientation of the building (azimuth) and the aspect ratio (ratio of south facing width to depth ratio). Both variables were tightly coupled to other design variables. The optimization of coupled variables is best handled in the EA.

Table 5.7: Search probability of design variable within MIHEA for Case Study

Variable	Description	Search Probability (%)
pv_eff	PV efficiency	5.4
pv_area	PV area	5.3
roof_slope	Roof and PV angle	5.1
set_heat	Heating setpoint	4.8
set_cool	Cooling setpoint	4.7
aspect	Aspect ratio	1.6
azi	Building orientation	0.6

Box-whisker (BW) plots compared the distribution of optimization results for each optimization algorithm (Fig. 5.3). BW plots allow for side-by-side comparisons of the convergence characteristics of each algorithm using five important statistical properties of the optimization datasets. In the BW plots, the dashes represent extremes of the data points (starting point of initial population and final optimized population). The thick line inside the box represents the mean quartile of the set. The lines of the box represent the lower and upper quartiles of the set where 50% of data points reside. The algorithm with the lowest mean fitness has the best convergence properties. Bean plots (Kampstra, 2008) were superimposed onto this Figure to show the individual fitness distribution throughout the search using Gaussian kernel density functions (Scott, 1992). The three dotted lines represent the global maximum, minimum and mean of the dataset. These lines are intended to simplify visual comparison of results.

Figure 5.3 shows the convergence analysis results for the case study using 20 optimization runs.

Both EA and MIHEA found better optimal designs and evolved more individuals

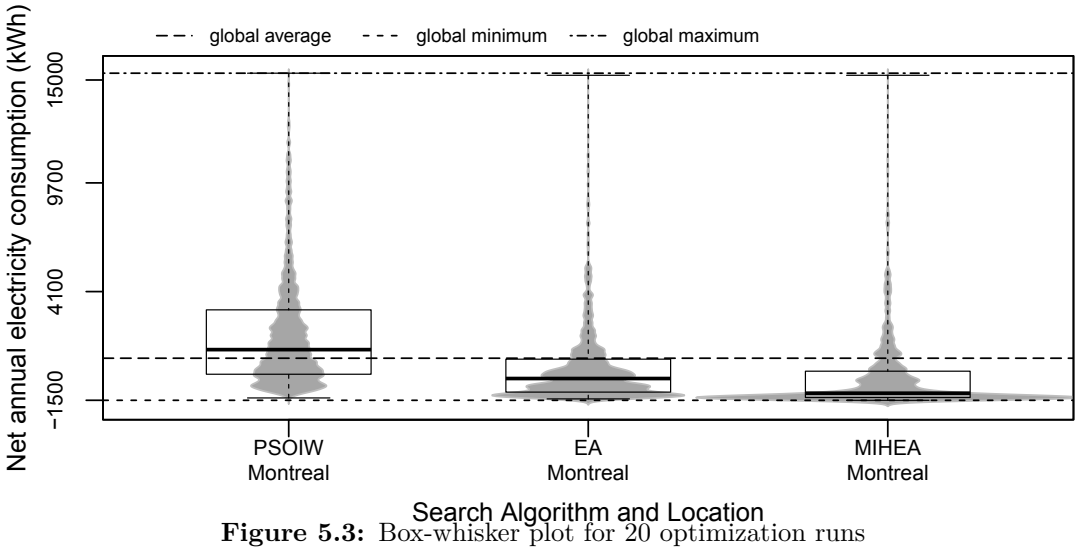

Figure 5.3: Box-whisker plot for 20 optimization runs

closer to the optimal landscape than the PSOIW. Note, the best individual from repeated PSOIW optimization was close to the EA solution; however both EAs were able to converge to the near-optimal landscape using fewer fitness evaluations which led to surplus individuals, as illustrated by spiking in the distribution. Note that this spike is absent in the PSOIW algorithm. MIHEA identified optimal solutions using only 22 generations compared to the 35 required by the proposed EA and PSOIW.

5.6 Conclusions

In this paper a hybrid evolutionary algorithm is proposed for minimizing solar building energy consumption. A net-zero energy house was used as a case-study to demonstrate the algorithm. Optimization approaches are required to identify cost-effective trade-offs between passive solar design and renewable energy generation. The MIHEA algorithm utilized information regarding variable interactions during the optimization process to identify opportunities for deterministic searches. This augmentation is valuable as EAs are strong at optimizing interdependent variables but have difficulties optimizing weakly coupled design variables—a strength of deterministic searches. Results suggest that this approach improves the reproducibility of near optimal solution set while requiring less computational resources.

The proposed MIHEA algorithm is applicable to any problem that involves various strengths of design variable interactions including several weakly interacting design

variables. Building energy simulation tools used for performance evaluations of solar buildings, such as ESP-r or EnergyPlus, are ideal case studies as they involve solving sets of sparse matrices (Clarke, 2001) or iterative solvers applied to loosely-coupled heat balance equations (DOE, 2011b). However, the proposed algorithm may be useful for other fields. Furthermore, using mutual information calculations to identify variables that may be susceptible to deterministic searches is not specific to an evolutionary algorithm. The approach could have equally been integrated into the PSOIW algorithm or a different algorithm entirely.

The information gained using the proposed optimization strategy is applicable to practicing energy modellers. For example, knowing which sets of design variables require simultaneous tuning and which design variables can be selected in isolation is useful information for energy modellers attempting to model high performance buildings.

Chapter 6

A Methodology for Identifying the Influence of Design Variations on Building Energy Performance

> "Never again will scientific life be as satisfying and serene as in days when determinism reigned supreme. In partial recompense for the tears we must shed and the toil we must endure is the satisfaction of knowing that we are treating significant problems in a more realistic and productive fashion."
>
> –*Richard Bellman*

> "The greatest value of a picture is when it forces us to notice what we never expected to see."
>
> –*John Tukey*

6.1 Overview

In building performance simulation, understanding the potential for parameter variations to cause a disproportionately large change in a performance metric is an important aspect of the modelling and design process. This is especially true if the proposed building is expected to meet a performance target such as net-zero energy consumption. This chapter proposes a methodology to identify influential variations around a performance criterion. This methodology aids in the understanding of possible discrepancies between predicted and realized building performance. This chapter uses the archetype solar home that combines passive solar design, energy efficiency measures including a geothermal heat pump and a building-integrated photovoltaic system

proposed in chapter 4. The proposed methodology was accepted for publication with revisions in the Journal of Building Performance Simulation (Bucking et al., 2013c).

6.2 Background

This chapter proposes a methodology to estimate the effect of variations around a performance criterion. This methodology aids in the understanding of discrepancies between predicted and realized building performance. A case-study demonstrates the methodology by identifying system level variations which significantly affect the net-energy consumption of a NZEH. This information is useful to designers of NZE buildings wishing to ensure that as-built designs equal or exceed preliminary performance estimates from models. As discussed later, such information could be used to streamline quality control processes.

The next section describes the methodology and a case study.

6.3 Methodology

This section proposes a methodology to estimate the effect of variations about a performance criterion. In a later section, the methodology is used to identify system level variations which most greatly affect the net-energy consumption of a NZEH.

To accomplish this, the methodology required the following distinct steps: (i) an optimization training dataset was formed using an optimization algorithm, (ii) discrete PDFs were created from this dataset for designs which satisfied the NZE performance criterion, (iii) new designs were created from independent random samplings of these PDFs and simulated using an objective function (due to system level effects, not all of these samplings resulted in NZEHs), (iv) a back-tracking search identified the variations responsible for non-NZE compliant samples.

Based on the literature review, presented in section 2.6.2, a MCA was selected for uncertainty propagation. Based on the recommendations of Macdonald (2009), a random sampling method was selected for the MCA to allow for an unbiased sampling of the solution space. To explore influences of input variations for a performance criterion such as NZE requires experimental evidence or expert knowledge. Associating arbitrary

PDFs to model inputs, such as normal or triangle distributions, offers no indication that sampled designs represent or fall within the desired performance range. To overcome this problem, optimization techniques extracted PDFs from the solution space of acceptable designs. Most of the sensitivity techniques used in literature were not suitable to extract and rank the relative importance of variation combinations to model inputs while retaining a performance criterion such as NZE. Based on the reviewed papers, only Monte Carlo Filtering techniques using regression analysis met this restriction. However, Monte Carlo Filtering is only suitable to explore first order effects (Saltelli et al., 2008). A back-tracking search, proposed in section 3.3.8.1, is used to explore first and higher order effects.

The methodology is divided into three sections described by the following components: (i) creation of optimization dataset using an Evolutionary Algorithm and extraction of PDFs, (ii) a Monte Carlo analysis using samplings of discrete PDFs, and (iii) importance factor calculations using back-tracking searches.

6.3.1 Formation of PDFs from an Optimization Training Dataset

This section describes the steps required to build PDFs from a training dataset built using an optimization algorithm; this training dataset will be used within a MCA.

The steps, summarized in Figure 6.1, are as follows: (i) model formation, (ii) discretization of variables, (iii) formation of optimization training dataset using a customized evolutionary algorithm (Bucking et al., 2010, 2013b), and (iv) extraction of PDFs for each model variable from compliant designs in the optimization training dataset. These steps are described in greater detail below.

Before proceeding, it is assumed that a model exists to evaluate the performance criterion. Simulation of this model allowed for comparisons of design performance.

The methodology requires discrete variables. This step is beneficial as it improves the convergence properties of the optimization algorithm. Furthermore, the resolution of most variables in building applications is finite in application. Although continuous parameters would result in higher resolution estimates of variability, they require additional binning which is sensitive to bin size. Thus, the methodology requires that appropriate design parameter increments be selected.

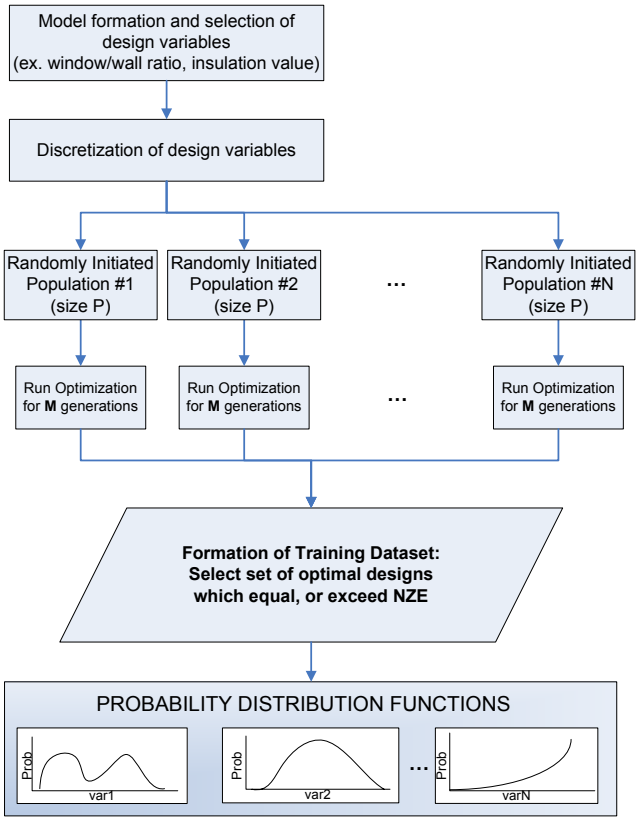

Figure 6.1: Formation of PDFs from the optimization dataset

In a MCA, attributing representative distributions with physical interpretations to the input parameters of the model is difficult. There is no evidence that samplings of common distribution functions such as normal or triangle distributions will represent a performance criterion or fall within a desired performance range. To overcome this difficulty, a training dataset was utilized based on searches from an optimization algorithm.

Optimization algorithms identify which sets of design parameters resulted in a NZEH. The selection of the optimization tool will not affect the training dataset if: (i) the algorithm can optimize large solution spaces involving interacting variables, and (ii) pathways leading to optimal regions can be queried from a database. For the case study, an evolutionary algorithm (Bucking et al., 2010; Eiben and Smith, 2003) was selected to navigate the design space. Training data was built by running the optimization tool, starting with a randomly selected initial population, at least N times for M generations using a population of P designs to approach optimal landscapes from different directions. Wright and Alajmi (2005) suggested a population size, P, of 10 to 15 is appropriate for most building simulation applications. The selection of the number of generations, M,

is problem specific and must be large enough to allow for convergence to global optimums. Finally, repeating optimization runs, N, at least 20 times is a sufficient sample size of optimization results to build PDFs. Therefore, the procedure requires $N \cdot M \cdot P$ simulations to build the training dataset. After navigating the design space, the training dataset was formed by selecting a subset of designs from the database which equalled or exceeded a specified performance criterion.

A SQLite database (SQLite, 2012) stored data originating from the optimization tool; SQL queries formed the training dataset. SQLite allows for concurrent writes from simultaneous simulations originating from multi-core and distributed computers. To save computation time, a database query confirmed if a set of parameters has yet to be simulated before calling the simulation tool. SQL queries allowed for the quick recollection of design parameter sets which exceeded the NZE performance criterion.

PDFs were extracted by: (i) selecting all combinations of variables that equalled or exceeded the NZE performance criterion from the training dataset, (ii) counting the number of occurrences of each discretized interval, and (iii) normalizing the sum of counts to equal one. For the case study, the performance criterion was NZE or better, i.e. all building designs where the on-site renewable energy generation equalled or exceeded on-site energy consumption over one year. To aid in visualizing the limits of and weightings of PDFs, kernel density functions (Scott, 1992) smoothed and interpolated the data, see Figure 6.2. However, discrete probabilities were used for samplings in the MCA.

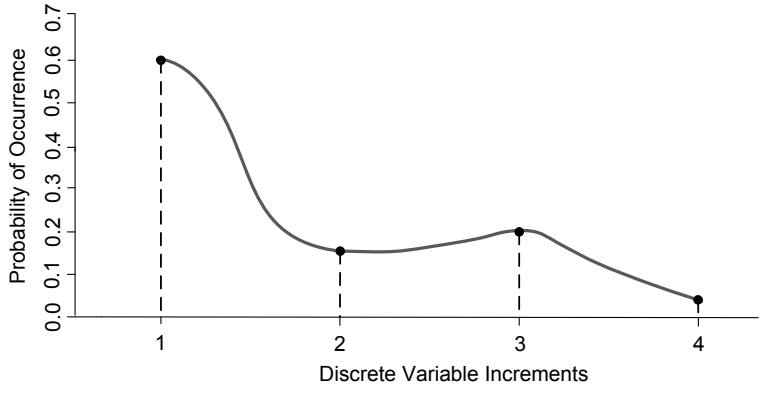

Figure 6.2: Kernel density function fitted to discrete probabilities of one variable

The extraction of PDFs from the training dataset ensured that all variable distributions were representative of NZEHs. An immediate benefit is the identification of parameter limits and most probable values for each variable. This is discussed more in

the results section. Logically, one expects the sampling of a set of trained PDFs to result in a NZE compliant design since the PDFs were extracted from a population of NZE compliant designs. However, due to variable couplings, this is not always true. This became evident if the Monte Carlo samplings from trained PDFs resulted in some non-NZE compliant designs. In fact, by intentionally sampling model variables as though they were independent variables indirectly identifies non-linear effects and inter-variable interactions which cause non-NZE compliant designs.

The optimization dataset offered many insights into variations which caused a performance criterion to be exceeded. Using the trained PDFs as an input, a Monte Carlo analysis enabled the exploration of model variations around this performance criterion.

6.3.2 Monte Carlo Analysis

A Monte Carlo analysis was selected to identify the global effects of variations on the previously defined PDFs. A MCA does not require modifications to the model and can directly use the trained PDFs from the optimization training dataset for samplings. Monte Carlo analyses are commonly referred to as uncertainty analyses since they estimate the cumulative effect of sampling uncertain input distributions. For this chapter, a MCA conducts a variability study since the input distributions represent parameter sets of NZE buildings and not physical uncertainties in model inputs.

Figure 6.3 summarizes the steps required to estimate the global variability of a model. A random sampling technique of trained PDFs was used for the MCA, based on the recommendations of previous studies comparing sampling methods (Lomas and Eppel, 1992; Macdonald, 2009). This methodology used sample sizes of 1000—ten times more than the recommended sample size to estimate mean and variance of the outcome distribution (Macdonald, 2009). Larger sample sizes helped to explore the effect of sample size on importance factor convergence as discussed in section 6.3.3. In a MCA, larger sample sizes tend to yield more normal distributions, due to the central limit theory of statistics. Otherwise, they do not affect Monte Carlo outcomes.

Monte Carlo methods rely on the sampling of predefined input distributions to estimate the cumulative variability of a model. Data points are formed by simulating samplings using a performance objective. The binning of all sampled data points forms

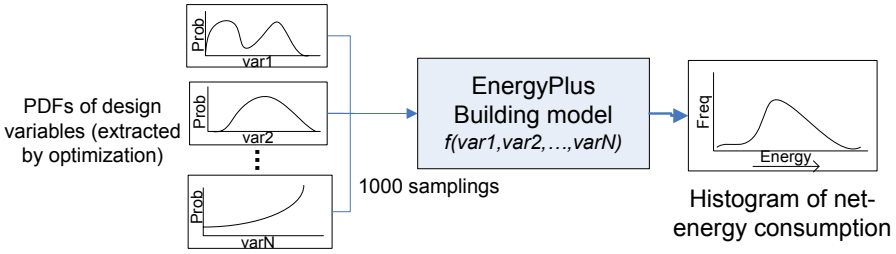

Figure 6.3: Monte Carlo analysis

an outcome distribution which represents the cumulative effect of input variability on the model output. The expected variation within a confidence interval, typically 95%, can be extracted from the outcome distribution and indicate the importance of potential variations. Regions of the outcome distribution that result in unacceptable performance are of particular interest.

However, the MCA is unable to identify which variations to model inputs cause non-compliant Monte Carlo samples. A separate back-tracking analysis is proposed for this purpose.

6.3.3 Calculation of Importance Factors using Back-tracking Searches

A back-tracking search ranked the relative importance of variations to model inputs for Monte Carlo samplings that were non-NZE compliant. This search identifies input variations which caused non-compliant Monte Carlo samples.

In this section, importance factors are introduced to represent the relative significance of variations to each variable affecting a performance criterion. A variable with an importance factor of zero indicates that variations to this variable do not affect the performance criterion. The sum of all importance factors equals one; thus, each factor is the relative contribution of each variable to unexpected changes in the performance criterion.

A back-tracking search requires a reference design. Selecting the optimal design, a positive NZEH with maximum production, as a reference point ensures that the extraction of steepest objective function gradients is consistent across the entire solution set. This is because the optimal design is unique for a single objective optimization problem. Furthermore, using the optimal design as a reference point also ensures that back-tracking searches identify all influential variations in the solution space. Note that the back-tracking of incremental improvements of the initial design to the reference

design is equivalent to the back-tracking of incremental degradations of the reference design to the initial design.

Figure 6.4 shows the method for calculating importance factors using back-tracking searches. Designs of interest, shown as shaded region in histogram, refers to candidate building designs for the back-tracking searches, i.e. designs which are non-NZE compliant. To calculate importance factors, using each design of interest ($j = 1, \cdots, M$): (a) perform a back-tracking search from the design of interest to the reference building to identify steepest performance gradients and incremental performance improvements for each variable change; (b) calculate *local* importance factors by dividing the incremental objective function gradient of each variable ($E_{\text{grad } i,j}$ where $i = 1, \cdots, N$) by the difference in the objective functions between the design of interest (E_{DOI}) and the reference building design (E_{Ref}), see equation 6.1; (c) continue to the next design of interest and repeat from step (a) until all non-NZE compliant designs have been back-tracked; finally, (d) calculate and rank *global* importance factors by normalizing all local importance factors calculated in steps (a–c), see equation 6.2. The sum of global importance factors for all variables should be equal to one. These factors are global in the sense that they represent the average effect of variations on non-compliant Monte Carlo samples.

$$IF_{\text{local } i,j} = \frac{E_{\text{grad } i,j}}{E_{DOI} - E_{Ref}} \tag{6.1}$$

$$IF_{\text{global } i} = \frac{\sum_j IF_{\text{local } i,j}}{\sum_i \sum_j IF_{\text{local } i,j}} \qquad \text{where, } \sum_i IF_{\text{global } i} = 1 \tag{6.2}$$

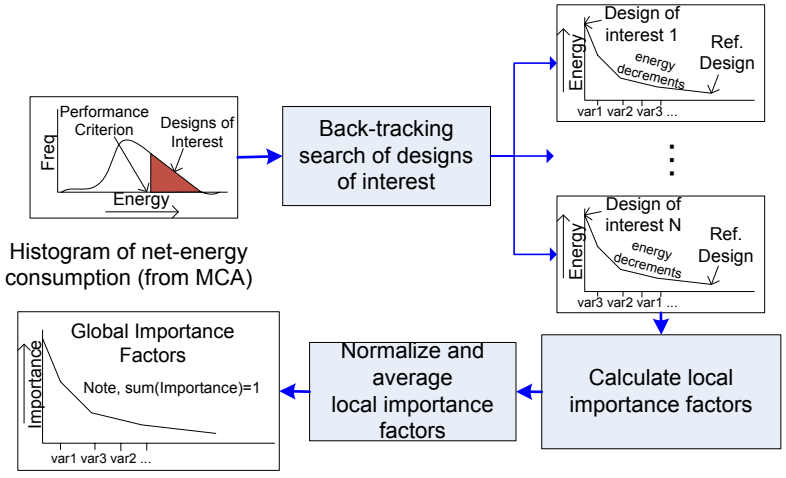

Figure 6.4: Calculation of importance factors using back-tracking searches

Algorithm 3 shows the psuedo-code for the back-tracking search.

Algorithm 3 Back-tracking sensitivity analysis

Precondition: **D** are the designs of interest from the MCA

```
1  function BACK-TRACK(D)
2      a ← getRefDesign()          ▷ select optimal design from optimal training dataset
3      f1 ← calcPerformance(a)          ▷ calculate performance of optimal design
4      i ← 0
5      for d in D do                    ▷ for each design in 'designs of interest'
6          f2 ← calcPerformance(d)
7          e[i], v[i] ← back_track(d, a)        ▷ e: energy increments, v: variable order
8          l[i] ← e[i]/|f2 − f1|                          ▷ l: local importance factors
9          i ← i + 1
10     g ← scaleLocalIF(e, v)        ▷ calc. global importance factors by averaging and
   normalizing local importance factors
11     return g
```

To investigate if the back-tracking of all designs of interest were required, a convergence analysis of importance factors was performed. After back-tracking each additional design of interest, the average of all local importance factors for each variable was recorded. The calculation of importance factors converged if the inclusion of results from additional back-tracking searches does not change the average of local importance factor for each variable. This characteristic is important in understanding how many back-tracking searches are required to confidently calculate global importance factors.

Importance factors have the following advantages: (i) they identify, rank and give the relative importance of changes to influential variables using a performance criterion, (ii) they identify the significance of first order and second order effects, (iii) they are generalized for a set of design considerations and climate zone, and (iv) they estimate the impact of variations for Monte Carlo samplings which unexpectedly do not equal or exceed a performance criterion.

Important factors have several useful properties. In addition to identifying which variations can cause large deviations from the NZE target, it is possible to identify the significance of primary and secondary effects of variations. Global importance factors, or averaged local importance factors, determine the overall influence of the variable on the output. The standard deviation of local importance factors estimates the ensemble effects of variations. Ensemble effects are caused by non-linearities and/or interactions

with other variables. An importance factor with a large variance indicates that the effect of variations is strongly affected by the values of other parameters. By contrast, low values imply that the effect is almost independent of other sampled parameters. Note that primary effects are de-emphasized in this methodology since back-tracking searches are intentionally conducted on designs with sufficient system-level interactions to cause non-NZE building designs. Similar to the Morris method (Morris, 1991), the mean and standard deviation of importance factors can be plotted against each other to visualize primary and secondary effects.

The following section presents a case study to demonstrate the proposed methodology.

6.4 Case Study

The proposed methodology was applied using an energy model described in chapter 3. The archetype solar building design presented previously in chapter 4 was used for the case-study. This case study used twenty-six discrete variables, summarized in Table 6.1. Note that some variables may depend on circumstances which the designer might not have control over such as construction air-tightness, orientation and occupant behaviour. Variable descriptions are shown for the south orientation only; also, the PV slope is equal to the roof slope since the house has a building-integrated photovoltaic system that covers the south-facing roof. The performance objective selected was the net-annual electricity consumed (Net) during a typical meteorological year, i.e. the energy balance of building energy consumption with renewable energy (RE) generation, see equation 6.3. Negative values of net-energy indicate a greater production of electricity compared to consumption. Thus, satisfying or exceeding the NZE criterion can be stated succinctly as Net ≤ 0 or RE $\geq$ Consumption.

$$\text{Net} = \text{Consumption} - \text{RE} \tag{6.3}$$

An evolutionary algorithm minimized the annual net-energy consumption of the house. The algorithm used a population size P of 10 with 30 generations (M) within each optimization run. To ensure that the optimal landscape was approached from different

Table 6.1: Sample of influential model variables for a NZEH

Variable	Units	Min.	Max.	No. Steps	Description
aspect	–	0.7	2.2	16	Aspect ratio (south facing width to depth ratio)
azi	degrees	-45	45	32	Building orientation/azimuth
wall_ins	m^2K/W	3.5	13.0	8	Effective resistance of wall insulation
ceil_ins	m^2K/W	5.6	15.0	8	Effective resistance of ceiling insulation
base_ins	m^2K/W	0.0	7.0	8	Effective resistance of basement wall insulation
slab_ins	m^2K/W	0.0	2.3	4	Effective resistance of slab insulation
heating_sp	°C	18	25	4	Heating setpoint
cooling_sp	°C	25	28	4	Cooling setpoint
infil	ACH	0.025	0.179	8	Natural infiltration rate
occ_loads	% CAD_{avg}	50	80	8	Occupant loads (percent of Canadian average consumption)
ovr_south	m	0.00	0.45	4	Width of Southern Window Overhangs
pv_area	%	0	90	8	Percent of PV area on roof
pv_eff	%	12	15	4	PV efficiency
roof_slope	degrees	30	47	8	South facing roof/PV slope
wwr_s	%	5	80	8	Percent of window to wall ratio, south (also N,E,W)
GT_s	–	1	4	4	Glazing type, south (also N,E,W)
FT	–	1	2	2	Window Framing Types (1:Wood, 2:Vinyl)
slab_th	m	0.1	0.2	8	Concrete slab thickness
vwall_th	m	0.00	0.35	8	Concrete wall thickness (basement)
zone_mix	L/s	0	400	4	Air circulation rate between thermal zones

angles, 20 optimization runs (N) were executed using randomized initial populations; thus, 6000 EnergyPlus simulations were required ($P \cdot M \cdot N = 6000$). Approaching the optimal landscape from different pathways ensured that the extracted PDFs represented a variety of interactions present in the building model.

6.5 Results

Figure 6.5 shows the PDFs extracted from the optimization training set. Table 6.1 provides longer descriptions of short-form notations. The probabilities of each variable, shown in the y-axis, are normalized to one.

Each PDF resulted in a NZE compliant design given a specific set of other variable combinations. Two-dimensional contour maps are more appropriate to visualize discrete combinations of variables that resulted in NZE compliant designs. For example, Figure 6.6 shows a probability contour plot, based on several near-optimal designs from the training dataset, for the southern window glazing to wall ratio (WWR) and for the amount of wall insulation. The shaded region shows variable combinations that resulted in a NZE compliant home for this particular case study (RE $\geq$ Consumption). Shading indicates the probability that the combination of parameters appeared in the training dataset; darker shading indicates an increased probability of occurrence.

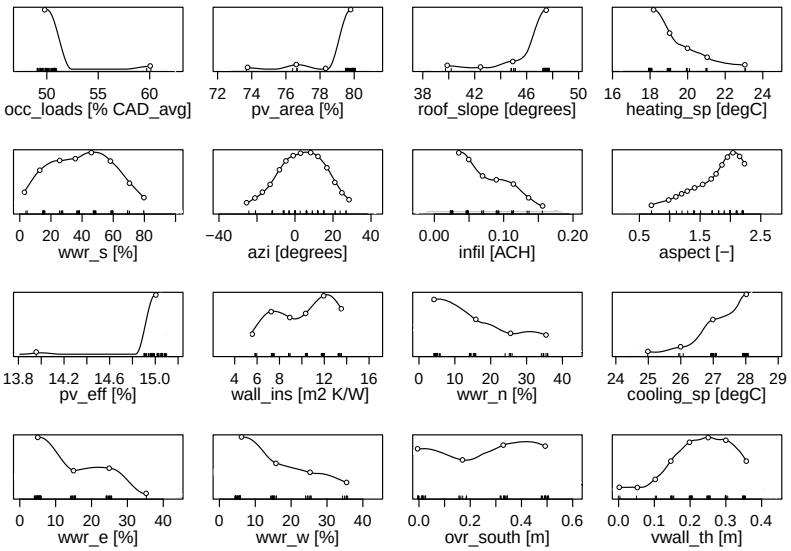

Figure 6.5: Sample of PDFs extracted from the training dataset

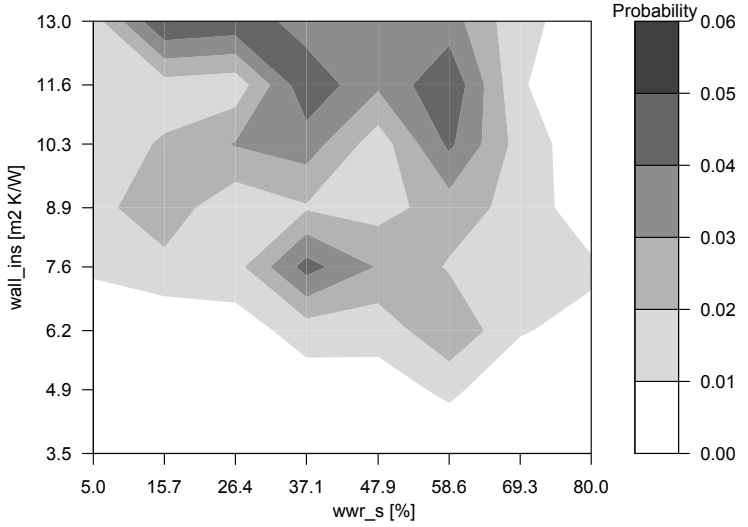

Figure 6.6: Probability of occurrence for southern WWR and wall insulation parameters resulting in homes that are NZE compliant

One important observation from Figure 6.6 is that some combinations of wall insulation and WWR preferentially appeared in clusters due to coupling; for example, a range of southern WWRs of 31.8–47.9% correlated with wall insulation levels of 6.9–8.3 m^2K/W indicating that these variable pairings has a high probability of occurrence in the NZEH training dataset. Additional pairings can be found for higher wall insulation and lower southern WWRs. This important result demonstrates two very different approaches to design a NZEH: (i) super insulated walls with more variable southern WWR, and (ii) a design with relatively lower wall insulation and appropriately sized southern WWR for passive solar design. Both are valid design strategies to achieve the NZE performance criterion. This result quantifies these two different approaches that

until now were described qualitatively: super insulate and be conservative in window areas versus insulate well—but not excessively—and use larger window areas. The second approach was used in the design of the ÉcoTerra house, but the first approach was used in some of the other EQuilibrium houses.

Once the PDFs were extracted from the optimized training dataset, a MCA was performed which resulted in a histogram of the accumulated effects of design variations, as shown in Figure 6.7. If all variables were weakly interacting, the sampling of trained PDFs from NZE compliant design in a MCA would result in all NZE compliant design. However, the shaded area in Figure 6.7 identifies designs where renewable energy generation did not offset the building energy consumption. This is due to variable interactions and non-linearities. The histogram satisfied a hypothesis test for a long-tail distribution (Venables and Ripley, 2002). Long-tailed distributions represent rare events—meaning that deviations from NZE require more than one variable change. The back-tracking analysis proposed, described in section 6.3.3, identifies the variations responsible for long-tail events.

If one was to approximate a mean and variance, assuming a normal distribution, the expected net annual electricity consumption given all variations would be $-400 \pm 850\ kWh$ using a 95% confidence interval. Negative values of energy indicate the net-production of electricity. For this case study, the combined variations is enough to cause building energy consumption to be larger than renewable energy generated in 20.4% (204/1000) of sampled designs, i.e. RE < Consumption.

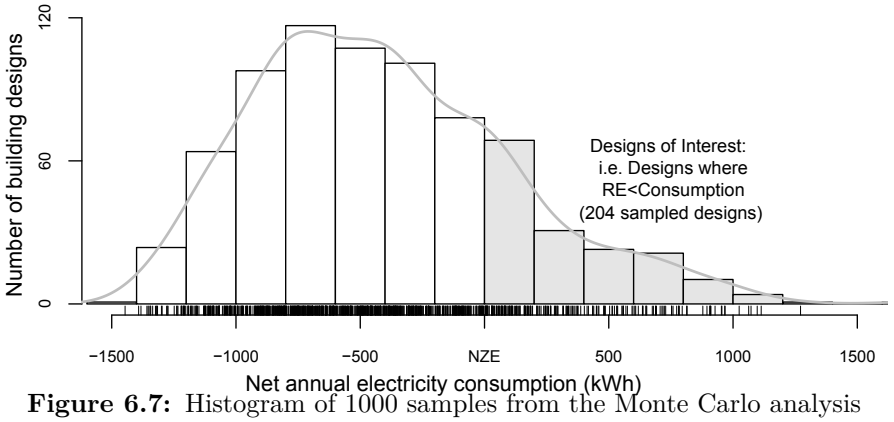

Figure 6.7: Histogram of 1000 samples from the Monte Carlo analysis

Importance factors were calculated for input variables responsible for NZE non-compliance. As shown in Figure 6.7, 20.4% of the sample was non-NZE compliant. Im-

portance factor calculations involved back-tracking each variable to find which variation caused the largest change in net-energy consumption relative to the reference building, see Figure 6.8 for the result of one back-tracking search. The reference building used was the optimal design found from the training dataset. The relative importance for each variable was calculated by normalizing each incremental improvement by the performance difference between each design of interest and the reference building. EnergyPlus simulations determined the incremental variable improvements, the performance of the design of interest and reference building.

Consider the back-tracking of a particular design of interest, as shown in Figure 6.8. Note the net-energy consumption of the design of interest was 374 kWh. A positive NZEH with maximum production was used as the most desirable outcome, and therefore the performance of the reference building was -1446 kWh. The steepest gradient of 797 kWh was obtained by varying the southern WWR from a starting value of 5% to 48.2%, see Table inside Figure 6.8. The local importance factor for variable wwr_s was calculated to be $797/(374 + 1446) = 0.4381$. A local importance factor of 0.4381 indicates that the variation to southern WWR is responsible for about 44% of the net-energy consumption difference of this particular design of interest relative to the optimal reference building.

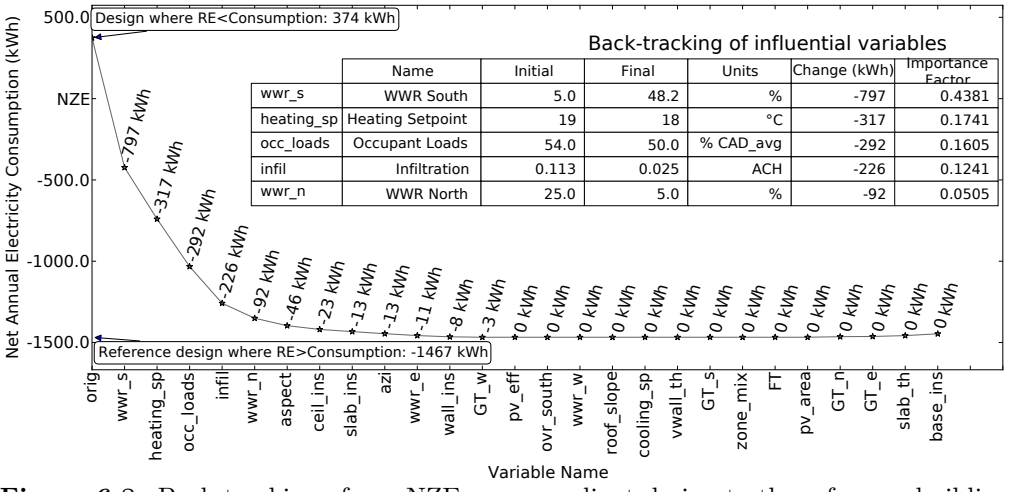

Figure 6.8: Back-tracking of one NZE non-compliant design to the reference building

Table 6.2 presents the influential global importance factors for 204 designs of interest. Recall that global importance factors refer to the averaging of all local importance factors; local importance factors were calculated using a single back-tracking search.

The average net-change presented in this table is the expected change in net-energy consumption found in the back-tracking search for all 204 designs.

Table 6.2: Importance factors for influential variables

Variable	Units	Description	Mean Importance Factor	Importance Factor Deviation	Average Net-Change (kWh)
occ_loads	% CAD_{avg}	Occupant Loads (percentage of Canadian Average consumption)	0.1420	0.1258	253
pv_area	%	Percent area of PV on roof	0.1104	0.1490	200
roof_slope	%	Roof slope	0.1043	0.1627	197
heating_sp	°C	Heating setpoint	0.0993	0.1233	182
wwr_s	%	Percent of window to wall ratio, south	0.0868	0.1280	154
azi	degrees	Building orientation/azimuth	0.0828	0.1200	150
infil	ACH	Natural infiltration rate	0.0705	0.0931	129
pv_eff	%	PV efficiency	0.0445	0.1238	82

Table 6.2 is applicable to other NZEHs with similar variables, RE generation technology, site and situational constraints and climate type as the case study. For different studies, users should repeat the proposed methodology. Calculating the effect of combinations of variations is achieved by adding the average net-changes. This linear assumption may approximate some local non-linear phenomena but is generally acceptable since net-changes originated from the solution space.

Figure 6.9 shows a plot of importance factor mean and standard deviation. Recall that the mean importance factor represents the overall influences of each variable on the non-compliant MC samples shown in Figure 6.7. The importance factor standard deviation represents the effect of non-linearities or inter-variable couplings of each variable. This figure shows three clusters of importance factors: (i) cluster A called influential variables, (ii) cluster B, variables with intermediate influence, and (iii) cluster C, non-influential variables. Based on this plot, only 8 of the 26 variables examined were considered influential.

Figure 6.10 shows the convergence characteristics for the five most influential variables over the back-tracked home designs found to greatly influence the NZE objective. It was found that the calculation of importance factors converged after back-tracking approximately 150 of the 204 building designs. For instance, the value at 50 building designs is the average importance factor calculated for back-tracked building design no. 1 through no. 50. Similarly, the value at 100 building designs is the average of importance factor from design no. 1 through no. 100.

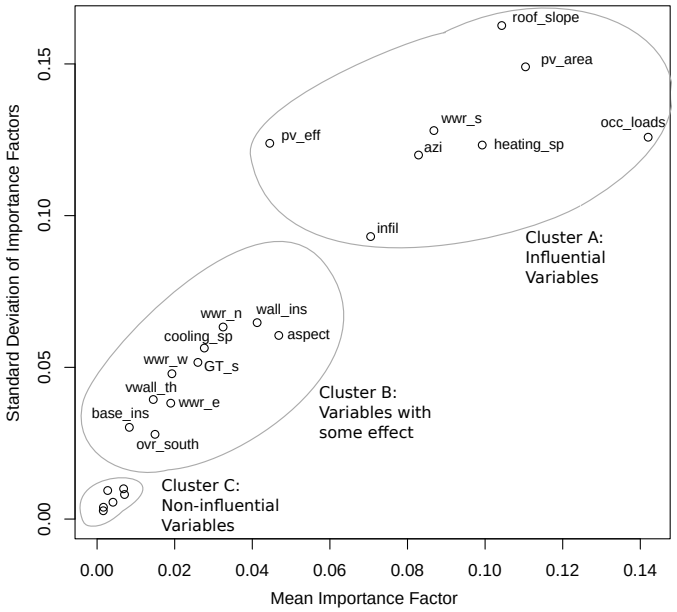

Figure 6.9: Plot of importance factor mean and standard deviation

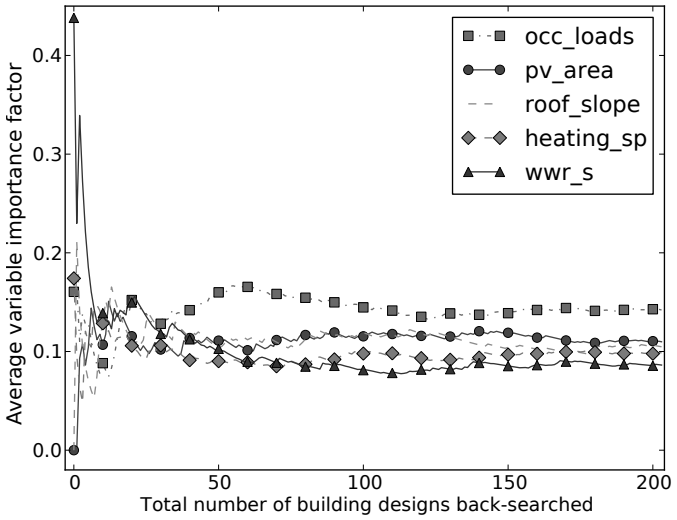

Figure 6.10: Convergence characteristics for the five most influence variables towards a constant importance factor

6.6 Discussion and Conclusion

This chapter proposed a methodology to identify influential variations around a performance criterion. A net-zero energy house case-study demonstrated the methodology. Although the methodology is catered towards NZE buildings, it is applicable to other high performance building studies. The remainder of this section discusses results from the case study and areas of future work.

The application of the methodology to a NZEH identified several design restrictions specific to the case study. From the set of PDFs shown in Figure 6.5, limits in variable ranges that resulted in NZE were identified. For instance, if occupants consumed more

than 60% of Canadian national electricity averages for appliance, DHW and lighting loads, achieving NZE was not practically possible, i.e. PDFs equalled zero. Other similar design restrictions were noted for the building azimuth angle and PV sizing. For example, NZE compliance is difficult to achieve when the main solar collecting surface of the building is oriented greater than 30 degrees of south. Note that these results are for a particular location and a set of modelling assumptions but they are expected to be valid for similar climatic conditions. For this case study, cut-offs originated due to a limited amount of roof space for PV-based electricity generation. Regardless, Figure 6.5 shows a remarkable variety of design combinations with the potential to reach NZE. Figure 6.6 identified that some combinations of wall insulation and WWR preferentially appeared in clusters. For example, a range of southern WWRs of 31.8–47.9% correlated with wall insulation levels of 6.9–8.3 m^2K/W. This result represents two very different design approaches to a NZEH: (i) super insulated walls with more variable southern WWR, and (ii) a design with relatively lower wall insulation and appropriately sized southern WWR for passive solar design. Identifying variable restrictions and optimal combinations of variations in the early design stages of a NZE building will facilitate the quantitative design process.

The convergence of importance factors exhibited an asymptotic relationship regardless of the order of the back-tracked population (see Figure 6.10). The convergence analysis indicated that at least at least 150 back-tracking searches were required to build confident estimates of global importance factors.

In the case study, importance factors indicated that only a few design variables associated with a NZEH significantly affect net-energy consumption. In fact, only thirty percent of the variables examined in the case study were influential. Energy related occupant behaviour (occ_loads) was the most influential variable. Occupant behaviour carried more significance than design variations affecting heating and cooling loads due to the COP effect of the heat pump which reduced electricity used by 1/COP. Monitored data from a set of NZEHs would be more appropriate to extract the importance of occupant behaviour. For this study, ranges of occupant behaviour were based on monitored data of a NZEH and average energy consumption data for Canada. Since the occ_loads importance factor was based on these assumptions of occupant behaviour, these results

are applicable to the case-study only.

Variations related to renewable energy generation, particularly, the roof slope (roof_slope), PV efficiency (pv_eff), building orientation (azi) and percentage of roof coverage with PV (pv_area), were the next most influential variables in the case study. Note that the azimuth and roof slope are factors in energy generation since PV is integrated into the roof surface. Although the significance of PV related variables is not surprising given that roof-based PV being the only source of renewable energy used to offset energy consumption, the relative importance of these variables is not immediately obvious. For example, results suggest that the assurance of PV specifications should have equal or greater prioritization than envelope air-tightness.

Streamlined quality assurance processes guided by importance factors can be used in the design of high performance buildings to identify and prevent costly design mistakes before they occur. By definition, importance factors identify which variables changes are likely to cause a non-compliant performance level for a given climate and building type. Importance factors allow for the prioritization of quality control to focus on the design aspects which most significantly affect a desired performance target. Larger importance factors indicates that changes to the given variable have a greater effect. Also, the size of the anticipated changes can be estimated, as shown in Table 6.2. Similarly, in the commissioning of new buildings, importance factors could aid in identifying and resolving the causes of discrepancies between predicted and realized building performance.

An area for future work is to utilize PDFs and importance factors to improve energy design guidelines by providing a scientific basis for establishing an optimal combination of design variables. Several approaches used in this chapter are applicable in creating more flexible performance-based design guides. For example, PDFs encapsulate all design parameters extracted from an optimized solution set which result in the desired performance level. This can be useful to select parameters which are constrained for the given location. For example, as found by the optimization algorithm, Figure 6.5 shows that wall insulation, wall_ins, must be greater than 6 m^2K/W in Montréal for a house to be NZE. However, the added flexibility of recommending ranges of individual design variables results in a new problem. As shown in this chapter, combining sets of high-performing design variables with the assumption that the combination should

result in a high performing design is circumstantial due to influential variable linkages and couplings. Importance factors, by definition, identify which design variable changes are responsible for such discrepancies. From the perspective of a design guide, the smaller the importance factor of a design variable, the more confidently it can be used in combination with other design variables.

The presented methodology is directly transferable to multiple objectives such as life-cycle cost or embodied energy. The database query requires an additional lower or upper bound for each additional performance objective.

It is likely that annual climatic variations such as variations in solar radiation, exterior wind speed and air temperature will also affect the energy performance of a NZEH. By including climatic factors, the proposed methodology can be applied to establish if the building model, used to inform design decisions, represents the monitored energy operations of the building. If the monitored energy consumption of the building falls within the estimated uncertainty ranges while considering variations in occupant behaviour, design variations and climatic factors, the building is compliant with preliminary energy models. The ability to determine if a predicted building model represents the operations of a building also has implications toward building rating systems, retro and on-going commissioning of buildings, and NZE building compliance checking. These topics will be explored in future research.

Chapter 7

Optimization Methodology to Evaluate the Effect Size of Incentives on Life-Cycle Cost for NZEHs

> "But humankind has a great capacity for finding technological solutions to seemingly intractable problems, and this will likely be the case for global warming. It isn't that the problem isn't potentially large. It's just that human ingenuity—when given proper incentives—is bound to be larger. Even more encouraging, technological fixes are often far simpler, and therefore cheaper, than the doomsayers could have imagined."
>
> *–Steven D. Levitt, SuperFreakonomics*

7.1 Overview

This chapter proposes a methodology to compare the effect of various incentives on optimized building design. The goal of the methodology is to identify incentives structures which improve the economics of performance-optimized building design. The best incentive structures are further investigated in the next chapter. This methodology was presented at an International conference on building simulation (Bucking et al., 2013d).

7.2 Background

The adoption of net-zero energy buildings, like any new technology, is inhibited by cost. An initial cost premium for a NZEB is expected due to the higher initial costs associated with balancing on-site energy generation against energy conservation and efficiency measures. Essentially, NZEB owners pre-purchase their future energy needs before occupying the building. Undoubtedly, there is motivation to move towards high performance buildings due to dwindling fossil fuel reserves and climate change, as well as the superior comfort and low operating costs these buildings provide. Given that it is technologically feasible to achieve NZEBs in most climates (Voss and Musall, 2012), perhaps, the factor limiting the wide-spread adoption of NZEBs is the capacity of consumers to manage higher upfront costs. Economists see such stalemates as perfect opportunities for economic incentives.

In Canada, the cost premium for specialized material and equipment of a net-zero energy home (NZEH) is thought to be between $50,000–90,000 depending on location (CMHC, 2008). Leckner (2008) suggested a NZEH in Montréal had an initial cost premium of $34,300 (excluding solar energy generation) over a typical house, constructed in 1994, and achieved cost payback after 37 years; the embodied energy had a payback of 8.4 years. Patil (2010) indicated that a NZEH in Montréal achieved embodied energy payback after 9 years for PV, 7 years for PV/T and cost payback (including solar energy generation) within a 50 year time horizon. This research indicated that embodied energy payback is relatively short compared to life-cycle cost payback.

If the immediate target of NZE for buildings is too ambitious, then what performance target is economically attractive? Can incentives be developed to encourage the transition towards a NZE building stock? What is the relationship between a cost-optimal building and an energy-optimal building? This chapter examines the opportunity for economic incentives to establish pathways towards cost-optimal NZEBs. It also further develops key concepts from previous cost and energy optimization research.

The BEOpt development team proposed “swoosh” curves to represent cost-optimal improvements relative to a Building America reference building (DOE, 2010), see Figure 7.1.

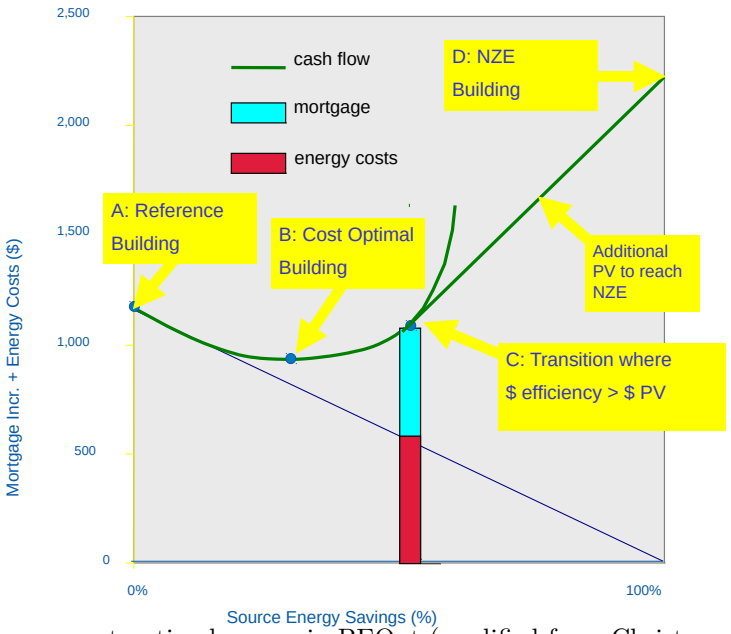

Figure 7.1: Energy-cost optimal curves in BEOpt (modified from Christensen et al. (2004))

The BEOpt team utilized a cost-optimization technique which identified all intermediate designs starting from a reference building to a cost optimal design and eventually a NZEH (Christensen et al., 2004). BEOpt optimal cost curves, shown in Figure 7.1, have several interesting features. The reference building, intended to represent the present housing stock, is marked by point (A). Several design improvements can be made to this reference design to identify a cost-optimal point, the most economically attractive building design, shown by point (B). The sequential search used always prioritizes cost-improvements over energy performance improvements (Horowitz et al., 2008). The transition point (C), is the point where energy generation becomes more cost effective than improvements to energy efficiency and energy conservation. To attain the NZE performance target, point (D), from the transition point (C), a specified number of PV panels are used. The line from point (C) to point (D) is straight due to a linear cost assumption of PV panel costs.

This energy-cost optimal curve has also appeared in European building performance targets. In 2009, EU nations set a target that all new buildings should be NZE after 2020. One peculiarity in establishing this ambitious target is that no clear definitions were given regarding what a NZEB was. Furthermore, no practical guidance was given on how designers and contractors could achieve this target. It was later through the energy performance building directive recast that a firm definition of the NZEB target

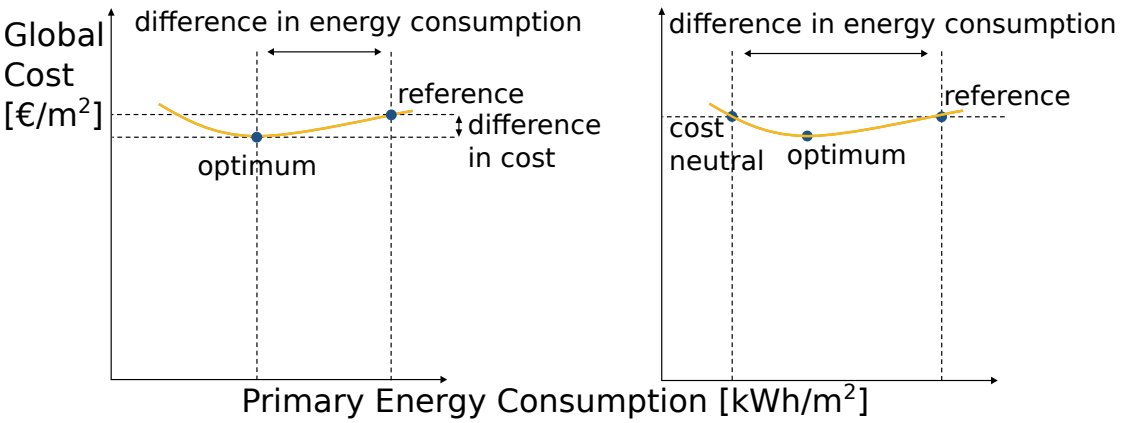

Figure 7.2: Identification of cost optimal and cost neutral buildings (modified from BPIE (2010))

was formed (Kurnitski et al., 2011). The EU now mandates that all new buildings should be nearly net-zero energy (nNZEB) after 2020 (EU Parliament, 2010). A nNZEB is the cost-optimal building using a life-cycle cost analysis on the optimized pathway to a NZEB, see Figure 7.2 (BPIE, 2010). The reference building suggested is defined in EN15316-1 (2007). The nNZEB performance target is less ambitious and favours cost-feasibility to dictate design. Regardless, optimization approaches are influential in forming energy-cost optimal curves.

The Building Performance Institute Europe (BPIE) recommended that designers pursue cost neutral or cost equivalent designs, see Figure 7.2. A cost neutral design has similar life-cycle costs but resides on opposing limit of energy use intensity reductions on the energy-cost optimal curve. They found that economic optimums involved a minor reduction in energy use intensity (EUI) and cost compared to present energy standards. To encourage further reductions in EUI, it was recommended that new buildings be cost neutral with present standards. This means that a given building should be no more expensive, using a life-cycle analysis, than the reference building but have significantly reduced energy consumption. Reference buildings can be a particular energy code or customized to represent a particular building stock. Although it has not been discussed in literature, it is possible that economic incentives may positively effect energy-cost curves.

The remaining chapter presents a methodology for identifying incentive opportunities which create cost-optimal pathways towards NZEB design.

7.3 Method: Evaluating in Effect Size of Incentives on NZEH Design Optimization

This section proposes a methodology to evaluate the effect of several financial incentives on cost-optimal pathways towards NZEBs. In addition, the relationship between cost and energy optimized buildings are examined. To accomplish these goals, the energy-cost curves introduced in the previous section measured the effect of incentives. The following incentive types are explored: (i) incentives which reduce the initial cost premium of a NZEH; (ii) incentives which create revenue streams for part of the life-cycle period; and (iii) disincentives to a typical reference building which indirectly incent the NZE objective.

The proposed methodology and results build from the tools and design concepts presented in previous chapters. To exemplify the approach, a NZEH located in Montréal, as described in section 3.4 was used. Two objective functions are used. Objective function 1 (obj. 1) is the net-energy consumption described by equation 3.13 in section 3.4. Objective function 2 (obj. 2) is the life-cycle cost described by equation 3.17 in section 3.5.

To identify the effect of incentives on pathways towards NZEBs, several objectives are identified: (i) formation of a reference building; (ii) creation of energy-cost performance curve using no incentives (base case); (iii) implementation of incentives by post-processing energy simulation results; (iv) evaluation of incentive effects on energy-cost performance curves; (v) identification of a reference, cost optimal, cost-equivalent and energy optimal building on all energy-cost performance curves; (vi) measurement of effect size by comparing the incentivized energy-cost curve to the base case energy-cost curve from step (ii).

In order to establish a pathway toward cost-optimal and cost-equivalent building designs, a point of reference is required. A reference building represents a business as usual scenario. The method for determining the reference building is shown in Table 7.1. Values in Table 7.1 are specified from the following resources: (i) locally enforced building codes, and (ii) a database of 180 thousand audited Canadian homes (NRCan, 2012; Swan, 2010). For example, envelope air-tightness is not specified by local building codes.

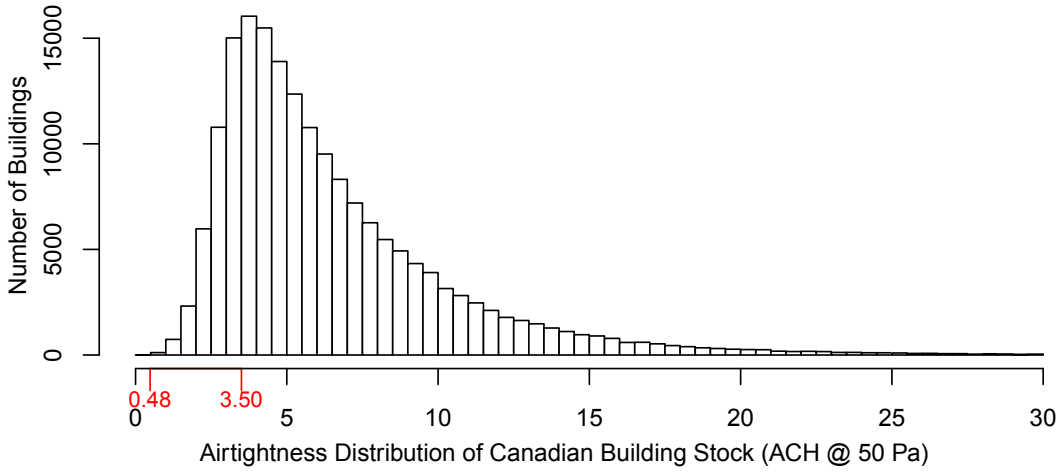

Figure 7.3: Distribution of air-tightness in the Canadian housing stock

Instead, physical measurements from a standardized blower-door test were used, see Figure C.2. The most probable air-tightness value for a home in Canada is around 3.5 ACH at 50 Pa. This value was used for the reference infiltration rate. Similarly, other values were determined from this dataset if they could not be determined from building code.

Values of Table 7.1 are based on Appendix C. The cost-performance metric is the relative life-cycle cost function, as described in section 3.5, compared to the reference design using a 30 year time horizon. A summary of the life-cycle cost parameters are shown in Table 7.2.

The cost-equivalent performance criterion was defined by identifying buildings which have the same life-cycle cost as the reference building, but resides on the opposing limit of net-energy consumption of the energy-cost optimal curve, see Figure 7.4.

The incentive effect is the shift in net-energy consumption of the energy-cost curve with an incentive relative to the baseline energy-cost curve without an incentive, see Figure 7.5. The larger the shift, the more beneficial the incentive is for the NZE objective.

The next step is to identify several performance points on the cost-energy curve. The optimization tool, described in section 3.2 and chapter 3, was used to find: (i) the design with lowest net-energy consumption, or the energy optimal design (obj. 1); (ii) the cost optimal design relative to the reference building (obj. 2); and (iii) the set of Pareto optimal designs, or designs with trade-offs with respect to obj. 1 and obj. 2. Included in this set is the cost-equivalent design.

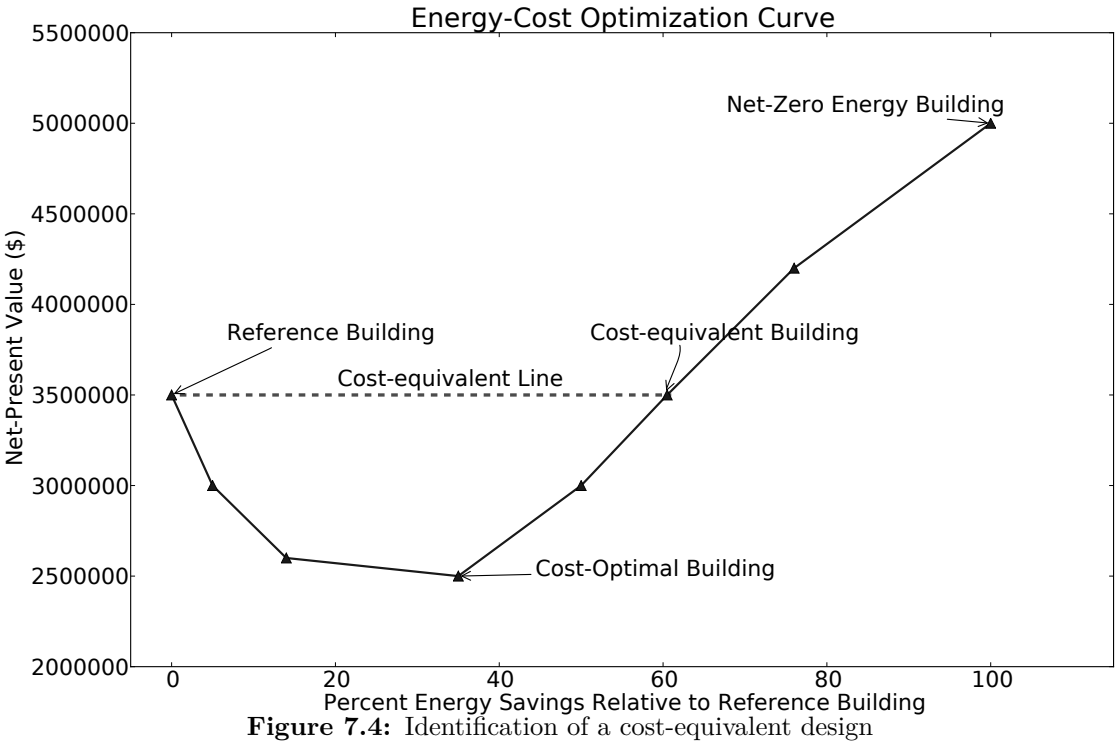

Figure 7.4: Identification of a cost-equivalent design

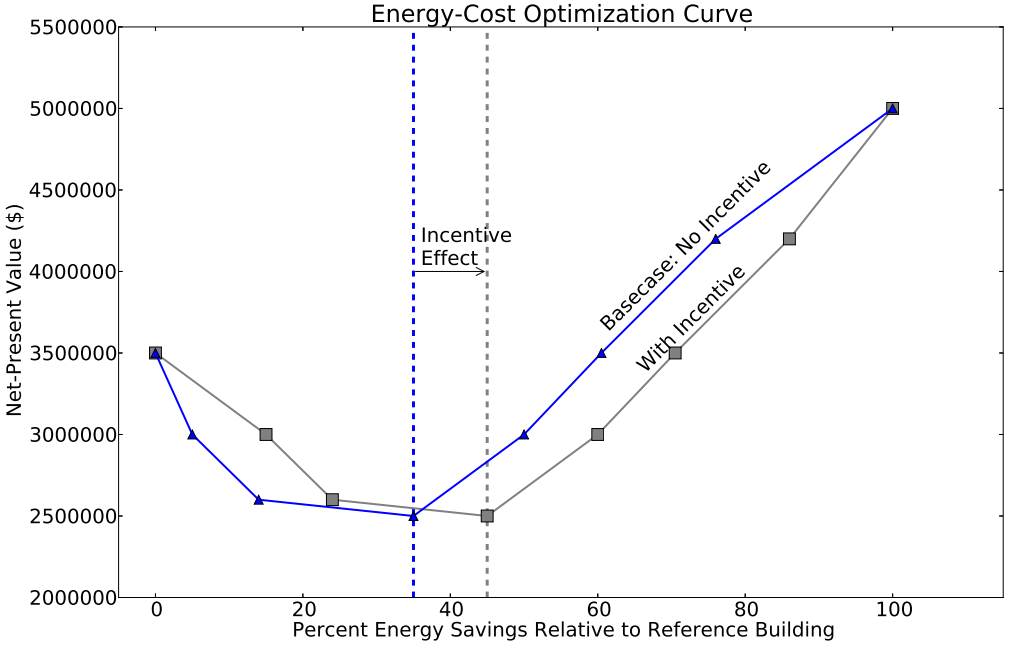

Figure 7.5: Incentive effect using a energy-cost diagram

Table 7.1: Definition of reference building

Variable	Description	Units	Reference Building Values
stories	Number of stories	–	same[a]
area	Total floor area	m^2	same[a]
azi	Building orientation/azimuth	degrees	0
aspect	Aspect ratio (south facing width to depth ratio)	–	1.4
wall_ins	Effective resistance of wall insulation	m^2K/W	4.4[c]
ceil_ins	Effective resistance of ceiling insulation	m^2K/W	8.8[c]
base_ins	Effective resistance of basement wall insulation	m^2K/W	3.5[c]
slab_ins	Effective resistance of slab insulation	m^2K/W	1.7[c]
ovr_south	Width of Southern Window Overhangs	m	0
occ_loads	Occupant loads (percent of Canadian average consumption)	% CAD_{avg}	same
pv_area	Percent of PV area on roof	%	0
pv_eff	PV efficiency	%	0
roof_slope	South facing roof/PV slope	degrees	30
wwr_s	Percent of window to wall ratio, south	%	25[b]
wwr_n	Percent of window to wall ratio, north	%	10[b]
wwr_e	Percent of window to wall ratio, east	%	10[b]
wwr_w	Percent of window to wall ratio, west	%	10[b]
GT_s	Glazing type, south (also N,E,W)	–	2
heating_sp	Heating setpoint	°C	18
cooling_sp	Cooling setpoint	°C	26
FT	Window Framing Types (1:Wood, 2:Vinyl)	–	2
slab_th	Concrete slab thickness	m	0.05
vwall_th	Concrete wall thickness (basement)	m	0.05
zone_mix	Air circulation rate between thermal zones	L/s	50
infil	Natural infiltration rate	ACH	0.175[b]

a: value is same as the compared design.
b: value is taken from Canadian home dataset.
c: value is dictated by building code.

Table 7.2: Summary of life-cycle cost parameters

Cost Parameter	Setting
Inflation	2.00%
Bank rate	2.14%
MARR	4.18%
Life-cycle period	30 years

Energy-cost optimal curves were created for each incentive scenario and for a no-incentive scenario. Creating energy-cost curves required the following steps: (i) create datasets by running the multi-objective algorithm for each incentive (algorithm settings are summarized in Table 7.3 and were discussed in detail in section 3.2); (ii) remove all designs with energy performance less than the reference building; and (iii) from the remaining data, identify four points (reference, cost optimal, energy optimal and cost-equivalent buildings). The optimization algorithm was run separately for each incentive. This ensured that the algorithm could exploit cost-saving aspects such as renewable energy rebates to reduce life-cycle cost. Multi-objective optimizations were run ten

times to ensure the solution space was fully explored.

Table 7.3: Summary of multi-objective algorithm configuration

Algorithm Parameter	Setting
Representation	66 bit grey-coded binary string
Solution Space Size	1.84^{19} unique designs
Objective 1	Net-energy consumption (kWh)
Objective 2	Life-cycle cost over a 30 year period ($)
Population Size	10 growing to 40, i.e. generation gap of 25%
Recombination	50% bit-by-bit Uniform, 50% variable Uniform
Recombination Prob	100%
Mutation	40% bit-by-bit mutation, 60% differential mutation
Mutation Prob	2.0%
Parent Selection	Non-dominated sorting (NSGA-II)
Elitism?	Yes, built into NSGA-II
No. of Children	10
Survivor Selection	Best parents and children, $(\mu + \lambda)$, using crowded comparison operator
Diversity Control	None required since using NSGA-II

The effect of the following incentives were explored: (i) PV feed-in tariff; (ii) preferential mortgage rates; (iii) rebate on renewable energy technology; and (iv) TOU electricity billing.

A FIT incents the creation of on-site renewable electricity generation. This income is intended to provide an attractive return on investment for homeowners to accept the financial cost of additional material and labour associated with the PV system install. The intent is to financially reward those who participate in the distributed generation of renewable energy. Ideally, if electricity is generated during peak periods, distributed generation can preclude the need for additional centralized generation. For this study, a tariff of 54.9 ¢/kWh was used for 20 years of the life-cycle based on a incentive program incentive program in Ontario (OPA, 2013). Feed-in tariffs have been successfully implemented in other countries such as Germany and Spain.

Fixed-rate mortgages were used to reduce initial costs by amortizing them over a set 25 year term. The intention is to provide preferential mortgage rates to clients purchasing a NZEH. Since NZEHs have lower operational costs, owners should be more capable of making monthly mortgage payments; thus lenders should incur less risk for issuing mortgages to NZEH owners. Due to this reduced risk, NZEH homeowners should be eligible for preferential mortgage rates. A preferential mortgage fixed-rate of 3% was

assumed.

A rebate was explored as a possible mechanism to reduce the cost premiums incurred by NZEH owners. A rebate essentially offsets the initial costs required to purchase a given good; rebates can be in the form of tax deductions, Government issued grants, or provincial sales tax rebates. In order to have a measured effect, the incentive must be significant. In 2008, the US Government offered tax rebates of 30% of initial PV system costs (USGOV, 2008). For this study, a similar rebate of 30% is explored. Rebates absorb some of the cost premiums associated with renewable energy generation technologies by reducing the initial price at year zero of the life-cycle cost analysis.

Finally, TOU electricity billing creates a disincentive to use electricity during peak electrical use periods, typically 7am to 7pm. This disincentive may be beneficial since a NZEH uses considerably less electricity compared to a reference building during peak hours. Higher operation cost for other building options may incent homeowners to purchase a NZEH. Section 3.5.7.3 described the TOU schedule used.

The effect of these aforementioned incentives on the cost-optimal and cost-equivalent point relative to a reference building are shown in the following results section.

7.4 Results and Discussion

Figure 7.6 shows the energy-cost curve for a no-incentive scenario.

This plot shows a sample of non-optimal designs in the optimization search using black hollow circles. The reference, cost-optimal, energy-optimal and cost-equivalent designs are shown using large solid circles. These results are used to measure the effect size of incentives. The cost-optimal point has an energy performance of approximately 10,000 kWh. Note the cost-equivalent design is a NZEH. This implies that a NZEH costs approximately the same as the reference building over a 30 year life-cycle.

Figure 7.7 shows the four points from Figure 7.6 as well for all other incentives.

TOU had little effect on the energy-cost curve. As expected, disincentives increased the NPV of reference building designs. PV system rebates reduced the cost of the cost-optimized design but did not significantly shift the energy-cost curve. Incentives such as FIT and a FIT combined with a preferential mortgage rate had a large incentive effect.

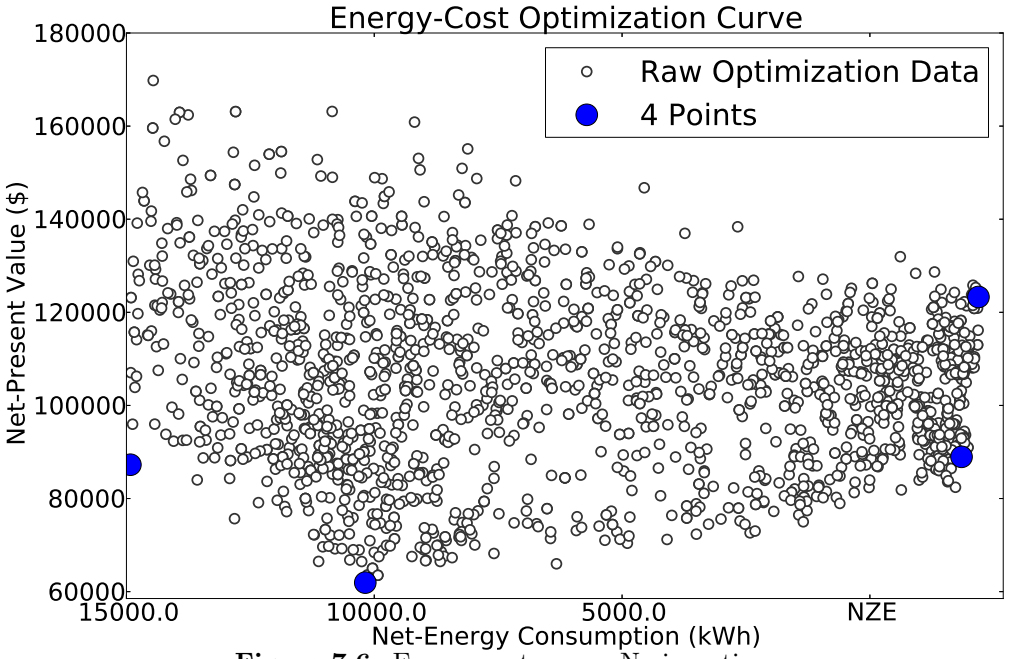

Figure 7.6: Energy-cost curve: No incentives

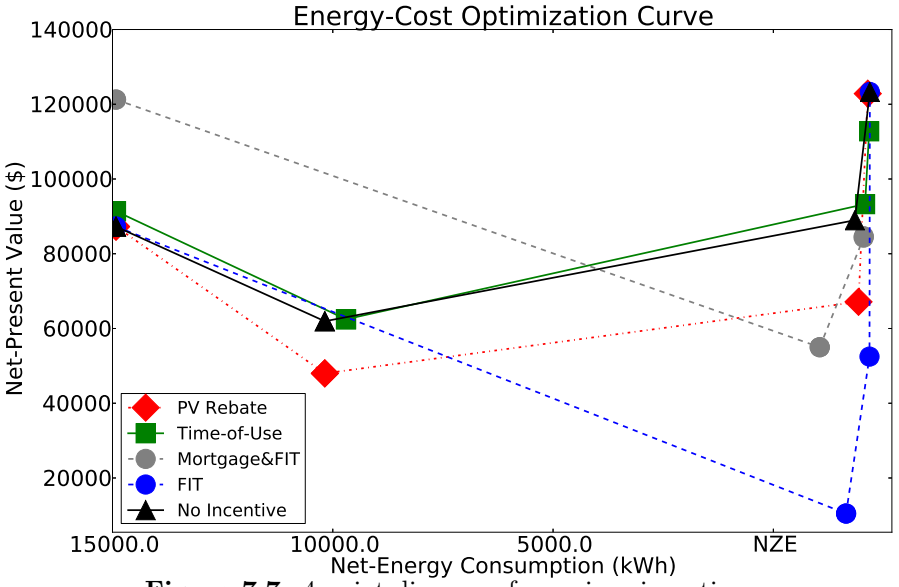

Figure 7.7: 4-point diagrams for various incentives

In fact, the use of a FIT is sufficient to move the cost-optimal point very close to the energy-optimal design. Figure 7.8 shows the raw data used to create the energy-cost optimal curve for the FIT incentive. Note that separations in raw points are caused by discrete variables in the optimization analysis.

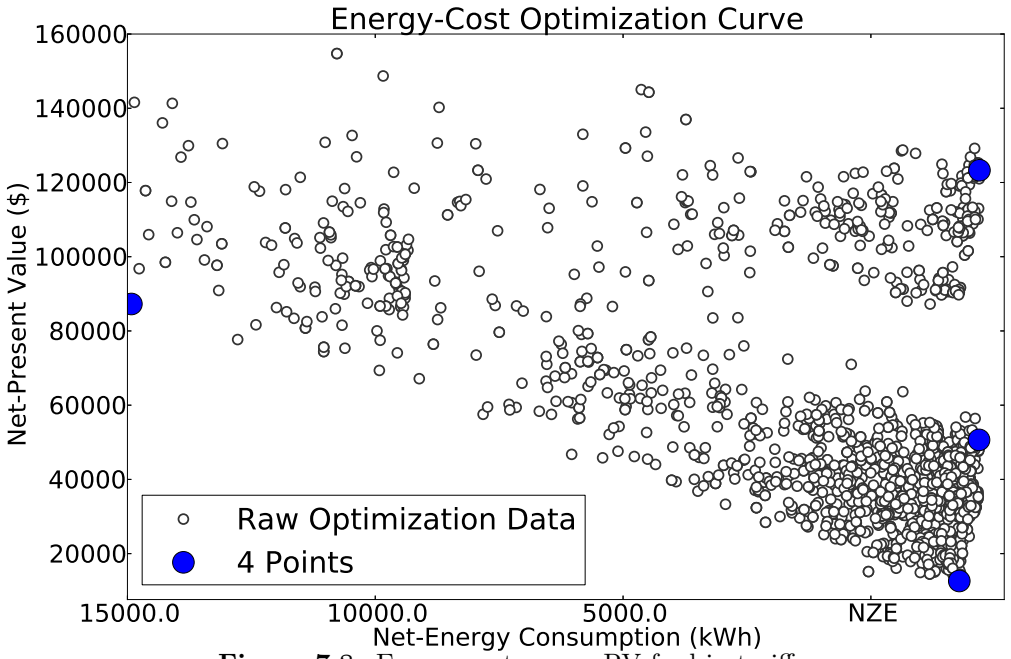

Figure 7.8: Energy-cost curve: PV feed-in tariff

Note there is a large disparity in Figure 7.8 of almost $120,000 difference between the cost-optimal and energy optimal design over the life-cycle. This suggests that optimization studies can greatly aid in identifying pathways to cost-optimal NZEHs. Furthermore, since some NZEHs can cost up to 50% more than a cost-equivalent NZEH design, a life-cycle cost analysis is needed in addition to an energy analysis.

Table 7.4 shows the optimal NZEH parameter set for the cost-optimal individual in Figure 7.8.

This optimal design generated a net of 1053 kWh of electricity. To achieve this level of performance required a balance of passive solar strategies, such as: air-tight envelopes (0.05 ACH), high envelope insulation values (8.56 m^2K/W), appropriate south-facing window-to-wall percentage (48%), sufficient circulation of thermal gains (133 L/s) and sizing of thermal mass (0.251 m central thermal storage wall in basement). Note that the algorithm found diminishing returns for ceiling, wall and slab insulation.

Table 7.5 shows the raw results form Figure 7.7. This table also shows the incentive

Table 7.4: Cost optimal design using the PV FIT incentive

Variable	Description	Units	Optimal Values
azi	Building orientation/azimuth	degrees	0
aspect	Aspect ratio (south facing width to depth ratio)	–	1.3
wall_ins	Effective resistance of wall insulation	m^2K/W	8.93
ceil_ins	Effective resistance of ceiling insulation	m^2K/W	10.97
base_ins	Effective resistance of basement wall insulation	m^2K/W	5.08
slab_ins	Effective resistance of slab insulation	m^2K/W	1.39
ovr_south	Width of Southern Window Overhangs	m	0.34
pv_area	Percent of PV area on roof	%	90
pv_eff	PV efficiency	%	15
roof_slope	South facing roof/PV slope	degrees	45
wwr_s	Percent of window to wall ratio, south	%	48
wwr_n	Percent of window to wall ratio, north	%	10
wwr_e	Percent of window to wall ratio, east	%	10
wwr_w	Percent of window to wall ratio, west	%	10
GT_s	Glazing type, south (also N,E,W)	–	2
FT	Window Framing Types (1:Wood, 2:Vinyl)	–	2
slab_th	Concrete slab thickness	m	0.2
vwall_th	Concrete wall thickness (basement)	m	0.251
zone_mix	Air circulation rate between thermal zones	L/s	133
infil	Natural infiltration rate	ACH	0.025
Fitness of Individual (kWh)			-1491

effect, or the shift in the cost-optimal building for each incentive from the no-incentive scenario as previously described by Figure 7.5.

Table 7.5: Energy and cost values for reference cost optimal and cost equivalent buildings

Incentive	Reference Building		Cost Equivalent Building		Cost Optimal Building		Incentive Effect (kWh)
	Obj. 1 (kWh)	Obj. 2 ($)	Obj. 1 (kWh)	Obj. 2 ($)	Obj. 1 (kWh)	Obj. 2 ($)	
None	14920.36	87262.47	-1849.18	88959.54	10180.96	61937.14	–
Time of Use	14920.36	91386.38	-2081.73	93271.2	9699.66	62462.79	481
PV Rebate	14920.36	87262.47	-1933.64	67132.59	10180.23	47990.89	0
Feed-in Tariff	14920.36	87262.47	-2181.88	50646.65	-1783.34	12626.34	11964
Mortgage and FIT	14920.36	119467.28	1129.29	76601.43	-2135.04	125167.93	12316

Table 7.6 shows the initial cost of the cost optimal building and the life-cycle cost for each incentive. Homeowners are sensitive to the first cost of a home. Incentives which reduce the initial cost may be desirable. Ideally, incentives should reduce the initial cost and the life-cycle cost. This was achieved by combining a PV FIT with a preferential mortgage. Note that mortgage loans decrease the initial cost but increase the life-cycle cost. PV system rebates decrease both. Feed-in tariffs reduce the life-cycle cost but do not significantly effect initial costs. The optimization algorithm did not select PV systems for the TOU and base case cost-optimal buildings. This explains the lower initial costs for these scenarios. All life-cycle values were positive indicating that payback was not achieved for the desired rate of return.

Table 7.6: Initial cost premiums for cost-optimal design using various incentives

Incentive	Initial Cost Premium	Life-Cycle Cost
None	27103.00	61937.14
Time of Use	26400.00	62462.79
PV Rebate	21800.00	47990.89
Feed-in Tariff	58900.00	12626.34
Mortgage and FIT	45061.00	125167.93

7.5 Conclusion

Given the proper incentive, a NZEH can also be a smart financial opportunity. Incentives which generate revenue over the life-cycle period, such as feed-in tariffs for PV generated electricity, have a large effect on shifting the energy-cost optimal curve. As shown by Table 7.6, higher initial costs can be reduced using mortgage loans but at the trade-off of increasing life-cycle costs.

The shape and behaviour of energy-cost curves depends on available incentives. The proposed methodology can influence EU NZEB initiatives. Recall that the EU downgraded the target that all new buildings should be NZE by 2020 to nearly-NZE. However, using incentives the cost-optimal target can also result in an energy-optimal target. Carefully selected incentives can assist EU member states in achieving their 2020 goals.

Multi-objective building optimization using energy and cost objectives is a problem of context. The results presented are dependent on location, climate and time. The economic scenarios found in various countries will affect results. The local climate will dictate the energy performance limits of the building. New technologies will affect the potential performance of any building. Furthermore, future economic circumstances, such as inflation and fuel costs are constantly fluctuating. Likely, optimization outcomes will change every few years due to these circumstances. Thus, the proposed methodology can aid in identifying new opportunities for a cost-effective building stock. The results should not be viewed as being static and final. The issue is highly dynamic and depends on economic situations as well as the needs and wants of different countries. This emphasizes the importance of an optimization methodology over optimization results.

In this chapter, net-zero energy performance was made possible using a mix of passive solar design, improved mechanical efficiency and renewable energy generation using photovoltaic panels as determined by an optimization algorithm. Further technological

advances will undoubtedly improve thermal storage, reduce peak loads, improve controls and enable distributed grids. However, without further economies of scale or strong economic incentives, net-zero energy buildings will likely remain a small fraction of the building stock due to their additional upfront costs.

Further research is needed to identify incentives which reduce initial and life-cycle costs by generating revenue over the life-cycle period. These types of incentives greatly improve the life-cycle cost outcome. Further work should focus on collaborating with policy makers to ensure that future buildings are both cost and energy optimal.

Chapter 8

Effect of a Time-of-Use Feed-In Tariff on Optimal Net-Zero Energy Home Design

> "In some ways I think that scientists have misled themselves into thinking that if you collect enormous amounts of data you are bound to get the right answer. You are not bound to get the right answer unless you are enormously smart. You can narrow down your questions; *but enormous data sets often consist of enormous numbers of small sets of data*, none of which by themselves are enough to solve the thing you are interested in, and they fit together in some complicated way."
>
> –*Bradley Efron*

8.1 Overview

This chapter builds on successful incentives proposed in the previous chapter, in particular, the effect of a feed-in tariff on optimal NZEH design. As recommended in the previous chapter, technology costs are amortized in life-cycle cash flows. This assumes that roof-installed PV panels are considered by mortgage lenders as part of the property value. A time-of-use FIT is explored to investigate cash-flow improvements and how such an incentive affects optimal buildings design. This section demonstrates the utility of conservation and efficiency measures to reduce the net-payback of a NZEH. However, projected future PV panel costs suggest that this relationship may change in the coming decade. To achieve this, archetype solar home proposed in chapter 4 is used in the case-study. The optimization methodology and approach proposed is important in identifying future interactions using yet unknown economics. In this chapter, large sets of interacting optimization data are reduced to simple economic metrics, in order to

better understand the relationship between energy conservation measures and renewable energy generation in optimal building design.

8.2 Background

In the last 10 years, the PV industry has undergone a significant transformation. PV panel prices have dropped much more quickly than anticipated. The IEA PVPS (2013) anticipated that global price of PV would approach $1/W by 2017. Globally, a PV panel is manufactured at $1.15/W in 2012 and is predicted to decrease to $0.85/W by 2014 (IEA PVPS, 2013). Furthermore, the cost of manufacturing PV panels is decreasing by 20% per year (Breyer and Gerlach, 2010) with conversion efficiencies approaching 25%. At the beginning of this PhD (2009), market-ready PV was sold at almost $4/W (not installed) and was only 14% efficient! The DOE SunShot initiative aims to provide opportunities to facilitate innovation in the market and reduce installed PV panel costs at 25% efficiency to $0.5/W and total installed costs (including panel price) to $1/W by 2020 (DOE, 2013). The SunShot initiative is offering a ten million dollar prize to the first company who achieves this task. At the $1/W installed price point, it is believed that PV can compete directly with all other forms of electricity generation in the US even with subsidies to fossil fuels. The PV industry is now projected to achieve this goal by 2020. The idea that solar energy will be cheaper than fossil fuels is not surprising. Fossil fuels require exploration, environmental review, processing, transportation and management and without carbon capture and containment scrubbing they negatively impact the environment. Solar energy originates from an efficient nuclear fusion process which is abundant, free to use and a virtually inexhaustible form of renewable energy. However, it is not possible yet to achieve net-zero energy using renewable energy alone.

Rapidly falling PV prices complicates the relationship between improved energy conservation approaches to building design, improved mechanical efficiency and renewable energy generation in optimal building design. For example, at what PV price point is it more economical to invest in generation over more insulation? From a different perspective, is it possible that investment gains from cheap, efficient PV might be reinvested into further efficiency measures to reduce net-energy consumption? Methodologies, not

rules-of-thumb are necessary to navigate such complex and constantly fluctuating interactions.

This chapter explores the effect of a TOU FIT incentive and falling PV prices on optimal building design. The capital payback of a NZEH case-study previously shown in Chapter 5 is further expanded upon. The relationship between energy conservation measures and PV generation at different price points is explored using this model.

8.3 Method

A Feed-in-Tariff was developed to create positive cash-flow for PV integrated into the envelope of a NZEH. Feed-in tariffs for renewable energy generation have been available since 2009 in Ontario (OPA, 2013). Peak electricity consumption in some large Canadian cities, such as Toronto, is directly correlated with summer cooling (Toronto Hydro, 2011). Cooling loads are caused by peak solar radiation which could be offset using PV generated electricity. To create a disincentive for electricity use during peak periods, some provinces in Canada have implemented time-of-use electricity charges. Since electricity is sold at a higher rate during peak periods, logically, so too should it be purchased at a cost premium. The largest incentive is provided when electricity is needed the most. Such incentives may cause sub-optimal orientation to improve PV generated revenue and better reduce peak-grid loads. Utilities benefit since they do not require expansion of centralized generation to meet peak electricity demands and PV system owners generate additional revenue during the equipment's expected lifetime. This incentive structure improves a criticism of the present FIT program that tax-payers pay cost premiums for PV generated electricity when electricity is not at peak demand.

Table 8.1: Time of use Feed-in Tariff

FIT Schedule	Hours	Peak	Incentive, ¢/kWh
Summer Weekdays	21:00–07:00	off-peak	36.6
	07:00–11:00	mid-peak	54.9
	11:00–17:00	on-peak	72.2
	17:00–21:00	mid-peak	54.9
Winter Weekdays	21:00–07:00	off-peak	36.6
	07:00–11:00	on-peak	72.2
	11:00–17:00	mid-peak	54.9
	17:00–21:00	on-peak	72.2
Weekends and Holidays	00:00–24:00	off-peak	36.6

Table 8.1 shows the implemented time-of-use feed-in tariff over a 20 year period. Note that peak electricity mid-purchase rates are based on the microFIT program offering of 54.9¢/kWh in Ontario (OPA, 2013). The off-peak rate was determined by a reduction multiplier of 1.5. The on-peak rate was set as 2.5 times the off-peak rate.

Using this incentive, along with the energy model proposed in Chapter 3 and the multi-objective optimization methodology proposed in Chapter 7 a near cost-optimal design on the Pareto front was identified. Note that economic metrics such as payback are compared to a reference building as defined in Appendix C.

The next section presents results and a discussion.

8.4 Results and Discussion

A TOU FIT was found to increase annual cash-flows by 20% (approximately $1000) with a 3% increase in net-energy consumption. The optimal design found in this analysis is shown in Table 8.2.

Table 8.2: Optimization Results for ÉcoTerra Complete Redesign

Variable	Description	Units	Optimal Values
azi	Building orientation/azimuth	degrees	12 (SSE)
aspect	Aspect ratio (south facing width to depth ratio)	–	1.4
wall_ins	Effective resistance of wall insulation	m^2K/W	8.56
ceil_ins	Effective resistance of ceiling insulation	m^2K/W	10.57
base_ins	Effective resistance of basement wall insulation	m^2K/W	5.08
slab_ins	Effective resistance of slab insulation	m^2K/W	1.39
ovr_south	Width of Southern Window Overhangs	m	0.34
pv_area	Percent of PV area on roof	%	90
pv_area_e	Percent of PV on east facade	%	0
pv_area_w	Percent of PV on west facade	%	0
pv_eff	PV efficiency	%	15
roof_slope	South facing roof/PV slope	degrees	45
wwr_s	Percent of window to wall ratio, south	%	48
wwr_n	Percent of window to wall ratio, north	%	10
wwr_e	Percent of window to wall ratio, east	%	10
wwr_w	Percent of window to wall ratio, west	%	10
GT_s	Glazing type, south (also N,E,W)	–	2
heating_sp	Heating setpoint	°C	18
cooling_sp	Cooling setpoint	°C	28
FT	Window Framing Types (1:Wood, 2:Vinyl)	–	2
slab_th	Concrete slab thickness	m	0.25
vwall_th	Concrete wall thickness (basement)	m	0.15
zone_mix	Air circulation rate between thermal zones	L/s	133
infil	Envelope air-tightness (natural infiltration rate)	ACH	0.025
$f(\mathbf{x})$	Net-Energy Consumption of Individual	kWh	-3150
$g(\mathbf{x})$	Net-Present Value of Individual	$	32,000

Interestingly, the TOU FIT caused very few design changes compared to previous chapters. The largest change is the sub-optimal orientation 12 degrees east of south.

Further inspection found that the algorithm was increasing cash-flow by generating more electricity during peak periods while slightly reducing the energy performance of the home. Here, 12 degrees east of south was identified as the optimal trade-off in lost performance to improve payback. The design strategies found in previous chapters were equally applicable under the context of sub-optimal orientations.

Figure 8.1 shows the breakdown of cash flow for the FIT incentive and amortization of initial costs.

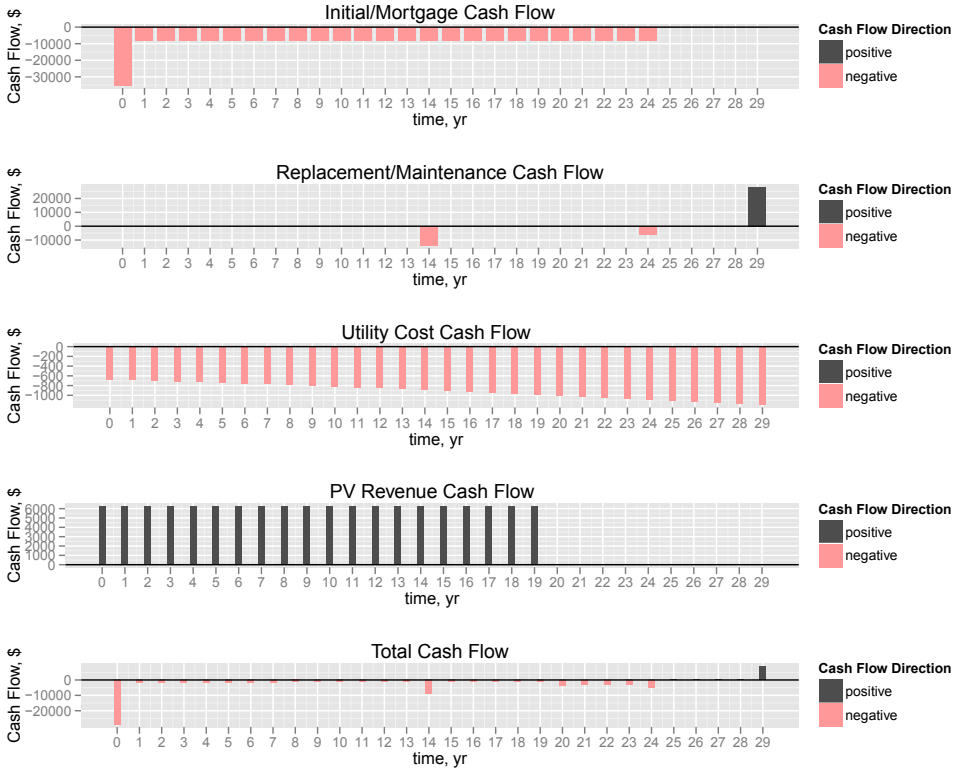

Figure 8.1: Cash flow diagram of optimal design using FIT incentive and mortgage

Figure 8.2 shows total cash flow for the optimal design compared to the total cash flow of the reference design. The cumulative sum shows the optimal NZEH has a capital payback of 9 years. The internal rate of return for this cash flow difference is 5%.

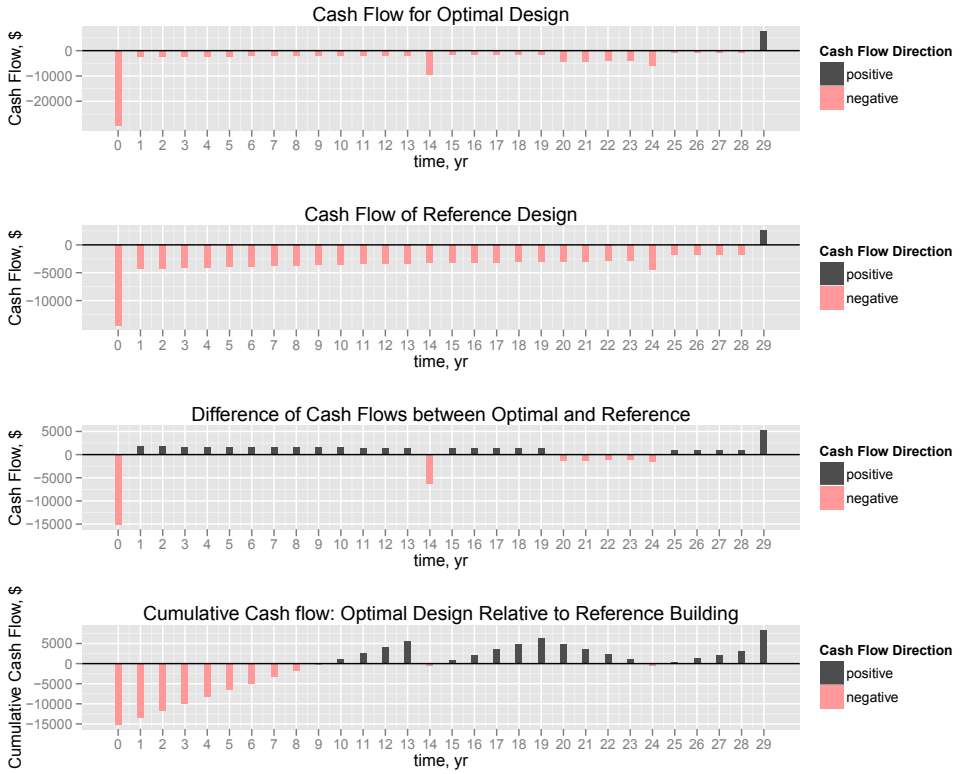

Figure 8.2: Cash flow diagram: Optimal design compared to reference building

Table 8.3 shows the capital payback of various conservation measures relative to the reference home.

Table 8.3: Sample of capital payback of design upgrades from reference to optimal design

Variable	Description	Reference	Optimal	Units	Payback, yr
pv_area	Percent of PV area on roof	0	90	%	10.5
GT_s	Glazing type, south	dbl-glaze	dbl-glaze EStar	–	2.5
ceil_ins	Effective resistance of ceiling insulation	8.8	10.57	m^2K/W	10
wwr_s	Percent of window to wall ratio, south	25	48	%	3.0
wall_ins	Effective resistance of wall insulation	4.4	8.56	m^2K/W	3.9
blind_irr	Incident solar radiation for blind deployment	0	150	W/m^2	3.8
Combined payback from reference to optimal					9.1

Under present economic scenarios, the capital payback of conservation measures are less than the capital payback of PV panels. Effectively, conservation measures reduced the net-payback of PV panels relative to the reference building. For example, better insulation and improving solar access had economic paybacks in the sub five year range whereas further improving ceiling insulation and adding solar panels had paybacks nearer to 10 years. Combining both measures under one capital investment had a net-payback

of 9.1 years.

The following figures explore scenarios for increasing utility costs and reduced PV panel costs. Figure 8.3 shows total cash flow for the optimal design compared to the total cash flow of the reference design with electricity prices at 14¢/kWh. Under the scenario of electricity prices at 14¢/kWh, payback is achieved after 6.5 years.

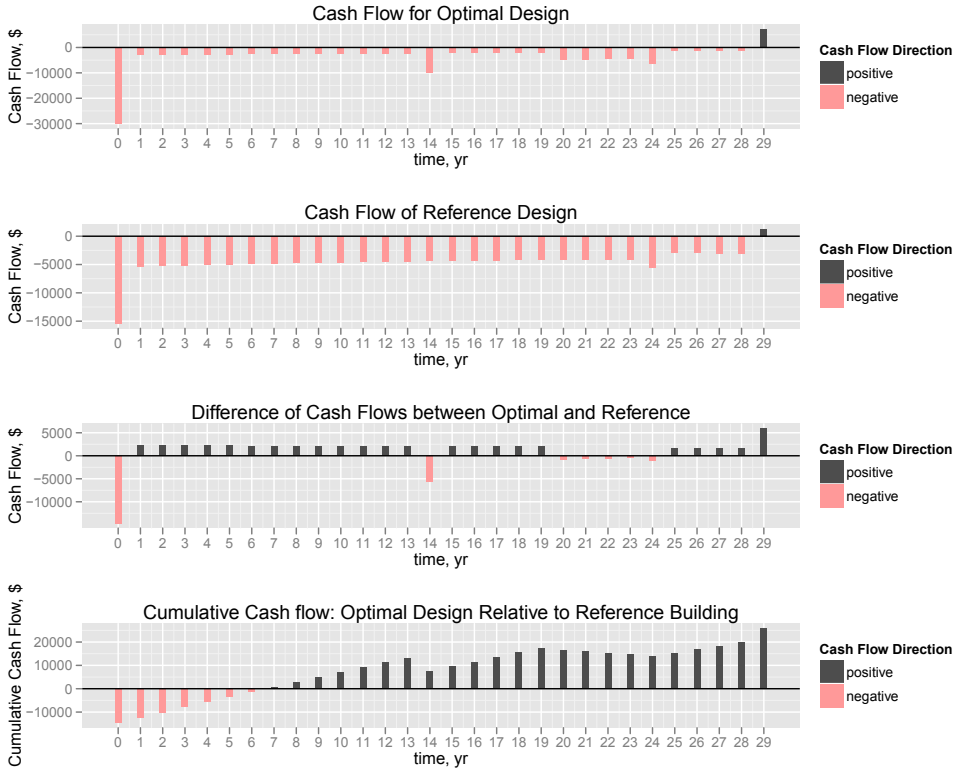

Figure 8.3: Cash flow diagram: Optimal design compared to reference building. Utility prices at 14¢/kWh.

Figure 8.4 shows total cash flow for the optimal design compared to the total cash flow of the reference design with PV panel prices at 1.0$/W or 2.5$/W installed and electricity prices at 14¢/kWh. Under the scenario of electricity prices at 14¢/kWh and PV panel installed costs of $2.5, capital payback of 3 years is achieved.

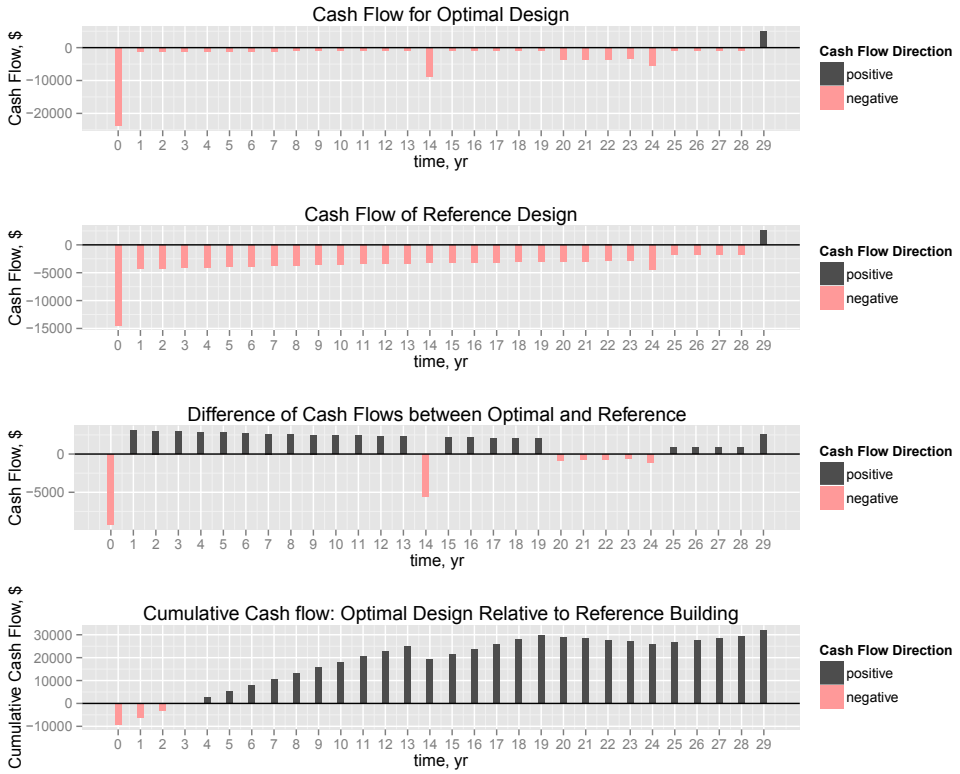

Figure 8.4: Cash flow diagram: Optimal design compared to reference building. PV prices at 1.0$/W and electricity prices at 14¢/kWh.

8.5 Conclusion

With targeted incentives, NZEH can have an payback that is more attractive and stable than other market options. Typically, consumers and business will act on investments with capital paybacks in the 5–7 year range. Given the projected future cost of PV, the net-payback of such technology could be less than five years in the coming decade.

Using a TOU FIT incentive, the algorithm found that it was more cost-effective to orientate the primary solar collector twelve degrees east of south rather than orientating directly south and using solar panels on the east or west facades. This design choice had two benefits: (1) more energy was generated during peak times which increases annual income, and (2) the slightly east-oriented passive solar glazing surface was able to reduce the heating-system dependency when transitioning from a nightly set-back schedule to the morning heating schedule. This reduced heating system peak-loads without significantly changing annual heating consumption. West-facing glazing surfaces were not selected since they typically resulted in overheating of living spaces.

The relationship between economic payback from energy conservation and efficiency

measures with electricity generation is changing quickly. Presently, energy conservation measures reduce the burdensome investment of more expensive renewable energy investments in PV panels. Given the rapid reduction of PV panel price, this relationship may inverse in the near future, where energy generation technology aids in the payback of energy conservation measures. Methodologies that are those useful which aid designers in understanding the energy and cost paybacks in building design under quickly changing markets.

Chapter 9

Conclusion

> "Automate the mundane—liberate the creative.
> –*Drew Crawley (on the future of building energy modelling)*"

9.1 Summary

THIS thesis explored the following research areas: (i) performance enhancements to optimization algorithms applied to building research; (ii) use of optimization algorithms in uncertainty analysis around performance criterion; (iii) potential for economic incentives to affect energy-cost optimal curves; and (iv) effect of economic incentives on optimal NZEH design.

This thesis was structured as follows. Chapter 3 provided the design concepts used in this thesis. Chapter 4 showed a multi-objective design of an archetype solar home using the optimization algorithm, cost and energy model presented in Chapter 3. The archetype NZEH which combined passive solar design, energy efficiency measures including a geothermal heat pump and building-integrated photovoltaics was used in later chapters. Chapter 5 elaborated on how information obtained from previous simulations can be used to improve search convergence properties and optimization results using deterministic searches coupled with an evolutionary algorithm. The improvements in convergence speed and accuracy allowed for repeated optimization runs to build statistical significance in later chapters. Chapter 6 introduced a methodology to estimate the influence of building design parameter variations on the performance an energy model. This analysis improved the robustness of a design in meeting the NZE criterion by vi-

sualizing which design variations most significantly affect the archetype NZEH design. Chapter 7 describes an optimization methodology to establish and compare potential policies which incentivize cost optimal net-zero energy buildings. Using the incentive structures proposed in Chapter 7, Chapter 8 explores the effect of a time-of-use feed-in tariff and reductions in PV panel costs on optimal NZEH design.

Optimization methodologies in building simulation is an important research area. The reality is that no single optimization result can be generalized for all potential design scenarios. For example, custom home-builders have different framing billing-rates and time-requirements than pre-fabrication builders. Also, the energy costs and weather conditions are specific to the building location. Furthermore, the cost of photovoltaic panels is dropping quickly and becoming cost-competitive with energy efficiency measures. Thus, this thesis focused on methodologies to generate results quickly for any location with emphasis on facilitating the identification of optimal design opportunities that combine energy efficiency measures with building integrated solar systems such as passive solar systems and building integrated photovoltaics.

The proposed algorithm performance enhancements reduced the time requirements from 40–50 hours, see chapter 2, to less than two hours on a personal laptop. This made it possible to explore repetitive optimization analysis and to extract statistical information from the solution space into a database. The information stored in the database made it possible to extract PDFs for use in a variability analysis. The variability analysis identified potential changes which significantly effect the net-zero energy performance criterion. Finally, the effect of economic incentives on energy-cost optimal curves was explored. It was identified that under certain incentive structures, a cost-optimized building could be synonymous with a performance-optimized building with capital paybacks approaching 5 years.

In achieving these research goals, several unexpected tools were identified. PDFs enabled the visualization of design trade-offs around the NZE performance objective. Using PDFs, design variable limits were identified for several influential variables such as energy-related occupant behaviour, solar orientation of the building, wall insulation levels and window-to-wall ratios. Back-tracking searches identified steepest gradient pathways from reference buildings to performance-optimized buildings. Energy-cost

curves were found to be an ideal tools to identify effective incentives. In addition to these tools, several contributions were made to the field of building engineering.

9.2 Contributions

This thesis proposed a methodology to achieved robust performance-optimized net-zero energy buildings. The contributions of this thesis are roughly divided into four areas:

1. A methodology for integrating strategic deterministic searches into an evolutionary algorithm to improve solution quality and algorithm convergence speed for building optimization problems.

2. A methodology to approximate the uncertainty in building energy consumption due to cumulative variations in influential variables.

3. A methodology to determine the effect of policies and incentives to aid cost-optimal NZEHs.

4. Effect of a Time-of-Use Feed-In Tariff on Optimal Net-Zero Energy Home Design.

Several contributions to new performance-optimized simulation approaches are:

1. Development and demonstration of the use of probability density functions extracted from optimization results to identify performance opportunities and potential design summaries.

2. Development and demonstration of back-tracking searches to identify performance gradients between one-to-many and one-to-one building comparisons. Importance factors were introduced to summarize back-tracking results.

Contributions to optimization tool developments are:

1. Development of optimization tool and cost model for building simulation studies.

2. Extraction of variable interactions using mutual information for determining sub-population searches in an optimization algorithm.

3. Algorithm performance improvements specific to the needs of building research such as adaptive diversity control, preferential deterministic searches, use of generation gaps to grow multi-objective populations, parallel execution of building simulations and a differential mutation operator which resulted in factor of 10 time improvement over other tools used in building optimization research with better resolution of optimum solutions.

9.3 Future Work

There are many opportunities to further develop, refine and apply the scope of research proposed in this thesis. This section describes potential future work related to: (i) further improvements to optimization algorithms; (ii) other application areas of optimization research; (iii) implications of different occupant usage and a changing climate on performance-optimized buildings; (iv) integration of visual and thermal comfort as an additional objective or constraint; (v) cost model improvements; and (vi) energy model improvements.

There are still several potential opportunities to further improve algorithm speed and convergence performance, such as:

1. Applying simplified models to replace time-expensive building simulations using online training methods from previous simulation data. Several simplified modelling techniques could be explored such as artificial neural networks, decision tree ensembles, and regression models. Training of simplified models can further reduce the simulation requirements for building simulation and expedite the optimization process.

2. Further improvements to the diversity control within the optimization algorithm. The adaptive control method proposed, which modified selection pressure, can be greatly improved resulting in better algorithm convergence. For example, using specialized genetic operators depending on the convergence issue the algorithm is confronted with.

3. Further exploration on how previous optimization and building simulation data can be exploited to further improve decision making.

4. Expedite back-tracking searches by identifying non-full-factorial simulation approaches to reduce time and computational requirements.

5. Further elaboration on specialized sub-population searches using data extracting from previous simulations. For example, isolating clusters of interacting variables within sub-specialized searches. Further explore specialized deterministic searches for weakly interacting sub-clusters.

There are still many potential application areas for optimization tools and the methodologies proposed in this thesis within the scope of building research. For example:

1. Apply the proposed energy and cost optimization methodologies to commercial and industrial buildings. Identify incentive opportunities for cost-optimized industrial and commercial NZEBs.

2. Further validate the proposed methodologies by using the optimization tool developed for building retrofit. The goal would be to provide guidance on how to convert the existing residential or commercial building stock to NZE. Decision analysis would determine if energy measures should be performed now or in the near future. Analysis includes HVAC systems falling out of calibration and probabilistic projections of future economic scenarios.

3. Apply the optimization tool to larger problems with more than 50 variables such as a neighbourhood of NZEBs with centralized thermal and electricity storage.

It is likely that different occupant usage patterns and the changing climate will play a role in determining what a performance-optimized building is. The methodology could be expanded to identify compromises in design to best suit the uncertain climate change, occupant usage or economic scenarios. In present research probabilistic approaches are used to quantify uncertainty in occupant behaviour and climate change. An advantage in implementing probabilistic approaches is that variations in building usage can be better reflected in fitness functions used in the optimization analysis. This allows for variability in objective functions to be quantified and additional simulations are conducted. A disadvantage in this approach is that fitness evaluations would no longer be deterministic

which would complicated the extraction of information for strategic search techniques. Often this design approach is referred to as *robust design* where buildings are designed resilient to future unknown or uncertain circumstances. Optimized design could be viewed as trade-off decision, based on estimates of future scenarios.

The proposed methodology could benefit from the integration of a thermal comfort model applicable to NZEBs. In the PhD thesis of Carlucci (2012), over 25 thermal comfort models were evaluated for their suitability of use in a NZEH model. It was found that only particular thermal comfort approaches best evaluated thermal comfort of occupants across variations in locations and seasons. Comfort models could be integrated into the methodology as an objective function or a constraint to better quantify occupant comfort.

The energy model could be expanded to include better thermal zoning control using specialized mechanical systems in the house. For example, bedrooms are typically unoccupied outside of sleeping hours. Heating and cooling of these zones could be controlled based on occupancy. By only heating occupied rooms, heating and cooling loads could be further reduced. Mechanical equipment such as a variable refrigerant flow system or radiant floors with control valves could achieve such control.

The house energy model could be expanded to include other market-ready or near market-ready technologies, such as phase-change materials, masonry wood-stoves and daily and seasonal thermal storage cisterns. There are economies of scale for community-based storage systems that cannot realized on a single detached home basis. Many control strategies could be deployed for system-level and sub-system level control of: (i) charging of thermal storage; (ii) peak-load reductions via electrical storage or load shedding; and (iii) control of centralized and localized renewable energy production. Cost optimization research could be expanded to determine feasible price points for new building materials such as aerogel insulation or electrochromic windows. The integration of occupant comfort models into the energy model could be further explored.

There is opportunity to include advanced control strategies into net-zero energy building design. Such strategies might include: (i) model predicative control, (ii) modular conditioning of zones depending on occupancy, and (iii) model interactions with grid-signals to shed peak loads. For example, if excess renewable electricity was be-

ing generated in the grid, utilities could ask residential consumers to charge electric hot-water tanks to reduce later peak-electricity consumption.

9.4 Final Thoughts

> To imagine is to perceive many potential futures, select the most delightful possibility, and then pull the present forward to meet it.
>
> –*Imaginary Foundation*

This thesis demonstrated a methodology to achieve performance-optimized net-zero energy buildings. Optimization approaches explored and found optimal trade-offs between energy and cost optimized buildings. A variability analysis aided in better understanding the robustness of the NZEH design. In the last two chapters, previously developed tools were used to explore how incentives change the approach of optimal building design.

Optimization tools enhance our decision making capabilities. With these approaches, we can navigate complicated trade-offs in economics and performance, and can identify scenarios where uncertainty in unknown variables is significant. We can look at all possible paths, identify opportunities to best achieve our building performance objectives and make these opportunities a reality. By automating mundane simulation tasks, optimization tools enhance our decision making abilities by focusing our attention on significant design opportunities and away from repetitive energy simulation. Many benefits are achieved for this effort including: better occupant comfort, improved indoor air-quality, possible investment opportunities, and resilient investments to mitigate climate change and energy cost escalation. By identifying opportunities for performance-optimized buildings, optimization approaches enhance our imagination making us aware of achievable performance targets.

Recall the polarizing view regarding the application of optimization algorithms presented at the end of the introduction. One view is that only artificially-intelligent algorithms will design performance-optimized buildings of the future. No amount of human innovation can identify scenarios which both meet performance objectives while satisfying occupant comfort. On the opposing side is the view that algorithms cannot understand the cultural or social implications of a particular design, thus they result

in unusable information. It is possible that algorithms will never completely design a building. There are many cultural and æsthetics implications that an algorithm cannot yet, and may never, embody. However, there are areas that algorithms excel at. Herein lies their true potential. Optimization approaches are tools. Tools which sculpt potential solutions to unsolved and ill-defined problems. Optimization tools can propose unprecedented solutions to tough problems. Perhaps their potential has yet to be fully realized since the toughest problems are yet to come.

References

Abley, M., 1998. The Ice Storm: An Historic Record In Photographs of January 1998, 1st Edition. McClelland and Stewart.

Al-Homoud, M. S., 2005. A systematic approach for the thermal design optimization of building envelopes. Journal of Building Physics 29 (2), 95–119.

Amdahl, G., 1967. Validity of the single processor approach to achieving large-scale computing capabilities. In: Proceedings of AFIPS. New York, US, pp. 483–485.

Anderson, R., Christensen, C., Horowitz, S., 2006. Analysis of residential system strategies targeting least-cost solutions leading to net zero energy homes. ASHRAE Transactions 112 (2), 330–341.

Andre, D., Koza, J.R., 1998. A parallel implementation of genetic programming that achieves super-linear performance. Information Sciences 106 (3-4), 201.

Armstrong, M. M., Swinton, M. C., Ribberink, H., Beausoleil-Morrison, I., Millette, J., 2009. Synthetically derived profiles for representing occupant–driven electric loads in Canadian housing. Journal of Building Performance Simulation 2 (1), 15–30.

Arndt, D., Baringer, M., Johnson, M., 2010. Published on July 28, 2010 by the National Oceanic and Atmospheric Administration.
URL http://www.ncdc.noaa.gov/bams-state-of-the-climate/

ASHRAE, 2002. ASHRAE guideline 14: Measurement of energy and demand savings. Retrieved February 2013.
URL https://www.ashrae.org/standards-research--technology/standards--guidelines/titles-purposes-and-scopes#Gdl14

ASHRAE, 2011a. ASHRAE standard 62.2.
URL http://www.ashrae.org/standards-research--technology/standards--guidelines

ASHRAE, 2011b. ASHRAE standard 90.1.
URL http://www.ashrae.org/standards-research--technology/standards--guidelines

ASHRAE, 2011c. HVAC Applications. American Society of Heating, Refrigerating and Air-Conditioning, Atlanta, USA.

Athena, 2011. Athena impact estimator for buildings. Retrieved May 2011.
URL http://www.athenasmi.org/our-software-data/impact-estimator/

Athienitis, A., Santamouris, M., 2002. Thermal Analysis and Design of Passive Solar Buildings. James & James, London, UK.

Attia, S., Hamdy, M., OâĂŹBrien, W., Carlucci, S., 2013. Assessing gaps and needs for integrating building performance optimization tools in net zero energy buildings design. Energy and Buildings 60 (0), 110–124.

Aude, P., Tabary, L., Depecker, P., 2000. Sensitivity analysis and validation of buildings' thermal models using adjoint-code method. Energy and Buildings 31 (3), 267–283.

Audet, C., Dennis, J.E., 2002. Analysis of generalised pattern searches. SIAM Journal of Optimization 13 (3), 889–903.

Augenbroe, G., de Wilde, P., Moon, H. J., Malkawi, A., 2004. An interoperability workbench for design analysis integration. Energy and Buildings 36 (8), 737–748.

Balachandran, M., Gero, J. S., 1987. Dimensioning of architectural floor plans under conflicting objectives. Environment and Planning B 14, 29–37.

Balcomb, J. D., 1992. Passive Solar Buildings, 1st Edition. The MIT Press, Cambridge, USA.

Bank of Canada, 2009. Rates and Statistics: Interest rates, Canadian interest rates. Accessed January, 2013.
URL http://www.bankofcanada.ca/rates/interest-rates/

Beausoleil-Morrison, I., 1996. BASECALC: A software tool for modelling residential foundation heat losses. In: Proceedings of the Third Canadian Conference in Computing in Building and Civil Engineering.

Beausoleil-Morrison, I., 2000. The adaptive coupling of heat and air flow modeling within dynamic whole-building simulations. Ph.D. dissertation, University of Strathclyde.

Beausoleil-Morrison, I., Griffith, B., Vesanen, T., Weber, A., 2009. A demonstration of the effectiveness of inter-program comparative testing for diagnosing and repairing solution and coding errors in building simulation programs. Journal of Building Performance Simulation 2 (1), 63–73.

Beausoleil-Morrison, I., Macdonald, F., Kummert, M., McDowell, T., Jost, R., 2013. Co-simulation between esp-r and trnsys. Journal of Building Performance Simulation 0 (0), 1–19.

Beausoleil-Morrison, I., Macdonald, F., Kummert, M., McDowell, T., Jost, R., Ferguson, A., 2011. The design of an esp-r and trnsys co-simulator. In: Proc. Building Simulation. pp. 2333–2340.

Beccali, G., Cellura, M., Brano, V. L., Orioli, A., 2005. Is the transfer function method reliable in a european building context? a theoretical analysis and a case study in the south of italy. Applied Thermal Engineering 25 (2-3), 341–357.

Berggren, B., Hall, M., Wall, M., 2013. LCE analysis of buildings - Taking the step towards Net Zero Energy Buildings. Energy and Buildings 62 (0), 381–391.

Bledsoe, W. W., Browning, I., December 1959. Pattern recognition and reading by machine. pp. 225–232, the 1959 Eastern Joint Computer Conference for The National Joint Computer Committee.

Booth, A., Choudhary, R., 2013. Decision making under uncertainty in the retrofit analysis of the UK housing stock: Implications for the green deal. Energy and Buildings 64 (0), 292–308.

Borchiellini, R., Fürbringer, J.-M., 1999. An evaluation exercise of a multizone air flow model. Energy and Buildings 30 (1), 35–51.

BPIE, 2010. Cost optimality: Discussing methodology and challenges within the recast Energy Performance of Buildings Directive.
URL http://www.bpie.eu/cost_optimality.html

Breesch, H., Janssens, A., 2010. Performance evaluation of passive cooling in office buildings based on uncertainty and sensitivity analysis. Solar Energy 84 (8), 1453–1467.

Breyer, C., Gerlach, A., 2010. Global overview on grid-parity event dynamics. In: Proceedings of 25th EU PVSEC/WPEC-5. Valencia, ES, pp. 6–10.

Brohus, H., Frier, C., Heiselberg, P., Haghighat, F., 2012. Quantification of uncertainty in predicting building energy consumption: A stochastic approach. Energy and Buildings 55 (0), 127–140.

Bucking, S., Athienitis, A., Zmeureanu, R., 2011. Optimization of net-zero energy solar communities: effect of uncertainty due to occupant factors. In: Proceedings of ISES World Conference, Kassel, Germany.

Bucking, S., Athienitis, A., Zmeureanu, R., 2013a. Multi-objective optimal design of a near net-zero energy solar house. ASHRAE Transactions 0 (0), 1–26, accepted for presentation.

Bucking, S., Athienitis, A., Zmeureanu, R., O'Brien, W., Doiron, M., 2010. Design optimization methodology for a near net zero energy demonstration home. In: Proceedings of EuroSun International Conference on Solar Heating, Cooling and Buildings. EuroSun, Graz, Austria.

Bucking, S., Zmeureanu, R., Athienitis, A., 2013b. An information driven hybrid evolutionary algorithm for optimal design of a net zero energy house. Solar Energy 96 (0), 128–139.

Bucking, S., Zmeureanu, R., Athienitis, A., 2013c. A methodology for identifying the influence of design variations on building energy performance. Journal of Building Performance Simulation, 1–26.

Bucking, S., Zmeureanu, R., Athienitis, A., 2013d. An optimization methodology to evaluate the effect size of incentives on energy-cost optimal curves. In: Proceedings of Thirteenth International IBPSA Conference, Chambéry, France. pp. 1–8.

Buhl, W.F., Erdem, F.C., Winkelmann, F.C., Sowell, E.F., 1993. Recent improvements in SPARK: Strong component decomposition, multivalued objects, and graphical interface. In: Proceedings of Building Simulation, Adelaide, Australia. IBPSA.

Burhenne, S., Jacob, D., Henze, G., 2010. Uncertainty analysis in building simulation with monte carlo techniques. In: Proceedings of SimBuild, 3rd National Conference of IBPSA-USA New York, USA. International Building Performance Simulation Association, USA chapter.

Burhenne, S., Tsvetkova, O., Jacob, D., Henze, G. P., Wagner, A., 2013. Uncertainty quantification for combined building performance and cost-benefit analyses. Building and Environment 62 (0), 143–154.

Caldas, L., September 2001. An evolution-based generative design system: Using adaption to shape architectural form. Ph.D. dissertation, Massachusetts Institute Technology.

Caldas, L., 2008. Generation of energy-efficient architecture solutions applying GENE_ARCH: An evolution-based generative design system. Advanced Engineering Informatics 22 (1), 59–70.

Candanedo, J., 2011. A Study of Predictive Control Strategies for Optimally Designed Solar Homes. Ph.D. dissertation, Concordia University.

Candanedo, L., Athienitis, A., Candanedo, J., O'Brien, W., Chen, Y., 2010. Transient and Steady State Models for Open-Loop Air-Based BIPV/T Systems. ASHRAE Transactions 116 (1), 600–620.

Carlucci, S., March 2012. An automated optimization process to support the design of comfortable net zero energy buildings. Ph.D. dissertation, Dipartimento Di Scienza e Tecnologie Dell'Ambiente Costruito.

Castro-Lacouture, D., Sefair, J. A., Flórez, L., Medaglia, A. L., 2009. Optimization model for the selection of materials using a leed-based green building rating system in colombia. Building and Environment 44 (6), 1162–1170.

Chakraborty, U., 2008. Advances in Differential Evolution, 1st Edition. Springer-Verlag, Heidelberg, DE.

Charron, R., 2007. Development of a genetic algorithm optimisation tool for the early stage design of low and net-zero energy solar homes. Ph.D. dissertation, Concordia University.

Chen, Y., 2009. Modeling and design of a solar house with focus on a ventilated concrete slab with a building-integrated photovoltaic/thermal system. Master's thesis, Concordia University.

Chen, Y., Athienitis, A., Galal, K., 2010a. Modeling, design and thermal performance of a BIPV/T system thermally coupled with a ventilated concrete slab in a low energy solar house: Part 1, BIPV/T system and house energy concept. Solar Energy 84 (11), 1892–1907.

Chen, Y., Galal, K., Athienitis, A., 2010b. Modeling, design and thermal performance of a BIPV/T system thermally coupled with a ventilated concrete slab in a low energy solar house: Part 2, ventilated concrete slab. Solar Energy 84 (11), 1908 – 1919.

Chiras, D. D., 2002. The Solar House: Passive Heating and Cooling, 1st Edition. Chelsea Green, White River, VT .

Choudhary, R., Spring 2004. A hierarchical optimization framework for simulation-based architectural design. Ph.D. dissertation, University of Michigan.

Choudhary, R., Malkawi, A., Papalambros, P., 2003. A hierarchical design optimization framework for building performance analysis. In: Building Simulation. IBPSA, pp. 179–999.

Choudhary, R., Malkawi, A., Papalambros, P., 2005. Analytic target cascading in simulation-based building design. Automation in Construction 14, 551–568.

Chow, T. J., Hand, J., Strachan, P., 2003. Building-integrated photovoltaic and thermal applications in a subtropical hotel building. Applied thermal engineering 23 (16), 2035–2049.

Christensen, C., Barker, G., Horowitz, S., 2004. A sequential search technique for identifying optimal building designs on the path to zero net energy. In: Proceedings of the Solar 2004. American Solar Energy Society.

Clarke, J., 2001. Energy Simulation In Building Design, 2nd Edition. Butterworth-Heinemann, Oxford, UK.

CMHC, 2008. Canada Mortgage and Housing Corporation EQuilbrium Homepage. Retrieved July, 2013.
URL http://www.cmhc-schl.gc.ca/en/co/maho/yohoyohe/heho/eqho/index.cfm

CMHC, 2012. Accessed November, 2012.
URL http://www.cmhc-schl.gc.ca/en/corp/faq/faq_006.cfm

Coello Coello, C., 1999. An updated survey of evolutionary multiobjective optimization techniques: State of the art and future trends. In: Proceedings of the 1999 Congress on Evolutionary Computation. IEEE Press, Piscataway, NJ.

Coello Coello, C., 2002. Theoretical and numerical constraint-handling techniques used with evolutionary algorithms: a survey of the state of the art. Computer Methods in Applied Mechanics and Engineering 191 (11), 1245.

Coley, D. A., Schukat, S., 2002. Low-energy design: combining computer-based optimisation and human judgement. Building and Environment 37 (12), 1241–1247.

Corrado, V., Mechri, H., 2009. Uncertainty and sensitivity analysis for building energy rating. Journal of Building Physics 44 (6), 1538–1544.

Couchoulas, O., Spring 2003. Shape evolution: an algorithmic method for conceptual architectural design combining shape grammars and genetic algorithms. Ph.D. dissertation, University of Bath.

Cover, T., Tomas, J., 2006. Elements of Information Theory, 2nd Edition. Wiley, Hoboken, NJ.

Crawley, D., Huang, J., 1997. Does It Matter Which Weather Data You Use in Energy Simulations? Accessed Nov 2011.
URL http://simulationresearch.lbl.gov/dirpubs/1801_weath.pdf

Crawley, D.B., Hand, J.W., Kummert, M., Griffith, B.T., 2008. Contrasting the capabilities of building energy performance simulation programs. Building and Environment 43 (4), 661–673.

Crawley, D. B., Pedersen, C. O., Lawrie, L. K., Winkelman, F. C., 2000. Energyplus: Energy simulation program. ASHRAE Journal 42, 49–56.

Davis, L., 1987. Genetic algorithms and simulated annealing. Morgan Kaufman Publishers, Los Altos, USA.

Day4Energy, 2012. Day4Energy model 48MC Premium Photovoltaic Modules. Retrieved Nov 2012.
URL http://simulationresearch.lbl.gov/dirpubs/1801_weath.pdf

D'Cruze, N.A., Radford, A.D., 1987. A multicriteria model for building performance and design. Building and Environment 3 (22), 167–179.

D'Cruze, N.A., Radford, A.D., Gero, J.S., 1983. A pareto optimization problem formulation for building performance and design. Engineering Optimization 7, 17–33.

Deb, K., 2001. Multi-objective optimization using evolutionary algorithms, 1st Edition. Wiley, New York, USA.

Deb, K., Pratap, A., Agarwal, S., Meyarivan, T., 2002. A fast and elitist multiobjective genetic algorithm: NSGA-II. IEEE Transactions on Evolutionary Computation 6, 182–197.

Déqué, F., Ollivier, F., Poblador, A., 2000. Grey boxes used to represent buildings with a minimum number of geometric and thermal parameters. Energy and Buildings 31, 29 – 35.

De Wit, S., 2001. Uncertainty in predictions of thermal comfort in buildings. Ph.D. dissertation, Delft University.

De Wit, S., Augenbroe, G., 2002. Analysis of uncertainty in building design evaluations and its implications. Energy and Buildings 34 (9), 951–958.

De Wit, S., Augenbroe, G., 2004. Analysis of uncertainty in building design evaluations and its implications. Energy and Buildings 34, 951.

Diakaki, C., Grigoroudis, E., Kabelis, N., Kolokotsa, D., Kalaitzakis, K., Stavrakakis, G., 2010. A multi-objective decision model for the improvement of energy efficiency in buildings. Energy 35 (12), 5483–5496.

DOE, 2005. DOE Building America Benchmark Model. U.S. Department of Energy.
URL http://www.eere.energy.gov/buildings/building_america/docs/benchmark_2005.doc

DOE, 2007. Building Energy Software Tools Directory. Retrieved May 2011.
URL http://www.eere.energy.gov/buildings/tools_directory/

DOE, 2009. Buildings Energy Data Book, Chapter 1.2 Building Sector Expenditures. United States Department of Energy.

DOE, 2010. Building America Hompage. Retrieved November, 2010.
URL http://www.eere.energy.gov/buildings/building_america

DOE, 2011a. DOE Releases New Version of EnergyPlus Modeling Software. Retrieved May 2013.
URL http://apps1.eere.energy.gov/news/progress_alerts.cfm/pa_id=651

DOE, Oct. 10, 2011b. EnergyPlus Engineering Reference: The Reference of EnergyPlus Calculations (in case you need to know). U.S. Department of Energy.

DOE, 2013. The DOE SunShot Initiative. Retrieved July 2013.
URL http://www1.eere.energy.gov/solar/sunshot/

Doiron, M., 2010. Whole-building energy analysis and lessons-learned for a near net-zero energy, passive solar house. Master's thesis, Concordia University.

Doiron, M., O'Brien, W., Athienitis, A., 2011. Energy performance, comfort, and lessons learned from a near net zero energy solar house. ASHRAE Transactions 117 (2), 1–12.

Domínguez-Muñoz, F., Cejudo-López, J. M., Carrillo-Andrés, A., 2010. Uncertainty in peak cooling load calculations. Energy and Buildings 42 (7), 1010–1018.

Doty, S., Turner, W. C., 2012. Energy management handbook. The Fairmont Press, Inc., 8th Edition.

Eco-Indicator-99, 2009. Product ecology consultants. Retrieved April 2011.
URL http://www.pre.nl/eco-indicator99/default.htm

Eiben, A. E., Rudolph, G., 1999. Theory of evolutionary algorithms: a bird's eye view. Theoretical Computer Science 229 (1-2), 3–9.

Eiben, G., Smith, J., 2003. Introduction to Evolutionary Computing, 1st Edition. Springer, London, UK.

Einstein, A., 1905. Concerning an heuristic point of view toward the emission and transformation of light. Annal der Physik 131 (17).

Eisenhower, B., O'Neill, Z., Fonoberov, V. A., Mezič, I., 2011. Uncertainty and sensitivity decomposition of building energy models. Journal of Building Performance Simulation 5 (3), 171–184.

Elbeltagi, E., Hegazy, T., Grierson, D., 2005. Comparison among five evolutionary-based optimization algorithms. Advanced Engineering Informatics 19 (1), 43–53.

EN15316-1, 2007. Heating systems in buildings - Methods for calculation of system energy requirements and system efficiencies.
URL http://www.buildup.eu/publications/6244

EN15459, 2010. EN 15459: Energy performance of buildings—economic evaluation procedure for energy systems in buildings.

EnergyPlus, 2011. DOE Building Technologies Homepage. Retrieved April, 2011.
URL http://apps1.eere.energy.gov/buildings/energyplus/

EPA, 2012. EPA EnergyStar Benchmark Homepage. Accessed Nov 2012.
URL http://www.energystar.gov/index.cfm?c=assess_performance.benchmark

ESP-r, 2011. Energy Simulation Program - Research Homepage. Retrieved May 2011. URL http://www.esru.strath.ac.uk/Programs/ESP-r_overview.htm

EU Parliament, 2010. Directive of the European Parliament and of the council on the energy performance of buildings (recast). Accessed Nov 2012. URL http://www.eceee.org/buildings/EPBD_Recast

Feoktistov, V., 2006. Differential Evolution: In search of solutions, 1st Edition. Springer, New York, USA, Chapter 9.

Friedberg, R. M., November 1958. A learning machine: Part i. IBM Journal of Research and Development 2 (1), 2–13.

Frischknecht, R., 2003. Ecoinvent2000, code of practice, data v1.01. Ecoinvent report no. 2, Dubendorf.

Fritzson, P., Engelson, V., 1998. Modelica- A unified object-oriented language for system modeling and simulation. Vol. 1445. Springer-Verlag, London, UK, lecture Notes in Computer Science.

Glicksman, L., Gouldstone, J., Lehar, M., Urban, B., 2011. MIT design advisor website. URL http://designadvisor.mit.edu

Goos, P., Jones, B., 2011. Optimal Design of Experiments: A Case Study Approach, 1st Edition. Wiley.

Green, M. A., 2001. Third generation photovoltaics: Ultra-high conversion efficiency at low cost. Progress in Photovoltaics: Research and Applications 9 (2), 123–135.

Hachem, C., September 2012. Investigation of Design Parameters for Increased Solar Potential of Dwellings and Neighborhoods. Ph.D. dissertation, Concordia University.

Haltrecht, D., Zmeureanu, R., Beausoleil-Morrison, I., 1999. Defining the methodology for the next-generation HOT2000 simulator. In: Building Simulation. Kyoto, Japan, pp. 61–68.

Hand, J., Dec. 2, 2010. The ESP-r cookbook: Strategies for deploying virtual representations of the build environment. Energy Systems Research Unit Department of Mechanical Engineering University of Strathclyde, Glasgow, UK. URL http://www.esru.strath.ac.uk/Documents/ESP-r_cookbook_dec_2010.pdf

Hasan, A., Vuolle, M., Sirén, K., 2008a. Minimisation of life cycle cost of a detached house using combined simulation and optimisation. Building and Environment 43 (12), 2022–2034.

Hasan, A., Vuolle, M., Siren, K., 2008b. Minimisation of life cycle cost of a detached house using combined simulation and optimisation. Building and Environment 43 (12), 2022–2034.

Heiselberg, P., Brohus, H., Hesselholt, A., Rasmussen, H., Seinre, E., Thomas, S., 2009. Application of sensitivity analysis in design of sustainable buildings. Renewable Energy 34 (9), 2030–2036.

Henderson, S., Roscoe, D., 2010. Solar Home Design Manual for Cool Climates, 1st Edition. EarthScan, London, UK.

Hensen, J., Lamberts, R., 2011. Building Performance Simulation for Design and Operation, 1st Edition. Spon Press, London, UK, chapter 1, Introduction.

Heo, Y., Augenbroe, G., Choudhary, R., 2011. Risk analysis of energy-efficiency projects based on bayesian calibration of building energy models. In: Proceedings of 12th International IBPSA Conference, Sydney, Australia. pp. 2579–2586.

Heo, Y., Choudhary, R., Augenbroe, G., 2012. Calibration of building energy models for retrofit analysis under uncertainty. Energy and Buildings 47 (0), 550–560.

Hickey, R., 2012. Clojure programming language homepage. Accessed May, 2012.
URL http://www.clojure.org/

Holst, J., 2003. Using whole building simulation models and optimizing procedures to optimize building envelope design with respect to energy consumption and indoor environment. In: Building Simulation. IBPSA, pp. 507–514.

Hooke, R., Jeeves, T.A., 1961. 'Direct search' solution of numerical and statistical problems. Journal of the Association for Computing Machinery 8 (2), 212–229.

Hopfe, C., Hensen, J., 2011a. Uncertainty analysis in building performance simulation for design support. Energy and Buildings 43 (10), 2798–2805.

Hopfe, C., Struck, C., Kotek, P., van Schijndel, J., Hensen, J., Plokker, W., 2007. Uncertainty analysis for building performance simulation–a comparison of four tools. In: Proceedings of the 10th IBPSA Building Simulation Conference. pp. 1383–1388.

Hopfe, C. J., Hensen, J. L., 2011b. Uncertainty analysis in building performance simulation for design support. Energy and Buildings 43 (10), 2798 – 2805.

Horowitz, S., Christensen, C., Brandemuehl, M., Krarti, M., 2008. An enhanced sequential search methodology for identifying cost-optimal building pathways. In: Proceedings of SimBuild, 3rd National Conference of IBPSA-USA Berkeley, CA, USA. International Building Performance Simulation Association, USA chapter.

Hu, H., Augenbroe, G., 2012. A stochastic model based energy management system for off-grid solar houses. Building and Environment 50 (0), 90–103.

Hydro-Québec, 2010. Hydro-Québec: Annual Report 2010. Accessed January, 2013.
URL http://www.hydroquebec.com/publications/en/annual_report

IEA, 2010. World Energy Outlook, 2010th Edition.
URL http://worldenergyoutlook.org/

IEA, 2013. International Energy Agency Annex 21–26 Homepage. Accessed July 2013.
URL http://www.iea-eces.org/annexes/ongoing-annexes.html

IEA/ECBCS, 2013. International Energy Agency Task 40/Energy Conservation in Building and Community Systems Annex 52 Homepage. Accessed March 2013.
URL http://task40.iea-shc.org/

IEA PVPS, 2013. Photovoltaic power systems annual report 2012. Tech. rep.

IEEE, 2012. Power Systems of the Future: The Case for Energy Storage, Distributed Generation, and Microgrids.
URL http://smartgrid.ieee.org/images/features/smart_grid_survey.pdf

Janak, M., 1997. Coupling building energy and lighting simulation. In: Proceedings of the 5th international IBPSA conference, Prague, Czech Republic. pp. 313–319.

Jo, J. H., Gero, J. S., 1998. Space layout planning using an evolutionary approach. Artificial Intelligence in Engineering 12 (3), 149–162.

Judkoff, R., Neymark, J., 1995. International energy agency building energy simulation test (BESTEST) and diagnostic method.

Kämpf, J., December 2009. On the modelling and optimisation of urban energy fluxes. Ph.D. dissertation, École Polytechnique Fédérale de Lausanne.

Kämpf, J. H., Robinson, D., 2007. A simplified thermal model to support analysis of urban resource flows. Energy and Buildings 39 (4), 445–453.

Kämpf, J. H., Robinson, D., 2010. Optimisation of building form for solar energy utilisation using constrained evolutionary algorithms. Energy and Buildings 42 (6), 807–814.

Kämpf, J. H., Wetter, M., Robinson, D., 2010. A comparison of global optimization algorithms with standard benchmark functions and real-world applications using EnergyPlus. Journal of Building Performance Simulation 3 (2), 103–120.

Kampstra, P., 2008. Beanplot: A boxplot alternative for visual comparison of distributions. Journal of Statistical Software 28 (1), 1–9.

Kazuhiro, I., Nishiwaki, S., Yoshimura, M., Nakamura, M., Renaud, J. E., 2008. Enhanced multiobjective particle swarm optimization in combination with adaptive weighted gradient-based searching. Engineering Optimization 40 (9), 789–804.

Kennedy, J., Eberhart, R., Shi, Y., 2001. Swarm Intelligence, 1st Edition. Morgan Kaufmann Publishers, San Francisco, USA.

Kennedy, J., Eberhart, R. C., 1997. A discrete binary version of the particle swarm algorithm. In: Proceedings of IEEE, International Conference on Neural Networks, Indianapolis, USA. pp. 4104–4108.

Kicinger, R., Arciszewski, T., De Jong, K., 2005. Evolutionary computation and structural design: A survey of the state-of-the-art. Computers and Structures 83, 1943–1978.

Kim, H. M., Michelena, N. F., Papalambros, P. Y., Jiang, T., 2003. Target cascading in optimal system design. Transaction of ASME: Journal of Mechanical Design 125, 481–489.

Kim, S. H., Augenbroe, G., 2013. Uncertainty in developing supervisory demand-side controls in buildings: A framework and guidance. Automation in Construction 0 (0), 1–20, in Press, Corrected Proof.

Kleijnen, J. P. C., Sargent, R. G., 2000. A methodology for fitting and validating metamodels in simulation. European Journal of Operational Research 120 (1), 14–29.

Klein, S.A., Beckman, W.A., Duffie, J.A., 1976. TRNSYS - a transient simulation program. ASHRAE Transactions 82, Part 1, 623–633.

Krarti, M., 2011. Energy Audit of Building Systems, 2nd Edition. CRC Press, Boca Raton, FL.

Kurnitski, J., Allard, F., Braham, D., Goeders, G., Heiselberg, P., Jagemar, L., Kosonen, R., Lebrun, J., Mazzarella, L., Railio, J., Seppänen, O., Schmidt, M., Virta, M., 2011. How to define nearly net zero energy buildings nZEB. Accessed Nov 2012.
URL http://www.rehva.eu/en/374.how-to-define-nearly-net-zero-.energy-buildings-nzeb

Langton, C., 1990. Computation at the edge of chaos: Phase transitions and emergent computation. Physica D 42, 12–37.

LBNL, 2001. User's Guide to the Building Design Advisor, Version 3.0. Building Technologies Department Environmental Energy Technologies Division Ernest Orlando Lawrence Berkeley National Laboratory (LBNL).
URL http://gaia.lbl.gov/BDA/bda3help.pdf

LBNL, 2011. Radiance Homepage. Retrieved May 2011.
URL http://radsite.lbl.gov/radiance/

LBNL, 2012. Window 6.3 software. Accessed November, 2012. Berkeley, CA.
URL http://windows.lbl.gov/software/window/6/index.html

Leckner, M., 2008. Life Cycle Energy and Cost Analysis of a Net Zero Energy House (NZEH) Using a Solar Combisystem. Master's thesis, Concordia University.

Lehar, M. A., June 2005. A branching fuzzy-logic classifier for building optimization. Ph.D. dissertation, Massachusetts Institute Technology.

Lewis, N., Nocera, D., 2006. Powering the planet: chemical challenges in solar energy utilization. In: Proceedings of the National Academy of Sciences. Vol. 103. pp. 15729–15735.

Liggett, R.S., 1985. Optimal spatial arrangement as a quadratic assignment problem. Design Optimization, 1–40.

Liggett, R.S., Mitchell, W.J., 1981. Optimal space planning in practice. Computer-Aided Design 13 (5), 277–288.

Liu, J. S., 2001. Monte Carlo Strategies in Scientific Computing (Springer Series in Statistics), 1st Edition. Springer.

Lomas, K., Eppel, H., 1992. Sensitivity analysis techniques for building thermal simulation programs. Energy and Buildings 19 (1), 21 – 44.

Lstiburek, J., 2009. Moisture control for new residential buildings. Tech. rep.
URL http://www.buildingscience.com/documents/digests/bsd-012-moisture-control-for-new-residential-buildings

Luke, S., 2009. Essentials of Metaheuristics. Lulu, available for free at http://cs.gmu.edu/ sean/book/metaheuristics/.

Macdonald, I., 2002. Quantifying the effects of uncertainty in building simulation. Ph.D. dissertation, University of Strathclyde.

Macdonald, I., 2009. Comparison of sampling techniques on the performance of monte carlo based sensitivity analysis. In: Proceedings of Eleventh International IBPSA Conference, Glasgow, Scotland. p. 992.

Macdonald, I., Clarke, J., 2007. Applying uncertainty considerations to energy conservation equations. Energy and Buildings 39 (9), 1019–1026.

Macdonald, I., Strachan, P., 2001. Practical application of uncertainty analysis. Energy and Buildings 33 (3), 219–227.

Magnier, L., 2009. Multiobjective optimization of building design using artificial neural network and multiobjective evolutionary algorithms. Master's thesis, Concordia University.

Magnier, L., Haghighat, F., 2010. Multiobjective optimization of building design using TRNSYS simulations, genetic algorithm, and artificial neural network. Building and Environment 45 (3), 739–746.

MathWorks, 2011. Matlab homepage.
URL http://www.mathworks.org/

Matsumoto, Y., 2013. Ruby homepage.
URL http://www.ruby-lang.org/

McKinsey, 2009. Reducing US Greenhouse Gas Emissions: How Much at What Cost?
URL http://www.mckinsey.com/clientservice/electricpowernaturalgas/downloads/US_energy_efficiency_full_report.pdf

Michalek, J., Choudhary, R., Papalambros, P., 2002. Architectural layout design optimization. Engineering Optimization 34 (5), 461–484.

Michalewicz, Z., Schoenauer, M., 1996. Evolutionary algorithms for constrained parameter optimization problems. Evolutionary Computation 4 (1), 1–36.

Mitchell, W.J., Steadman, J.P., Liggett, R.S., 1976. Synthesis and optimization of small rectangular floor plans. Environment and Planning B 3, 37–70.

Morris, M. D., 1991. Factorial sampling plans for preliminary computational experiments. Technometrics 33 (2), 161–174.

NASA, 2009. Article: The day the sun brought darkness. Accessed January, 2013.
URL http://www.nasa.gov/topics/earth/features/sun_darkness.html

Nassif, N., Kajl, S., Sabourin, R., 2004. Evolutionary algorithms for multi-objective optimization in hvac system control strategy. In: Fuzzy Information, 2004. Processing NAFIPS '04. IEEE Annual Meeting, Vol.1. Vol. 1. pp. 51–56.

Nelder, J.A., Mead, R., 1965. A simplex method for function minimization. The Computer Journal 7 (4), 308–313.

NIBS, 2011. National building information model standard (nbims).
URL http://www.nibs.org/?page=standards

Nicol, J. F., Humphreys, M. A., 2002. Adaptive thermal comfort and sustainable thermal standards for buildings. Energy and Buildings 34 (6), 563–572.

NIST, 2013. Security Management & Assurance. Retrieved August, 2013.
URL http://csrc.nist.gov/groups/STM/index.html

Norton, P., Christensen, C., 2008. Performance results from a cold climate case study for affordable zero energy homes. ASHRAE Transactions 114 (1), p218–229.

NRC, 1997a. Model National Energy Code for Buildings (MNECB). Institute for Research in Construction (IRC) National Research Council Canada (NRC).

NRC, 1997b. Model National Energy Code for Homes (MNECH). Institute for Research in Construction (IRC) National Research Council Canada (NRC).

NRCan, 2012. Ecoenergy homepage. Accessed November, 2012.
URL http://oee.nrcan.gc.ca/residential/6551

NRCan-OEE, 2009. Energy use data handbook. Accessed Nov 2012.
URL http://oee.nrcan.gc.ca/publications/statistics/handbook09/pdf/handbook09.pdf

NREL, 2011. Opt-E-Plus Software for Commercial Building Optimization, retrieved April 2011.
URL www.nrel.gov/docs/fy10osti/45620.pdf

NREL, 2013. NREL Commercial Buildings Reserach and Software Development Homepage. Retrieved July, 2013.
URL https://openstudio.nrel.gov/getting-started-developer/getting-started-radiance

NZEH Coalition, 2012. Net-zero energy home coalition homepage. Accessed Nov 2012.
URL www.netzeroenergyhome.ca

O'Brien, W., 2011. Development of a solar house design methodology and its implementation into a design tool. Ph.D. dissertation, Concordia University.

O'Brien, W., Athienitis, A., Kesik, T., 2011. Parametric analysis to support the integrated design and performance modeling of net-zero energy houses. ASHRAE Transactions 117 (1), 1–16.

O'Brien, W., Kennedy, C., Athienitis, A., Kesik, T., 2010. The relationship between net energy use and the urban density of solar buildings. Environment and Planning B: Planning and Design 37 (6), 1002–1021.

OCA, 2007. Air Quality Issues Fact Sheet no. 24: Reducing Peak Demand.
URL http://www.cleanairalliance.org/files/active/0/fs24.pdf

Ooka, R., Komamura, K., 2009. Optimal design method for building energy systems using genetic algorithms. Building and Environment 44 (6), 1538–1544.

OPA, 2013. Ontario power authority feed-in tariff program. Accessed January, 2013.
URL http://fit.powerauthority.on.ca/fit-program

Oracle, 2013. Java 6 platform standard: Class SecureRandom. Retrieved August, 2013.
URL http://docs.oracle.com/javase/6/docs/api/java/security/SecureRandom.html

Ouarghi, R., Krarti, M., 01 2006. Building shape optimization using neural network and genetic algorithm approach. ASHRAE Transactions 112 (1), 484–491.

Pacala, S., Socolow, R., August 2004. Stabilization wedges: Solving the climate problem for the next 50 years with current technologies. Science 305 (5686), 968–972.
URL http://www.sciencemag.org/cgi/content/abstract/305/5686/968

Page, L., 2012. Perl homepage.
URL http://www.perl.org/

Papamichael, K., Chauvet, H., LaPorta, J., Dandridge, R., 1999. Product modeling for computer-aided decision-making. Automation in Construction 8 (3), 339–350.

Parry, M., Canziani, O., Palutikof, J., van der Linden, P., Hanson, C. (Eds.), 2007. Fourth Assessment Report: Climate Change 2007: The AR4 Synthesis Report. Geneva: IPCC.
URL http://www.ipcc.ch/ipccreports/ar4-wg1.htm

Parsopoulos, K.E., Vrahatis, M.N., 2002. Recent approaches to global optimization problems through particle swarm optimization. Natural Computing 1, 235–306.

Patil, R., 2010. Impact of climate change on an r-2000 and a net zero energy home. Master's thesis, Concordia University.

Pedersen, C.O., Liesen, R.J., Strand, R.K., Fisher, D.E., Dong, L., Ellis, P.G., 2000. A toolkit for building load calculations [user manual], ASHRAE, Alanta, GA.

Peippo, K., Lund, P., Vartiainen, E., 1999. Multivariate optimization of design trade-offs for solar low energy buildings. Building and Environment 29 (1), 189–205.

Pike Research, 2012. Zero Energy Buildings: Global Market, Regulatory, and Technology Analysis for Energy Efficiency and Renewable Energy in Commercial and Residential Buildings.
URL www.pikeresearch.com/research/zero-energy-buildings

Poli, R., Langdon, W. B., McPhee, N. F., 2008. A field guide to genetic programming.
URL http://www.gp-field-guide.org.uk

Price, K., Storn, R., Lampinen, J., 2005. Differential Evolution: A Practical Approach to Global Optimization, 1st Edition. Springer-Verlag, Heidelberg, DE.

Purdy, J., Beausoleil-Morrison, I., 2001. The significant factors in modeling residential buildings. In: Proceedings of Seventh International IBPSA Conference, Rio de Janeiro, Brazil.

R Foundation, 2012. R project for statistical computing homepage.
URL http://www.r-project.org/

Radford, A.D., Gero, J.S., 1980. Tradeoff diagrams for the integrated design of the physical environment in buildings. Building and Environment 15 (2), 3–15.

Ramesh, T., Prakash, R., Shukla, K., 2010. Life cycle energy analysis of buildings: An overview. Energy and Buildings 42 (10), 1592–1600.

Reddy, M. J., Kumar, D. N., 2007. An efficient multi-objective optimization algorithm based on swarm intelligence for engineering design. Engineering Optimization 39 (1), 49–69.

Reddy, T. A., 2011. Applied data analysis and modeling for energy engineers and scientists. Springer Science.

Reddy, T.A., 2005. Literature review on calibration of building energy simulation programs: Uses, problems, procedures, uncertainty, and tools. ASHRAE Transactions 115, Part 1, 226–240.

Robbins, H., Monro, S., 1951. A stochastic approximation method. Annals of Mathematical Statistics 22 (3), 400–407.
URL http://projecteuclid.org/euclid.aoms/1177729586

RSMeans, 2012. RSMeans Electrical cost data. RSMeans Company, Kingston, MA.
URL http://www.rsmeans.com

RSMeans, 2013. RSMeans building construction cost data. Retrieved April 2013.
URL http://www.rsmeans.com

Russell, S., Norvig, P., 2010. Artificial Intelligence: A Modern Approach, 3rd Edition. Pearson Higher Education, New Jersey, USA.

Rysanek, A., Choudhary, R., 2013. Optimum building energy retrofits under technical and economic uncertainty. Energy and Buildings 57 (0), 324–337.

Sadineni, S. B., Atallah, F., Boehm, R. F., 2012. Impact of roof integrated pv orientation on the residential electricity peak demand. Applied Energy 92 (0), 204–210.

Sahlin, P., Bring, A., 1991. IDA solver - a tool for building and energy systems simulation. In: Proceedings of IBPSA Conference, Nice, France. IBPSA.

Saltelli, A., Chan, K., Scott, E., 2000. Sensitivity analysis, 1st Edition. John Wiley & Sons.

Saltelli, A., Ratto, M., Andres, T., Campolongo, F., Cariboni, J., Gatelli, D., 2008. Global Sensitivity Analysis: The Primer, 1st Edition. John Wiley & Sons.

Scott, D. W., 1992. Multivariate Density Estimation. Theory, Practice and Visualization, 1st Edition. Wiley, New York.

Shannon, C., Weaver, W., 1947. The Mathematical Theory of Communication, 1st Edition. Univ. Illinois Press, Urbana, IL.

Sobol, I. M., 1993. Sensitivity estimates for nonlinear mathematical models. Mathematical Modelling and Computational Experiments 1 (4), 407–414.

Spitz, C., Mora, L., Wurtz, E., Jay, A., 2012. Practical application of uncertainty analysis and sensitivity analysis on an experimental house. Energy and Buildings 55 (0), 459–470.

SQLite, 2012. SQLite homepage. Accessed April 2012.
URL http://www.sqlite.org/

Storn, R., Price, K., 1995. Differential evolution âĂŞ a simple and efficient adaptive scheme for global optimization over continuous spaces. Tech. rep., International Computer Science Institute, Berkley, USA:.

Struck, C., Kotek, P., Hensen, J., 2006. On incorporating uncertainty analysis in abstract building performance simulation tools. In: Proceedings of 12th International Symposium for Building Physics, Dresden, Germany. pp. 193–205.

Sun, Y., Heo, Y., Tan, M. H., Xie, H., Wu, C.F. Jeff., Augenbroe, G., 2013. Uncertainty quantification of microclimate variables in building energy models. Journal of Building Performance Simulation 0 (0), 1–16.

SunPower, 2013. Sunpower homepage. Retrieved May 2013.
URL http://www.sunpowercorp.com

Swan, L., 2010. Residential Sector Energy and GHG Emissions Model for the Assessment of New Technologies. Ph.D. dissertation, Dalhousie University.

Taylor, R., Pedersen, C., Lawrie, L., 1990. Simultaneous simulation of buildings and mechanical systems in heat balance based energy analysis programs. In: Proceedings of the 3rd International Conference on System Simulation in Buildings, Liege, Belgium.

Thevenard, D., Driesse, A., Pelland, S., Turcotte, D., Poissant, Y., 2010. Uncertainty in long-term photovoltaic yield predictions. Tech. rep., CanmetENERGY, Varennes Research Center, Natural Resources Canada, report no. 2010-122 (RP-TEC).

Thevenard, D., Pelland, S., 2011. Estimating the uncertainty in long-term photovoltaic yield predictions. Solar Energy.

Tian, W., 2013. A review of sensitivity analysis methods in building energy analysis. Renewable and Sustainable Energy Reviews 20 (0), 411–419.

Tian, W., de Wilde, P., 2011. Uncertainty and sensitivity analysis of building performance using probabilistic climate projections: A UK case study. Automation in Construction 20 (8), 1096–1109.

Torcellini, P., Pless, S., Deru, M., Crawley, D., June 2006. Zero energy buildings: A critical look at the definition. In: ACEEE Summer Study. NREL, pp. 1–12.

Toronto Hydro, 2011. 2011 Annual Report.
URL http://www.torontohydro.com/sites/corporate/InvestorRelations/FinancialReports/Documents/FinancialReports/2011Interactive/pdf/2011AR.pdf

Torres, S. L., Sakamoto, Y., 2007. Facade design optimization for daylight with a simple genetic algorithm. In: Building Simulation. IBPSA, pp. 1162–1167.

Trane, 2013. Trane Trace Homepage. Retrieved January 2013.
URL http://www.trane.com/COMMERCIAL/DNA/View.aspx?i=1136

Trčka, M., Hensen, J., Wetter, M., 2010. Co-simulation of innovative integrated HVAC systems in buildings. Retrieved April 2011.
URL http://simulationresearch.lbl.gov/people/wetter-michael

Tuhus-Dubrow, D., Krarti, M., 2009. Comparative analysis of optimization approaches to design building envelope for residential buildings. ASHRAE Transactions 115 (1), 554–561.

Tuhus-Dubrow, D., Krarti, M., 2010. Genetic-algorithm based approach to optimize building envelope design for residential buildings. Building and Environment 45 (4), 1574–1581.

Tzempelikos, A., July 2005. A methodology for integrating daylighting and thermal analysis of buildings. Ph.D. dissertation, Concordia University, dAI-B 66/11, May 2006.

UN, 2013. Department of economic and social affairs population division. Accessed January, 2013.
URL http://www.un.org/esa/population/

UNEP-SBCI, 2007. Buildings Can Play Key Role in Combating Climate Change. United Nations Environment Program.
URL http://www.unep.org/Documents.Multilingual/Default.asp?DocumentID=502&ArticleID=5545

USGBC, 2011. Leadership in energy and environmental design (LEED) green building rating system.
URL http://www.usgbc.org

USGOV, 2008. The emergency economic stabilization act of 2008. Tech. rep., retrieved September, 2012.
URL http://www.energy.gov/media/HR_1424.pdf

van Rossum, G., 2011. Python homepage.
URL http://www.python.org/

Venables, W. N., Ripley, B. D., 2002. Modern Applied Statistics with S, 4th Edition. Springer.

Verbeeck, G., 2007. Optimisation of extremely low energy residential buildings. Ph.D. dissertation, Catholic University Leuven.

Vieira, R. K., Cummings, J. E., Fairey, P. W., Hannani, K., 1998. How to calculate financial information for home energy raters, lenders and savvy home buyers. In: Proceedings from the 1998 ACEEE Summer Study on Energy Efficency in Buildings, Washington, D.C. America council for an energy-efficient economy (ACEEE), pp. 7.335–7.346.

Voss, K., Musall, E., 2012. Net Zero Energy Buildings: International Comparison of Carbon-Neutral Lifestyles, 1st Edition. Walter de Gruyter.

W3C Consortium, Apr. 2011. XML consortium homepage.
URL http://www.w3.org/XML

Walker, I., Wilson, D., 1998. Field validation of equations for stack and wind driven air infiltration calculations. HVAC&R Research 2 (2).

Wang, L., Mathew, P., Pang, X., 2012. Uncertainties in energy consumption introduced by building operations and weather for a medium-size office building. Energy and Buildings 53 (0), 152–158.

Wang, W., 2005. A simulation-based optimization system for green building design. Ph.D. dissertation, Concordia University.

Wang, W., Beausoleil-Morrison, I., 2009. Integrated simulation through the source-code coupling of component models from a modular simulation environment into a comprehensive building performance simulation tool. Journal of Building Performance Simulation 2 (2), 115–126.

Wang, W., Rivard, H., Zmeureanu, R., 2006. Floor shape optimization for green building design. Advanced Engineering Informatics 20 (4), 363–378.

Wang, W., Zmeureanu, R., Rivard, H., 2005. Two-phase application of multi-objective genetic algorithms in green building design. In: Building Simulation. IBPSA, pp. 1323–1330.

Weise, T., Mar. 9, 2009. Global optimization algorithms - Theory and application, 2nd Edition. Self-Published.
URL http://www.it-weise.de/

Wetter, M., Spring 2004. Simulation-based energy optimization. Ph.D. dissertation, University of California, Berkeley.

Wetter, M., 2005. BuildOpt–a new building energy simulation program that is built on smooth models. Building and Environment 40 (8), 1085–1092.

Wetter, M., 2010. Co-simulation of building energy and control systems with the building controls virtual test bed. Journal of Building Performance Simulation.

Wetter, M., 2011a. GenOpt, generic optimization program. Retrieved April 2011.
URL http://gundog.lbl.gov/GO/index.html

Wetter, M., 2011b. GenOpt, generic optimization program, user manual, version 3.1.0. Technical report, Lawrence Berkeley National Laboratory, Berkeley, CA.
URL http://gundog.lbl.gov/GO/index.html

Wetter, M., Haves, P., 2008. A modular building controls virtual test bed for the integration of heterogeneous systems. In: Proceedings of SimBuild, 3rd National Conference of IBPSA-USA Berkeley, CA, USA. International Building Performance Simulation Association, USA chapter.

Wetter, M., Polak, E., 2004. Building design optimization using a convergent pattern search algorithm with adaptive precision simulations. Energy and Buildings 37, 603–612.

Wetter, M., Wright, J., 2003. Comparison of a generalized pattern search and a genetic algorithm optimization method. In: Building Simulation. IBPSA, pp. 1401–1408.

Wetter, M., Wright, J., 2004. A comparison of deterministic and probabilistic optimization algorithms for nonsmooth simulation-based optimization. Building and Environment 39 (8), 989–999.

Wolfram, S., 1984. Universality and complexity in cellular automata. Physica D 10, 1–35.

Wolfram, S., 1994. Cellular Automata and Complexity: Collected Papers, 1st Edition. Addison-Wesley, Reading, MA.

Wolpert, D., Macready, W., 1997. No free lunch theorems for optimization. IEEE Transactions on Evolutionary Computation 1, 67.

World Energy Council, 2007. Survey of energy resources. Published by the World Energy Council.

Wright, J., Alajmi, A., 2005. The robustness of genetic algorithms in solving unconstrained building optimization problems. In: Proceedings of Ninth International IBPSA Conference, Montréal, Québec. pp. 1361–1368.

Wright, J., Farmani, R., 2001. The simultaneous optimization of building fabric construction, HVAC system size, and the plant control strategy. In: Proceedings of Seventh International IBPSA Conference, Rio de Janeiro, Brazil. pp. 865–872.

Wright, J., Loosemore, H.A., 2001. The multi-criterion optimization of building thermal design and control. In: Proceedings of Seventh International IBPSA Conference, Rio de Janeiro, Brazil. pp. 873–880.

Wright, J.A., Loosemore, H. A., Farmani, R., 2002. Optimization of building thermal design and control by multi-criterion genetic algorithm. Energy and Buildings 34 (9), 959–972.

Yudelson, J., 2008. Green Building Through Integrated Design, 1st Edition. McGraw-Hill Professional, NY, USA.

Zang, H., Zhang, S., Hapeshi, K., 2010. A review of nature-inspired algorithms. Journal of Bionic Engineering 7, S232–S237.

Zitzler, E., Deb, K., Thiele, L., 2000. Comparison of multiobjective evolutionary algorithms: Empirical results. Evolutionary Computation 8 (2), 125.

Appendix A

Uncertainty and Sensitivity Analysis of Cost Model

This appendix describes an uncertainty and sensitivity analysis on the cost-model defined in section 3.5 and used in Chapters 4–8. The goal of this appendix is to complement the variational analysis of the energy model presented in Chapter 6 by showing sensitivity and influential variables in the cost-model. Note that the formation of PDFs differs entirely from the previously proposed approach. Probability distributions represent the uncertain quantities in the economic model used whereas the PDFs of Chapter 6 represented the probability of achieving the NZE criterion. A discussion of uncertainty and sensitivity of the cost model is presented in the next section.

A.1 Method

Table A.1 describes the 26 variables used in the analysis. Variable types included: (i) life-cycle economic variables such as inflation and discount rate; (ii) variations of initial and replacement costs using multipliers; (iii) duration of expected material serviceable life-times; (iv) duration of incentive offerings such as feed-in tariffs; and (v) utility, mortgage and feed-in tariff rates.

All uncertainties were described using normal distributions. The mean parameter was specified as the value used in the cost model. The standard deviation was calculated such that 95% of values fall with in the select range of variables. However, the

Table A.1: Sample of influential cost model variables for a NZEH

Variable	Units	Min.	Max.	No. Steps	Mean	Description
infla	%	1.0	3.0	8	2.0	Inflation rate
elec_esc	%	2.4	3.6	8	3.0	Excalation of electricity utility cost
disc	%	1.0	3.0	8	2.14	Discount rate or bank-rate
t_fit	yr	16	24	8	20	Time-period for Feed-In Tariff
t_lcc	yr	24	36	8	30	Time-period for life-cycle analysis
rate_fit	$\$/kWh$	0.439	0.658	8	0.549	Feed-In Tariff rate
rate_elec	$\$/kWh$	5	8	8	7.0	Utility rate of electricity
rate_mort	%	4.8	7.2	8	6.0	Amortization rate
cost_pvwatt	\$/W	1	3	8	1.5	Unit cost of PV Panels
cost_pvmisc	\$/W	2.746	4.119	8	3.432	Unit cost of misc. PV materials/installation
cost_inv	\$/W	0.68	1.02	8	0.85	Unit cost of inverter
cost_shinmul	–	0.8	1.2	8	1.0	Cost multiplier factor for shingles
cost_roofmul	–	0.8	1.2	8	1.0	Cost multiplier factor for roof slope
cost_wallmul	–	0.8	1.2	8	1.0	Cost multiplier factor for wall cost
cost_ceilmul	–	0.8	1.2	8	1.0	Cost multiplier factor for ceiling cost
cost_bwallmul	–	0.8	1.2	8	1.0	Cost multiplier factor for basement wall
cost_conmul	–	0.8	1.2	8	1.0	Cost multiplier factor for concrete
cost_ovrmul	–	0.8	1.2	8	1.0	Cost multiplier factor for overhangs
cost_tightmul	–	0.8	1.2	8	1.0	Cost multiplier factor for air-tightness
cost_winmul	–	0.8	1.2	8	1.0	Cost multiplier factor for windows
cost_slabmul	–	0.8	1.2	8	1.0	Cost multiplier factor for slab
repl_pv	yr	32	48	8	40	Replacement time-period for PV panels
repl_inv	yr	12	18	8	15	Replacement time-period for inverter
repl_win	yr	32	48	8	40	Replacement time-period for windows
repl_shin	yr	20	30	8	25	Replacement time-period for shingles
repl_wallcell	yr	20	30	8	25	Replacement time-period for wall insulation
repl_ceilcell	yr	20	30	8	25	Replacement time-period for ceiling insulation

distribution was re-weighted such that the sum of the PDF is one. Note that for some variables the distribution is shifted to model specific scenarios. For example, the PV panel costs were shifted to have a higher weighting for more expensive panel costs to explore this effect on the cost model. Upper and lower limits were typically within 20% to 50% of estimated mean values.

Variations in cost model parameters were calculated for a single optimal design, as presented in Chapter 8. Thus, the sensitivity is calculated in the solution space where important conclusions about optimized building design are drawn. Conducting a similar analysis on other non-optimal individuals might be inappropriate due to partial usage of some cost parameters. For example, partial roof coverage of PV panels may lessen the significance of initial cost for PV material and FIT tariff offerings.

Similar to Chapter 6, a Monte-Carlo approach conducted the uncertainty analysis. A sample size of 500 individuals ensured statistical significance in the conclusions drawn from this analysis. As previously mentioned, PDFs were specified from user defined values using normal distributions described in Table A.1. The sensitivity of variables

within the MCA was calculated using a generalized linear model (GLM) regression approach.

A GLM is a generalized approach for calculating regression models using generalized least squares (Reddy, 2011). GLMs calculate many interesting statistical metrics including: (i) student t-tests and p-values indicating the significance of a variable in the GLM, (ii) parameter fitting of the regression model to training data; (iii) coefficient of determination of the fit (R^2); (iv) the F-statistic which tests for significance of the overall regression model; (v) fitting using linear, higher-order terms and interacting regressor values; and (vi) ability to fit non-linear data (not-discussed). The p-values were used to rank a variables influence in the Monte Carlo results.

The uncertainty methodology was conducted on two economic indicators: net-present value and capital payback. The goal was to compare the effect of uncertainty on each of these indicators used in the thesis. Since we are dealing with economic aspects which also affect the base-case building, reference buildings were used to calculate incremental NPV and capital paybacks. Discussion of these economic indicators were conducted in the cost methodology section in Chapter 3.

Incremental NPVs and paybacks were calculated using reference buildings as defined in Appendix C using identical economic parameters as defined in the proposed optimal building. As a final step, the difference from the varied incremental economic model and the baseline economic model (values used for economic estimates in Chapters 4–8) were used for all uncertainty estimates in the model. This ensures that uncertainty is measured from the varied economic model relative to the assumptions in the the baseline model used in the thesis. It is expected that uncertainty results will be centered around zero due to this subtractive approach.

Results of the uncertainty and sensitivity analysis are presented in the next section.

A.2 Results and Discussion

Figure A.1 shows the uncertainty distribution for the net-present values economic metric using a Monte Carlo with distributions defined in Table A.1.

Table A.2 shows the ranking of variables used in the NPV uncertainty analysis. The

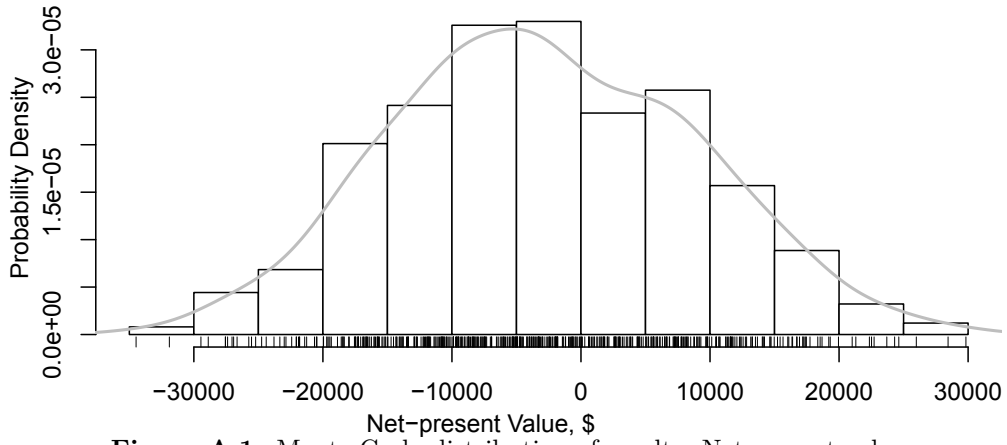

Figure A.1: Monte Carlo distribution of results: Net-present value

regression analysis matched 10 variables with p-values less than 5%. The coefficient of determination was $R^2 = 0.97$. Variations in the economic model as described in Table A.1 caused NPV to vary by $\$ - 2277 \pm 18613$ relative to the reference building over the evaluated life-cycle. The slight negative bias indicates that cash flows are underestimated relative to the reference economic model. The most sensitive variable in the model is the amortization rate. If the additional technology costs of a net-zero energy home are amortized over a long period this can create a divergence in cost model results.

Table A.2: Ranking of influential variables in cost model for a NZEH using NPV

Rank	Variable	Units	Description
1	rate_mort	%	Amortization rate
2	t_lcc	yr	Time-period for life-cycle analysis
3	rate_fit	$\$/kWh$	Feed-In Tariff rate
4	t_fit	yr	Time-period for Feed-In Tariff
5	rate_elec	$\$/kWh$	Utility rate of electricity
6	repl_pv	yr	Replacement time-period for PV panels
7	cost_pvmisc	\$/W	Unit cost of misc. PV materials/installation
8	cost_pvwatt	\$/W	Unit cost of PV Panels
9	cost_inv	–	Unit cost of inverter
10	cost_tightmul	–	Initial cost multiplier factor for air-tightness

At a first look, the differences in NPV may seem significant. However, these values are taken over the entire 30 year life-cycle indicating that uncertainty in the economic model is approximately ±\$500 given a single years cash-flow. This analysis is repeated using capital payback as an economic metric.

Figure A.1 shows the uncertainty distribution for the capital payback economic metric using a Monte Carlo with distributions defined in Table A.1.

Table A.3 shows the ranking of variables used in the capital payback uncertainty

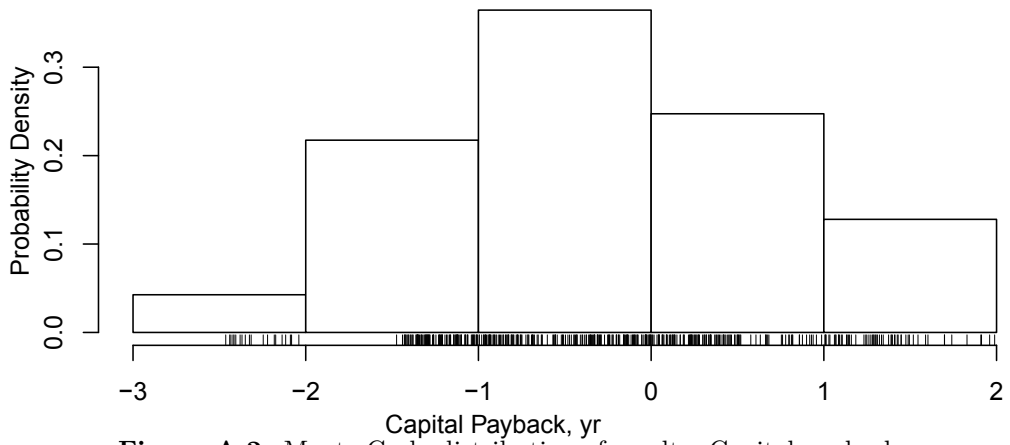

Figure A.2: Monte Carlo distribution of results: Capital payback

analysis. The regression analysis matched 10 variables with p-values less than 5%. The coefficient of determination was $R^2 = 0.85$. Variations caused the total capital payback to vary by -0.28 ± 1.16 years. The slight negative bias indicates that paybacks are under-estimated relative to the reference economic model. The most sensitive variable in the model again is the amortization rate. Not surprisingly, the FIT rate and the miscellaneous installation costs of PV panels are also significant.

Table A.3: Ranking of influential variables in cost model for a NZEH using capital payback

Rank	Variable	Units	Description
1	rate_mort	%	Amortization rate
2	rate_fit	$\$/kWh$	Feed-In Tariff rate
3	cost_pvmisc	\$/W	Unit cost of misc. PV materials/installation
4	cost_tightmul	–	Initial cost multiplier factor for air-tightness
5	disc	%	Discount rate or bank-rate
6	cost_inv	–	Unit cost of inverter
7	repl_inv	yr	Replacement time-period for inverter
8	rate_elec	$\$/kWh$	Utility rate of electricity
9	t_fit	yr	Time-period for Feed-In Tariff
10	repl_pv	yr	Replacement time-period for PV panels

A.3 Conclusion

This analysis builds confidence in our economic model and payback estimates. It can be concluded that results originating from capital paybacks should be given the most confidence. The most sensitive variables are typically well known. For example, fixed-mortgage rates, FIT rates and initial costs can be estimated near precisely at the late design stage. However, some care should be taken in identifying appropriated values for

early stage designs.

Using the distributions defined in Table A.3, it is estimated that predictions on paybacks can be made with an uncertainty of ± 1.16 years. This is well within the acceptable range to make economic decisions.

Appendix B

Description of Optimization Software

B.1 Overview

This appendix describes the software development approached used in this thesis. Excluding software used for simulating energy models and data visualization, over four thousand lines of code was developed for this thesis. Many of the algorithms explored were not used in the proposed methodologies. Due to the exploratory nature of this research, the algorithms shown in source code could be refactored to improve readability and simplicity.

B.2 Software Structure

The optimization methodology was developed using a functional programming paradigm. Unlike other programming paradigms, such as procedural or object orientated, functional programming relies solely on the deconstruction of larger problems into smaller, more tractable problems. Each smaller problem is solved using a single function. Results from each function are passed directly to the next function. Functional programming limits side-effects by avoiding states and mutable data.

The Clojure programming language was selected to develop the methodology (Hickey, 2012). Clojure is built on the Java virtual machine and thus has all the functionality of Java with the expressive terseness of LISP. For example, building on the Java virtual machine allowed for simple implementation of a cryptographically strong random num-

ber generator based on NIST standards which improves algorithm functionality (NIST, 2013; Oracle, 2013). Like other LISP dialects, Clojure expresses functions using lambda calculus. A function $f(x)$ is now expressed by `(f x)`, where the function f is said to operate on variable x.

A major advantage in using a LISP dialect is the terseness in which software can be developed. For example, consider the skeleton code for developing an evolutionary algorithm shown below. A loop represents the evolutionary cycles. New children populations are formed by cascading the following functions: parent selection, crossover, mutation, fitness evaluation, and survivor selection. The entire algorithm, excluding fitness evaluations, can be reduced to less than 60 lines of code with comments. Note that comments are marked using the '`;;`' characters.

```
;; Description of namespace and namespace dependencies
(ns validate.ea
    (:gen-class)
    (:use [validate.math])
    (:use [validate.binary])
    (:use [validate.discrete])
    (:use [validate.epistasis])
    (:use [validate.utils])
    (:use [validate.database])
    (:use [validate.detsearch])
)

;; Load up algorithm configuration.
(load-file "src/validate/parameters.clj")

(defn run-ea [num-iter]
  "Function to run evolutionary algorithm."
  ;; EA algorithm loop
  (loop [
         ;; initialized population
         population (initial-population-fn population-size)
         iter num-iter ;; Number of evo-cycles to perform]

         ;; terminate EA if max cycles reached
         (if (= iter max-cycle)
           (terminate-fn)
         )

         ;; let function defines variables
         (let
         [

         ;; Formation of child population:
         ;;  Order of operations: 1) parent select, 2) crossover
         ;;    3) mutation
         child (map
                 #(mutation-fn % mutation-rate)
                   (crossover-fn
                     ;; k: size of tournament for parent selection
                     (parent-sel-fn population num-parent-needed k)
```

```
                    )
                )

            ;; evaluate fitness of new children population
            fitness (eval-fit-fn child)

            ;; join old parent population with new children population
            joined-population (join-fn children population)

            ;; select new population (using fitness evaluation)
            new-population (survivor-sel-fn joined-population fitness)
            ]

            ; Begin next EA cycle
            (recur
              new-population ;; Pass new population to next iteration
              (dec iter) ;; Decrement number of iterations to perform by 1
            );; End Recur function
            );; End let function
    );; End loop function
) ;; End run-ea function
```

Listing B.1: Exemplar Clojure Code for EA

The optimization methodology was deconstructed using several modules, called namespaces in Clojure. Table B.1 describes each namespace. Namespaces form a hierarchy with the core module, the dispatcher namespace, at the top of the dependency tree. Lower level modules, such as the `math` and `util` namespace, provide functionality for all intermediate namespaces. Finally, Figure B.1 shows the dependencies between each namespace.

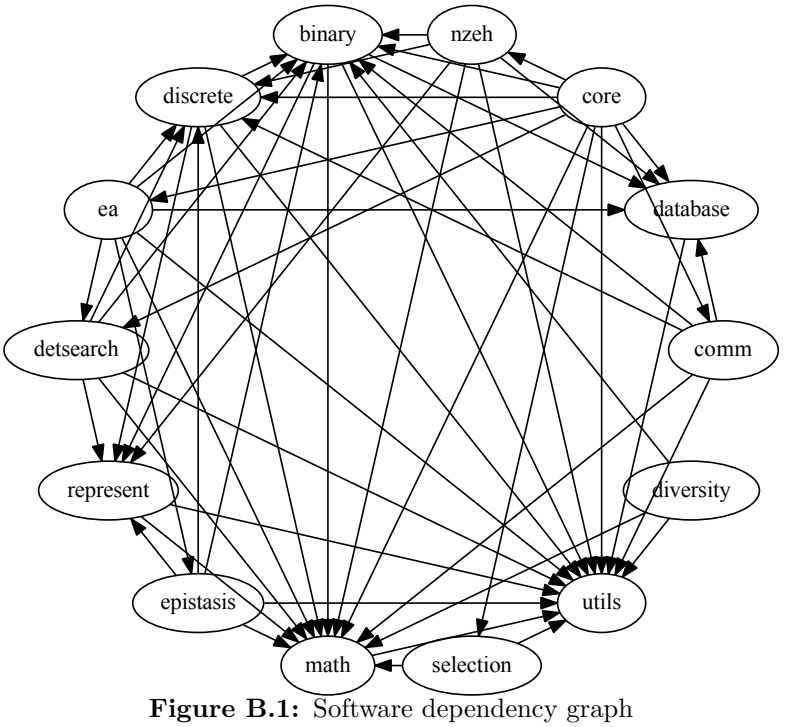

Figure B.1: Software dependency graph

Table B.1: Description of software modules and module dependencies

Module Name	Module Dependencies	Description
utils	–	Utility functions for all modules.
math	utils	Math utility module
represent	math, utils	Core representation functions common to both representation types.
binary	represent, math, database, utils	Module for binary representation.
discrete	math, utils, represent, binary	Discrete representation module.
selection	math, utils, represent, binary	Selection operators used in EA.
database	utils	Database module used for SQL interactions.
diversity	binary	Diversity calculation functions.
epistasis	math, utils, represent, binary, discrete	Module for mutual information calculations.
comm	math, binary, discrete, database, utils	Commercial building module.
nzeh	represent, math, binary, discrete, database, utils	NZEH module.
detsearch	math, represent, binary, discrete, utils	Deterministic search module.
ea	math, binary, discrete, epistasis, utils, database, detsearch	Evolutionary algorithm module.
core	math, utils, binary, discrete, selection, detsearch, nzeh, comm, ea, database	Core module which pulls all components together.

B.3 Algorithm Scalability Tests

This section describes a scalability comparison of the proposed evolutionary algorithm, without augmentation of information data-mining, to the particle swarm inertial weight algorithm (PSOIW) in the GenOpt optimization suite. Information driven data-mining was not employed since this would give the EA an immediate advantage of strategic deterministic searches over the PSOIW algorithm.

A scalability test shows how an optimization algorithm reacts to increasing problem sizes to find a known optimal solution. Particularly, this test compares the average number of algorithm iterations or generations to solve a building optimization problem with a given number of design variables.

Figure B.2 shows typical scalability test comparing two different algorithms. In this case, algorithm B outperforms algorithm A for smaller problem sizes and the reverse is true for larger problem sizes. Extrapolations of this graph can be valuable in estimating how the optimization algorithm scales with problem sizes beyond those tested. Since this test compares iterations, rather than time, it is independent of computer speed and

type.

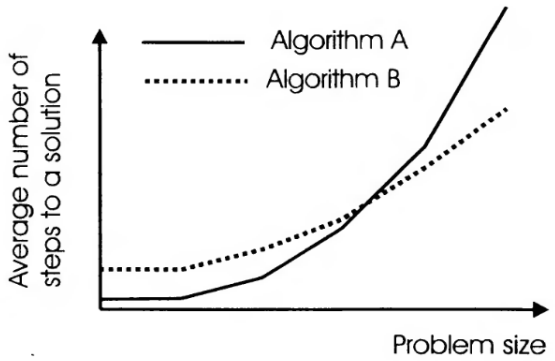

Figure B.2: Approach for optimization algorithm scalability test (Eiben and Smith, 2003)

The following section describes the method to perform this test for building optimization problems.

B.3.1 Method

A single objective optimization problem using 26 design variables, as described in Chapter 4 was used. The optimization process was run initially to identify the optimal solution. A termination criterion specified that the optimization process would stop if an individual was found within 3% of this optimal solution.

The optimization algorithm was started with the full optimization problem. The number of generations was recorded to meet the termination criteria. A sequence of 16 variables were randomly selected for removal. The optimization process was repeated, removing the first variable in the sequence and setting it to the optimal value in the parameter configuration file. This step ensured that the termination criterion was valid while scaling back the optimization problem. Again the number of generations was recorded once the termination criterion was met. This process was repeated until only 10 variables were left. At this point, the algorithm required only a few iterations to identify the optimal solution. This test was repeated 15 times to ensure a significant sample size.

It is imperative that variables be randomly removed while decreasing the problem size and that a large sample size be used. As discussed in Chapter 5, some variables are weakly and tightly coupled which leads to varying algorithm performance.

The identical logic was implemented in GenOpt. Several challenges were overcome.

First, GenOpt does not support a termination criterion that stops the algorithm if an individual was found within 3% of this optimal solution. Furthermore, the source-code in GenOpt did not allow for an easy implementation of such termination criterion. As a work around, logic was hard-coded in to the energy simulation script to write an error message into the GenOpt log file. GenOpt immediately terminates the algorithm if error messages are found. The number of generations to reach the termination criterion is then simply extracted from the results file. The randomization of variables both in initialization and in removal had to be scripted and tested.

The following section shows the scalability test and discusses results.

B.3.2 Scalability Results and Discussion

The scalability test is shown in Figure B.3. The curves were not smooth due to random removal of design variables. Statistical tests indicate that both algorithms require exponentially more generations to reach the optimal solution as problem size increases.

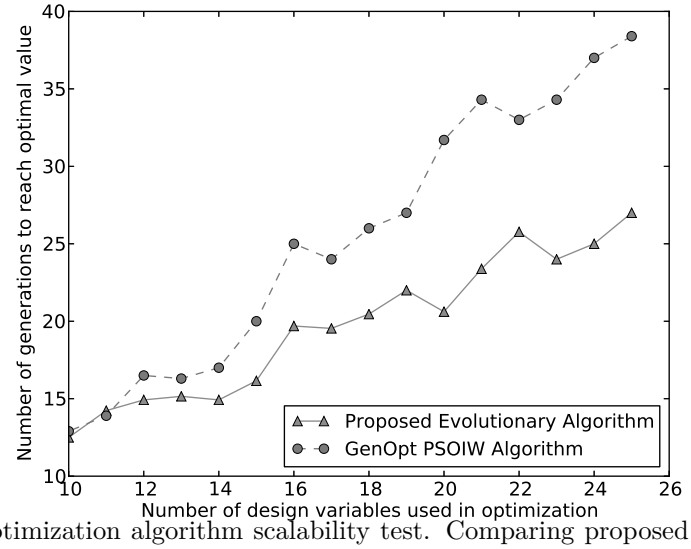

Figure B.3: Optimization algorithm scalability test. Comparing proposed evolutionary algorithm to GenOpt PSOIW

Both algorithms require approximately the same number of generations for smaller design problems. The proposed optimization algorithm required 12 less generations for larger problem sizes. This indicates that the proposed evolutionary requires 10 fewer algorithm iterations for problem sizes greater than 25 design variables. Given the exponential fit, this difference will become exponentially more significant for larger problem sizes.

Appendix C

Formation of Reference Building

C.1 Overview

THE goal of this appendix is to define the reference building used in the case-studies. When creating a reference building it is important to look at both codes and the existing building stock. Three building standards were considered: model national code of Canada (NRC, 1997b), ASHRAE 90.2 (ASHRAE, 2011b), EnergyStar (EPA, 2012) and dataset of 180,000 homes constructed in Canada. NRCan provided the dataset collected through the ecoEnergy programme (NRCan, 2012). This dataset was originally used for the PhD research of Swan (2010).

Consider the statistical trends found using the NRCan dataset shown in Figures C.1–C.7. Looking at how existing homes are constructed is the best resource for creating a reference building. Not all contractors rely on energy standards for constructing homes. Furthermore, energy codes represent minimal suggested values—builders may exceed these values significantly depending on the needs of their clients or their willingness to innovate the market.

Figure C.1 shows the distribution of construction dates in the dataset. Only detached homes built in Quebec and Ontario were used in this analysis to ensure similar climate zones. Note, the average home in the dataset was built around 1975.

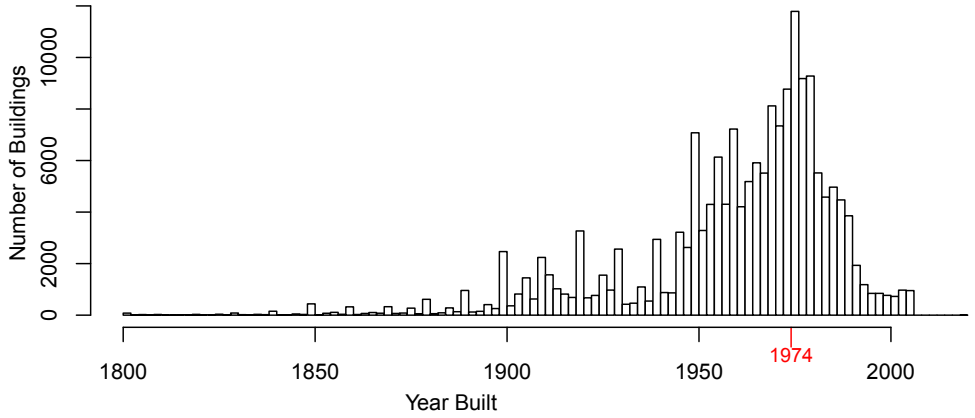

Figure C.1: Distribution of construction dates

One area of interest is how air-tight the existing building stock is. Figure C.2 shows blower door measurements for all 180,000 homes. The average home has an air-tightness around 3.5 ACH at 50 Pa.

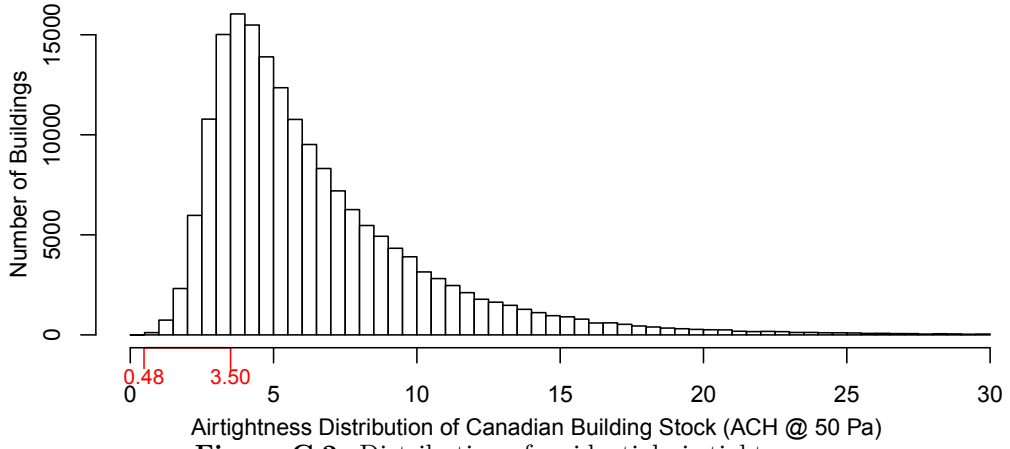

Figure C.2: Distribution of residential air-tightness

One difficult variable to specify from building codes are window-to-wall ratios. Figure C.3 shows the WWR trends observed in the present housing stock. To ensure similar comparisons, slices of data were used for the plot. For example, data is show for homes where the front is south facing. South was selected as front facing as this is the primary orientation of a passive solar home. Note that year of construction is binned into the nearest five year interval. This was performed due to the smaller sample size of homes on an annual basis.

In Figure C.3, one immediately notices the relatively small WWR of east and west faces. Likely this is due to closely spaced homes in urban areas. Another result is that

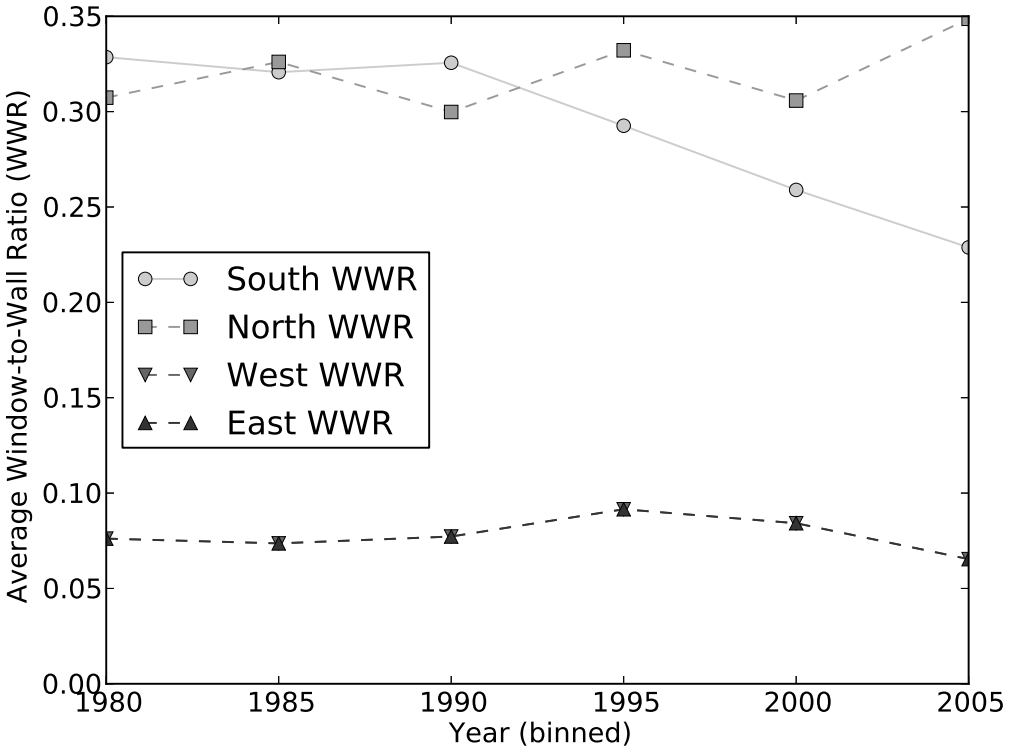

Figure C.3: Window-to-Wall ratio trends for homes constructed after 1980

southern WWRs appear to be decreasing over time from almost 35% in 1980 to less than 25% in 2005 however northern WWRs stay approximately the same. Based on this plot, the following WWRs were selected for reference buildings: (i) south facing WWR of 25%; (ii) east and west facing WWR of 10%; and (iii) north facing WWR of 10%. A conservative value of 10% was selected for the north WWR. Likely, the higher value of 35% found in the database preserved the back view of the home. This effect was not included to better evaluate the passive solar performance of the house. In doing so, the economic and energy savings is underestimated.

The following four graphs present common insulation values. The values vary considerably depending on the age of construction. To ensure insulation graphs reflect recent construction practices, a subset of homes from 1990 to present where selected.

Figure C.4 shows the distribution of wall insulation values in the dataset. Largely, homes are constructed with the minimal code value of 3.7 RSI or roughly R20 of insulation. This is likely limited by the size of a 2x6" wall cavity.

Figure C.4: Distribution of wall insulation

Figure C.5 shows the distribution of attic insulation values in the dataset. There is a much larger distribution of ceiling values with some homes with more than 8 RSI of insulation.

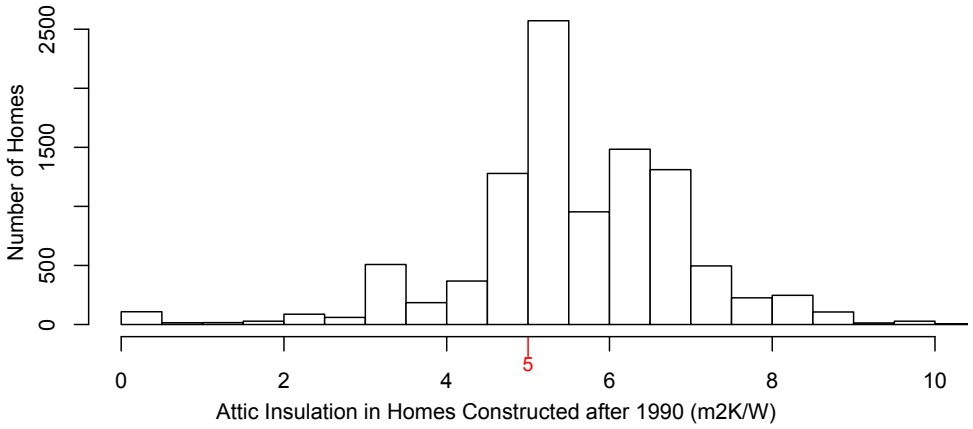

Figure C.5: Distribution of attic insulation

Figure C.6 shows the distribution of basement insulation values in the dataset. Although the majority of basements are uninsulated, many homes have around 2 RSI of insulation.

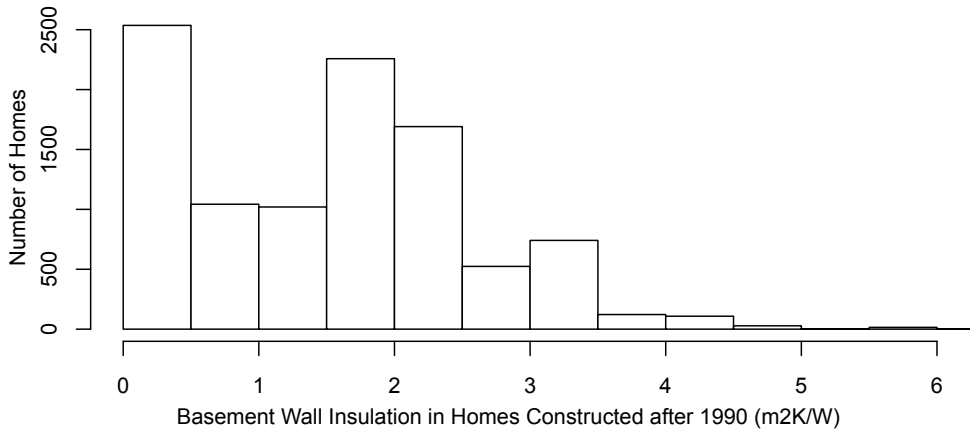

Figure C.6: Distribution of basement wall insulation

Finally, figure C.7 shows the distribution of slab insulation values in the dataset. As shown in this figure, the majority of homes in Canada have uninsulated basement slabs.

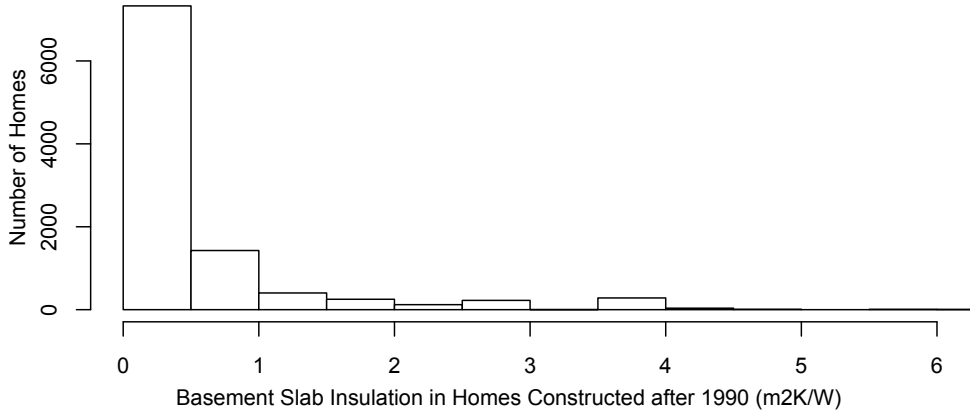

Figure C.7: Distribution of slab insulation

Table C.1 shows construction values recommended by various codes and standards and summarizes values from the NRCan dataset.

Table C.1: Code requirements for reference building

	MNECH-1997	ASHRAE 90.2-2007	EnergyStar	NRCan Dataset	Value Used
Attic Insulation (m^2K/W)	8.8	8.6	7.7	5	8.8
Wall Insulation (m^2K/W)	4.4	3.7	3.8	3.5	4.4
Below-grade walls (m^2K/W)	3.5	1.4	1.7	1.7	3.5
Below-grade slab (m^2K/W)	1.9	–	0.88	0	1.9
Envelope Tightness (ACH@50Pa)	–	–	2.5	3.5	3.5

When selecting reference building values, first energy standards were considered. However, values from the NRCan dataset were used if energy standard values were not common. For example, consider insulation values for slabs. Although standards recommended values of 0.8 to 1.9 RSI, these rarely found in the NRCan dataset. However it might be that insulation of slabs is difficult to ascertain for energy auditors so energy standards were used for slab insulation. Although present building codes specify 8.8 RSI of attic insulation, this would not commonly found in the NRCan dataset. This likely due to settling of blown-in insulation or deterioration of existing value. Regardless, a value of 8.8 RSI from standards was used for ceiling insulation.